A Finite Element Analysis Study of the Trans-femoral Residuum

Alex van Heesewijk

This thesis is submitted to the University of Surrey for the degree of Doctor of Philosophy

2020

Centre for Biomedical Engineering

University of Surrey, Guildford, Surrey, GU2 7XH

ABSTRACT

The current method for prosthetic socket design is a lengthy and costly process which is highly dependent on the experience of the prosthetist. Finite Element (FE) modelling has the potential to improve the efficiency of the socket design process.

The aim of this project was to investigate the interaction between the trans-femoral residual limb and prosthetic socket using FE simulations. FE models of the residual limb were created and used to simulate standing and walking loads. The studies were conducted over three separate chapters to allow for objective examination of several novel aspects of the modelling setup.

Firstly, the effect of introducing the pelvic bone was examined. The results show that pelvic bone shifted the peak interfacial stresses from the distal end, when the bony geometry was only simulated as the residual femur, to the proximal medial region of the residuum.

Secondly, the effect of prosthetic liners was examined in terms of its friction coefficient, thickness, and stiffness values. Experimental testing of prosthetic liners showed that the friction coefficient for all liners decreased in wet conditions compared to dry conditions. Higher peak interfacial stresses were found in the FE models with increase friction coefficient levels at both the residuum-liner and liner-socket interfaces. Furthermore, the results showed that the muscle stiffness, liner stiffness and liner thickness were all statistically significant in terms of the resultant interfacial stresses on soft tissues.

Finally, the effect of socket tightness of fit and different socket types was considered. Increased fit tightness for the socket significantly reduced the peak interfacial stress and increased average pressures producing more optimal conditions. With two different prosthetic socket designs the results from bipedal stance were examined against soft tissue damage thresholds. The studies showed that the amount of tissue at risk of viability was related to the socket design.

Acknowledgements

I would like to express deep gratitude to my academic supervisors, Dr W. Xu, Prof. A. Crocombe and Dr S. Cirovic for their guidance, supervision, and support that made this research possible.

I am incredibly grateful to the support and guidance obtained from both the EU H2020 Socket Master project and ProActive Prosthetics Ltd which has helped me explore this incredibly interesting field of study.

Finally, I would like to express my appreciation to my girlfriend, family, and friends, all of whom gave unfathomable backing and encouragement.

Declaration of Originality

This thesis and the work to which it refers are the results of my own efforts. Any ideas, data, images, or text resulting from the work of others (whether published or unpublished) are fully identified as such within the work and attributed to their originator in the text, bibliography or in footnotes. This thesis has not been submitted in whole or in part for any other academic degree or professional qualification. I agree that the University has the right to submit my work to the plagiarism detection service TurnitinUK for originality checks. Whether or not drafts have been so assessed, the University reserves the right to require an electronic version of the final document (as submitted) for the assessment as above.

Signed: Alex van Heesewijk

Table of Contents

Table of Figures

Table of Tables

1. INTRODUCTION

1.1 Background

There are approximately 1.6 million individuals in the United States living with an amputation (Ziegler-Graham et al. 2008), with an estimated 22.4% yearly increase in the number of annual amputations (Sugimoto 2013). Trans-femoral amputation has been reported to account for up to 46.4% of all major amputations (Davie-Smith et al. 2018).

A trans-femoral amputation, also known as above-knee (AK), is amputation of the lower limb through the femoral bone. Similar to other types of limb loss, people with a trans-femoral amputation experience a loss of mobility. Diabetes and peripheral arterial disease are the two major causes for lower-limb amputation, with over 75% of all amputations occurring due to diabetes and peripheral arterial disease related (Heyer et al. 2015; Narres et al. 2017). A planned amputation is typically not considered to be a challenging surgical procedure. The outcome can provide good functional results provided that surgical consideration is given to the knowledge of prosthetic design, preoperative planning and the patient's expectations following the amputation (Morris et al. 2015).

The amputation process has a substantial cost and burden on national and private healthcare, with an annual cost of £55 million for the National Health Service (NHS) (Kerr et al. 2014) and additional costs associated with hospitalisation and after care. The socket design and fabrication is a costly and lengthy process: over a five-year period after amputation, the cost of a single lower limb prosthesis ranges between £28,100 and £48,300 with an average of 32% of the costs relating to the labour of the prosthetist (Frossard et al. 2017). On average, only 63% of patients are issued with a prosthetic socket within six months of amputation and individuals often reporting inadequate coupling between residual limb and prosthetic socket (Jordan et al. 2012).

Lower limb amputees have reported up to three skin problems each month, consequently 25% reported limited use of their prosthesis and 28% felt inhibited from social functions (Meulenbelt et al. 2011). Further, up to 98.4% of lower limb amputees have reported falling within the past 12 months, for the majority these falls occurred during normal ambulation activities (Chihuri and Wong 2018).

1.2 The Need for Work

When designing a prosthetic socket for a person with a lower limb amputation, the prosthetist must rely on their clinical experience and knowledge to determine the most appropriate socket design and fit for each individual. This is currently a lengthy and costly process, requiring numerous iterations of the socket to be designed, fabricated, and tested, before a suitable socket fit is deemed comfortable and useable by the patient. This drawn out process entails large scope for human error as the process is highly dependent on the artisan nature of the prosthetists techniques which are based off knowledge that differs between prosthetists. A notable drawback of the current technique is the uncertainty that the final socket iteration provides a truly optimal fit between the socket and residual limb. The manner in which the socket design has been carried out has direct influence on the performance of the socket. When the fit of the socket over the residual limb is not suitable, excessive stresses occur on the residual limb causing problems to arise. For example, a socket fit that is too tight over a pressure sensitive region will cause, the patient high levels of discomfort and potential tissue damage.

The use of finite element (FE) modelling is potentially very attractive and is a useful way of providing qualitative guidance for prosthetists in a clinical setting with potential for improving the socket design process. Using the tool of FE modelling could allow the prosthetist to determine the internal and interfacial loading distribution for different residual limb soft tissues when combined with several different socket designs. This improved process would enable rapid prototyping of a subject specific socket design that considers the patients individual residuum characteristics. This would significantly reduce the number of 'check' sockets required, which would make this process more feasible to budget constraints in the UK and NHS hospitals. Providing savings in both time and money for the service provider and patient. Furthermore, this modelling method would gather additional information such as areas of potential soft tissue damage and the most suitable liner properties to be paired with the patient's residual limb.

Clinically and commercially, these developments are desirable as they provide the potential benefits of:

- Greater process simplicity, sharing the expertise and tacit knowledge for socket design. A computational design process would allow potential modifications of the socket design to be quickly implemented within computer-aided design (CAD) software and the results examined via finite element analysis (FEA) simulations.
- Improved patient satisfaction with the fit of their prosthesis.
- Reduced cost for the prosthetist spent on fabrication multiple socket iterations, with quicker patient turn around for socket design.
- Overall improvement of the design process with greater likelihood that an optimal socket fit would be achieved.

Therefore, the research aim of this thesis is:

"To evolve the finite element modelling of the trans-femoral residual limb for accurate simulation of the interaction between the lower limb prosthetic components"

This is a necessity to enable the above benefits to be realised for further developments in computational trans-femoral socket design. For this to be done, areas for improvement in the current FE modelling setup will be reviewed and studied in separate chapters. The overarching research aim can be met by achieving five objectives:

- Conduct a literature review summarising previous FEA studies of the residual lower limb.
- Construct and pilot three-dimensional residual limb models.
- Assess the effects of the pelvis on the outputs of the residual limb FE model by comparing the results of FE models with and without the pelvic bone.
- Analyse changes in several liner variables including friction coefficient at soft tissue-liner and liner-socket interfaces, liner stiffness, liner thickness and residual soft tissue

stiffness. Use the process to develop a preliminary framework for a liner prescription database.

- Evaluate the socket modelling process by simulating the initial phase of socket volume reduction and altering the socket brim contours to create distinctly different socket variations.

1.3 Overview

This introductory chapter provides a summary background on the current state for those individuals living with a lower limb amputation, the necessity for the work to be conducted in this thesis, and an overview of the remaining chapters.

The second chapter provides an in-depth background research in the form of a literature review. The components of a lower limb prostheses are reviewed along with the research that has been conducted previously. An overview of the conventional socket design process is given, and how this process may be adapted to the emerging trends and abilities of computation simulation is explored. This chapter includes with a review of previous research on the interface between residual limb and socket gathered by both FE modelling and experimental transducers. This chapter also highlights the areas of required improvement in the current field of study and lays out what was subsequently studied and the reasoning for them. The examination of these modelling issues was conducted separately over the three following chapters to allow for objective examination of several specific aspects of the modelling setup.

Chapter three describes the end-to-end processes used to develop the FE models to be used for the subsequent chapters. This includes the software used, how the models were modified and verified, as well as preliminary results obtained.

Chapters four and five continue the development of the pilot FE models from chapter three. The models were used to conduct theoretical work on novel aspects relating to the residual limb bone geometry and prosthetic liners. Chapter six builds on the work of chapters four and five to produce a developed FE model which was used to conduct theoretical work on the socket geometry to aid the design process for socket design. Each chapter includes the methodologies used, results, discussion, limitations, and conclusions drawn. The conclusions are also given in terms of clinical relevance.

The final chapter reviews chapters four, five and six to provide and overall summary of the important findings. This chapter recommends future work in the form of several ideas on how to expand the area of study to further enhance the computational methods for socket design.

2. LITERATURE REVIEW

2.1 Soft Tissue Damage

The use of a prosthesis enables the individual to regain mobility loss. For this, the remaining soft tissue of the residual lower limb needs to be intimately coupled with a prosthetic socket. However, unlike the plantar tissues of the foot, the soft tissues of the residuum are not designed to sustain ambulatory loads. The inherent mismatch of this interface is the basis for regular occurrences of soft tissue breakdown, creating a persistent challenge for lower limb amputees (Paterno et al. 2018). The prosthesis fit, mobility and avoidance of blistering, sores and rashes have been recorded as the most important factors for individuals living with a lower limb amputation (Legro 1999; Pascale and Potter 2014). Indicating that soft tissue health of the residuum is an important factor in the patient's satisfaction with their prosthesis, as without the maintenance of good skin health, the skin can become damaged preventing the use of the prosthesis for a period of time (Meulenbelt, et al. 2011).

The residuum-prosthesis interface is the site at which the majority of the complications are observed following on from surgery and during rehabilitation. Previous studies have reported between 41% and 74% of lower limb amputees having one or more skin problems within the month prior to the studies (Dudek et al. 2005; Koc et al. 2008; Meulenbelt et al. 2011) with 54% having a reduction of prosthesis use as a result (Meulenbelt et al. 2011). The most common skin problems experienced within that month were typically related to eczema (50%), blisters, abrasions, and other mechanically induced skin problems (43%) or skin problems caused by occlusion such as pimples or profuse sweating (51%). More serious skin injuries had also been experienced by these patients at some point, including pressure ulcers (57%), infections (35%) and open wounds (31%). These problems have a detrimental effect on the patient's well-being and mental health. The aetiology of the majority of the soft tissue injuries are as a result of the mechanical coupling and transferring of forces between the residual limb and socket (Meulenbelt et al. 2009).

2.1.1 Mechanical Loading of Soft Tissues

Mechanical loading of the soft tissues refers to the equivalent pressure, shear and friction applied to the skin. It is commonly accepted that prolonged or high intensity compressive and shear stresses are the major causes for soft tissue damage (Agam and Gefen 2007). Compression stresses are applied perpendicular to the soft tissues and shear stress is parallel to the soft tissues. For example, during the stance phase, predominantly compression stresses are exerted on the residual limb, at the ischium and/or distal end, with smaller amounts of shear stresses supporting the load. Similar quantities of shear stresses are applied during the swing phase as friction is supporting the contact between prosthetic socket and residual limb preventing it from slipping or falling off (Laszczak et al. 2016).

Superficial tissue damages such as abrasion are often the result of inadequate levels of friction to maintain an intimate fit between skin and contacting material. Deeper tissue damage is caused by a combination of cell deformation and ischaemia, which jeopardises essential supply of oxygen and nutrients to the tissues as well as removal of metabolic waste. These lead to detrimental changes in membrane stresses, volumetric changes, and cytoskeletal reorganisation (Bouten et al. 2003; Defloor 1999). However, the exact processes and stress magnitude that cause soft tissue damage is still debated. Various methods of simulating soft tissue damage have been used including: substitute animal models (Dinsdale 1973; Goldstein and Sanders 1998; Linder-Ganz et al. 2006; Oomens et al. 2010), artificial muscles (Gefen et al. 2008), silicone models (Sparks et al. 2015) and finite element models (Shaked and Gefen 2013; Oomens et al. 2010; Linder-Ganz et al. 2007). Consequently, general trends may be noted, but it is difficult to compare them, and often specific values are not consistent between studies (Bader 1990).

Substantial data has been collected by previous studies to suggest that pressures of at least 200 mmhg (26.7 kPa) are required to produce soft tissue breakdown (Husain 1953; Kosiak 1961; Dinsdale 1973; Nola and Vistnes 1980; Salcido et al. 1995). A study by Linder-Ganz et al. (2006) exposed rat skeletal muscle tissues to pressures of varying magnitude and time. The histopathology results obtained were used to indicate cell death, loss of cross-striation in the muscle tissues, or no damage, cross-striation was unaffected by the pressures. Their results were compiled with previous studies also conducted using rat models to determine a sigmoid curve threshold to describe the relationship between pressure intensity and duration (see Figure 2-1). Their results determined that the magnitude of pressure was the dominant factor for cell death in exposure durations shorter than 60 minutes (32 kPa) and greater than 120 minutes (9 kPa). For the period between 60 and 120 minutes, the magnitude of pressure needed to cause cell death was strongly dependant on the time of exposure as the magnitude of pressure dropped significantly during this period.

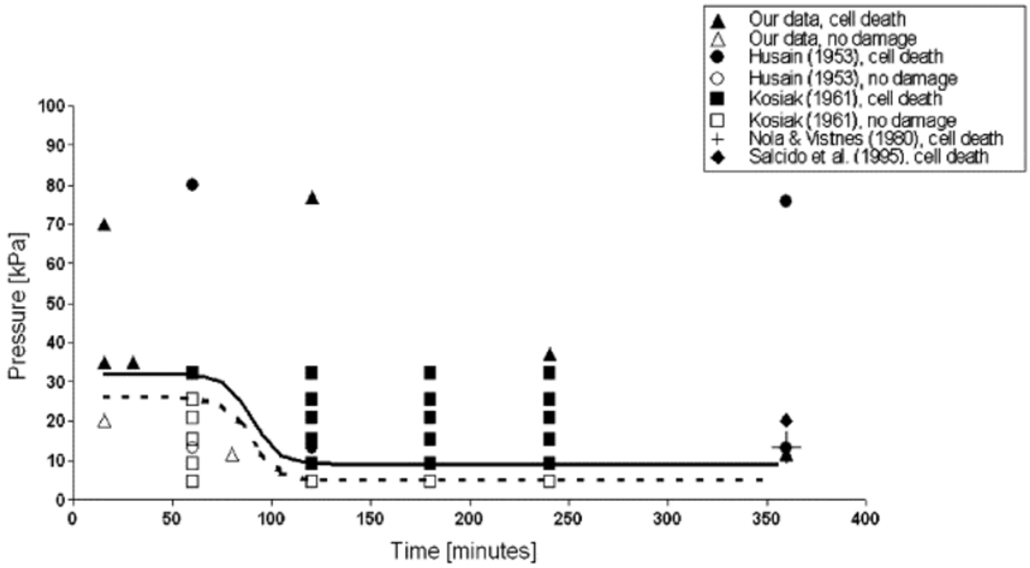

Figure 2-1: Pressure-duration cell death threshold for muscle tissue of albino rats reported by Linder-Ganz et al. (2007). Sigmoid curve fitting for cell death (solid line) and no damage (dashed line) were developed from a combination of their results and previous studies where solid markers depict cases of cell death, hollow markers depict cases of no cell damage.

In real-life conditions, shear can only exist in the presence of compression, therefore pressure remains the primary factor with shear stress being a potential by-product. However, studies have shown that shear stress appears to enhance the destructive capabilities of pressure. Goldstein and Sanders (1998) reported tissue breakdown with a pressure of 250 kPa and shear stress of 45 kPa, however when increasing the shear stress to 71 kPa, a pressure of only 125 kPa was required to induce the same tissue breakdown. These results agreed with a study by

Defloor (1999) concluded that shear stress plays a significant part in the occlusion of blood vessels, but shear alone is not capable of causing soft tissue breakdown. However, when in the presence of sufficient shear, the amount of pressure required to induce vascular occlusion is halved when compared to without shear stress.

In relation to the mechanical loads within a prosthetic socket, the average pressures exerted on the residual limb have been reported as being between 25.0 and 42.9 kPa during single leg stance phase (Kahle and Highsmith 2013). These values are higher than those reported to have caused soft tissue damage in previous studies (Husain 1953; Kosiak 1961; Dinsdale 1973; Nola and Vistnes 1980; Salcido et al. 1995; Linder-Ganz et al. 2006). However, the stresses exerted on the residual limb are often cyclic (applied for significantly short durations) and repetitive due to the ground reaction forces of the gait cycle, and the pressures applied by these studies were applied continuously. This limits the amount of direct comparison that can be undertaken.

Additionally, a study by Li and colleagues (2011) used a contact pressure of 17.7 kPa and reciprocating sliding distance of ±5.0mm to simulate the residuum skin-prosthetic socket interface and the sliding that may occur if a socket continually rubs against the skin, commonly known as 'pistoning'. Testing was conducted on rabbit skin for durations of 30 minutes with rehabilitation periods of 14 days between tests. This contact caused skin trauma including, erythema, oedema, exudation, and bleeding. As a result, skin underwent histological changes and self-adaption, which over time reduced its susceptibility to skin traumas. Therefore, indicating that the interface between residual limb and socket has a direct influence on the health of the residual tissues.

Conversely, studies have recommended the use of internal tissue strain to develop tissue damage thresholds more accurately for pressure ulcers (Linder-Ganz et al. 2007; Gefen et al. 2008; Oomens et al. 2010). More recently it has been understood that there are three main contributors to cell death as a result of strain: the main contributor being direct deformation, the inflammatory response and finally ischemia, with each beginning sequentially at a different time point (Gefen 2018). Continual and extreme forces cause sustained cell deformation, damaging the integrity of the cellular structure and membrane leading to eventual loss of cell homeostasis and cell apoptosis (cell death) (Gefen and Weihs 2016). The initial inflammatory response dilates capillaries and increases the permeability of capillary walls allowing leucocytes to migrate to the site of cell death (Moore et al. 2017). This inadvertently increases interstitial pressure which can be damaging in cases where the surface is being continually compressed with no relief, such as during extended periods of bipedal stance for prosthesis users. Deformation and inflammatory responses culminate in ischaemic damage, where restriction of blood supply to the tissues causes a build-up of cellular waste and shortage of oxygen required for regular cellular metabolism (Leopold and Gefen 2013). Determining the load state of the cellular tissues is dependent on the complex, structural and mechanical interactions occurring at various dimensional scales between the tissues and supporting surfaces. These interactions are affected by intrinsic factors (such as tissue composition, tissue stiffness, and an individual's internal anatomy) and extrinsic factors (such as supporting surface material, the mode of contact and medications) (Gefen 2018).

Similar to the work by Linder-Ganz and colleagues (2007), a strain-time cell-death threshold was also developed by Gefen and colleagues (2008) using bio-artificial muscles (BAM). Their compressive strain distributions were calculated under the assumptions of a flat tissue surface, frictionless contact and infinitesimal deformations, and the calculated contact parameters of material thickness, indentor radius, indentation depth and contact radius being derived from Ning et al. (2006). Their results showed the BAM cultures could tolerate compressive strains below 57% for up to a 60-minute duration, with the tolerable compressive strain dropping to 42% after a period of 180 minutes. There was a transition period between these two durations.

Sparks et al. (2015) used silicone models to simulate deep tissue injuries, revealing similar stress distribution patterns at deep and superficial locations. Whilst the magnitude of the pressures in the deep tissue adjacent to the bony prominences was higher (approximately 1.5 times) than those recorded in superficial tissue the tissue depth and tissue properties were believed to be important factors. Furthermore, the role of temperature in the facilitation of tissue damage has been scarcely examined, but previous studies agree that higher temperatures (ranging between 25ºC and 45ºC) make soft tissue more susceptible to damage. This is caused by the increased temperature increasing the metabolic requirements (nutritional and oxygen) of the tissues and subsequently reducing the durational onset of ischemia (Kokate et al. 1995; Patel et al. 1999).

2.2 Prosthetic Components

A prosthesis, or artificial limb, is the principle element in the rehabilitation process following a lower limb amputation, allowing the individual to often regain a substantial amount of mobility. Lower limb prosthetics typically consist of; a prosthetic socket, a prosthetic liner and additional components such as pylons, connectors, prosthetic knee, and foot (see Figure 2-2). Suspension of the socket to the residuum is often achieved via suction, also known as vacuum method, with more traditional sockets using straps to achieve suspension (Paterno et al. 2018). The prosthetic components are aligned for the individual user and are often cosmetically finished to match the desired appearance.

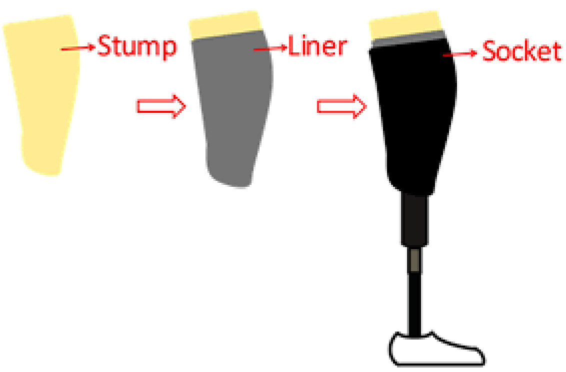

Figure 2-2: Prosthetic components of a lower limb prosthesis (taken from Paterno et al. 2018)

Lower limb prosthetic components have advanced dramatically in recent decades to enable individuals with amputations to regain high levels of function and mobility. Despite this, there remains numerous reports of residuum soft tissue problems relating to the prosthetic interface involving the prosthetic liner and socket (Meulenbelt 2010).

2.3 Prosthetic Liners

As shown in the previous section, protecting the soft tissues of a residual limb is often a challenge for a lower limb prosthetic user. Prosthetic liners have therefore been developed to further facilitate improving the stress transfer and distribution between residual limb and socket. A prosthetic liner is a protective cover made of cushioning material. It is worn over the residual limb to provide a complete fit between the residuum and prosthetic socket. Prosthetic liner types can be tailored to work with different suspension systems.

A liner may reduce the peak pressures, shear stresses and soft tissue displacement experienced by the residuum, creating a more uniform stress distribution (Sanders, et al. 2004; Palace, et al. 2014; Boutwell, et al. 2012). This was demonstrated as early as 1970 by Sonck and colleagues who measured pressures at four sites within a trans-tibial socket for 26 amputees over three conditions; (i) no liner, (ii) soft insert (called Kem-Blo), and (iii) a silicone liner. Their results suggested the silicone liner had the ability to distribute pressures evenly over the residuum as it demonstrated reduced pressures at all sites compared to the other conditions.

The use of a liner is a personal choice and can depend on the individuals' needs and uses. Previous survey studies have reported 50% to 85% of all lower limb amputees use a prosthetic liner (Meulenbelt 2010; Whiteside 2015). There are a wide variety of liners available and the properties can vary greatly between them, meaning they may be prescribed to meet an individual's need. However, whilst the properties provided by a liner are in most cases beneficial to the user's comfort and soft tissue health, a failure to appropriately match a liner to a user may cause a variety of clinical problems. For example, pairing a user having a residuum containing excessive adipose tissue with a softer liner may result in greater levels of displacement between the residual limb and socket, known as pistoning (Cagle et al. 2017).

Presently, there are in excess of 70 liner products available on the market, but there is currently a paucity in the information on the performance of these liners (Hafner et al. 2017). Studies that have examined the performance of liners have either included a limited number of products (Boutwell et al. 2012; Gholizadeh et al. 2012; Ali et al. 2014; Cavaco et al. 2016; Cagle et al. 2017) or products that are no longer available on the market (Emerich and Slater 1998; Covey et al. 2000). A recent study by Hafner et al. (2017) concluded that a prosthetist prescribing a liner will routinely use fewer than three liner products from a wide variety available on the market. Though the liner property information is available to the prosthetist, the authors suggested it was due to this information seldomly being objective and comparable. This has caused prosthetists to typically be reliant on information provided by individual liner manufactures and feedback from their patients to inform future prescribing decisions.

2.3.1 Prosthetic Liner Types, Materials and Properties

Prosthetic liner technology has evolved from simple open and closed cell foams, such as Pelite and Nickelplast, to more sophisticated materials with urethane, silicones, or thermoplastic elastomers (TPEs), also known as copolymers (Kistenberg 2014). The correct application of a liner is dependent on appropriate selection of materials and their properties.

A widely regarded and cited study by Sanders et al. (2004) conducted tensile testing (up to 60% strain) on a range of 15 liners: one single urethane liner and the remaining fourteen silicone elastomers, silicone gels, or a combination of the two. The results showed linear responses for all materials tested with a stiffness range of 30 kPa to 249 kPa. The data was easily classified into groups for the products tested. The highest stiffness value was obtained from the urethane liner, and the lowest values from the silicone gels. When comparing test results of liners with and without the fabric backing, it was noted that the effect of the liner fabric backing was negligible. Similar values of 124 kPa to 353 kPa were reported from tensile testing on numerous liners up to 100% strain by Cagle et al. (2017). Additionally, Cagle and colleagues also conducted compression testing up to 60% strain on the same liners. They reported a range of 96 kPa to 458 kPa for compression testing. Contrary to the comments of Sanders et al. (2004), Cagle et al. (2017) reported the fabric backing of liners increased a liners compressive stiffness by up to 50%.

The compressive stiffness of a liner should be a consideration for providing cushioning on bony or sensitive areas of the residuum, whilst the tensile stiffness, when coupled with adequate friction, would provide good suspension of the prosthesis during the swing phase of the gait cycle. It is therefore important to consider the stiffness values of the liners in terms of compression and tension.

The studies by Sanders et al. (2004) and Cagle et al. (2017) both performed tests on new ‘fresh state’ liners. An interesting study by Cavaco et al. (2015) examined the mechanical characteristics of three liners over an aging period of 90 days. To simulate the aging process caused by exposure to sweat, the samples were continuously soaked in a synthetic sweat bath. Compressive testing to 40% strain reported stiffness values between 112 and 275 kPa for the copolymer and silicone elastomer liners tested. The silicone liners exhibited a lower stiffness in their fresh state, with increasing stiffness over the 90-day testing duration (up to 159% of their fresh state). Conversely, the stiffness of the copolymer liner reduced to 84% of its fresh state over the 90-day duration. Between the fresh state (day 1) and day 30, all liners displayed an initial increase in stiffness. This study highlights the potential for degradation of the liner properties over their lifespan, however the results may be considered exaggerated due to the continuous exposure to the synthetic sweat not being a true representation of the liner conditions. It is recommended that liner products are cleaned daily/weekly with mild detergent to help maintain their integrity (Ossur 2017; Blatchford 2019). To the best of the author’s knowledge, there is currently no literature on the effect of liner degrading from repeated loading.

The study by Sanders et al. (2004) concluded that a softer liner would be more suitable for a bony residuum to provide cushioning, conversely a stiffer liner would suit a residuum with excessive soft tissue. Both situations would require sufficient friction to maintain suspension of the prosthesis and prevent slippage. The thickness of the liner has been thought to affect the liner performance and should therefore be considered in these situations. The thickness of a liner is dependent on the level of amputation along with the amount of padding required to cushion the residuum. Trans-tibial liners are typically between 3mm and 9mm in thickness and are normally thicker than trans-femoral liners which range between 3mm and 6mm (Ossur 2011; WillowWood, 2018; Ottobock, 2015). These can also be tapered to provide greater thickness, and hence cushioning, to protect the sensitive tissue in the distal end of the residual limb. Boutwell et al. (2012) found that a thicker liner within a trans-tibial socket reduced peak pressures and increased all participants’ perceived comfort. However, a liner with 9mm thickness altered the gait characteristics of the amputees although this variation was not enough to be considered statistically significant. A liner to be used with a trans-femoral residuum is typically thinner compared to a liner to be used with a trans-tibial residuum. This is because the trans-tibial residuum is typically thinner with bonier prominences that require the additional padding and comfort provided by a thicker liner. Whereas the trans-femoral user typically has a bulkier residuum and therefore requires a thinner liner to help maintain the user's proprioception of the limb during ambulation (Boutwell et al. 2012).

Changes in the residuum volume and shape, which are common in early post-operative periods as well as a mature residuum, can lead to problems creating and maintaining a comfortable socket fit (Sanders and Fatone 2011). In addition to changing the liner thickness to accommodate this change, a study of 16 trans-tibial amputees found the volume increase of the residuum from muscle contraction was reduced from an average of 5.8% to 3.5% when a liner was worn (Lilja et al. 1999).

2.3.2 Friction Coefficients

The friction between two surfaces is generally quantified by the coefficient of friction (COF). The COF is dependent on a combination of two components, adhesion, and deformation. The deformation comprises of contributions from elastic deformation and hysteresis (Chen 2014).

There are two types of adhesion, practical and fundamental adhesion. Practical adhesion is concerned with the magnitude of force or energy required to break adhesive bonds. Fundamental adhesion is concerned with the force and mechanisms at molecular level that are involved in making the adhesive bonds. Therefore, the concepts of fundamental adhesion are a prerequisite for practical adhesion. Currently there are four theories of adhesion: adsorption theory, mechanical theory, electrostatic theory, and diffusion theory (Packham 2011). Each of these theories emphasises aspects of more comprehensive models, which principally relate molecular characteristics of the interface being examined to macroscopic properties. The deformation component of friction is caused by the bulk deformation of the contacting materials. This leads to deformation of the surface asperities, hysteresis and ploughing of softer materials causing energy loss.

At the lower limb prosthetic interfaces, friction can be both beneficial but also damaging. Friction on the skin surface of the residuum produces stresses on the skin and underlying soft tissues which may be damaging. Alternatively, friction between the prosthetic interfaces plays an important role in supporting the load of the amputee during ambulation (Zhang et al. 1995). However, achieving an optimum friction value at the residual limb interface is still to be achieved, with many studies concluding a balancing act between too low friction with slippage occurring, or too high friction with the possibility of skin/soft tissue damage.

A prosthetic liner is in contact with both the residual limb and the socket. Commonly these contact interfaces have different materials and conditions and will be examined individually at a practical level. Although not all the previous studies have been conducted with the interfaces being skin-liner and liner-socket, there are some results for materials similar to these interfaces and will be mentioned for completeness.

2.3.2.1 Residual Limb and Liner Interface

Sanders et al. (1998) performed static friction testing between skin and six commonly used liner materials, including Nickelplast, Pelite and silicone-based materials. Testing was performed against human skin (on the medial tibial flare) of ten volunteers and a woollen sock. A bidirectional force-control device was used to control the loading and motion of a loading pad against the skin to achieve pre-set normal and shear force values. Instead of applying a normal force and incrementally increasing the shear force as conducted by other studies (Zhang and Mak 1999; Sanders et al. 2004; Cavaco et al. 2016), Sanders and colleagues (1999) used a repeating cyclic shear force and a stepwise decreasing normal force until slip at the interface occurred. The COF ranged from 0.60 (±0.05) to 0.89 (±0.09) across all liners against both skin and woollen sock. The results of this study show a small scatter of COF across the range of liners and contacting material. Four out of the six liner materials produced a lower COF against the woollen sock compared to the human skin. Prosthetic sockets have previously been used to accommodate daily residuum volume fluctuations and help ease the residuum into the prosthetic socket. However, as highlighted by Sanders et al. (1998) the reduced COF compared to prosthetic liner materials results in a higher potential to induce slippage at the prosthesis interfaces.

Zhang and Mak (1999) examined the COF of numerous materials against six anatomical locations including the anterior and posterior middle leg of eight participants. The silicone material tested reported a higher COF range of 0.35 - 0.68 across the participants compared to 0.30 - 0.53 for the Pelite. Overall, there was no significant difference between the anterior and posterior leg locations, but differences were exhibited by individuals.

The most extensive liner friction coefficient study to date, conducted by Sanders et al. (2004), evaluated the static friction coefficient between 15 liners and a skin-like material (leather) using a custom-made jig. Pressures of 25.3, 53.7, 100.8 and 195.8 kPa were used, with shears at 4.3 kPa increments up to 142.8 kPa and the threshold at which slip occurred was recorded. The results showed a reduced friction coefficient with increasing force across all liners; however, this trend was more evident in certain liners. The liners were categorised in terms of their friction properties with the only urethane liner exhibiting a friction coefficient of up to 1.6 at pressures of 53.7 kPa and 0.8 at 195.8 kPa. This was significantly higher compared to the other liners, which had COF ranges of approximately 0.35 - 0.8 at 53.7 kPa and 0.18 - 0.6 at 195.8 kPa. Sanders et al. (2004) concluded that the use of a liner with a high friction coefficient against skin would help reduce localised shear stresses and therefore hypothesised that the urethane liner tested would be best paired with a residuum containing soft tissue that was sensitive or susceptible to skin breakdown.

In contrast to these studies, research by Cavaco et al. (2016) reported much higher values for copolymer (1.75 ±0.30), silicone gel (1.67 ±0.26) and silicone elastomer (1.94 ±0.28). Testing was performed with a handheld probe against the palm of the hand for four participants. Similarly, Cagle and colleagues (2017) reported peak static COF up to approximately 5.5 for three liners of urethane, silicone and TPE against a leather surface. Their static COF appears inconsistent with the other studies. A significantly higher COF may have potentially been caused by testing parameters applying low normal force over a larger surface area with substantial levels of adhesion at the liner interface. Unfortunately, limited information on the test protocol was provided, including the contact area and normal force applied. Further, the static COF was only reported for two out of three liners. The liner for which the static COF was not reported, had a dynamic COF as low as 0.3. Cagle and colleagues (2017) found distinct differences in dynamic COF across the three liner materials and hypothesised that the differences were characteristic of the chemical adherence as a result of each liner material. Whereas Sanders et al. (2004) were unable to consistently correlate their friction results with material (unlike their stiffness measurements), thus believed the manufacturing process of the liner controlled the friction coefficient more than the actual material itself.

2.3.2.2 Liner and Socket Interface

The use of a liner also introduces an interface between the external surface of the liner and the internal surface of the socket. This interface has been of less importance than the residual limb and liner interface as currently no studies have directly reported on the friction coefficient at this interface.

A study by Li et al. (2011) reported the friction coefficients for prosthetic socks consisting of cotton, nylon, silk, and wool against a human residual tibia. For a contact pressure of 39.8 kPa, friction coefficients were approximately 0.059 for cotton, 0.075 for silk, 0.125 for wool and 0.178 for nylon. These COF variations were closely related to the fabric weave parameters, fibre sizes and material compositions. Three out of the four materials tested by Li et al. (2011) including wool, cotton and nylon are commonly used as a fabric backing to the external surface of the liner (Ossur 2011; WillowWood, 2018; Ottobock, 2015). Sanders et al. (1998) also reported a mean COF of 0.53 ±0.09 when testing a wool sock against the tibial tuberosity skin of 10 participants. The friction results for a woollen sock by Sanders et al. (1998) were considerably higher than the 0.125 reported by Li et al. (2011). For their testing parameters, Sanders and colleagues secured the woollen sock to a load pad made of Pelite using epoxy resin which can be considered more representative of the external surface of a liner compared to a prosthetic sock. Sanders and colleagues did not report on the wool information preventing comparison of fabric parameters between the studies. Both studies tested the fabric surface against human skin. However, the fabric backed external surface would be in contact with the prosthetic socket and therefore the contacting material against the fabric should be common materials used to make a prosthetic socket rather than human skin.

2.3.2.3 Testing variations

These studies have demonstrated a variation of the COF between tissue and the various liner materials (Sanders et al. 1998; Zhang and Mak 1999; Sanders et al. 2004; Cavaco et al. 2016; Cagle et al. 2017). However, skin friction is complex and the variation of friction coefficients measured is dependent on the testing conditions (such as contact parameters and environmental factors), the contacting surface, as well as the variety of inherent tribological parameters related to the skin including hirsuteness, moisture, surface topography, anatomical location, age, gender and condition of health (Masen 2011; Veijen 2013; Tomlinson et al. 2007; Li et al. 2008).

Two similar studies conducted by Restrepo et al. (2014) and Ramirez et al. (2015) both concluded the factors of hirsuteness and moisture as being significant factors for the friction coefficient between a common prosthetic socket material, polypropylene, and human skin. Both studies reported similar COF ranges (0.186 to 0.545 for Restrepo et al. 2014, and 0.22 to 0.45 for Ramirez et al. 2015). Interestingly both studies reported the highest COF value when no hair and no moisture was present, and the lowest value was found with the presence of moisture.

The effect of moisture on skin friction has been expressed as a bell-curve behaviour by Derler et al. (2015) informed by previous studies. This represents a COF increase for moist skin compared to dry skin up to a maximum value, attributed to the swelling and softening of the stratum corneum (Tomlinson et al. 2011). The increase, up to the maximum value, is followed by decreasing COF with excessive water in the interface indicating a transition from boundary to mixed lubrication friction conditions. Although there is evidence for the bell-curve behaviour, the values for changes in COF to occur are not known. This bell-curve effect of moisture on skin friction is highly important in terms of the residual limb. A known negative affect from the use of a liner is the increased levels of humidity and perspiration of the residual limb. The build-up of moisture from perspiration and lack of ventilation will alter the friction between skin and liner during periods of use. Therefore, it can be assumed the COF against an initially dry residuum would firstly increase as the levels of moisture increased along with the duration of prosthesis use. After which, if there are sufficient levels of moisture to exceed the maximum value, a reduction in the friction levels may occur and allow for excessive slippage.

Six different anatomical locations including hand, forearm and leg measured by Zhang and Mak (1999) against various materials showed a higher COF at the palm of the hand (0.62) compared to the leg and forearm (0.40-0.46). Their study did not report on the surface topography of the skin testing sites. However, it has been demonstrated that at low levels of surface roughness on the skin there is little difference between the COF of contacting materials, however as the surface roughness increases so does the COF up to a point of plateau (Tomlinson et al. 2009). Additionally, the friction coefficient against skin has been shown to reduce by up to 50% when exposed to continuous friction contact and periods of rehabilitation (Li et al. 2011).

As shown, these friction parameters can greatly alter the friction experienced. It is therefore likely that the discrepancies in values reported by the studies testing liner COFs discussed in this section may be caused by the variations in testing parameters. This is similar to the substantial variations of skin friction coefficients assessed across several studies in a review paper by Derler and Gerhardt (2012).

2.4 Prosthetic Sockets

The prosthetic socket is often considered the most important prosthetic component as it provides mechanical coupling between the individual's residuum and the prosthesis. A study of 368 unilateral trans-femoral amputees concluded socket fit (72.9%) and gait/manoeuvrability (88.4%) as being dominant functional characteristics of the prosthetic socket (Berry et al. 2009). The socket is responsible for many aspects of proper prosthesis function, including allowing the amputee to bear weight on their prosthesis.

Without a proper socket shape and fit, the prosthesis will become uncomfortable, or even unusable, and cause pain, sores, or blisters. The socket fit should be balanced to allow for blood circulation in the residual limb and socket tightness to prevent the socket falling off during ambulation. Prosthetic sockets are commonly fabricated with thermoplastic, thermoset and composite materials such as polypropylene and polyethylene, which provide durable, flexible, lightweight, and high strength properties (Andrysek and Eshraghi 2017). Currently, the socket design and suspension system for the patient are decided by the prosthetist taking into consideration the patient's residual limb characteristics, age, lifestyle and activity level, but it is often based on the prosthetists previous experience and personal preference rather than objective information (Paterno et al. 2018).

2.4.1 Principles

Professor Radcliffe is widely regarded as the grandfather of prosthetic biomechanics. One of his greatest scientific contributions was a biomechanical description of walking, from which he established principles for prosthetic alignment and socket transfer through the gait cycle resulting in the pioneering of the Quadrilateral socket (Radcliffe 1955). Later, Hall (1964) summarised previous work on the design of prosthetic sockets into five important principles:

1. The socket walls should be contoured to provide adequate relief for remaining functioning muscles.
2. The stabilising pressures should be focused on skeletal structures as much as possible and avoided in areas of remaining functioning muscles.
3. Where possible, maximum power of the remaining functioning muscle may be achieved by altering the resting position of the socket to stretch the musculature to slightly greater than its length at the rest position of the residuum.
4. Properly applied pressure can be tolerated by structures of the neurovascular system.
5. Force is best tolerated by the residual limb when distributed over the largest area available.

These principles were originally intended as objectives for the design of Quadrilateral sockets but remain equally applicable to the numerous socket variations.

2.4.2 Prosthetic Socket Designs

There are various socket designs currently available. These originate from two primary socket designs: i) the sub-ischial Quadrilateral socket (Quad) and ii) the Ischial Containment (IC) socket. Whilst both these socket designs take into consideration the principles mentioned by Hall (1964), the resulting socket design differs significantly.

The Quad socket pioneered by Radcliffe (1955) was the first socket concept to be widely adopted. The quadrilateral term refers to the socket shape when viewed in the transverse plane (see Figure 2-4) due to the socket having considerably narrowed anterior-posterior (AP) dimension compared to the medial-lateral (ML) dimension. Weight bearing in the Quad socket is primarily achieved through the ischium with support provided by the gluteal musculature. The ischium sits on top of the wide posterior socket wall which acts as a seat parallel to the ground. Stability is achieved through tightly containing the remaining thigh musculature within the four distinct walls, with the tight anterior wall creating a posterior directed force intended to stabilise the ischium on the posterior seat (Schuch 1992).

A study by Ivan Long (1975) investigated the femoral alignment of above-knee amputees in quadrilateral sockets and found the residual femur showed adduction of up to 20 degrees in 94 out of 100 patients fitted with a Quad socket. The alignment of the residual limb was the initial focus of Long (1975), from which the concept of ‘Long’s Line’ was developed. This stated the normal adduction angle of the femur may be approximated by drawing a straight line down from the centre of the hip joint, through the distal end of the residuum to the centre of the prosthetic foot heel (see Figure 2-3). Later work by Long developed the first ischial containment socket concept as the Normal Shape Normal Alignment (NSNA) socket (Long 1985). The shape of the IC socket is configured more to align with the shape of the individual’s pelvis compared to the shape of the Quad socket (see Figure 2-4). All variations of the IC socket aim to provide medio-lateral stability during single leg phase of the gait cycle. This is achieved by contouring the socket brim to narrowing the medio-lateral dimension of the socket while also containing the medial aspects of the ischial tuberosity within the medial socket wall. In contrast to the Quad socket, the IC socket variations aim to achieve a greater degree of hydro static weight bearing, of the volume region of the residuum, and lessen the direct ischial weight bearing. As such, all trans-femoral socket variations require the volume of the residual limb tissue to be appropriately contained. The region for obtaining this is commonly referred to as the ‘volume region’ of the residuum, located approximately 4cm distal to the ischium, and 4cm proximal to the distal end of the residuum (Radcliffe 1955; Long 1985; Pritham 1990).

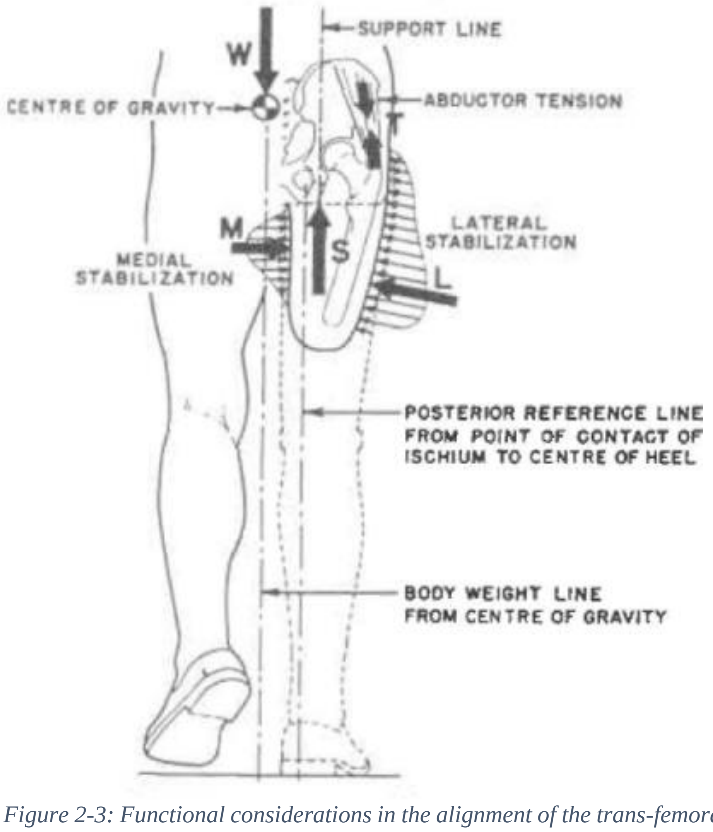

Figure 2-3: Functional considerations in the alignment of the trans-femoral socket for lateral stabilisation (Radcliffe 1970).

Both the Quad socket and IC socket have total surface bearing (TSB) and non-distal loading variations. The TSB socket suggests that the weight of the individual is as evenly distributed over the total surface area of the residual limb as possible. This is achieved by the weight being shared by loading on the skeletal anatomy and hydrostatic compression of the soft tissues from the tightness of socket fit. However, there are areas of the residuum which are more pressure tolerant than others, such as the distal end of the residuum commonly being pressure sensitive due to amputation scars (Lee et al. 2007). Non-distal loading sockets do not have an intimate fit between socket and residuum at the distal end, instead they usually contain a vacuum at the distal end and are coupled with a variety of vacuum assisted suspension systems (Paterno et al. 2018).

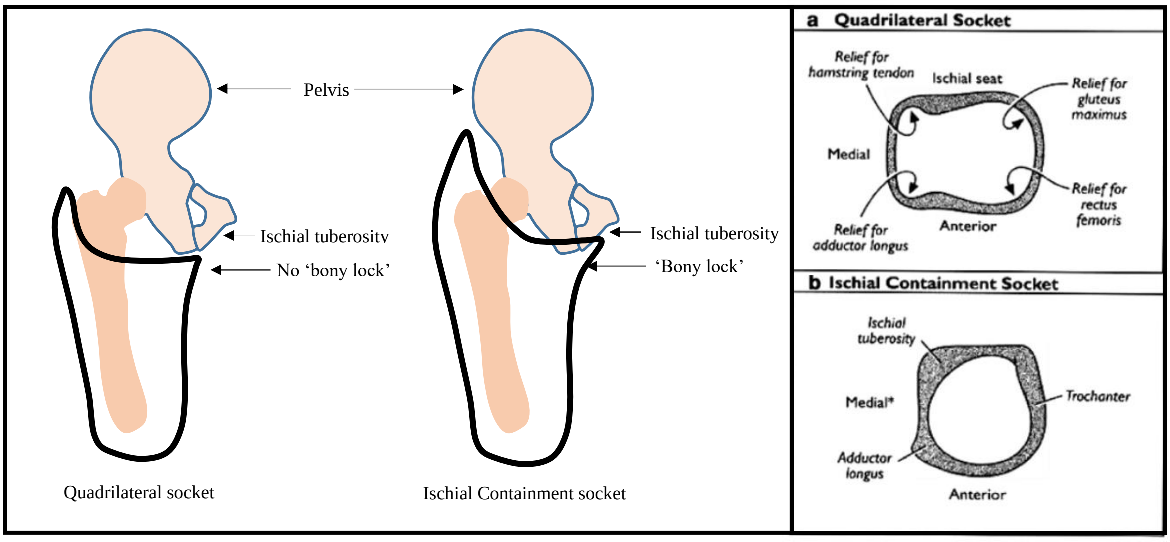

Figure 2-4: (right) Differences between the Quad socket and IC socket (left) transverse plan view of (a) Quad socket and (b) IC socket (adapted from Munarriz et al. 2003).

Prosthetic socket concepts have been continually evolving as more studies have been conducted. Following the findings by Long (1985) and the popularity of the IC socket concept there have been new developments made in the design of sockets allowing them to be developed in different concept variations from the traditional IC socket such as; Contoured Adducted Trochanteric-Controlled Alignment Method (CAT-CAM) (Sabolich 1985), Marlo Anatomical Socket (MAS) (Garrick and Fatone 2013) narrow Medio-Lateral and Northwestern ICS (Schuch 1992). Recently new additions to the sub-ischial concept have been proposed in the form of; sub-ischial Northwestern (Fatone and Cadwell 2017) and High Fidelity (Alley et al. 2011) sockets. Fundamentally, the aim of all prosthetic sockets is to achieve sufficient support and stability through the appropriate coupling and load transfer between socket and residual limb. The socket variations (such as sub-ischial and ischial containment) utilise different approaches to achieve this, but the principles to enable this (Radcliffe 1955) remain constant throughout all variations and have evolved over time in response to successful fittings and experimental observations indicating there is no standard socket design.

2.4.3 Socket Fabrication Process

The conventional process for fabricating a prosthetic socket involves taking a plaster impression of the individual's residual limb to produce a positive mould. The mould shape and walls are then adapted (rectified) according to the required socket design paradigms to create the desired prosthetic socket. The rectifications are performed by a prosthetist who, through their established tacit knowledge and artisan techniques, lessen the pressures in sensitive areas of the residuum and divert these pressures to more pressure-tolerant regions to determine an appropriate socket shape and volume (Pirouzi et al. 2014). The pressure tolerant and pressure sensitive regions are illustrated in Figure 2-5. The socket fitting is an iterative cycle, with feedback from the amputee being provided to the prosthetist after a socket has been created, and the feedback being used to inform an updated socket design. This cycle can have numerous repetitions being time consuming and costly. On average, at least nine adjustment iterations are required in the first 12 months alone following amputation (Pezzin et al. 2004).

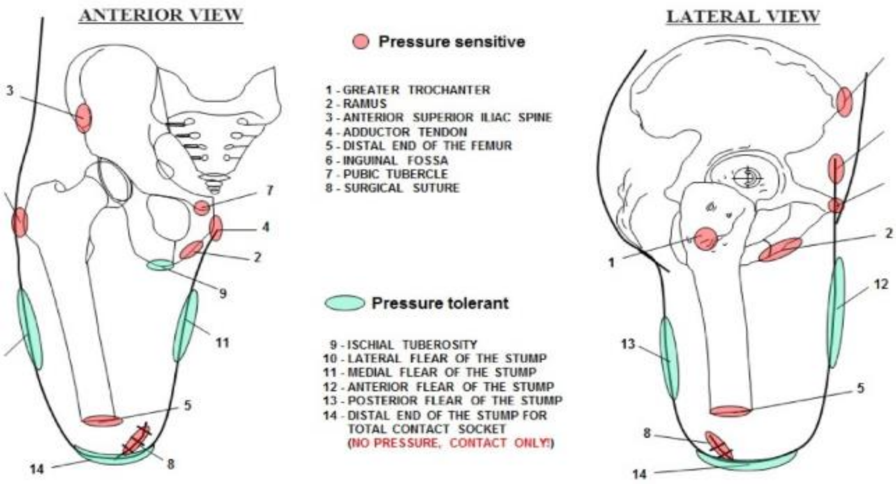

Figure 2-5: Pressure sensitive and pressure tolerant regions of the trans-femoral residuum (Physiopedia 2018).

Throughout recent history, and continuing to the modern day, the most common method of socket design and development has been conducted by a prosthetist palpitating the residual limb to ascertain areas of high-pressure and low-pressure tolerance. This design and manufacturing method, shown in Figure 2-6, is the 'As Is' method of socket design. This process requires multiple phases of measurement, cast preparation, socket creation and modification by a feedback loop with patient testing.

Recommended guidelines on how specific socket types should be cast by a prosthetist are available (Steeper Group 2011). However, the prosthetist is required to ascertain the factors of socket design and rectification given their individual clinical experience, knowledge about the patient's lifestyle, mobility, soft tissue characteristics and most importantly visual and verbal feedback during socket fittings (Wernke et al. 2017). Therefore, this process is highly dependent on both the skill and experience of the prosthetist, and patient feedback (Paterno et al. 2018), without any prediction of socket fit prior to the socket being manufactured. Because of this, the resulting socket designed for an individual can vary dramatically. For example, if ten prosthetists were tasked with designing a specific socket type, such as a Quad socket, for a single trans-femoral amputee, the ten sockets designed would all vary dramatically but all should contain characteristics of a Quad socket.

This subjectivity has led to longstanding inconsistencies in producing satisfactory sockets due to inadequate training and differing techniques which have been acknowledged historically and continually up to the modern day (Murdoch 1965; Jensen 2005; Wyss et al. 2015). Wyss et al. (2015) concluded the level of prosthetist training and skill was a critical factor in achieving a successful socket fit, with levels as low as 52% of cases achieving a good prosthetic fit.

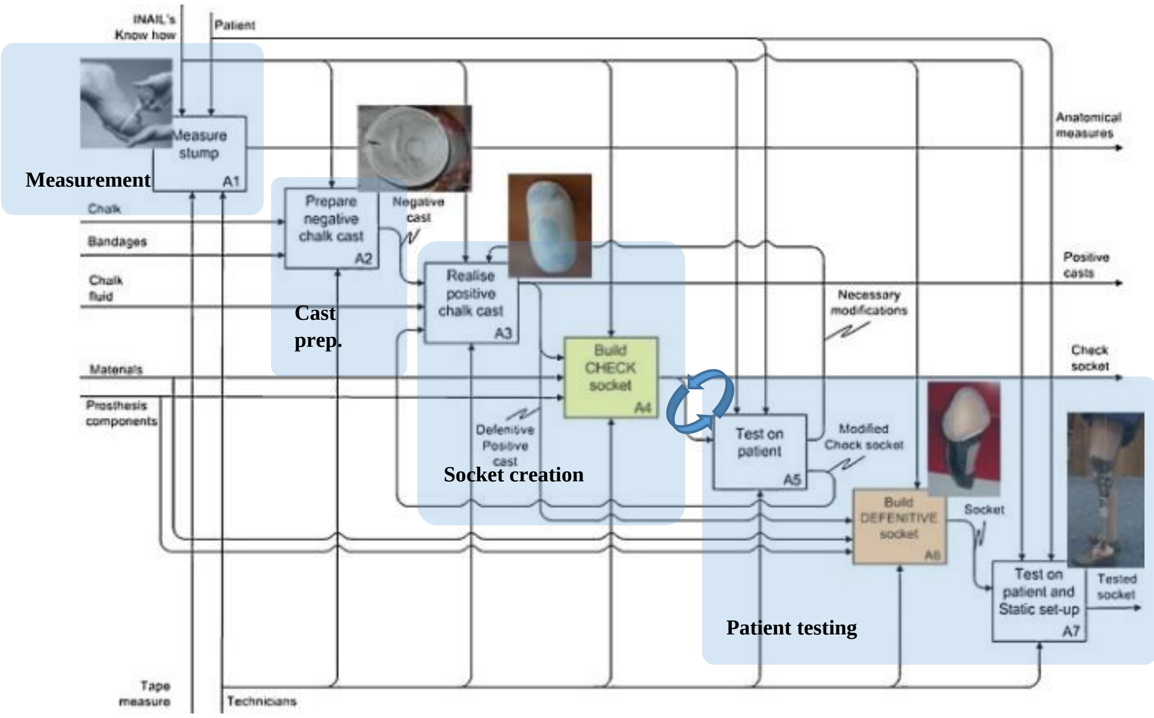

Figure 2-6: Current 'As Is' socket design method (figure adapted from Colombo et al. 2010).

Subsequently, alternative methods of designing and casting a prosthetic socket that are less reliant on the prosthetist's knowledge, have been progressed recently. The hydro-casting socket techniques have been advocated as an alternative to the hand-casting (hands-on) socket method described above (Kristinsson 1993; Safari et al. 2013; Buis et al. 2017; Cutti et al. 2018). Hydro-cast sockets are based on the hydrostatic principle of load transfer to achieve a uniform pressure distribution, which Kristinsson (1993) argued would achieve the most effective socket and that through application of a controlled pressurised casting technique a 'near' hydrostatic equilibrium point could be achieved. Safari et al. (2013) compared the conventional and hydro-casting techniques using twelve trans-tibial amputees. They found more consistent sockets were created using the hydro-casting technique, whereas greater inconsistencies were found for the conventional technique which was greatly influenced by the prosthetist's skill and dexterity. Hydro-casting is widely used in trans-tibial socket casting, preliminary work has recently demonstrated a feasible approach to trans-femoral casting (Buis et al. 2017, Cutti et al. 2018) in an attempt to provide more repeatability and reduce the errors during traditional plaster modification.

2.5 Finite Element Analysis

Finite Element Analysis (FEA) is a numerical computational technique used to approximate solutions to problems with complex geometries, loading and material properties. FEA replaces the single complicated shape with an approximately equivalent network of simple elements. The overall pattern of the elements is referred to as the finite element mesh.

The accuracy of the Finite Element (FE) model will be determined by the number of elements and their shape measure, with a higher number of elements producing more accurate results. Unfortunately, more elements also mean more calculations to be computed and greater solving times. Therefore, a compromise between just enough elements to achieve adequate accuracy, within a reasonable computational time is required. The points used to define the elements are known as nodes. The nodes of an element are free to move unless constrained in movement by a boundary condition. A load may be applied to the FE model to deform the nodes and induce stresses and strains within the element. The material properties for each part of the FE model must be specified to define how the material will react to the applied boundary conditions and loads. To analyse the socket and residuum combination, general purpose FE packages have been used; Abaqus, Ansys, LS-Dyna, Nastran, and Marc (Dickinson et al. 2017).

2.5.1 Application of FEA

As early as the 1980's, there has been the idea for the socket design process to be implemented in a more efficient and effective way using a range of computational software. Studies began to use computer-controlled methods for socket fabrication (Lawence et al. 1983, Lawrence et al. 1984), reconstruction of anatomical shapes from digital images (Saunders 1982), and preliminary socket modelling by FEA (Reynolds and Rodwell 1984). These studies built the necessary groundwork for future studies to combine these capabilities in the form of computer-aided design (CAD) for socket design. A study by Krouskop et al. (1987) used ultrasonic measuring techniques to create a generalised FE model of the trans-femoral residuum which was used to fabricate and fit Quadrilateral sockets for two individuals. The FE model used in this study was basic, but nonetheless it was one of the first studies to demonstrate the feasibility of using a CAD process to design and fabricate a socket. Torres-Moreno et al. (1990) used anthropometric measurements taken from an amputee and compared them against anthropometric measurements of 27 different residual limbs based on skeletal structure (brim size), residuum length and soft tissue mass to design a socket shape reflecting the individual's residuum characteristics. Initial discrepancies with the socket were modified interactively using CAD. Interestingly, the authors compared the socket dimensions between the final fabricated CAD socket and the individual's traditional socket and found significant shape differences. It was concluded that the two distinct shapes both provided support and comfort to a good degree of fit.

Over recent years there have been advances in technology capability and sufficient development in software processing that has enabled an increasing advancement in related studies. An innovative study by Colombo et al. (2010) presented a new 3D paradigm for the design and development of subject specific sockets. The paradigm presented is applicable to all custom fit lower limb sockets, but their study confirmed the process for trans-tibial sockets. The socket design methodology presented by Colombo et al. (2010) is shown in Figure 2-7 and referred to here as the 'To Be' methodology. This new 'To Be' methodology alters the traditional multiple phases of socket design to produce stages that can be categorised into three phases; measurement, computational design and computational confirmation (as shown in Figure 2-7). Using this method, the measurements are achieved from digital scans such as computed tomography (CT) or magnetic resonance imaging (MRI) scans and imported to software programmes to carry out the computational design of the socket. The designed socket is confirmed by simulating the socket and residuum interaction, commonly undertaken by FEA, to test and verify the internal socket shape. If an unfavourable outcome is achieved by the FEA output, which may be assessed by the stresses exerted on the residual limb (Liner-Ganz et al. 2006; Lee et al. 2007), the socket shape is modified interactively within the computational design phase and the confirmation carried out again until a favourable result is achieved. Finally, rapid prototyping technologies are used to fabricate the final socket shape.

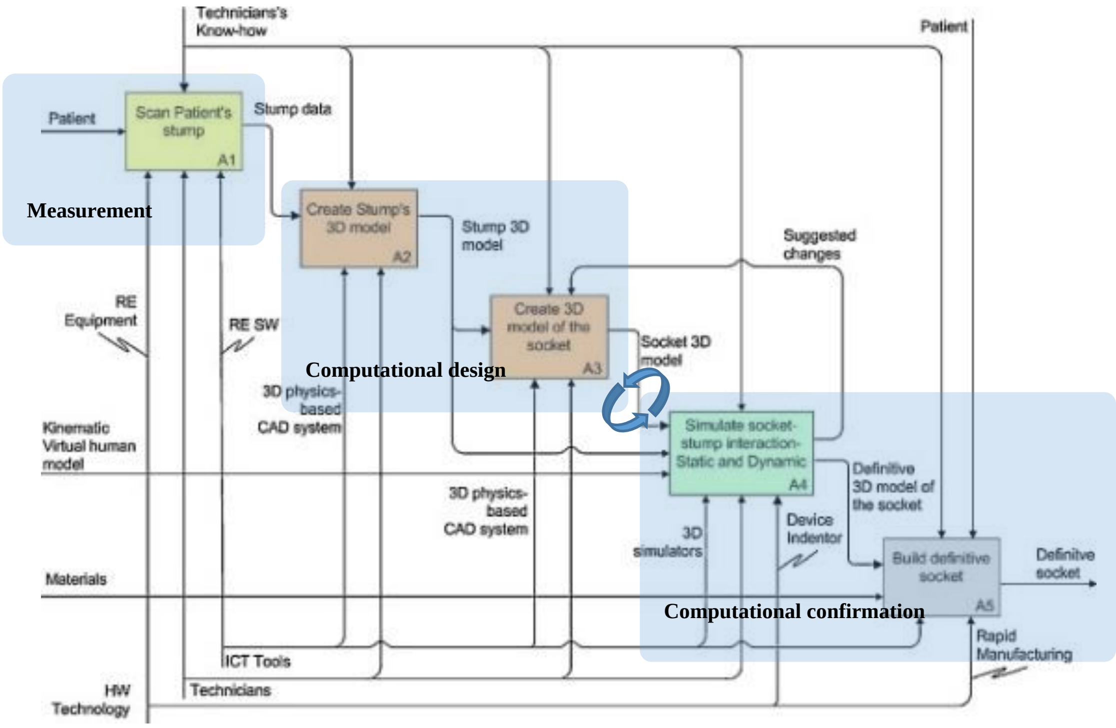

Figure 2-7: New 'To Be' socket design methodology using computational software (adapted from Colombo et al. 2010)

Morotti et al. (2015) implemented the new socket design method presented by Colombo et al. (2010) for a trans-femoral case study. They conducted three simulations of residuum and socket interaction, with each simulation using a different technique (3D scanning, MRI images and CAD modelling) to acquire the residuum and socket geometry. The three different FE simulations results were compared to experimental data obtained from Tekscan F-Socket System for the individual. This showed the predicted stresses were approximately twice the value of the experimental values. The authors concluded the protocol used was accurate, however the main criticalities and future developments should be focused on the accuracy of the numerical analysis with improvement of the boundary contact conditions.

More recently, work has been conducted by Steer and colleagues (2019) utilising the super computer capabilities at the University of Southampton to develop a parametric modelling process for trans-tibial socket fit, in hopes to tackle the current lengthy simulation solver times experienced in FE simulations. Their surrogate modelling techniques provide a faster solving time compared to FE simulations; however significant FE simulations were still required and used as a method to validate the preliminary surrogate models.

Comparing both the ‘As Is’ and ‘To Be’ methods show they both have a feedback loop to implement suggested changes to the socket geometry and of process of evaluation for these changes with numerous iterations before a suitable socket is designed. For the ‘As Is’ method this feedback loop is obtained between the phases of socket creation and patient testing (see Figure 2-6), and computational design and computational confirmation for the ‘To Be’ method (see Figure 2-7). If correctly implemented, the new ‘To Be’ method of socket design alters the feedback loop to require fewer check socket (physical prototypes) iterations to be fabricated, resulting in lower cost, testing time and travel time from the user. Instead, the feedback loop is conducted within computational software with the results being analysed by qualified professionals to determine the suitability of the socket.

However, due to the large number of variables and inputs that can be processed by FEA, it is of paramount importance that the model and inputs being used are highly accurate and credible to ensure a truthful output. According to Zhang et al. (1998) for complex three-dimensional models, the accuracy of the solution may be affected by:

- Geometry accuracy of the residual limb parts models in comparison to their true geometry.
- Difficulty in 3D arrangement of the interacting residual limb parts.
- Non-linear behaviour of soft tissues which are required to undergo large deformation.
- Contact constraints/conditions between the interacting residual limb parts.
- Magnitude and direction of the loading.

Because of this, the reliability and accuracy of FE models may come into question. Therefore, the task of establishing guidelines is a necessity for FE model development and dissemination, but also a difficult task for complex models. Recommended considerations for Finite element analysis studies have been published by various authors for studies in biomechanics (Erdemir et al. 2012), soft tissue modelling (Freutel et al. 2014) and clinical relevance (Viceconti et al. 2005), with the accumulative goal of enabling researchers to critique and better understand a model’s value. These recommendations are focused on the correct use of model verification and validation. For a model, verification is concerned with “solving the equations right”, whereas validation is “solving the right equations”. Therefore, verification is used to ensure the procedures used to solve the model are appropriate and repeatable. Whereas, validation ensures the model accurately predicts the results of the phenomenon it was designed to replicate.

Since inception, and extensively throughout the previous two decades, there have been numerous changes and improvements in the FE modelling practices of the lower residual limb and socket interface to implement FE ‘best practice’ recommendations and overcome various modelling limitations.

2.5.2 Review of Previous FEA Studies

This section conducts a systematic literature review considering the application of FEA to analyse the residual amputated limb, and their interface with prosthetic components of liners and sockets. Both TT and TF levels of amputation will be included in this literature review as research on both levels of amputation have been used to inform, develop, and continually build upon the modelling techniques employed. This review was conducted to capture original research and identify their objectives, modelling approaches (material properties, loads and boundary conditions), geometries, and outcomes of recent studies to better inform the future studies undertaken within this research.

Numerous database platforms were used to identify and obtain the reviewed studies. Keywords involved in the searches included: *finite element analysis, FEA, amputation, trans-femoral, trans-tibial, above-knee, and below-knee.* Cases where articles were deemed not eligible included, full text of the article was not accessible (Steege et al. 1987; Steege and Childress 1988; Seguchi et al. 1989; Brennan and Childress 1991; Torres-Moreno 1992), the article FEA methodology or results did not contain sufficient information (Krouskop et al. 1987; Reynolds and Lord 1992; Torres-Moreno 1999; Peery et al. 2006) and articles identified as review articles (Zhang et al. 1998; Mak et al. 2001).

The results show an observed trend of greater focus on trans-tibial studies compared to trans-femoral, with 20 trans-tibial (TT) and 10 trans-femoral (TF) articles yielded. The articles have been grouped on a level of amputation basis and chronological order. There was a historical focus on TT research during the early years of FEA research (see Figure 2-8), with more research being conducted on TF analysis in more recent years. The TF and TT research articles from this literature review are summarised in Table 2-1.

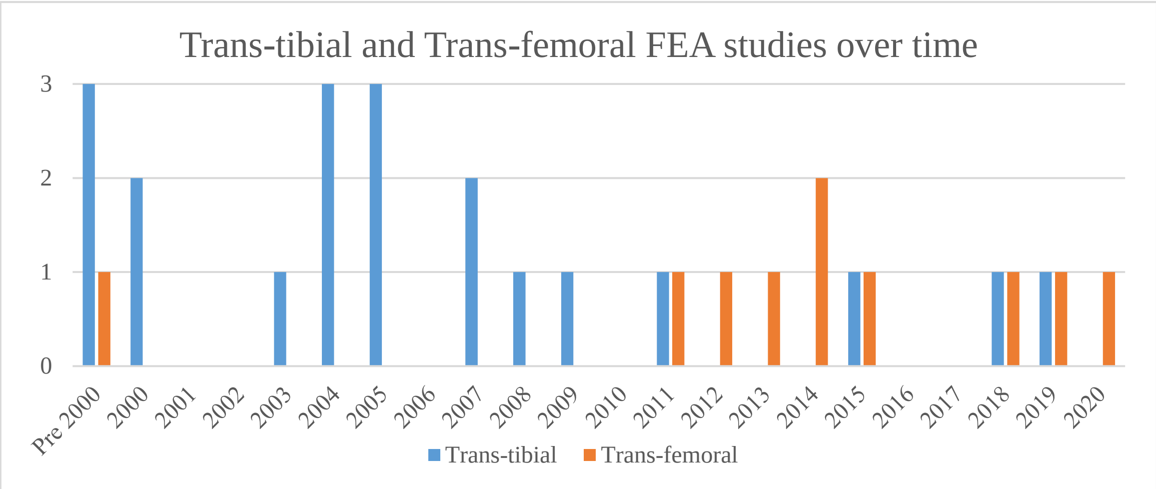

Figure 2-8: Research articles and publication years categorised by amputation level.

Over time, the modelling techniques of the research articles on this topic have been continually improving. The main contributors for this can be considered as improvement in topic knowledge and increasing computational power which have developed in parallel; new and improved ideas have been established and are able to be included in the modelling with additional computational power allowing more complex finite element simulations to be completed. Evidence of this is shown in a series of modelling conditions which will be described along with their subsequent studies under the prominent headings below, and is summarised in Table 2-1.

Table 2-1: Results of lower limb amputation FEA studies literature review

Information			Model	n	Boundary conditions and loading	Material Properties				Interfaces	Notable outcomes
Reference	Aim of study	Type				Bone	Soft tissues	Liner	Socket		
Trans-femoral (TF)											
Zhang and Mak (1996)	Examination of the roles of interface friction and distal-end boundary conditions	TF	2D sagittal plane model of assumed residuum and socket profile	3[a]	Donning: radial displacement to the nodes on the external socket surface Loading: axial load of individual BW	*E* = 15 GPa *v* = 0.3	*E* = 150 kPa *v* = 0.45	N/A	*E* = 15 GPa *v* = 0.3	Bone-soft tissue, tied Residuum-socket, μ = 0 – 0.9	Outcome: Increasing COF reduces the amount of load supported by pressure and increases the amount of load supported by shear. Peak pressure: 65 kPa at the distal end of the residuum. Peak shear: approximately 20 kPa
Lacroix and Patino (2011)	Examination of explicit donning process simulation	TF	3D Bone and ST geometry from CT scan Socket geometry from external scan of residuum	5	Donning: soft tissue deformed from axial socket donning Loading: N/A	*E* = 15 GPa *v* = 0.3	Hyperelastic, 3-parameter Mooney-Rivlin C10 = 4.25 kPa C11 = 0 kPa D01 = 2.36 MPa-1	N/A	*E* = 1 5 GPa *v* = 0.3	Bone-soft tissue, tied Residuum-socket, μ = 0.415	Outcome: Implemented an accurate method of simulating the donning process Peak pressure: 1.54 – 5.61 kPa Peak shear: 0.23 – 0.93 circumferential, 0.57 – 2.00 longitudinal
Ramirez and Velez (2012)	Examination of boundary condition between bone and soft tissue	TF	3D Bone and ST geometry from CT scan Socket geometry from external scan of residuum	4	Donning: soft tissue deformed from axial socket donning (unexplained) Loading: axial load of half BW	*E* = 15 GPa *v* = 0.3	*E* = 200 kPa *v* = 0.475	N/A	*E* = 1.5 GPa *v* = 0.3	Bone-soft tissue, tied/ μ = 0.3 Residuum-socket, μ = 0.415	Outcome: Stress and strain values and distribution affected by boundary condition between bone and soft tissue Peak strain: 85 - 163% compressive, 26 - 118% tensile
Zhang et al. (2013)	Examination of interfacial residuum and socket stresses	TF	3D Bone and ST geometry from CT scan Unrectified socket made from residuum external contours	1	Donning: 50N axial load Loading: 3 stance phases, heel strike, mid-stance and toe-off taken from Lee et al. (2004)	*E* = 15 GPa *v* = 0.3	Hyperelastic, 2-paramenter Mooney-Rivlin C10 = 85.5 kPa C01 = 21.4 kPa *v* = 0.459	N/A	*E* = 1.5 GPa *v* = 0.3	Bone-soft tissue, tied Residuum-socket, μ = 0.5	Outcome: 3 stance phase loading simulation Peak pressure: 119.3 kPa, at socket brim Peak shear: 25.7 kPa longitudinal, 103.6 kPa circumferential, at socket brim
Morotti et al. (2014)	Examination of experimental data to evaluate FEA model generation methods	TF	3D Bone and ST geometry from MRI scan Rectified socket geometry from external scan	1	Donning: soft tissue deformed from axial socket donning (unexplained) Loading: axial full bodyweight (BW) load	*E* = 10 GPa *v* = 0.3	*E* = 200 kPa *v* = 0.49	N/A	*E* = 15 GPa *v* = 0.3	Bone-soft tissue, tied Residuum-socket, μ = 0.4	Outcome: Correlation of peak interfacial stress locations between experimental and FEA predicted. FEA values found to be much greater than experimental values Peak pressure: 240.0 – 573.8 kPa
Restrepo et al. (2014)	Examination of varying friction coefficient at residuum-socket interface	TF	3D Bone geometry from CT scan Residuum and socket geometry from external scan	4	Donning: soft tissue deformed from axial socket donning (unexplained) Loading: axial load up to 120% BW Relative motion between residuum and socket not considered	*E* = 15 GPa *v* = 0.3	Hyperelastic, 3-parameter Mooney-Rivlin Skin: C10=9.4 kPa, C11=82 kPa, D01=0 MPa-1 Fat: C10=0.14 kPa, C11=0 kPa, D01=70.2 MPa-1 Muscle: C10=8.08 kPa, C11=0 kPa, D01=1.24 MPa-1	N/A	*E* = 1.5 GPa *v* = 0.3	Bone-soft tissue, tied/ μ = 0.3 Residuum-socket, μ = 0.2 - 0.6	Outcome: Higher COF values produced higher average shear stress values which were proportionate to the COF. Average pressure was independent of the COF.

Information			Model	n	Boundary conditions and loading	Material Properties				Interfaces	Notable outcomes
Reference	Aim of study	Type				Bone	Soft tissues	Liner	Socket		
Velez Zea et al. (2015)	Examination of relationship between residuum length and interface stresses	TF	3D Bone and ST geometry from CT scan Socket geometry from external scan of residuum	5	Donning: soft tissue deformed from axial socket donning (unexplained) Loading: patient gait specific axial load	*E* = 15 GPa *v* = 0.3	*E* = 200 kPa *v* = 0.475	N/A	*E* = 1.5 GPa *v* = 0.3	Bone-soft tissue, tied Residuum-socket, μ = 0.415	Outcome: General trend of lower stresses with a longer residuum Peak pressure: 81.7 – 151 kPa, at socket brim Peak shear: 14.0 – 55.5 kPa
Ramasamy et al. (2018)	Examination of residual limb and socket interaction for individual muscles and fused muscles	TF	3D Bone and ST geometry from MRI scan Socket geometry from external scan of residuum Liner from external residuum contours	1	Donning: soft tissue deformed from axial socket donning Loading: bipedal stance phase (400N)	*E* = 15 GPa *v* = 0.27	Muscle, fat and skin modelled as hyperelastic and anisotropic based on Rohrle et al. (2017)	Hyperelastic, 2-parameter Neo-Hookean CL1=0.33 MPa CL2=0.01 MPa	*E* = 15 GPa *v* = 0.3	Bone-soft tissue, tied Soft tissue-liner, tied Residuum-socket, frictionless	Outcome: Individual muscle model produced greater stresses compared to the fused muscle model.
Jamaludin et al. (2019)	Estimation of pressure distribution between residuum and two socket types	TF	3D Bone and ST geometry from MRI images Socket geometries from MRI images	2	Donning: soft tissue deformed from axial socket donning Loading: bipedal stance phase (400N)	*E* = 17.7 GPa *v* = 0.3	Muscle, fat and skin modelled using a strain energy function based on Untaroiu et al. (2005)	N/A	*E* = 1.9 GPa *v* = 0.39	Bone-soft tissue, tied Residuum-socket, μ = 0.5	Outcome: Comparison between FE models and experimental data provided good correlation of pressures in the volume region of the residuum, but not at the distal or proximal regions. Peak pressure: 118.95 kPa at a proximal location, not on the socket brim
Henao et al. (2020)	Estimation of dynamic gait loading	TF	3D residuum and socket taken from laser scanner of residuum positive plaster cast. Bone geometry from previous CT scan	14	Donning: soft tissue deformed from axial socket donning Loading: dynamic 3D loads	*E* = 15 GPa *v* = 0.3	Hyperelastic Neo-Hookian C10 = 11.6 kPa D01 = 11.9 MPa-1	N/A	*E* = 15 GPa *v* = 0.3	Bone-soft tissue, tied Residuum-socket, μ = 0.37	Outcome: Dynamic loads produced higher pressures on the residuum for all but one participant model. Large variability between the stresses experienced on each participant model. Peak pressure: 88 to 710 kPa across all participant models. Peak shear: 0.2 to 231 kPa
Trans-tibial (TT)											
Zhang et al. (1995)	Examination of preliminary modelling work to residual limb and socket interface	TT	Residuum geometries taken from Reynolds (1988) Unrectified socket geometry	1	Donning: Radial displacement to external nodes of liner Loading: axial load of 800N	*E* = 10 MPa *v* = 0.49	*E* = 160 – 260 kPa (200 kPa average) *v* = 0.49	*E* = 380 kPa *v* = 0.49	Rigid, external nodes of liner fixed	Bone-soft tissue, tied Residuum-liner, μ = 0.5	Outcome: FE predicted results correlate with experimental data. Model assumptions and approximations believed to the analysis accuracy. Peak pressure: 226 kPa Peak shear: 53 kPa
Zhang et al. (1996)	Examination of frictional action at limb-socket interface	TT	3D Bone geometry from biplanar X-ray ST geometry digitised from CAD systems Liner assumed from ST geometry and external surface fixed for socket geometry	1	Donning: N/A Loading: axial 400N load	*E* = 15 GPa *v* = 0.3	*E* = 160 – 260 kPa *v* = 0.49	*E* = 380 kPa *v* = 0.3	Rigid, external nodes of liner fixed	Bone-soft tissue, tied Residuum-liner, μ = 0 – 1.0	Outcome: Increasing the COF at the residuum-liner interface reduced the average and maximum interfacial pressure Peak pressure: ~150 kPa
Silver-Thorn and Childress (1997)	Examination of FEA as a tool to quantify the prosthetic interface	TT	3D Residuum geometries approximated by standard geometric shapes Liner modelled on external ST surface Un rectified socket modelled on external liner surface	1	Donning: N/A Loading: Bipedal loading	Rigid, internal nodes of ST fixed	*E* = 0.6 – 110 kPa *v* = 0.45	*E* = 380 kPa *v* = 0.45	*E* = 1.5 GPa *v* = 0.3	Residuum-liner, tied	Outcome: FE predicted results correlate with experimental data. Both are susceptible to interface sensitivity to numerous prosthetic factors. Peak pressure: 105 kPa
Zachariah and Sanders (2000)	Examination of two contact element types (gap and automated) on	TT	3D Bone geometry from non-amputation CT scan Socket geometry from CAD file	1	Donning: N/A Loading: axial 800N BW load	*E* = 69 GPa *v* = 0.28	*E* = 965 kPa *v* = 0.45	N/A	*E* = 1 GPa *v* = 0.28	Bone-soft tissue, tied Residuum-socket, μ =	Outcome: automated contact elements better reflect effect of local shape differences compared to gap elements

Information			Model	n	Boundary conditions and loading	Material Properties				Interfaces	Notable outcomes
Reference	Aim of study	Type				Bone	Soft tissues	Liner	Socket		
	interfacial stresses									frictionless, 0.5, bonded	Peak pressure: 201.5 kPa (auto friction case) Peak shear: 33.2 kPa (auto friction case)
Zhang and Roberts (2000)	Examination of FE predicted and experimental interfacial stresses comparison	TT	3D Bone geometry from biplanar X-ray ST geometry digitised from CAD systems Liner assumed from ST geometry and external surface modified for rectified socket geometry	1	Donning: interference fit from overclosure between ST and liner Loading: axial 800N BW load	*E* = 15 GPa *v* = 0.3	*E* = 160 – 260 kPa *v* = 0.49	*E* = 380 kPa *v* = 0.3	Rigid, external nodes of liner fixed	Bone-soft tissue, tied Residuum-liner, μ = 0.5	Outcome: Good correlation between FE and experimental results. FE predictions were 11% (SD 9%) lower than experimental results. Peak pressure: 226 kPa Peak shear: 50 kPa
Wu et al. (2003)	Examination of socket design incorporating FEA, interface pressure and pain tolerance	TT	3D Bone and ST from CT scan Liner and socket shape from external scan	1	Donning: N/A Loading: Bipedal stance (235N) and single leg stance (470N) axial load	*E* = 15.5 GPa *v* = 0.28	*E* = 100 - 400 kPa *v* = 0.49	5mm thick *E* = 1000 kPa *v* = 0.49	Rigid, external nodes of liner fixed	Bone-soft tissue, tied Residuum-liner, μ = 0.5 – 0.6	Peak pressure: 250 kPa Peak shear: 130 kPa
Jia et al. (2004)	Examination of inertial loads on interfacial stresses	TT	3D Bone and ST geometry from MRI scan Liner geometry assumed from inside of unrectified socket cast	1	Donning: interference fit from overclosure between ST and liner Loading: quasi-dynamic knee force and moment sets from inverse dynamics (from kinematic motion analysis data)	*E* = 10 GPa *v* = 0.3	*E* = 200 kPa *v* = 0.49	*E* = 380 kPa *v* = 0.39	Rigid, external nodes of liner fixed	Bone-soft tissue, tied Residuum-liner, μ = 0.5	Outcome: Consideration of inertial effects during walking Peak pressure: ~340 kPa Peak shear: ~85 kPa
Lee et al. (2004)	Examination of pre-stress socket rectification on interfacial stresses	TT	3D Bone, ST and socket geometry from MRI scan Socket shape from MRI scan adapted in CAD software	1	Donning: 50N axial load Loading: quasi-static knee force and moment sets from inverse dynamics (from kinematic motion analysis data) for heel strike, mid-stance and toe-off	*E* = 10 GPa *v* = 0.3	*E* = 200 kPa *v* = 0.49	N/A	*E* = 1.5 GPa *v* = 0.3	Bone-soft tissue, tied Residuum-socket, μ = 0.5	Outcome: Rectified socket geometry caused greater normal and shear stresses over specific regions of the residual limb. Peak pressure: 185 kPa Peak shear: 67 kPa
Lin et al. (2004)	Examination of the effects of liner stiffness	TT	3D Bone, ST and socket geometry from CT scan Liner geometry assumed as 6mm inside socket contours	1	Donning: N/A Loading: axial 600N BW load	*E* = 15.5 GPa *v* = 0.28	*E* = 60 – 2490 kPa (including tendon) *v* = 0.45	6mm uniform thick *E* = 400 – 800 kPa *v* = 0.45	Rigid, external nodes of liner fixed	Bone-soft tissue, tied Residuum-liner, μ = 0.5	Outcome: Peak stresses did not show consistent trend with liner stiffness. Reduced downward bone displacement with increased liner stiffness. Peak pressure: 783 kPa Peak shear: 373 kPa
Faustini et al. (2005)	Examination of interface stresses on transtibial residuum with compliant socket	TT	3D Bone, ST, liner from CT scan Socket assumed as outer liner surface	1	Donning: N/A Loading: 800N axial load, and simulated GRF forces from reference gait study	*E* = 15 GPa *v* = 0.3	*E* = 200 kPa *v* = not stated	*E* = 380 kPa *v* = 0.39	*E* = 1.6 GPa *v* = 0.39	All interfaces modelled as tied	Outcome: Peak stresses occurred at 35% of gait cycle (heel strike). The horizontal forces of gait had a small effect on pressures. Peak pressure: up to 250 kPa
Goh et al. (2005)	Examination of CAD-FEA technique validated against experimental data	TT	3D Bone geometry assumed by anthropometric scaling data ST geometry from external scanner Socket geometry designed in CAD	1	Donning: N/A Loading: Nodal displacements applied to ST corresponding to 10%, 25% and 100% forces of measured gait cycle	*E* = 15.5 GPa *v* = 0.33	*E* = 105 kPa *v* = 0.49	N/A	Rigid, external nodes of liner fixed	Bone-soft tissue, tied	Outcome: FEA results validated against experimental data with reasonable accuracy. Limited accuracy believed due to boundary conditions applied. Peak pressure: ~110 kPa at 25% gait cycle

Information			Model	n	Boundary conditions and loading	Material Properties				Interfaces	Notable outcomes
Reference	Aim of study	Type				Bone	Soft tissues	Liner	Socket		
Jia et al. (2005)	As above, with inclusion of knee displacements during gait	TT	3D Bone and ST geometry from MRI scan Liner geometry assumed from inside of unrectified socket cast	1	Donning: interference fit from overclosure between ST and liner Loading: quasi-dynamic knee force and moment sets from inverse dynamics (from kinematic motion analysis data)	E = 10 GPa v = 0.3	E = 200 kPa v = 0.49	4mm thick E = 380 kPa v = 0.39	Rigid, external nodes of liner fixed	Bone-soft tissue, tied Residuum-liner, μ = 0.5	Peak pressure: 323 kPa
Lee and Zhang (2007)	Examination of computational simulation to predict socket fit with pressure sensitive data	TT	3D Bone, ST and socket geometry from MRI scan Socket shape from MRI scan adapted in CAD software	1	Donning: N/A Loading: axial 800N load	Rigid, internal nodes of ST fixed	E = 200 kPa v = 0.45	E = 380 kPa v = 0.3	Rigid, external nodes of liner fixed	Bone-soft tissue, tied Residuum-liner, μ = 0.5	Outcome: Socket fit evaluated on comparison of peak indentation pressure with perceived pain and FEA socket predicted pressure (from Lee et al. 2005). Peak indentation pressure was found to be greater than at socket interface (max 810 kPa). Peak pressure: 260 kPa
Liu et al. (2007)	Examination of socket properties on interfacial stresses	TT	3D geometry exported from pre-existing CAD software	1	Donning: N/A Loading: 5 loading phases of gait applied with unspecified amounts	E = 15 GPa v = 0.3	E = 60 kPa v = 0.49	N/A	E = 1.0 – 2.9 GPa v = 0.33 – 0.43	Not specified	Outcome: The interfacial stresses were reduced with increased socket wall thickness and material strength. Peak pressure: 771 – 1283 kPa Shear stress: ~ 100 kPa
Portnoy et al. (2008)	Examination of internal soft tissue mechanical conditions of the residuum	TT	3D Bone and ST geometry from MRI scan Unrectified socket geometry from external scan	1	Donning: N/A Loading: 0.9mm downward bone displacement corresponding to ~50% BW load	Rigid, internal nodes of ST fixed	Skin, hyperelastic 2-parameter: C_{10}=9.4 kPa, C_{11}=82 kPa Muscle, neo-Hookean, G^{ins}=8.5 kPa	N/A	E = 1 GPa v = 0.3	Residuum-socket, μ = 0.7	Outcome: Initial reporting of internal strain conditions of the residuum combined with interfacial stresses. Peak pressure: 65 kPa Peak shear: 51.9 kPa
Portnoy et al. (2009)	Examination of surgical and morphological factors	TT	3D Bone and ST geometry from MRI scan Skin assumed from external ST geometry Unrectified socket geometry from external scan	12[b]	Donning: N/A Loading: 1.6mm downward bone displacement corresponding to ~50% BW load	Rigid, internal nodes of ST fixed	Hyperelastic, 3-parameter Mooney-Rivlin Muscle: C_{10}=2.3-8.1 kPa, C_{11}=0 kPa, D_{01}=1.2-4.4 MPa^{-1} Fat: C_{10}=0.143 kPa, C_{11}=0 kPa, D_{01}=70.2 MPa^{-1} Skin (2mm): C_{10}=9.4 kPa, C_{11}=82 kPa, D_{01}=0 MPa^{-1}	N/A	E = 1 GPa v = 0.3	Residuum-socket, μ = 0.7	Outcome: Compiled guidelines for TT amputation surgery involving bone length, bone bevelment, bone osteophytes, muscle flap stiffness and surgical scarring.
Lenka and Choudhury (2011)	Examination of optimum socket by varying socket thickness and material	TT	CAD designed prosthetic socket		Donning: N/A Loading: nodal displacement relating to GRF applied to various locations over socket wall	N/A	N/A	N/A	E = 0.3 - 2.6 GPa v = 0.39 – 0.41	N/A	Outcome: Changes in socket thickness and stiffness can effectively reduce the von Mises at local areas around the socket.
Arotaritei et al. (2015)	Examination of liner and socket material properties	TT	3D Bone geometry unexplained ST, liner and socket geometry from external scan of residuum	1	Donning: 50N axial load Loading: axial load of 3 stance phases, heel strike, mid-stance and toe-off	E = 15 GPa v = 0.3	Hyperelastic, 3-parameter Mooney-Rivlin Skin: C10=9.4 kPa, C11=82 kPa, D01=0 MPa ST: C10=4.25 kPa, C11=0 kPa, D01=2.36 MPa	E = 380 kPa v = 0.3 & 0.39	E = 1.5 & 1.1 GPa v = 0.3 & 0.37	Bone-soft tissue, tied Residuum-liner, μ = 0.45-0.6 Liner-socket, μ = 0.65-0.75	Outcome: Comparison of sensor pressure and FEA predicted pressure at sensor location Peak pressure: ~490 kPa

Information			Model	n	Boundary conditions and loading	Material Properties				Interfaces	Notable outcomes
Reference	Aim of study	Type				Bone	Soft tissues	Liner	Socket		
Cagle et al. (2018)	Examination of FEA predicted interfacial stresses compared with locations of skin issues experienced by participants	TT	3D Bone, ST, liner and socket geometry from MRI scan	3	Donning: N/A Loading: axial load of 110% BW	Rigid, internal nodes of ST fixed	ST: E = 300 kPa v = 0.45 Patellar tendon: E = 150 MPa v = 0.45	6mm uniform thick Hyperelastic, Yeoh constitutive model	E = 19 GPa v = 0.1	Bone-soft tissue, tied Residuum-liner, μ = 2.0 Liner-socket, μ = 0.5	Outcome: Strong match between FEA results and locations of skin breakdown suggest appropriate modelling strategy Peak pressure: 98 kPa Peak shear: 50 kPa
Steer et al. (2019)	Examination of FEA-driven surrogate modelling	TT	3D Bone, ST from MRI scan Liner and socket geometry generated in CAD from external surface of ST	20[c]	Donning: interference fit from overclosure between liner and socket Loading: 400N axial load	E = 12 GPa v = 0.3	E = 35 – 55 kPa v = 0.49	Hyperelastic properties based on Sanders et al. (2004)	E = 1.5 GPa v = 0.3	Bone-soft tissue, tied Residuum-liner, μ = 2.0 Liner-socket, μ = 0.5	Outcome: Developed a framework to generate simplistic FE models to cover the geometry of TT population. Peak pressure: approximately 60 kPa

Key: n = number of geometry models used.

[a] One participant model was used and altered within FE software to generate 3 variations of the single model.

[b] One participant model was used and altered with FE software to generate 12 variations of the single model.

[c] One participant model was used and altered with FE software to generate 12 variations of the single model.

2.5.2.1 Boundary Conditions and Loading

In previous studies, the bone and socket have been modelled as rigid boundary conditions, due to the argument of these parts being significantly stiff compared to the contacting soft tissues. Due to the recent changes in socket materials including polypropylene, polyethylene, and copolymer, Liu et al. (2007) conducted research to examine the effect of altering the socket stiffness. As a result, they reported negligible changes in interfacial stresses due to changes in the socket material.

Earlier studies neglected the effects of donning the socket prior to applying a loading phase, this is believed to be due to the model complexity required to solve the donning and the limited computer power at the time. Variations of simulating the donning phase previously conducted include: radial node displacement, interference fits, axial pre-loading (50N) and an axial displacement method (push fit) (see Table 2-1). Lacroix and Patino (2011) were the first to examine the effects of the donning phase and establish a push fit method. For this, they modelled the residuum (bone and soft tissue) of five individuals with TF amputation and their corresponding sockets. The sockets were initially modelled axially distal to their corresponding location on the residuum and were moved proximally at a slow velocity to minimise the dynamic effects. The displacement of the soft tissue from this method of donning is considered to be the 'gold standard' for modelling donning. The push fit method displaces the tissues axially rather than the tissue being compressed from interference fit donning, which produces a more realistic tissue displacement compared to alternative methods (Dickinson et al. 2017).

The loading phase has previously been commonly modelled as half bodyweight load (bipedal stance phase) and full bodyweight load (single leg stance phase). These loads have often been given the value of 400N and 800N for half and full bodyweight respectively, regardless of the bodyweight for the participant. This is potentially due to lack of this information recorded in the study or to provide an element of continuity between studies. Later studies have increased this loading to use the peak GRFs from normal (Restrepo et al. 2014) and amputee (Cagle et al. 2018) ambulation as these conditions produce the highest potential for damage due to the increased transmitted forces and resultant residuum stresses and strains.

2.5.2.2 Soft Tissue

The material property used to represent the soft tissue is arguably the most important compared to the bone, liner, and socket. The soft tissue is often the focus as it is the location for potential damage. This requires an accurate representation of the soft tissue properties. Up until the late 2000's, a common simplification used in studies was the use of linear elastic material properties for soft tissues gathered from the experimental data available (Mak et al. 1994; Zhang et al. 1997; Choi and Zheng 2005). A wide variety of values have been previously used ranging between E = 0.6-965.0 kPa, with a more general trend ranging between E = 100-400 kPa and v = 0.45-0.49. This variety provides difficulty when comparing results between studies.

Notable effort and studies by Portnoy and colleagues (2008 & 2009) focused on improving the soft tissue material models used to characterise tissue displacement for below knee amputee models. These studies are widely regarded for popularising the transition from modelling the soft tissues as linear elastic to hyperelastic. This was done using Mooney-Rivlin strain energy function from recent developments in material property research (Hendriks et al. 2003; Palevski et al. 2006; Gefen and Haberman 2007; Hoyt et al. 2008) to depict the hyperelastic behaviour of soft tissues in future studies. The parameter values incorporated by Portnoy et al. (2009) have subsequently been employed in recent FEA studies (Lacroix and Patino 2011; Zhang et al. 2013; Restrepo et al. 2014; Arotaritei et al. 2015). The use of the same parameters between these studies aids comparison and introduces a uniformity between successive studies.

2.5.2.3 Geometries

Examples of the model geometries used in previous studies are shown in Figure 2-9. The soft tissues have most commonly been modelled to a height of distal to the lesser trochanter. This abrupt proximal cut off to the soft tissues has prevented the stresses around the proximal brim of the socket being reported (Zhang et al. 1996; Lacroix and Patino 2011; Ramirez and Velez 2012; Restrepo et al. 2014; Ramasamy et al. 2018; Jamaludin et al. 2019; Henao et al. 2020) with all of these studies reporting peak stresses at the distal end of the residuum. To some extent this issue is addressed by a minor number of studies where the soft tissue was modelled to a height proximal to the femoral head (for example, see Figure 2-9d). However, these studies have consistently modelled the bone geometry without the pelvic bone (Zhang et al. 2013; Morotti et al. 2015; Ramasamy et al. 2018). The trans-tibial FEA study by Portnoy et al. (2009) is the only study to have modelled scar tissue. This is potentially due to a combination of the difficulty in modelling scar tissue and the study by Portnoy et al. (2009) reporting a minimal impact in including it (less than a 7% change in normal and shear stresses).

Zhang et al. (1996) emphasised the importance of the conical angle of the external surface of the residual limb in determining the levels of supporting the load provided by normal and frictional force. Nonetheless, characteristics of the residual limb have seldomly been reported in previous studies, with only the individual’s height, bodyweight, and residuum length being reported (Lacroix and Patino 2011; Ramirez and Velez 2012; Restrepo et al. 2014; Velez Zea et al. 2015; Henao et al. 2020). Similarly, the attributes regarding the socket design, dimensions and rectification were omitted from all previous studies (Lacroix and Patino 2011; Ramirez and Velez 2012; Restrepo et al. 2014; Morotti et al. 2015; Velez Zea et al. 2015; Ramasamy et al. 2018; Jamaludin et al. 2019; Henao et al. 2020) apart from those where Boolean socket fit was used (Zhang et al. 1996; Zhang et al. 2013). As a result, the socket geometry used in previous studies would have differed substantially potentially leading to unfounded comparisons.

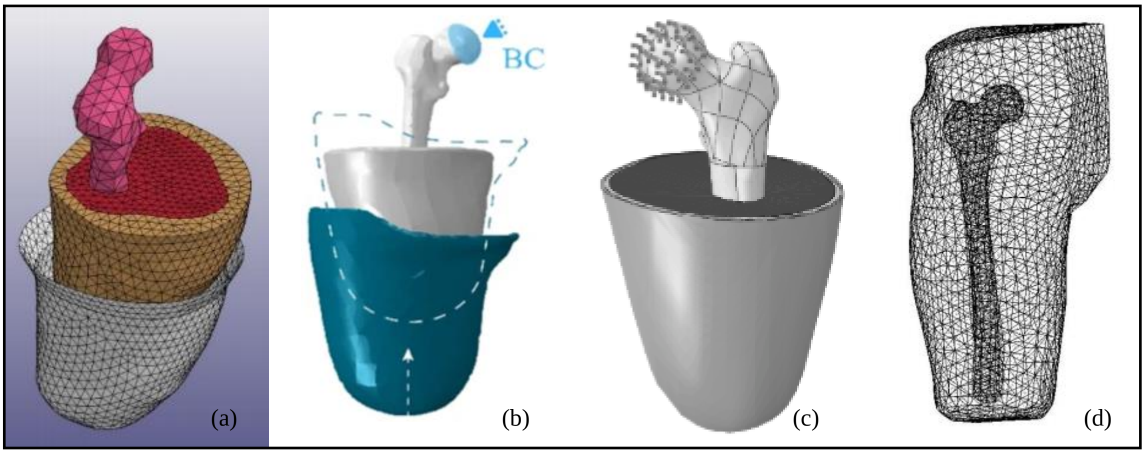

Figure 2-9: Comparison of model geometries used in previous studies; (a) Jamaludin et al. (2019), (b) Henao et al. (2020), (c) Restrepo et al. (2014) and (d) Zhang et al. (2013).

2.5.2.4 Interfaces

The bone-soft tissue interface is commonly modelled as tied or with the bone as a rigid body and the internal nodes of the soft tissue as fixed. This is potentially due to lack of sufficient data regarding this interface or for modelling simplicity. Ramirez and Velez (2012) examined the effects of altering the bone-soft tissue interface between tied and friction contact with a friction coefficient of 0.3 on the stress-strain state of the soft tissues. Ramirez and Velez (2012) used four 3D TF participant models and simulated donning and loading of half bodyweight for each whilst varying the bone-soft tissue interface conditions. The maximum von Mises stresses at the bone-soft tissue interface were located at the proximal region of the interface, potentially due to artefacts on the top surface caused by the tied interface condition, and located at the proximal and/or distal region of the interface for the friction condition. The friction condition resulted in increased von Mises stresses for all models except one. The peak principal strain values within the residuum followed the same magnitude and distribution trend as presented by the von Mises stresses for each model.

Zhang et al. (1996) was the first study to demonstrate the importance of including friction contact conditions at the external residuum interfaces. They used a simplified FE model with friction coefficients between 0.0 – 1.0 (0.25 increments) applied to the residuum liner interface whilst constraining the external nodes of the liner assuming rigid boundary conditions. Under the axial bodyweight load of the individual, the peak pressures were found to reduce with increasing friction, indicating that friction plays a critical role in supporting the bodyweight within the socket.

The number and type of residuum and socket interfaces are dependent on whether a prosthetic liner has been included in the model setup. Many of the previous studies which omitted a liner from the model setup used a generic friction coefficient of $\mu = 0.415$. This friction coefficient was popularised by Derler et al. (2007), however their study looked at the friction contact between a reference textile (wool) and a number of artificial skin substitutes, and is therefore not suitable for describing the contact between residuum and socket. Frictionless and tied contact assumptions have also been used for both the soft tissue-liner and liner-socket interfaces (see Table 2-1), with studies including a liner commonly applying friction contact to one interface, and applying tied or frictionless contact to the other interface. These simplifying assumptions are probably used to achieve convergence of the models being used in the studies.

Out of the eight trans-femoral FEA studies found in the literature review (see Table 2-1), five of the studies reported the peak interfacial stresses not along the brim of the socket, but commonly at the distal end of the residuum (see Figure 2-10). Whereas, only three of the studies reported peak stresses along the medial brim of the socket, including at the ischial support region (Zhang et al. 2013; Morotti et al. 2015; Velez Zea et al. 2015) (see Figure 2-11). Of these, Zhang et al. (2013) was the only study to comment on the boundary conditions applied

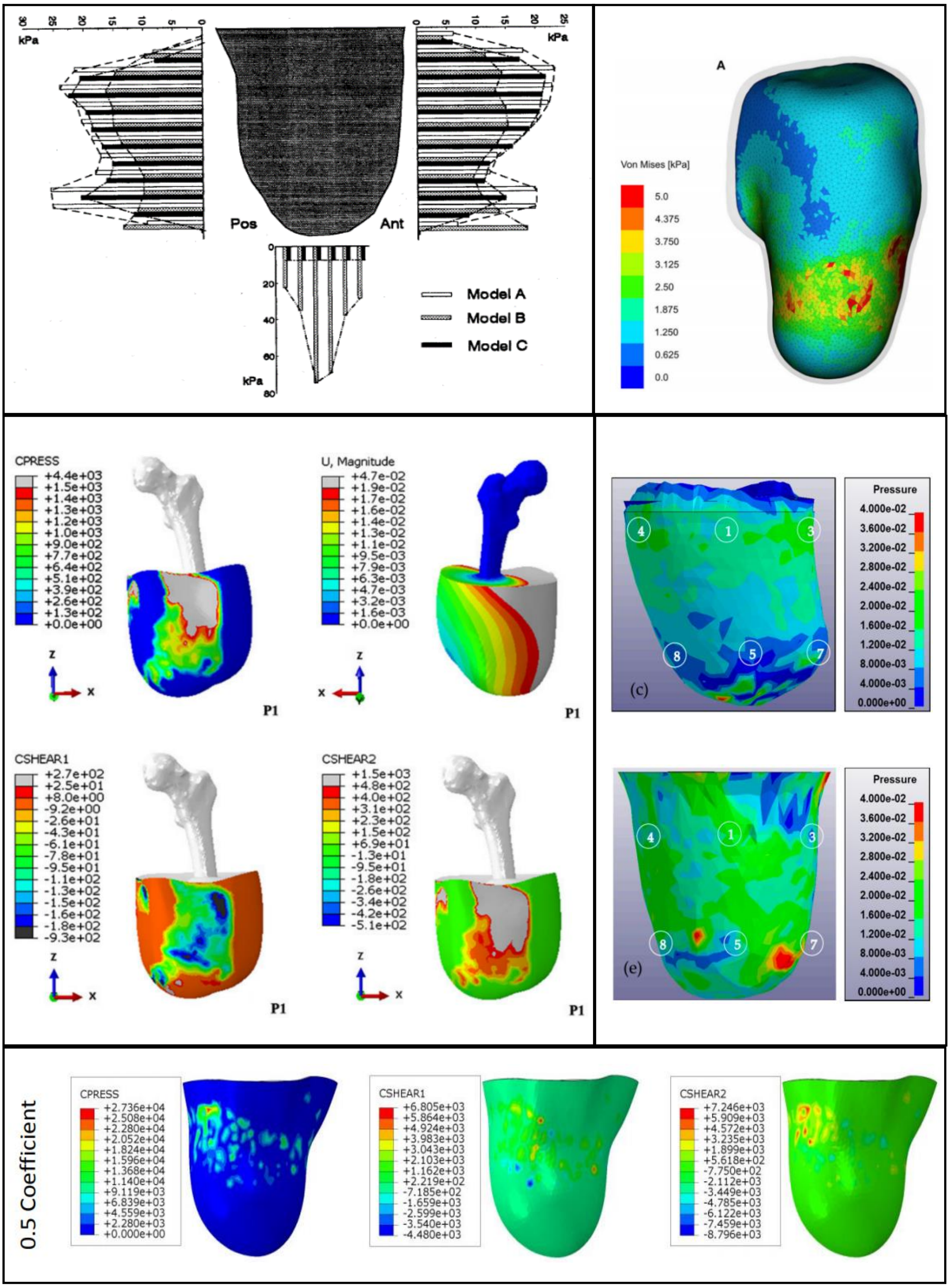

Figure 2-10: Stress distributions reported by FEA studies that have reported interfacial peak stresses not located at the proximal regions of the soft tissues; (top left) Zhang et al. (1996), (top right) Ramasamy et al. (2018), (middle left) Lacroix and Patino (2011), (middle right) Jamaludin et al. (2019), and (bottom) Restrepo et al. (2014).

to the soft tissues, in which they state the top surface of the soft tissue was fixed preventing movement. Fixing the top surface of the soft tissue would create artificial stresses along the brim of the socket by preventing the soft tissues from displacing. Whereas in clinical practice these would be caused by the bony geometry of the pelvis (Radcliffe 1955; Long 1985; Mulroy 2018). Information on the boundary conditions applied by Morotti et al. (2015 and Velez Zea et al. (2015) was not included but may be assumed to be the same as Zhang et al. (2013). Without fixing the top surface of the soft tissues, the stress distributions would have been similar to the other previous studies (see Figure 2-11).

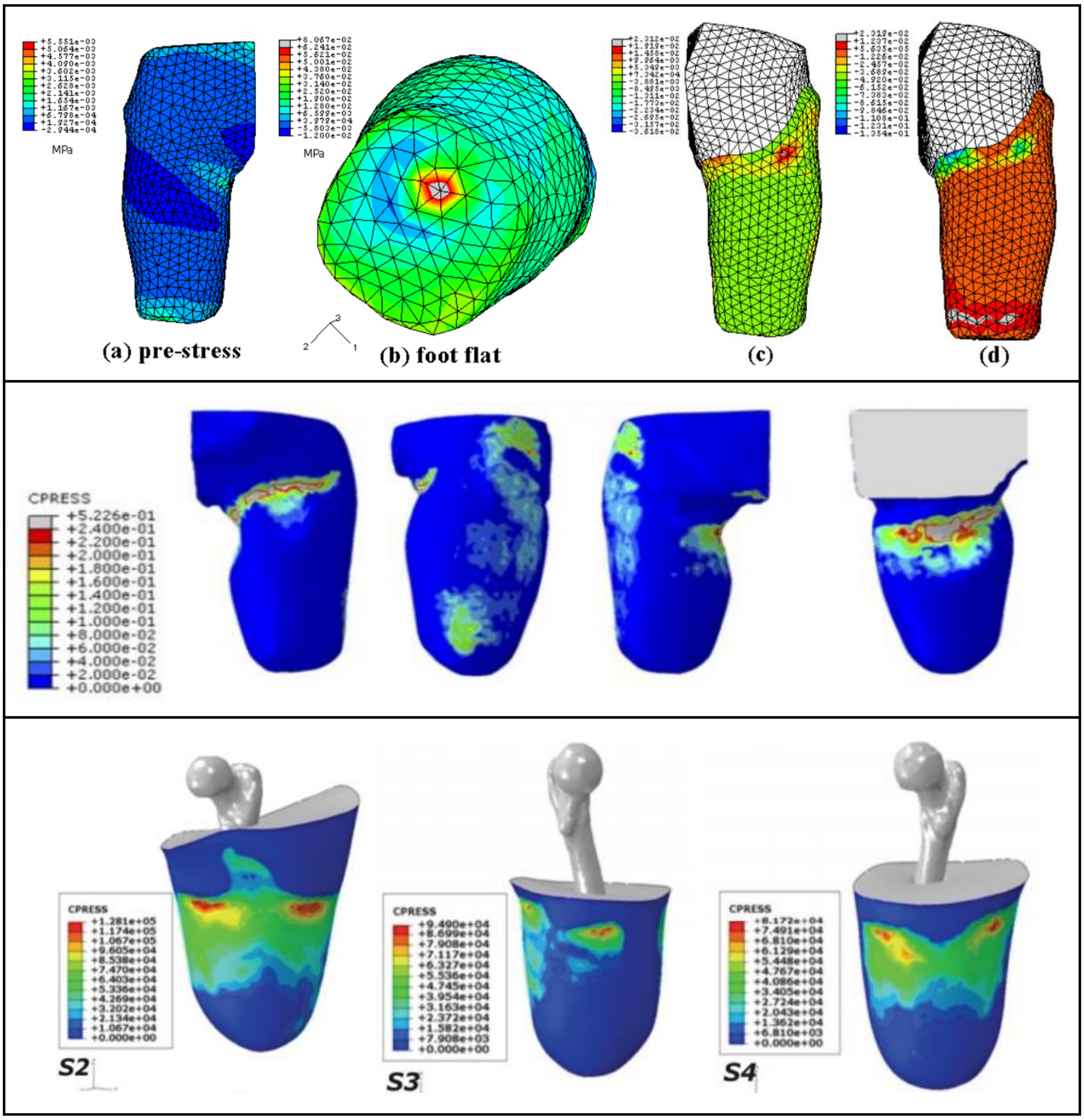

Figure 2-11: Stress distributions reported by FEA studies that have reported peak interfacial stresses at the proximal regions of the soft tissues; (top) Zhang et al. (2013), (middle) Morotti et al. (2015) and (bottom) Velez Zea et al. (2015).

Some previous FEA studies have incorporated experimental data acquisition alongside their FE models in an attempt to correlate the outputs from the FE models to the results of their experimental data (Silver-Thorn and Childress 1997; Zhang and Roberts 2000; Morotti et al. 2014), or as a method of validating the FE model outputs (Goh et al. 2005; Cagle et al. 2018).

2.5.3 Experimental Studies

Whilst FEA research into the prosthetic limb interfaces is incredibly useful and complex, results can be highly dependent on the multiple inputs available. Therefore, consideration should be made to compare FEA research to experimental data collected at these interfaces in the form of transducers (sensors). This comparison can act as a method of validating the models and outputs achieved from FEA.

Since the 1960's, research has been conducted to develop a variety of force transducers capable of accurately recording in vivo data of the pressure values and distribution at the residuum and socket interface. Several measurement techniques have been utilised including strain gauges, piezoresistive, capacitive, and optical fibre sensors (Al-Fakih et al. 2016). Transducers have commonly been mounted in various positions; embedded in the socket wall or liner, inserted in the socket, and mounted on the internal socket wall (Wheeler et al. 2016). Each transducer technique and mounting position has its own advantages and disadvantages. Depending on the combination used, possible advantages include, simplicity, flexibility, sensitivity, and accuracy. However, common disadvantages that can compromise the advantages include, bulky size, unidirectional measurement capability, easily damageable, and continual recalibration. A common disadvantage shared between nearly all types is the small sensing surface. Therefore, the placement of these transducers can be critical in accurately recording data.

The most commonly used types of transducers have been the Tekscan F-Socket System (Neumann et al. 2005; Kahle and Highsmith 2013; Morotti et al. 2015) and strain gauge transducers (Appoldt et al. 1969; Appoldt et al. 1970; Lee et al. 1997; Laszczak et al. 2016). A variety of these sensor types and their respective placements are shown in Figure 2-12. The Tekscan F-Socket System allows a large area of coverage and flexibility. The flexibility of the arrays allows them to fit directly between the residuum and socket making them suitable for the wide variety of residuum and socket shapes. This flexibility also enables the pressure arrays to cover the brims of the socket which have previously been noted as geometrically problematic regions (Silver-Thorn and Childress 1997). Unfortunately, the Tekscan F-Socket System is unable to measure shear stresses and is a considerable limitation as these stresses have been highly correlated to skin ulcers and soft tissue damage.

Strain gauge transducers are able to measure both normal and shear stress, however these transducers are more suited as a research tool rather than clinical use as they require the socket being examined to be permanently modified with holes created through the socket wall for transducer placement. Not only does this later render the socket unusable, but it is also a laborious task requiring prior knowledge of sensor placement as the sensors are only able to report activity within their limited area of coverage. This means the majority of the interface can be left unreported. Furthermore, the size of these sensors can be bulky with the required cables adding additional weight, impacting on an individual's normal ambulation, and altering the interfacial stresses being measured (Al-Fakih et al. 2016). Therefore, research by Xu et al. (2018) developed a dome-shaped tri-axial force sensor mounted on a flat plate for pressure and shear measurement for prosthetic socket design and used a numerically based reverse engineering method to establish the relationship between the sensor and the interfacial pressure. While the contact was within the dome area, the results indicated a linear relationship between sensor displacement and soft tissue stresses. However, the relationship becomes nonlinear after contact was made between the flat plate the sensor is mounted on and the soft tissue.

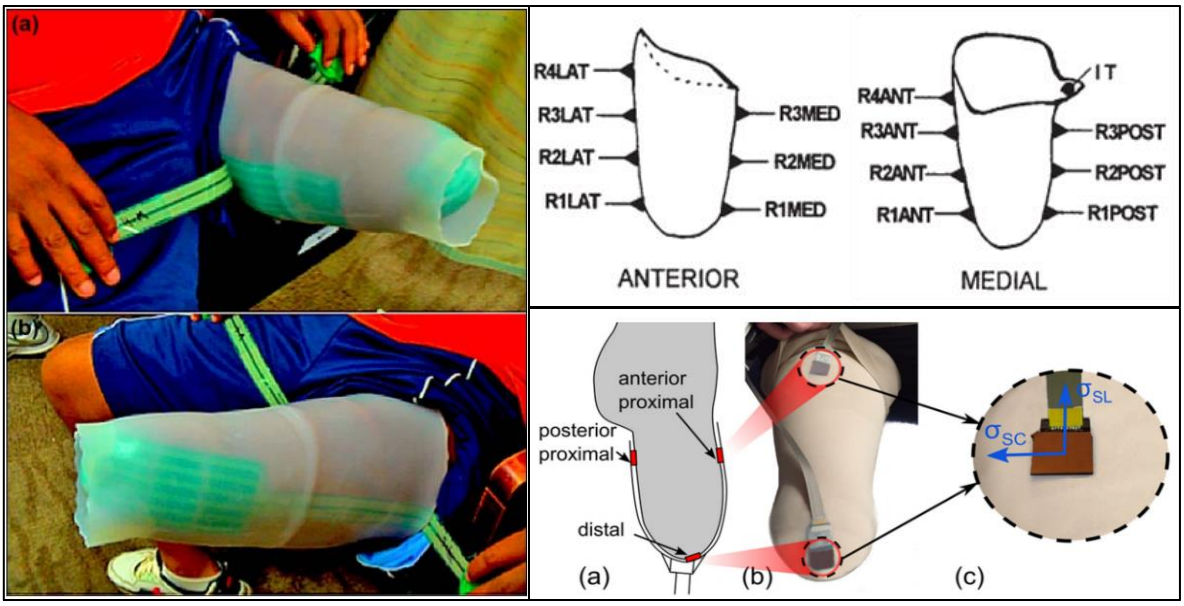

Figure 2-12: Sensor placement in previous studies. Left – Kahle and Highsmith (2013) Tekscan array placements of (a) proximal medial and (b) distal lateral. Top right – Lee et al. (1997) strain gauge cell locations mounted in socket wall. Bottom right - Laszczak et al. (2016) showing (a & b) schematic and image of sensor location, (c) coordinate system showing longitudinal and circumferential shear directions.

As both the FE and transducer method of determining the interfacial information have their own limitations, the results of both can be combined to form a basis of cross-checking and validation. This has already been undertaken by a number of FEA studies who have attempted to validate their models by transducer recordings (Zhang et al. 1995; Silver-Thorn and Childress 1997; Zhang and Roberts 2000; Goh et al. 2005; Morotti et al. 2014; Arotaritei et al. 2015). Care must be taken when validating FE model results against experimental data acquisition not to assume the experimental data to be entirely accurate, and therefore the limitations of each technique should be known. As with the previous FEA research, the majority of the experimental studies on amputated lower limbs has been focused at the TT level, often allowing comparison with FEA studies. The existing research on TF interfacial stress measurements by transducers will be discussed in this section.

A summary of the trans-femoral transducer studies is shown in Table 2-2 to allow for direct comparisons. Of these studies, the ones which report the resulting pressure distribution on the surface of the residual limb are shown in Figure 2-13.

Table 2-2: Summary table of trans-femoral transducer studies.

Reference	Aim of study	Type	n	Sensor type	Sensor coverage	Loading application	Liner application	Outcome recorded	Notable outcomes
Appoldt et al. (1969)	Comparison of two strain gauge mounting types within Quadrilateral socket	TF	4	Strain gauge transducers	Up to 29 locations (6.4mm sensor diameter) over entire socket area[a]	Self-selected walking pace	Not stated	Pressure	Outcome: Protruding strain gauges obtained larger pressure values than flush strain gauges. The peak pressure along all sensors at the medial brim (ischial seat) peaked at above 117.2 kPa Peak pressure: up to 186.2 kPa
Appoldt et al. (1970)	Sensor type developed to measure tangential pressure	TF	2	Strain gauge transducers	Up to 29 locations (6.4mm sensor diameter) over entire socket area[a]	Self-selected walking pace	Not stated	Shear	Outcome: Minimal shear (< 2.8 kPa) was detected at 20 test locations. Peak shear: up to 24.8 kPa
Lee et al. (1997)	To compare the pressure differences between Quadrilateral and IC sockets	TF	2	Strain gauge transducers	Entire socket area (apart from distal end) with 24-27 sensor locations (15mm sensor diameter)	Self-selected walking pace	Not stated	Pressure	Outcome: bipedal loading produced peak pressures of 23-34 kPa. The IC socket was favoured by the participants, which was attributed to the IC socket achieving a more even pressure distribution. Peak pressure: 92 kPa at ischial tuberosity
Neumann et al. (2005)	To develop a methodology for mapping a comfortable pressure distribution	TF	1	Tekscan F-Socket System	Entire socket area (apart from distal 4cm) in sections of 21.5x7.5cm[b]	Self-selected walking pace	Not stated	Pressure	Outcome: mean pressures between 13.3 – 40 kPa were obtained for most of the muscle compartments and all phases of gait. Mean pressure as high as 80 kPa recorded at the adductor longus, ramus and ischial areas. Peak pressure: 160.0 kPa at the ramus region
Kahle and Highsmith (2013)	To compare pressure values and distribution between brimless and IC sockets	TF	9	Tekscan F-Socket System	Medial proximal (7x20cm) and distal lateral (7x20cm)	Self-selected walking pace	Yes – sensors placed inside liner	Pressure	Outcome: All the participants favoured the brimless socket, which was attributed to the brimless socket producing reduced average pressure at the proximal medial region. Peak pressure: 112.1 ± 80.0 at the proximal medial for the IC socket, 109.2 ± 60.7 kPa at the proximal medial for the brimless socket.
Morotti et al. (2015)	To correlate automated simulation to experimental data acquisition	TF	1	Tekscan F-Socket System	Entire internal socket area apart from the distal end	Static full BW load on single leg stance	No	Pressure	Outcome: The experimental acquisition showed the posterior area was generally uniformly loaded except the ischium area which was loaded with peak pressure. The simulation results achieved similar pressure distribution to experimental data but with loading of the ischium area of up to 574 kPa Peak pressure: 240 kPa at ischium region
Laszczak et al. (2016)	Pilot test of a new pressure and shear sensor system on a knee disarticulate participant	TF	1	Strain gauge transducers	Three sensors (20x20mm) Placed at anterior proximal, posterior proximal and distal end locations	Self-selected walking pace	Yes – sensors placed outside liner	Pressure Circumferential shear Longitudinal shear	Outcome: The sensor system developed allowed for real-time feedback with a wireless approach. However, the results reported were from a limited sample area. Peak pressure: 58 kPa at distal end Peak circumferential shear: 27 kPa Peak longitudinal shear: 1.5 kPa
Jamaludin et al. (2019)	Examination of the pressure distribution by two IC sockets on the residual limb surface	TF	2	Strain gauge transducers	Eight sensors (unspecified size) placed at anterior, posterior, medial and lateral locations at both proximal and distal heights	Bipedal stance	Not stated	Pressure Circumferential shear Longitudinal shear	Outcome: Comparable pressure distribution between FEA model and sensor results. Peak pressure: 118.95 kPa at a proximal location, not along the socket brim Peak shear: No shear stresses reported even though the sensors were capable of recording them

Key; n = number of geometry models used.

[a] Data collected by four sensors at a time, requiring multiple walking trials.

[b] A single sensor with the location being changed between walking trials was used to cover the entire socket area. Results were not achieved for all sites.

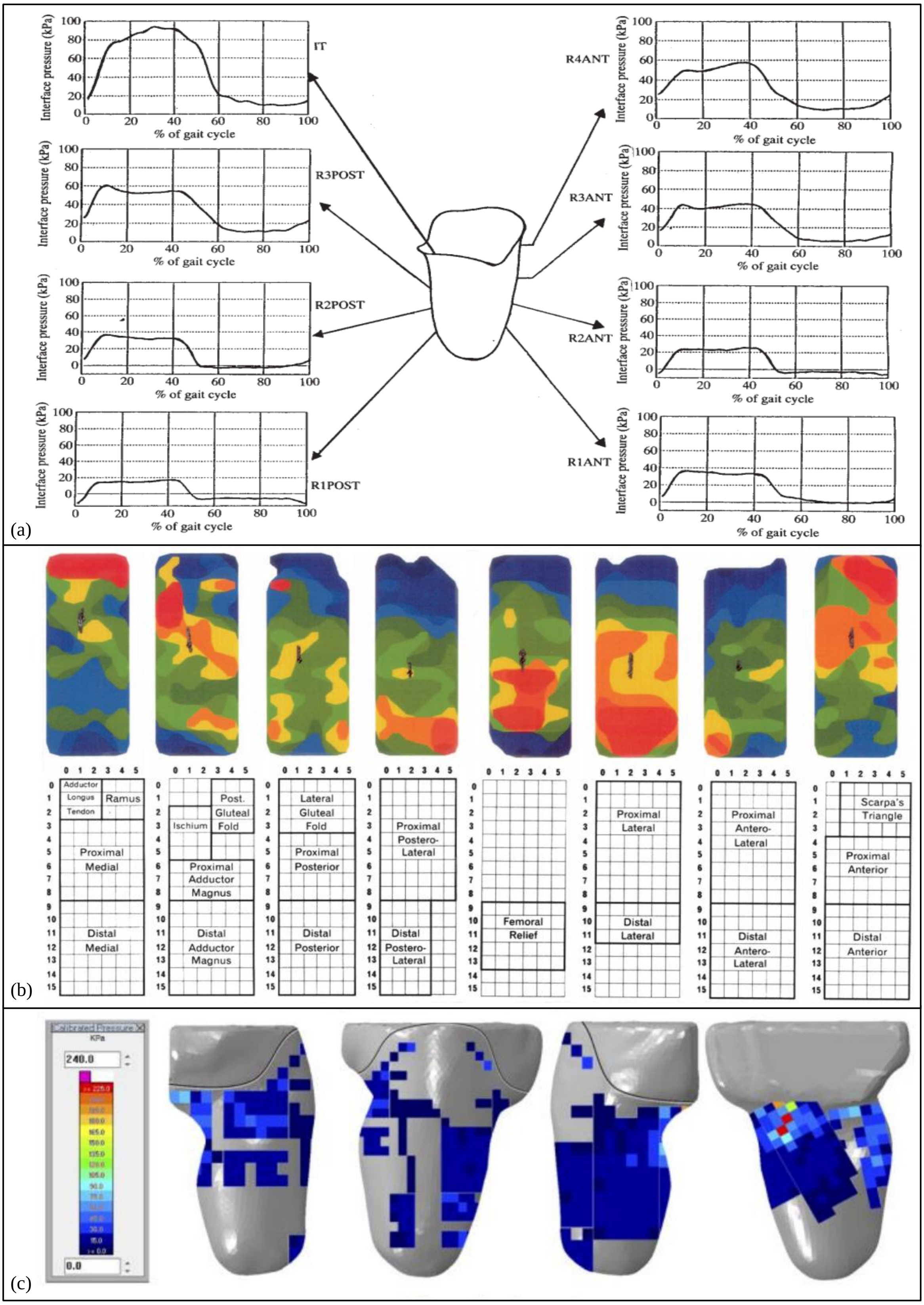

Figure 2-13: Pressure distribution on the residual limb surface reported by (a) Lee et al. (1997), (b) Neumann et al. (2005) and (c) Morotti et al. (2015).

Appoldt et al. (1969) conducted an early study of the pressures within a trans-femoral socket, examining the effects of mounting the strain gauge transducers flush within the socket wall or protruding. Testing was conducted on four amputees using subject-specific Quadrilateral total contact sockets whilst undergoing normal ambulation. The transducers mounted protruding from the socket wall were found to supply considerably larger pressures than those obtained from a flush mounted transducer. The data for a flush mounted transducer for one reported participant demonstrated a peak pressure range of 131.0-186.2 kPa (19-27 PSI) and was collected by the transducer located closest to the ischial seat of the socket.

Appoldt et al. (1970) developed their previous study further by including the recording of shear stresses between trans-femoral residuum and socket. The tangential transducer was created by cementing four strain gauges to thin steel bending beams and were arranged to load only along a specific axis. The shear stresses above a cut-off threshold of 2.8 kPa (0.4 PSI) were only detected at 20 out of the 29 tested locations for both participants. For the shear stresses that were detected, peaks of 8.3 kPa (1.2 PSI) and 24.8 kPa (3.6 PSI) were reported for the two participants.

Lee et al. (1997) studied the interfacial pressure differences between Quadrilateral and Ischial Containment sockets for two participants during normal walking with pressure transducers fitted flush to the socket wall. Only four transducers were used to record data at a time, meaning eight to nine different recordings were required for each participant and socket combination to obtain data readings for all transducer locations. This would have introduced potential variations between the number of data recordings. During the bipedal loading for standing tests, a peak pressure of ~23 kPa and 34 kPa was recorded for the IC and Quadrilateral sockets respectively, with both peak locations being recorded at the ischial tuberosity. For walking tests, the Quadrilateral socket produced the greatest peak of pressure, this was 70.1-92.0 kPa and located at the ischial tuberosity site for both participants. In comparison, the IC socket produced a more evenly spread pressure distribution, with the authors noting that the sloping medial socket wall brim of the IC socket reduced the loading at the ischium. The study concluded that the pressure distribution achieved by the IC socket was considered favourable by both participants.

Neumann et al. (2005) used the Tekscan F-Socket System to examine the interfacial pressure of an IC socket of a single participant. The participant had been using the socket examined for six years and had reported the fit of the socket as being comfortable. Pressure measurements were obtained at a comfortable walking pace. Numerous measurements were taken with the pressure array position being changed within the socket to cover the entire inner socket wall. They reported mean average pressures across the entire gait cycle of up to 80.0 kPa for the adductor longus, ramus and ischial areas of the residuum, with these pressures being nearly double the average pressures of the volume region. The greatest single peaks reached up to 160.0 kPa during mid-stance at the ramus region. The authors did not report on any feedback from the participant regarding the comfort of the socket during testing. It can be assumed the pressures experienced were comfortable given the prior statements made about the participants socket comfort.

The objective of a study by Kahle and Highsmith (2013) was to compare hip kinematics, socket position and interfacial pressures between IC and brimless sockets with vacuum assisted suspension. The brimless socket variant is not commonly used and was created with the same dimensions as the IC socket, but the proximal brim of the socket was removed. Therefore, similar to the Quad socket variant, the brimless socket is a sub-ischial socket variant and is not intended to contain the pelvis. The brimless socket requires the use of vacuum suspension to maintain an intimate contain with the residual limb. In their study, Kahle and Highsmith (2013) recruited nine participants who were fitted for the two socket types by the same prosthetist. Tekscan F-Socket System was used for pressure data capture during normal ambulation. Two pressure sensor arrays measuring 7x20cm were placed between the residuum and liner, one at the proximal medial region of the residuum and the other at the distal lateral. The peak averages and single greatest peaks reported by Kahle and Highsmith (2013) are shown in Table 2-3 below.

Table 2-3: Pressure results from Kahle and Highsmith (2013) study.

	IC socket	Brimless socket
Greatest stance average (kPa)		
Proximal medial	42.9 ± 28.0	25.3 ± 13.7
Distal lateral	25.1 ± 9.3	29.6 ± 15.1
Single greatest peak (kPa)		
Proximal medial	112.1 ± 80.0	109.2 ± 60.7
Distal lateral	72.4 ± 23.7	100.1 ± 74.9

All the participants favoured the brimless socket in comparison to the IC socket, this is interesting considering six out of the nine participants used IC sockets prior to the study. The authors correlated this unanimous preference to the reduced average pressure at the proximal medial region for the brimless socket in comparison to the IC socket.

A study by Morotti et al. (2015) attempted to implement an automatic simulation procedure with the goal of enabling a prosthetist to automatically run FE analysis to validate their socket design. They collected experimental acquisition data and compared it to three FE methods of model generation to determine the viability of each FE method. Tekscan F-Socket System was used for pressure acquisition at the residuum-socket interface whilst the patient was using the socket designed by the prosthetist and undergoing single leg standing for five seconds. The transducers area covered much of the proximal socket region but did not include the distal region of the socket. The experimental data showed the posterior area was generally uniformly loaded except for the ischium area, which was loaded considerably higher, with pressures up to 240 kPa. Comparatively, the FE methods of generating the residuum model by MRI scan and 3D scanning both predicted pressure maps of similar distribution and loaded areas. However, the predicted pressures in the proximal medial region of the thigh were significantly higher in comparison to the experimental data for both the MRI scan (pressures up to 522.6 kPa) and 3D scanning (pressures up to 573.8 kPa) methods. Whilst good comparative pressure distributions were attained, quantitative correlation between experimental and FE predictions was not achieved. The authors believed this was caused by the FE model differing geometrically to the true residuum shape and the simplistic linear elastic material properties assumed for the soft tissues.

To avoid the limitation of unobtainable shear data of the popular Tekscan F-Socket System, Laszczak et al. (2016) conducted a preliminary study using a capacitive interface stress sensor capable of measuring both normal and shear stresses. Clinical testing was conducted with a knee disarticulate amputee using their own regular prosthetic components. Three sensors were placed between the socket and a 6mm thick liner at the distal end, posterior proximal and anterior proximal locations. Data was captured over a self-selected walking pace. They reported peak pressures of up to 58 kPa, 38 kPa and 36 kPa at the distal end, posterior proximal and anterior proximal sensor locations, respectively. The observed peak shear stresses were greatest at the distal end sensor with a value up to 27 kPa, with the shear stresses at both the posterior proximal and anterior proximal locations peaking only up to 1.5 kPa. The study conducted by Laszczak et al. (2016) demonstrates a major improvement in sensors capability in capturing both the normal and shear stresses whilst remaining flexible and nonintrusive to the user. However, the use of knee disarticulate participant prevents direct comparisons to alternative studies as this type of amputation encourages loading at the distal end of the residuum as the method of weight bearing. This is demonstrated by the pressure distribution reported. The limited number, size and placement of the sensors can also be considered a limitation; the three sensors were placed along the sagittal plane of the residuum without consideration to the ischium. The sensors measured 20x20mm providing results from only a relatively small area of coverage. The combination of these limitations means only a partial amount of the interfacial stresses being recorded.

2.5.3.1 Assessment of Comfort

To investigate the relationship between pain tolerance and threshold, Lee et al. (2005) used a simplified FE indentation model, combined with physical indentation tests across 11 locations on the trans-tibial residuum of 8 individuals. They observed local differences in pain threshold (the minimum pressure to inducing pain) and pressure tolerance (the maximum tolerable pressure) levels. Their study demonstrated that comfort could be directly related to the pressures experienced on the residuum. The highest pain tolerance and pressure thresholds were found at known pressure tolerance areas of patellar tendon and tibial tuberosity, with the lowest pressure threshold at the residuum tip. The authors noted the importance of obtaining personalised information, with the two younger individuals in the study being capable of withstanding greater pressure and having a higher pain tolerance compared to the other individuals.

Arguably the most important benefit of the transducer experimental method of obtaining data is that it allows the authors to simultaneously receive feedback from the participant relating to the comfort provided and general satisfaction of the socket whilst also capturing data on the interfacial stresses. This participant feedback could prove to be invaluable in future FEA studies examining the interfacial stresses by relating perceived comfort in certain locations on the residual limb to the pressure outputs achieved.

This method of feedback was not reported by several of the transducer studies discussed (Appoldt et al. 1969; Appoldt et al. 1970; Neuman et al. 2005; Morotti et al. 2015; Laszczak et al. 2016). In the study conducted by Lee et al. (1997) both participants stated their use and preference for the IC socket prior to the study. After the study, the participants made a subjective preference again for the IC socket, however the reasoning for this was not provided. All the participants in the study by Kahle and Highsmith (2013) reported a preference for the brimless socket over the IC socket at the end of the study. The main narrative for this provided by the authors was the increased comfort during sitting and stationary standing. This justification for the preference was not correlated to the ambulatory pressures reported.

2.6 Summary

The work conducted in the literature review has encompassed an overview of the lower residual limb and the prosthetic components and a review of previous FEA and experimental sensor studies of the trans-femoral residuum. A review of the literature has highlighted the potential for the capability of FEA to be used in conjunction with other CAD software to design the prosthetic socket. This would advance the current socket design process from an 'As Is' state to a 'To Be' state. However, before this can be successfully achieved at trans-femoral level, a number of pitfalls in the modelling process that have been identified from the literature review need to be addressed and studied in order for more accurate models to be produced:

Pelvic Bone.

It has been demonstrated by numerous practitioners and studies that the pelvic bone is integral in the socket design process as it is the ischial region of the pelvis that supports a majority of the amputee's weight during ambulation. This has been demonstrated by numerous experimental studies on the interface pressures between residual limb and socket. Nevertheless, the pelvis has not been modelled in any trans-femoral FEA studies to date.

Prosthetic Liner.

Liners have been shown to greatly affect the stresses experienced by the residuum. This can be attributed to the properties of the liner such as friction coefficient, stiffness, and thickness. Therefore, the liner has great potential to not only improve, but also hinder the comfort and control the user has over the prosthesis as a result of these multiple variables. The effect of these variables should be examined to allow for a better pairing between residual limb and liner when prescribing a liner to a patient.

Prosthetic Socket.

The prosthetic socket design currently remains an extremely artisanal and individualised process to both the user and the prosthetist. Whilst there are guidelines for designing specific socket types (e.g. Quadrilateral and IC sockets) the process remains highly subjective to the prosthetist with the resulting socket shape being the main factor of the stress distribution and concentrations on the residual limb.

The next chapter of this thesis will detail the creation of FE models used to examine these three areas in order and in detail in the subsequent chapters. This will not only examine their effects, but also assess how they can be accurately modelled to collectively develop an optimised model that takes into consideration all these aspects.

3. FINITE ELEMENT MODEL CREATION

3.1 Introduction

According to the research reported in the previous chapter, the loading on the residuum can be accurately simulated using FEA. The geometry of the residuum significantly affects the stress and strain patterns obtained from the FE models (Morotti et al. 2015). As such, the more precise the models and geometry used, the more accurate the results will be. Therefore, reconstructing precise model geometry with appropriately refined mesh is essential.

In this study, the data from CT scans were used to generate three-dimensional residual limb models within the Materialise CAD packages Mimics version 19.0 and 3-Matic version 11.0 (Materialise, Leuven, Belgium). Finite element analysis of these models was carried out using ABAQUS CAE 2017 ®. The data analysis was performed in Microsoft Excel and MATLAB 2017 (MathWorks, Inc.). A flow diagram of the processing procedure and relevant software packages is shown in Figure 3-1.

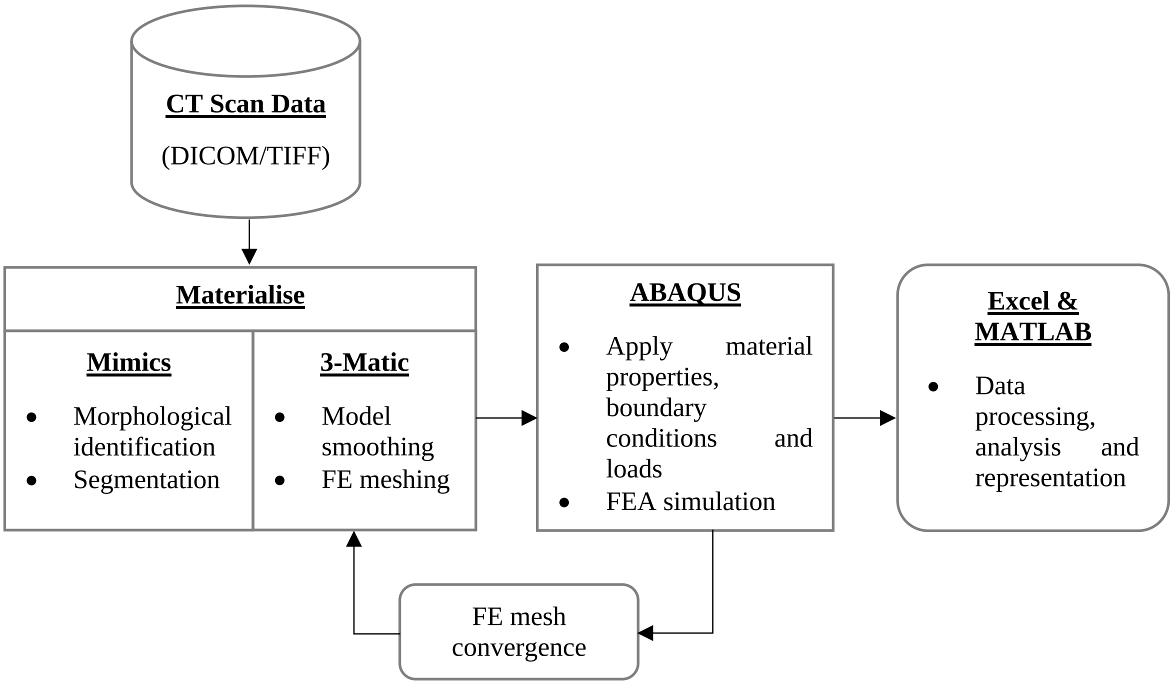

Figure 3-1: Flow diagram of software packages for the modelling process.

The work process outlined in this section was the general method for creating each model. If the method used was altered for a certain model type during this study, the details of this change will be stated in the relevant sections.

3.2 Three-Dimensional Model Creation

In this study, complex 3D residual limb models were reconstructed from three male participants with unilateral trans-femoral amputation. These individuals differed in age, weight, height, and residuum length. These details are shown in Table 3-1. To evaluate the consistency of the results in the later chapters, the three participants were chosen with each having varied residual limb characteristics: long conical, short conical and cylindrical.

Table 3-1: General information of the participating persons with a trans-femoral amputation.

Participant	Age (yrs)	Height (m)	Weight (kg)	Sex	Time since amputation (yrs)
Participant 1	55	1.80	70	M	10+
Participant 2	41	1.75	79	M	5+
Participant 3	39	1.73	74	M	5+

The geometries of the residual limb for each participant were collected via CT scans having a 512 x 512 pixel matrix, 0.703 mm pixel size, 1.25 mm slice increment and 0.0° gantry tilt. The scans were performed with the participants lying in a supine position without the application of a liner or socket. The scans were deemed usable if it encompassed the entire length of the amputated residuum up to the pelvic region. Once it was agreed that the scans were suitable, the modelling process outlined in Figure 3-1 was followed. The scans used in this thesis were collected during studies by Xu and Robinson (2008) and Xu et al. (2016). The ethical approval for the use of the images collected was also covered under these studies.

3.2.1 Segmentation and Mask Creation

The CT scan slices were imported into Mimics version 19.0© in the format of DICOM or TIFF image files. The Mimics software allowed the scans to be viewed in axial, sagittal and coronal slices. The scans were cropped to show only the area of interest. The bone geometry modelled was the residual femoral shaft and head, as well as the hemipelvis on the side of amputation. The height of the hemipelvis was limited due to the area within the scan, but included the ischium, pubis, and acetabulum. The medullary cavity, trabecular and cancellous bone were assumed to be a single entity. The muscle, fat and skin were also identified as a single soft tissue bulk entity. The approach of modelling the bone and soft tissue each as a single entity has been used in similar previous studies (Zhang and Mak 1996; Jia et al. 2004; Lacroix and Patino 2011; Ramirez and Velez 2012; Zhang et al. 2013; Morroti et al. 2014; Velez Zea et al. 2015). Within Mimics version 19.0©, masks were applied to the regions of bone and soft tissue. The built-in Hounsfield threshold values of 226 to 1713 for ‘Bone (CT)’ and -700 to 225 for ‘Soft Tissue (CT)’ were used to identify the desired regions. Areas where the built-in values did not readily identify between the bone and tissues were allocated to the appropriate mask by user discretion. Masks were applied to the regions on multiple axial slices using the ‘Multiple Slice Edit’ function.

The amount and location of scar tissue present on the scans varied between participants. This is inherent to the surgical procedure used as well as cause of amputation and is therefore unavoidable. During amputation, the myodesis process of suturing the remaining thigh musculature to the distal end of the residual femur can encourage bone remodelling. This is caused by changes in various signalling pathways and control mechanisms over time (Marghoub et al. 2019) and may occur in longer periods of time since amputation. To limit the complications of correctly modelling scar tissue and distal end bone remodelling, these were not included in the models. Instead, in the cases where scar tissue and distal bone remodelling were present, the residual limb geometry was approximated by the user to create a simpler geometry (see Figure 3-2). Using a small approximation method would prevent future complication in the meshing process and FE simulations.

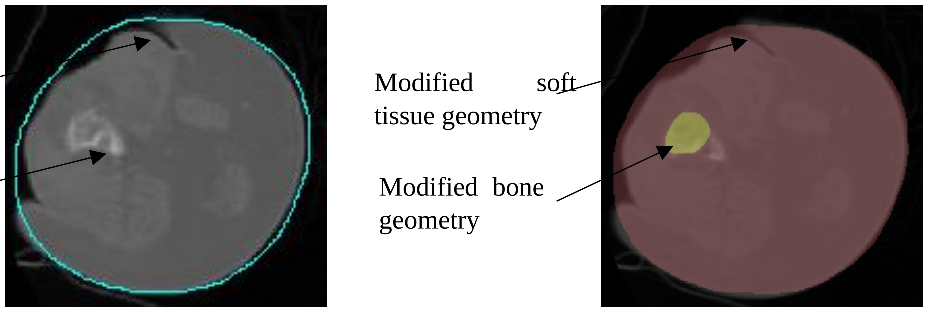

Figure 3-2: Approximation of soft tissue geometry within Mimics.

The final masks were transformed from 2D images to a 3D model within Mimics. As the masks were applied using an automatic thresholding tool. Any outliers existing beyond the desired area on the 3D model were identified and removed using the 3D Mask Editing tools. This included smoothing and wrapping to reduce the 'step' edging created from the scan pixel resolution which would cause problems later during the mesh process. Preliminary smoothing was applied with a smoothing factor of 0.3 and a minimum of 3 iterations. This smoothing factor was chosen as it allowed the step edging to be removed but did not significantly reduce the volume of the 3D mask. Wrapping was performed using the 'Wrap' tool which covered the outside of each part to fill any potential holes in the parts which could cause inaccuracies during meshing or FEA. Finally, the 'Edit Mask in 3D' tool was used to identify and remove any remaining unwanted areas on the calculated 3D model.

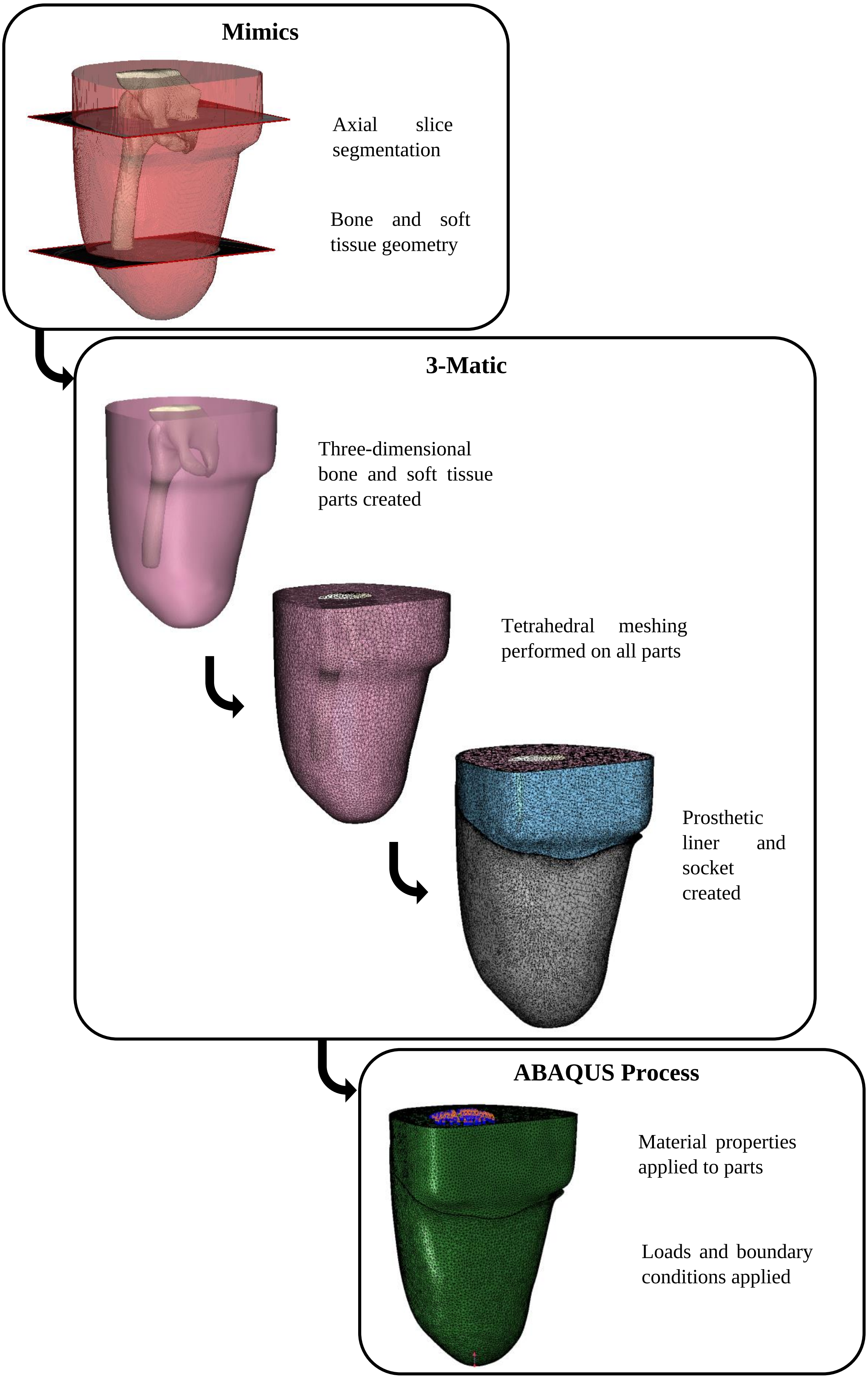

Figure 3-3: Global overview of the residual limb modelling process.

3.2.2 Solid Part Creation

The 3D models within Mimics were imported to 3-Matic to perform further operations. Within 3-Matic further smoothing was applied to the parts to prevent any sharp edges which may cause unwanted irregularly meshed elements and therefore unwarranted high stresses within the FE models. This was applied in the form of 'Global smoothing' to the parts with a smoothing factor of 0.3 and a minimum of 3 iterations. Following this, any areas which appeared to be unresolved by the global smoothing were smoothed locally using the 'Local Smoothing' tool until shape edges were removed to a suitable level.

The soft tissue masks used to create the 3D models within Mimics were solid entities without a hollow space to contain the bone geometry. Therefore, a subtraction Boolean operation was performed to remove the bone geometry from inside the solid soft tissue part. This allowed the two parts to fit together completely (i.e. with no gaps or overlaps).

Models within this thesis include a prosthetic liner and/or a prosthetic socket. Neither of these items were present during the CT scan of the residual limbs of the participants. These items were created and modified using the residual limb geometry and tools within 3-Matic. For this process, the outer surface of the soft tissue was copied to create a new part (see Figure 3-4). The surface was duplicated and adjusted relative to the X, Y & Z coordinate system using a scaling factor. The outer surface was adjusted until the desired distance between the copied outer surface and the scaled outer surface (i.e. the part thickness) has been achieved (Figure 3-4a & b). For example, this was most commonly 4mm for the prosthetic liner parts and 10mm for the prosthetic socket parts used in this study. The tool 'Fill Hole Normal' was used to create a solid part between the two surfaces (Figure 3-4c). This process was used to create prosthetic liners and prosthetic sockets that were an exact 'Boolean fit' with the outer surface of the soft tissue.

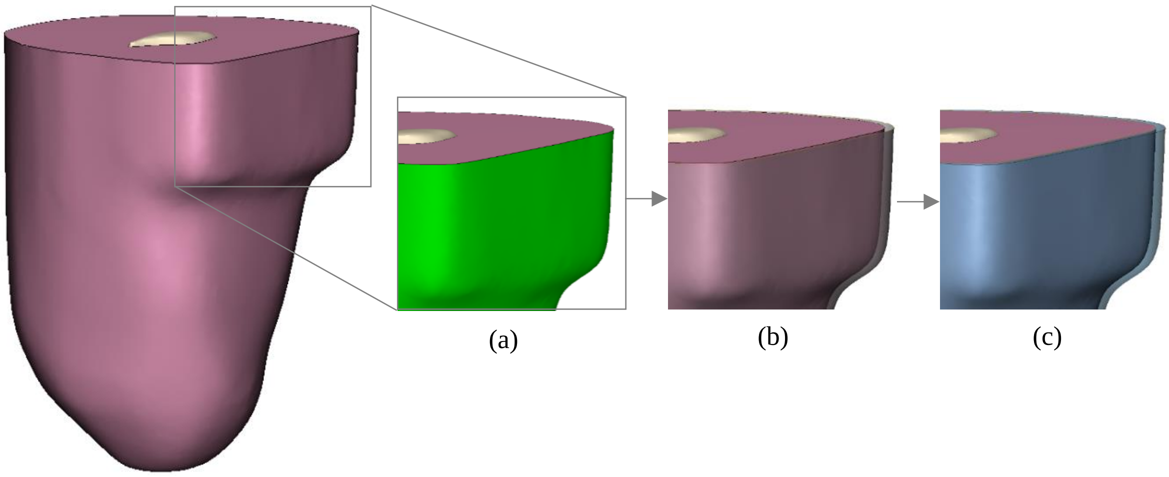

Figure 3-4: Process of creating a Boolean socket from the outer surface of the soft tissue; (a) highlights the external soft tissue surface, (b) which is duplicated and scaled (c) and then filled to create the additional part.

3.2.3 Meshing

Due to the complexity of the 3D geometry taken from the CT scans, 4-node Tetrahedral (Tet4) elements (C3D4) were used to mesh all parts. The meshing was performed using the adaptive meshing tool within 3-Matic version 11.0©. Hybrid elements C3D4H in ABAQUS CAE

2017® were assigned to the soft tissue to accommodate the use of hyperelastic material properties.

The adaptive meshing allows user control of the maximum and minimum triangle edge length. This technique is useful when meshing a small wall thickness or large planar areas; it allows smaller triangles to be allocated to thin parts (e.g. prosthetic socket/liner) and connecting interfaces whilst larger triangles to a bulk region to reduce the total number of elements. Adaptive Meshing was carried out with all model parts within a Non-Manifold Assembly (NMA). The NMA method creates matching surfaces between parts, removing gaps and overlap between parts and enforcing the same mesh size and node location at intersecting part connections (see Figure 3-5). This allows for easier computation with FEA at tied interfaces.

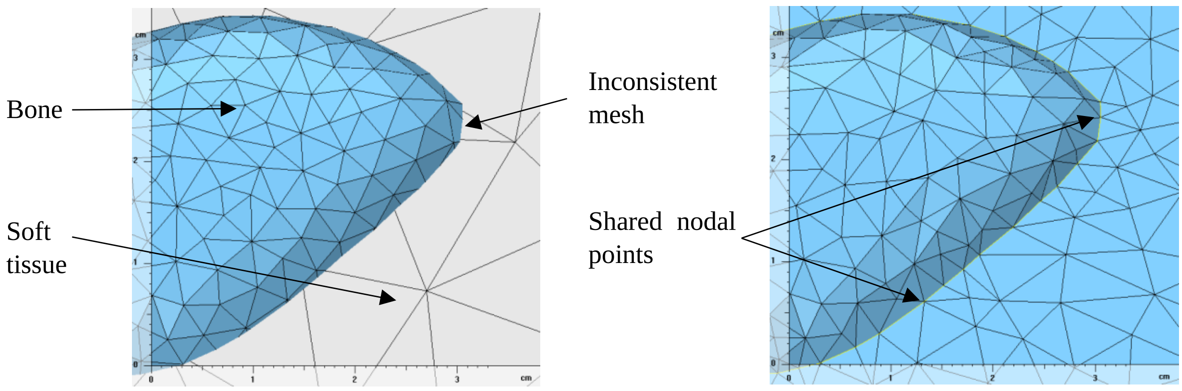

(a) (b)

Figure 3-5: (a) Meshing of separate parts (b) parts combined to a Non-Manifold Assembly and meshed within 3-Matic.

To ensure accurate results were achieved by the FE models, both aspects of good element shape measure and sufficient mesh density are required (Javidinejad 2012). To achieve an efficient shape measure of the elements, adaptive meshing was assessed by the shape measure of Height to Base (N). This parameter defines the quality of the triangles produced, with a value of 1.0 being a perfect equilateral triangle. A minimum shape measure threshold of 0.4 was enforced throughout surface and volume meshing to ensure accurate elements whilst avoiding extensive computational time. Therefore, only triangles with a shape measure (quality) higher than this were created during meshing. To limit the amount a re-meshed entity could deviate from the geometry of the original part in the meshing process, a maximum geometrical error value of 5% was enforced through-out the mesh process.

To ensure accurate elements and FEA output, the efficient shape measures stated above were used in combination with convergence testing (see Section 3.2.4), with the inference being the convergence testing determined a sufficient mesh density was mapped over the parts to produce valid outputs.

It should be acknowledged for the thin prosthetic liner part; the finite element solution was initially erroneous. This error occurred due to the standard Tet4 elements not accurately approximating the stresses and strains associated with bending. This artefact is known as "shear locking" as the elements report unphysical strains when examined (Bower 2009). This artefact can be simply solved by refining the mesh and avoided by using a sufficient mesh number. As a result of preliminary modelling, a minimum of three elements across the width of the liner part was found to eliminate the shear locking during preliminary modelling and was subsequently enforced throughout. It should be noted that the higher order 10-node Tetrahedral elements were considered for the liner part to eliminate the potential for shear locking (Li et al. 2019), however the higher order elements produced a negligible output change but at the cost of significantly increased computational solving time.

3.2.4 Convergence Testing

Prior to performing any critical analysis of the FE models of each participant, the FE models from each participants CT scans were verified by mesh convergence testing. The convergence testing was performed on the individual parts assembled as a residual limb model.

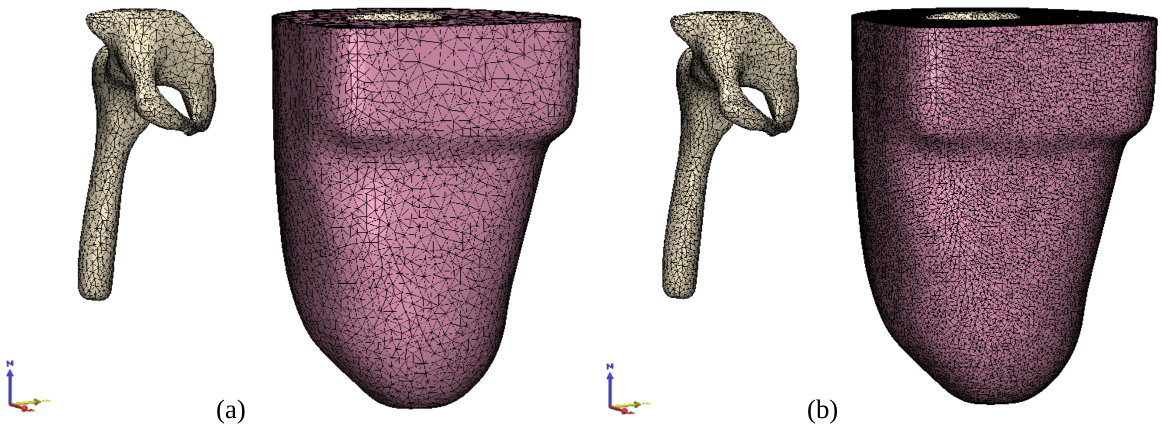

(a) (b)

Figure 3-6: Participant 1 bone and soft tissue part with a coarse mesh (a) and a dense mesh (b).

Various mesh densities of the residual limb models were obtained by adjusting the adaptive meshing parameters within 3-Matic. Two types of mesh refinement were used: global adaptive refinement and local adaptive refinement. Increasing the order of elements used (from Tet4 to Tet10) was not considered for the mesh convergence tests as it produced an unwarranted increase to the solving time. The highest and lowest possible element edge lengths used for the convergence test ranged between 30mm and 1mm, respectively. The shorter the edge length used, the denser the resulting mesh (Figure 3-6). Smaller element edge lengths were enforced at the part interfaces as these were shown to have been the location of previously reported peak stresses (see Table 2-1). For each of these meshes the quality parameters defined in Section 3.2.3 were enforced. The boundary conditions and loads applied during the convergence testing are described in Section 3.2.7.

Contact pressure at the soft tissue–prosthetic socket interface was chosen as the convergence test measure due to the prevalence of reporting this in previous studies and its importance in soft tissue damage (see Section 2.1). The peak deformation of the models was also considered but was not found to be as susceptible to the mesh changes as the contact pressure. The mesh density was increased for each model until less than a 3% percentage change in peak contact pressure at the soft tissue and prosthetic socket interface was measured. Increasing the mesh density further did not alter the contact pressure output significantly but did require a significantly greater computational cost and solving duration. Therefore, in the convergence test data show in Figure 3-7 and Table 3-2, the mesh with 428,008 elements was chosen.

The mesh convergence results for the models used in this study can be found in Appendix Chapter 3 Supporting Evidence.

Table 3-2: Example convergence results for P2 Pelvic model.

Number of Elements	Contact Pressure (kPa)	Percentage Change (%)	Solving Duration (h)
64,262	308.0	-	4.0
95,414	289.8	5.9	7.0
169,921	269.0	7.2	9.0
345,167	260.3	3.2	17.0
428,008	255.6	1.8	23.0
700,898	257.6	0.8	47.0

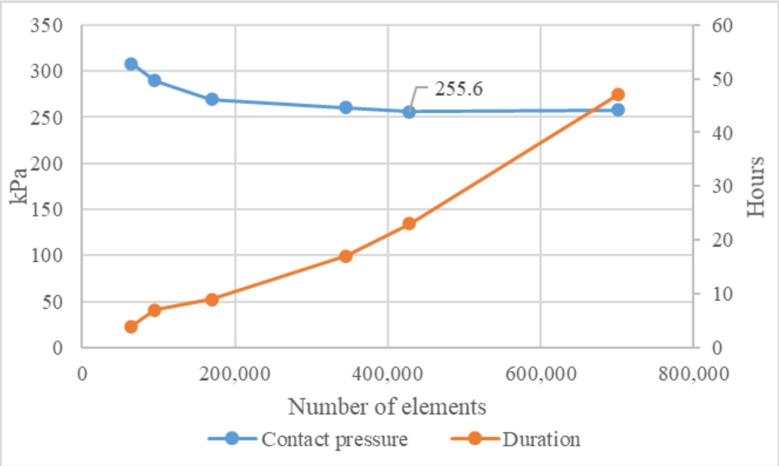

Figure 3-7: Convergence results for P2 Pelvic model with convergence result annotated.

Additionally, it should be noted that throughout the simulations of this work the simulation step size increments were controlled to aid in the simulation convergence. The maximum step size was limited to 5% of the total step duration. Smaller step sizes greatly increased the levels of convergence for all simulations, however this also required substantially greater computational solving time. To that end, smaller step sizes below 2% of the total step duration were applied to aid in convergence were required.

3.2.5 Model Dimensions

The residual limb models were created from three participants. The dimensions of each participant's residuum differed from one another. The dimensions of the residuum can alter the prosthesis design, recommendations, and individual's comfort. The dimensions of the participant's residual limb are shown in Table 3-3, these measurements were taken from the residuum models within 3-Matic. The residuum length (RL) was measured from the proximal region of the greater trochanter to distal part of the residuum. The femoral length (FL) was measured from the greater trochanter to the distal most part of the residual femur. The bone to soft tissue (BS) distance was measured as the distance between the distal most part of the residual femur and the residual limb. These measurements were taken in respect to the z axis (vertical) in the coronal plane (see Figure 3-8) without consideration to the x and y components.

Table 3-3 Residuum dimensions for each participant.

Attributes (mm)	P1	P2	P3
Amputation side	R	L	R
Residuum length (RL)	270.3	240.2	330.5
Femoral length (FL)	214.2	210.3	279.7
Bone to soft tissue (BS)	56.1	29.9	50.8

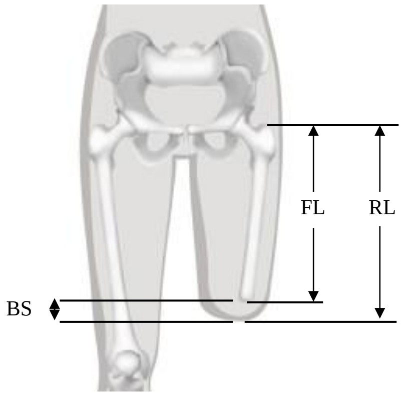

Figure 3-8 Residual limb measurements (Schematic adapted from Ottobock.co.uk 2015)

The prosthetic socket was given a global thickness of 10mm through the entirety of this study (Ottobock 2015). This thickness was chosen as it was within the thickness range for general prosthetic sockets (Ng et al. 2002). The thickness of the prosthetic liner was a variable in part of this study. Therefore, the value used ranged from 4mm to 6mm in thickness, however the exact thickness will be stated in the relevant section. The liner thicknesses were chosen from the actual thicknesses for trans-femoral use (Sanders et al. 1998, Sanders et al. 2004, Ossur 2011, Ottobock 2015, WillowWood, 2018). The inner surface of the prosthetic liner was continuously modelled as a 'Boolean fit' to the outer surface of the soft tissue to replicate the exact fit that the user would experience.

3.2.6 Material Properties

The material properties of the residual limb model will be detailed in this section. Should the material properties applied to a model differ from those mentioned here, it will be stated in the relevant section.

The mechanical properties of the bone, prosthetic liner and prosthetic socket were assumed to be linear elastic, isotropic and homogeneous and within the common values previously reported (Lee et al. 2004; Duchemin et al. 2008). The soft tissues of the residual limb demonstrate a complex biomechanical nature. Previously, the tissues have most commonly been modelled using linear elastic properties, however this does not accurately accomodate for the large deformation that occurs from ambulatory loads. Since the late 2000's hyperelastic models have been used to simulate the soft tissues (see Table 2-1), of which Mooney-Rivlin has been the most commonly adopted (Portnoy et al. 2008; Portnoy et al. 2009; Lacroix and Patino 2011; Restrepo et al. 2014; Zhang et al. 2013). Continued use of the same tissue model enables more clarity for inter-study comparisons to be made. The soft tissues during this study have been defined using the Extended Mooney-Rivlin strain energy function in the equation:

$$W = C_{10}(I_1 - 3) + C_{11}(I_1 - 3)(I_2 - 3) + \frac{1}{D_1}(J - 1)^2$$

where the invariants of the principal stretch ratios are $I_1 = \lambda_1^2 + \lambda_2^2 + \lambda_3^2$ and $I_2 = \lambda_1^{-2} + \lambda_2^{-2} + \lambda_3^{-2}$, the relative volume change is $J = \lambda_1\lambda_2\lambda_3$, and C_{10}, C_{11}, D_1 are the constitutive parameters. The constitutive parameters input to the above state equation will be stated in the relevant section. This equation is considered to be an accurate model for defining soft tissue characteristics (Dickinson et al. 2017). The soft tissue equivalent modulus for the constitutive parameters can be calculated by equations derived from the above calculation:

$$C_{10} = \frac{E}{4(1 + v)}$$

$$D_1 = \frac{6(1 - 2v)}{E}$$

where E and v are the elastic modulus and Poisson's ratio, and C_{10} and D_1 are constitutive parameters taken from the Extended Mooney-Rivlin strain energy function (see Table 3-4). Hybrid element types (C3D4H in ABAQUS CAE 2017®) were assigned to the soft tissue to accommodate the use of hyperelastic material properties. The common material properties used in this study for bone, soft tissue, liner and socket are shown in Table 3-4. These were determined from the material properties highlighted in the literature review and those used in previous studies (see Table 2-1).

Table 3-4: Material properties for all parts used in the bone geometry simulations.

Part	**Young's Modulus (MPa)**	**Poisson's Ratio**
Bone	15000	0.3
Liner	0.4	0.4
Socket	1500	0.3
Soft Tissue	C_{10} = 4.25 kPa, C_{11} = 0 kPa, D_1 = 2.36 MPa	

3.2.7 Boundary Conditions and Loads

The boundary conditions were applied within the FEA software package ABAQUS CAE 2017®. The boundary conditions chosen to apply interactions, constraints and loads to the models are detailed here. This is a general synopsis of the models, should a model have different boundary conditions than mentioned in this section it will be stated in the relevant section.

The bone and soft tissue interface were modelled as tied, simulating absolute bonding between the two surfaces. For simulations without a liner; the soft tissue and prosthetic socket interface were modelled with surface to surface frictional contact, preventing the nodes of the slave surface in the contact pair penetrating the master surface requiring the penetrating slave nodes to be moved to their corresponding tangent planes of the master surface. The outer soft tissue surface was identified as the slave surface whilst the inner prosthetic socket surface was identified as the master surface. For simulations with a liner, the soft tissue-liner and liner-socket interfaces were modelled with surface to surface frictional contact. The selected slave surfaces were the soft tissue (residuum) for the soft tissue-liner interaction, and liner for the liner-socket interaction.

A friction coefficient value can be assigned to this contact interface which controls the amount of relative movement between surfaces via the Coulomb friction model. The Coulomb friction model within ABAQUS assumes that surfaces will be considered as ‘slipping’ if the equivalent frictional stress, τ_{eq}, is equal or greater than the critical shear stress, τ_{crit},($\tau_{crit} = \mu p$):

$$\tau_{eq} = \sqrt{\tau_1^2 + \tau_2^2}$$

where τ_1 and τ_2 are orthogonal shear stresses on the contact surface, μ is the friction coefficient and p is the contact pressure. However, if $\tau_{eq} < \tau_{crit}$ no relative motion will occur, and the surfaces will be considered as ‘sticking’.

The finite element simulations were carried out in two phases. The initial phase was to simulate the pre-stresses that occur from donning the prosthetic socket onto the residuum, with the subsequent phase simulating ambulation (see Figure 3-9). Two methods were used to investigate the donning aspect:

a) For simulations where the socket and soft tissue shared the same geometry, a 50N axial force was applied to the proximal region of the bone (Lee et al. 2000; Zhang et al. 2013; Arotaritei et al. 2015). During this axial load, the movement of the socket was constrained fully. This loading was applied simply to stabilise the already perfectly fitting residuum within the prosthetic socket.
b) For simulations where there was overlap between the socket and soft tissue, otherwise known as socket rectification, a push fit was used. This involved the socket and residuum being separated during the initial step. A vertical displacement was then applied to the socket to move in into full contact with the residuum. During this solution, the constraints applied to the bone differed between non-pelvic and pelvic models. For the non-pelvic models, the femoral head was fully constrained, whereas in the pelvic models the proximal region of hemipelvis (ilium) was fully constrained.

During both donning simulation methods, the master-slave contact algorithm within ABAQUS was enforced. Therefore, stresses were developed on both the master and slave surfaces at points of overlapping.

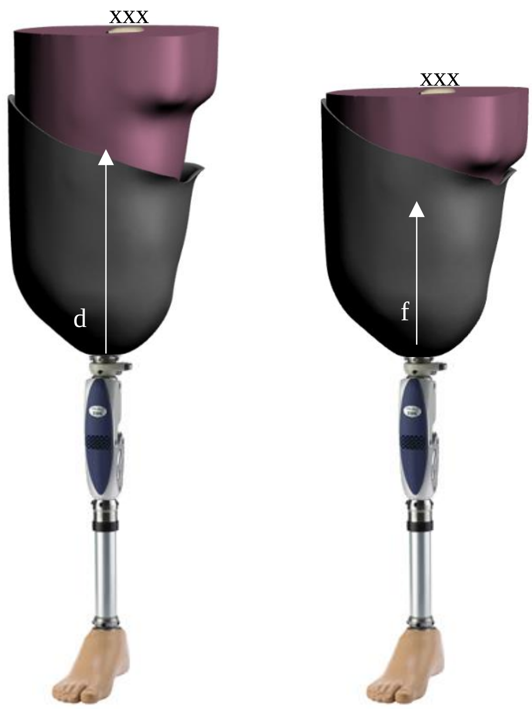

Figure 3-9: Boundary conditions for the two phases within FE analysis are shown here. The socket is donned over the residual limb by a displacement (d) in the initial phase (left). In the second phase (right) an upward GRF (f) is applied to the socket. Constraints are indicated by 'xxx' (image adapted from Ottobock.co.uk 2015)

The resultant stresses and deformation from the initial phase were retained in the second phase used to simulate the peak ground reaction forces (GRFs) during the gait cycle. Throughout the gait cycle the most significant GRF is the vertical component, which peaks during either heel strike and toe off occurring at approximately 20% and 75% stance (see Figure 3-10). As a result, the second phase of the simulation applied a vertical load to the distal end of the socket. The magnitude of this load was selected to be the equivalent of 110% of each participant's bodyweight. This load corresponds to the peak GRF reported for normal ambulation of prosthetic limb users (Vanicek et al. 2009). This corresponds to loads of 755N, 853N and 799N for participants 1, 2 and 3 respectively (see Table 3-1). During this phase, the proximal region of the bone was constrained preventing movement. The movement of the pelvis in relation to the femur was not simulated as the femur and hemipelvis were modelled together.

During the stance phase of the gait cycle, there are also forces applied in the transverse plane; anterior-posterior and medial-later (see Figure 3-10), additionally moments joint moments are created around the ankle, knee and hip joints. However, all the GRFs during the gait cycle do not peak simultaneously. At both heel strike and during bipedal stance, the moment of the hip joint is not significant, a greater hip joint moment only occurs during toe off when the stance phase leg is in flexion (Dijkstra and Gutierez-Farewik 2015). Additionally, the gait pattern has been shown to vary widely between trans-femoral amputees due to adaptions to their gait patterns to accommodate walking with the prosthesis (Wentink et al. 2013). As a result, the peak vertical GRF was chosen to be simulated, the forces in the transverse plane and joint moments were not included in the second phase of simulating the loading. This simplification was made due to the assumption the greatest stresses and strains produced on the residual limb, and therefore highest potential to cause tissue damage, throughout the gait cycle would occur from the vertical loading and further loading would significantly increase the required computational capacity.

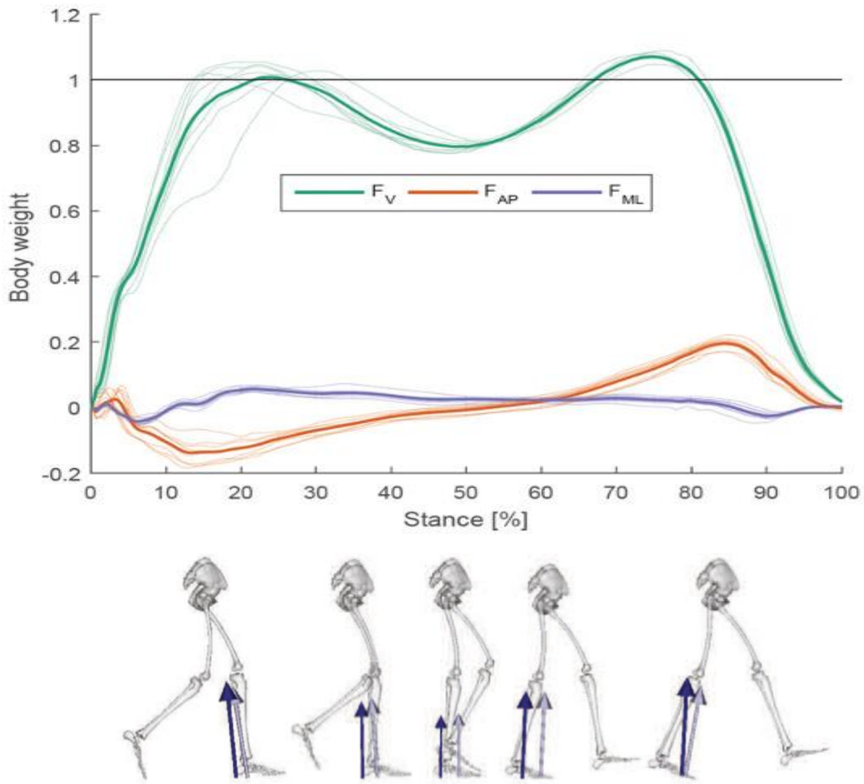

Figure 3-10: Ground reaction forces during the cycle normalised to bodyweight as reported by Dijkstra and Gutierez-Farewik (2015)

3.3 Preliminary Modelling Results

Anticipating the required complexity of the FE models displayed in this chapter, preliminary work was performed to ensure that a successful working process and desired application within ABAQUS could be achieved. The simplistic geometry for the preliminary modelling was created within SolidEdge© and imported to ABAQUS by .step files. The model dimensions were roughly matched to those taken from the CT scan of the residual limb for participant 1 (see Table 3-3). The model consisted of a straight cylinder to represent the bone, a conical shape tapered to the distal end to represent the soft tissues, a Boolean fitting external liner and a socket with a 1mm overlap between the internal socket surface and external liner surface (see Figure 3-11). Meshing was performed within Abaqus with Tet4 elements applied. A convergence test was performed for the preliminary model following guidelines in Section 3.2.3 to ascertain a suitable mesh size.

The preliminary modelling setup included a 1mm overlap between socket and liner. Two methods of solving this overlap during the donning procedure were simulated; an interference fit and a push-fit. After which a 400N axial load was used to simulate bipedal loading (Ramasamy et al. 2018; Jamaludin et al. 2019). The boundary conditions and loading applied to the models follow the guidelines shown in Section 3.2.7. The results of the donning comparison are shown in Figure 3-11 along with the resultant contact pressure from the bipedal loading phase.

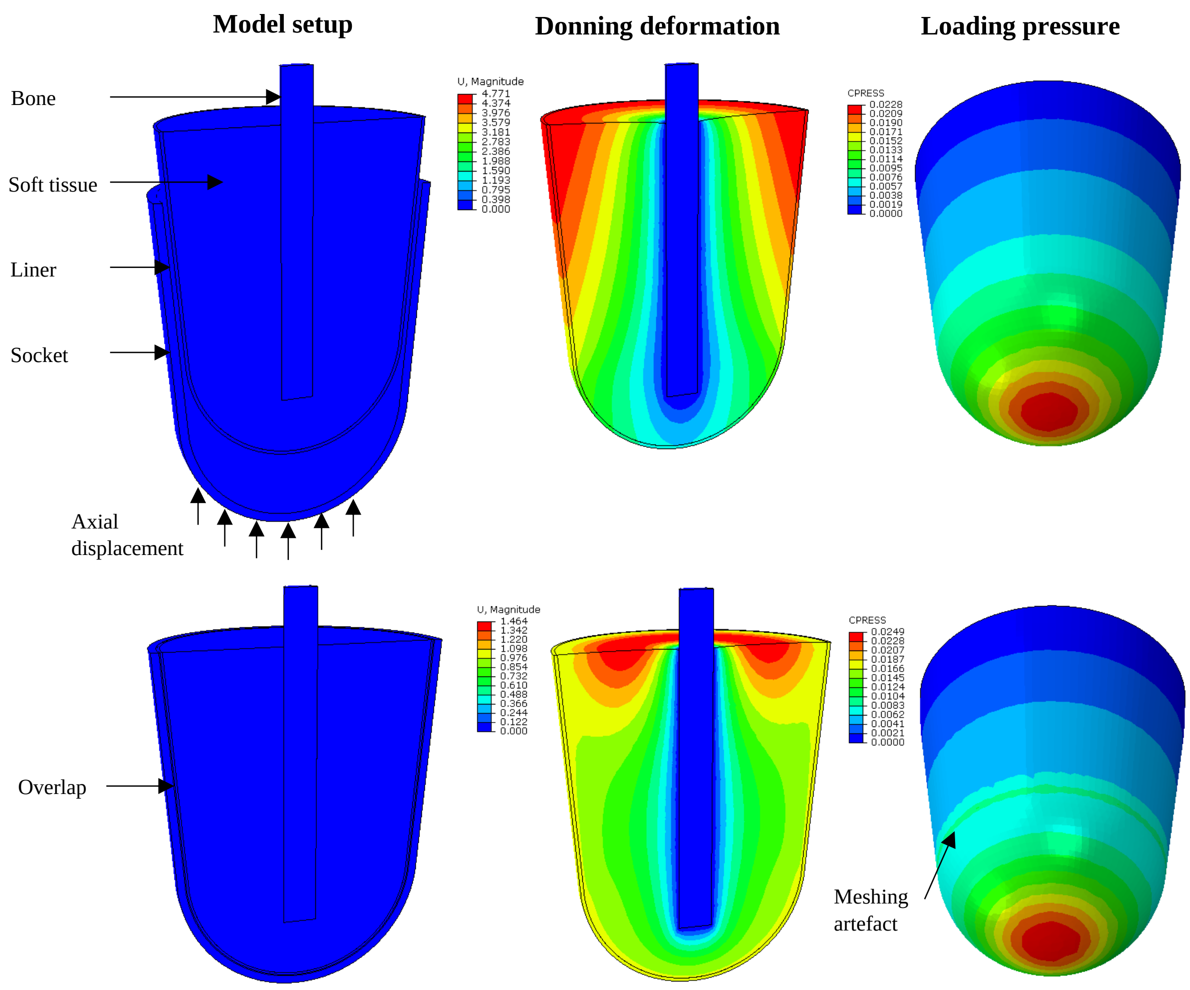

Figure 3-11: Preliminary 3D model donning and bipedal loading results.

The comparison of the donning simulations predicted a more realistic soft tissue deformation distribution occurring from a push fit method. For this method, there was an upward direction of deformation which is consistent with the ideology of pushing the residuum into a socket. The push fit method resulted in a higher maximal soft tissue deformation (4.8 mm) compared to the interference fit method (1.5 mm).

The deformation from the two donning process variations were carried over to a bipedal loading phase. The application of this loading resulted in similar peak pressures for both models being achieved at the distal end of the residuum, with 22.8 and 24.9 kPa for the push fit and interference donning models respectively (see Figure 3-11). The bipedal loading of the interference donning model showed an artefact of concentrated pressure around the lower part of the residuum above the distal end. This was believed to be an artefact caused by insufficient mesh sizing. Overall, even with the use of simplistic geometry the variations of donning simulation did cause variation in the outputs, with the push fit method being the more desirable method of simulation when there is overlap between the socket and liner parts.

The true geometry of a residual limb is complex and specific to the individual, therefore the predicted results from the preliminary models cannot be used directly due to the simplistic geometry used. However, the results of the preliminary modelling did provide an insight into the workflow and capabilities of the FE software which were required for later studies.

4. THE IMPORTANCE OF THE PELVIC BONE

4.1 Introduction

In this chapter, the effect of including the pelvic bone in the modelling process of the residual limb will be examined. This will be achieved by producing trans-femoral residuum FE models which do and do not include the pelvic region on the side of amputation. The effect of the pelvic bone will be evaluated by considering the stress-strain state on the residuum and at the soft tissue and prosthetic socket interface.

Previous studies have demonstrated the feasibility and reliability of using a FEA feedback method in simplifying the socket design process (Torres-Moreno et al. 1990; Colombo et al. 2010; Morotti et al. 2014). These studies concluded that correct and detailed geometry of the residuum was crucial to produce an effective prosthetic socket. However, given these advancements, currently all previous FEA studies of the trans-femoral residuum, have modelled the bony geometry of the residuum as only the femur without including the pelvis (Zhang and Mak, 1996; Lacroix and Patino, 2011; Ramirez and Velez, 2012; Zhang et al. 2013; Restrepo et al. 2014; Velez Zea et al. 2015; Morotti et al. 2015; Ramasamy et al. 2018) as shown in Figure 4-1.

However, the common concepts of weight bearing within a trans-femoral prosthetic socket involve providing a support beneath the ischium (see Figure 2-3) resulting in loading of the ischium support region. This ischial support region (ischial bearing) is classified as the use of a relatively horizontal surface directly inferior to the ischial tuberosity of the pelvis to provide the support of upwardly vertical forces from loading (Schuh and Pritham, 1999; Pritham, 1990) (see Section 2.4). The ischial tuberosity is the primary load bearing site, and the pelvic region is therefore integral in the design of trans-femoral prosthetic sockets and crucial to include in FE model of the trans-femoral residual limb.

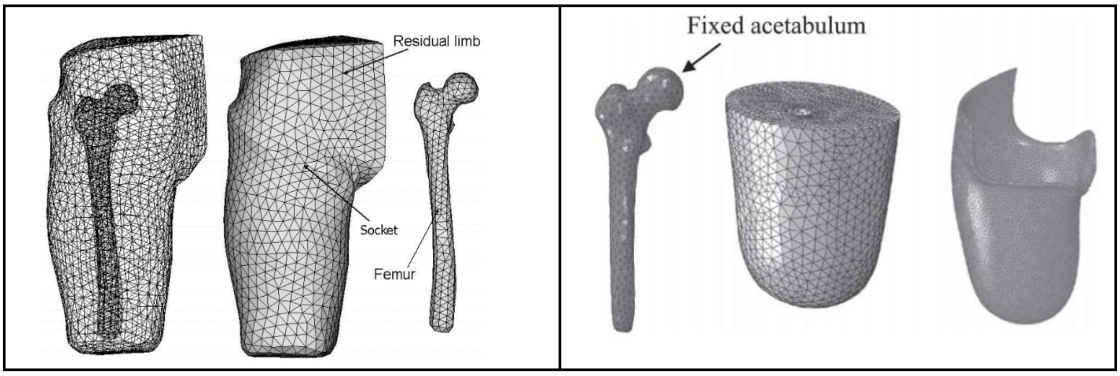

Figure 4-1: FEA components in previous FEA studies (left: Zhang et al. 2013) (right: Ramirez and Velez 2012) without the pelvic bone.

The objective of this chapter was to examine the effect the pelvic bone region has on the stresses experienced by the trans-femoral residuum. This was achieved using FE models to replicate the loading situation on the trans-femoral residuum. The initial methodology, results and discussions of this chapter are presented with idealised prosthetic socket geometry (see

Section 4.2). Subsequent methodology changes were applied to create and implement a realistic socket geometry, along with corrected results and discussion (see Section 4.5) for this new socket geometry.

4.2 Initial Modelling Method

For this chapter, two different residual limb models were created for each participant. The model acquisition and reconstruction of the three participant CT scans was performed using the methods detailed in Chapter 3.

The models constructed only differed by their bone geometry; (i) bone geometry modelled with only the residual femur shaft and femoral head (non-pelvic model) and (ii) bone geometry modelled with residual femur (shaft and head) and pelvis as a single unit (pelvic model). The pelvic bone geometry was chosen as the hemipelvis on the side of amputation and included the ischium, pubis, and acetabulum due to their involvement in loading support within trans-femoral prosthetic sockets. Differences have been shown to occur when modelling the hemipelvis compared to the entire pelvis. With the constraints applied in place of the pubic symphysis leading to an underestimation of bone displacement (Watson et al. 2017). Nonetheless, focus was to be applied to the residual limb-socket interface and hence modelling the entire pelvis would not have enhanced the model outputs but would have increased the computational time. To simplify the unity of femur and pelvis, the intermediary tissues within the acetabulum such as the acetabular fossa fat and connecting ligaments were considered to be bone (see Figure 4-2). Thus, the rotation of the pelvis in relation to the femur was not modelled. Two model types were created for each participant: non-pelvic and pelvic. A total of six models were created, the two model types for participant 3 are shown in Figure 4-3. The model creation process of the residual limb models used within this chapter are detailed within Chapter 3.

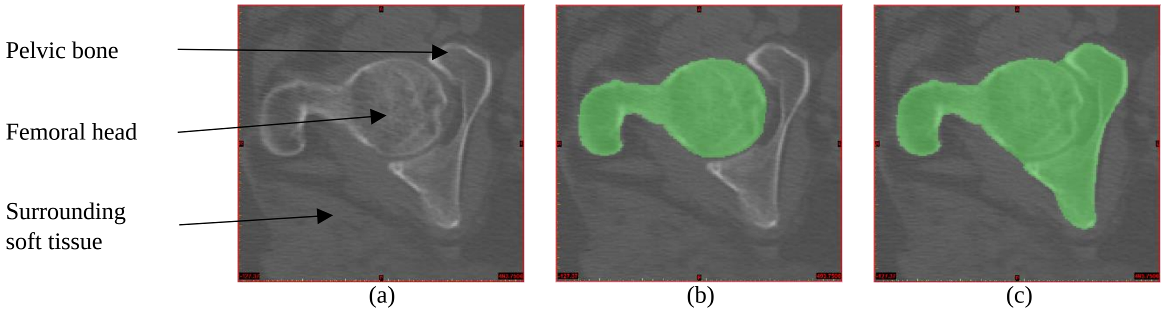

Figure 4-2: The modelling process showing the bone in situ (a), the bone geometry for the non-pelvic model (b) and the bone geometry for the pelvic model (c).

4.2.1 Convergence Testing

The FE models were verified by mesh convergence testing method as discussed in Section 3.2.4. The resulting approximate element size was 4mm for the soft tissue and 2mm for the bone and the socket. The mesh convergence results for the models used in this study can be found in Appendix Chapter 3 Supporting Evidence.

The average run time for the models was approximately 28 hours, using a Quad Core CPU i5-4590, 3.30 GHz and 8.0 GB RAM computer.

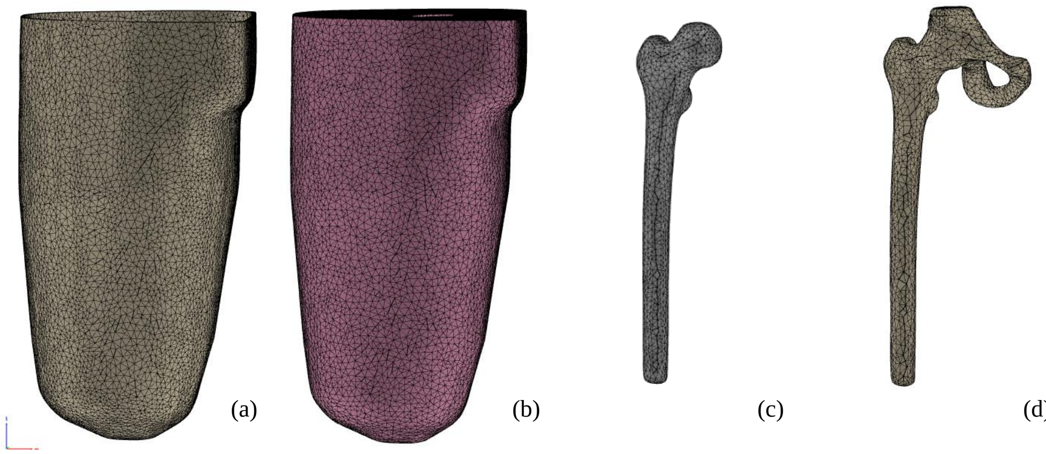

Figure 4-3: Finite element mesh of the prosthetic socket (a), soft tissue (b) and bone parts for the non-pelvic model (c) and the pelvic model (d) for participant 3.

4.2.2 Material Properties

The mechanical properties of the bone and socket were assumed to be linear elastic, isotropic and homogeneous. The soft tissues were defined using the Extended Mooney-Rivlin strain energy function with added compressibility. The material properties used in this chapter do not differ to those presented in Section 3.2.6.

4.2.3 Boundary Conditions and Loads

The boundary conditions and loading applied to these models follow the details outlined in Section 3.2.7. A friction coefficient of 0.45 was assigned to the soft tissue-socket interaction, this value was achieved between skin and polypropylene prosthetic socket material without the presence of sweat and skin hair at the interface (Ramirez et al. 2015). For the pelvic models, no movement of the pelvis in relation to the femur was included.

4.3 Results

The maximal stresses produced in the donning phase are shown in Table 4-1. For all participants and models, including the pelvic bone resulted in higher maximal shear stresses. The maximal contact pressure was higher in the pelvic models for participants 1 & 3, whilst it was greater in the non-pelvic model for participant 2.

Table 4-1: Maximal stresses for non-pelvic and pelvic models at the soft tissue-socket interface from donning phase.

Participant and Model		**Contact pressure (kPa)**	**Circumferential shear (kPa)**	**Longitudinal shear (kPa)**
Participant 1	Non-pelvic	5.2	1.1	1.1
	Pelvic	6.5	1.9	1.8
Participant 2	Non-pelvic	7.3	1.2	1.1
	Pelvic	5.9	1.8	1.4
Participant 3	Non-pelvic	3.5	0.4	0.5
	Pelvic	5.5	2.0	1.6

Table 4-2: Maximal stresses at the soft tissue-socket interface for non-pelvic and pelvic models from walking loads.

Participant and Model		**Contact pressure (kPa)**	**Circumferential shear (kPa)**	**Longitudinal shear (kPa)**
Participant 1	Non-pelvic	83.3	30.8	27.9
	Pelvic	330.2	91.3	57.4
Participant 2	Non-pelvic	141.8	30.6	39.3
	Pelvic	255.6	73.3	48.1
Participant 3	Non-pelvic	94.9	20.9	32.8
	Pelvic	364.4	78.1	38.9

The maximal normal stress (contact pressure) and shear stress values from application of 110% bodyweight for all participants, are shown in Table 4-2 for the non-pelvic and pelvic models respectively. The location of the maximal stresses for both phases were found distally for all non-pelvic models and underneath the ischial support for all pelvic models. The maximum stresses resulting from full loading were greater in the pelvic models compared to the non-pelvic models for all participants (see Table 4-2).

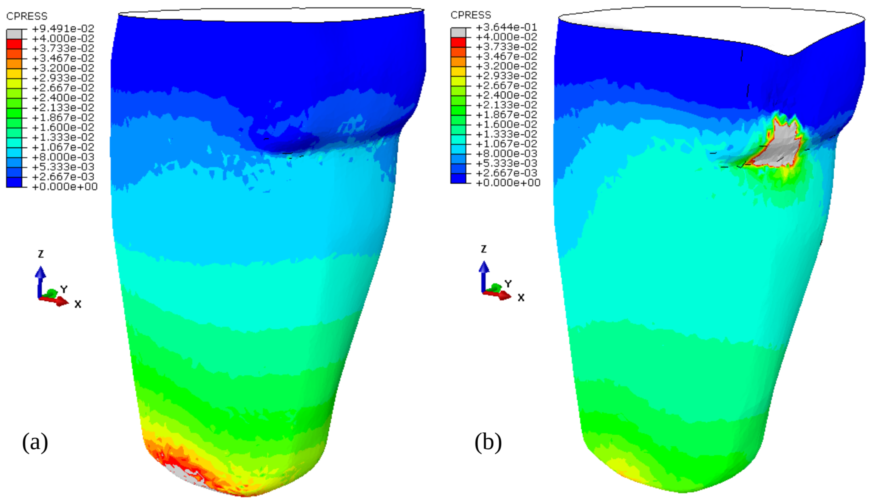

Figure 4-4: Contact pressure distribution for non-pelvic (a) and pelvic (b) models of participant 3.

The peak tensile (maximum) and compressive (minimum) principal logarithmic strain is shown in Table 4-3. The peak strains were located at the bone-soft tissue interface, at the distal end of the residual femur for the non-pelvic models and beneath the ischial region of the pelvic bone for the pelvic models.

Table 4-3: Peak tensile (maximum) and compressive (minimum) principal logarithmic strain.

Participant and Model		Tensile (%)	Compressive (%)
Participant 1	Non-pelvic	88.9	132.5
	Pelvic	160.0	325.1
Participant 2	Non-pelvic	118.3	150.7
	Pelvic	170.3	323.4
Participant 3	Non-pelvic	97.6	130.5
	Pelvic	168.7	306.4

4.4 Discussion

The results achieved by the non-pelvic models had similar peak pressures and distributions to previous studies that had not applied boundary conditions to the top surface of the soft tissues (see Figure 2-10). Whereas, the resulting peak contact pressure and strains values for the pelvic models achieved in the previous results section were much greater than expected, especially in comparison to previous studies transducer studies (see Table 2-2). It was hypothesised that the high concentrations of contact pressure and strain in the pelvic models were caused by the Boolean fit of the prosthetic socket part around the ischial tuberosity. The absolute fit of the socket provided direct load bearing and no relief between socket and the ischial support area. A midplane thickness analysis performed in 3matic (see Figure 4-5), reporting the soft tissue thickness between bone and socket, shows the soft tissue around the pelvis was less than 15mm in some areas.

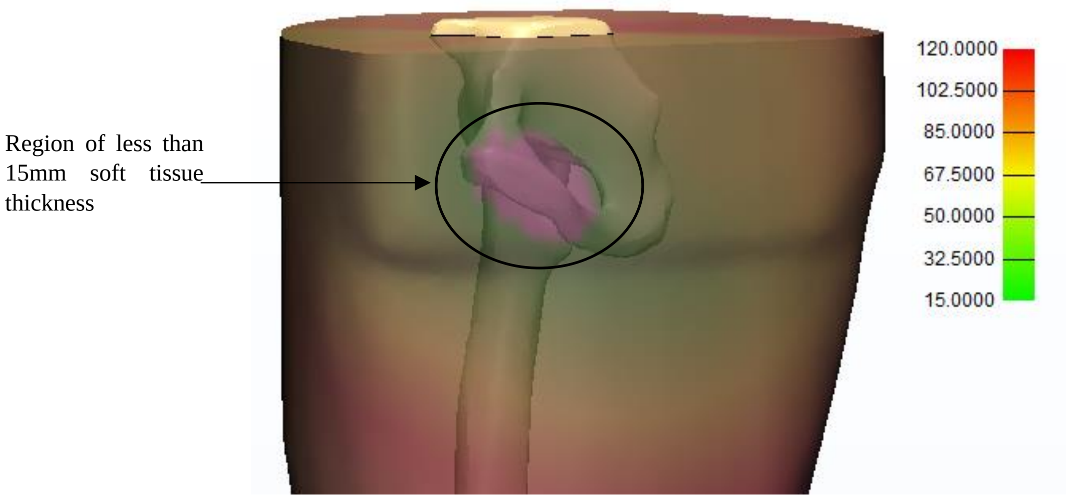

Figure 4-5: Soft tissue thickness around the ischial tuberosity shown by midplane thickness analysis for participant 3.

Generally, it is common practice in a clinical setting to modify a prosthetic socket to encourage pressure at pressure tolerant regions whilst reducing pressure at sensitive regions. The proximal medial brim of the prosthetic socket is contoured to provide relief by not loading the adductor longus tendon and pubic ramus, which are not pressure tolerant whilst encouraging the loading of the ischium. The prosthetic socket used in Section 4.2 (see Figure 4-3) was not rectified, meaning the proximal brim of the socket was not contoured, and therefore not realistic when compared to subject specific prosthetic sockets. The lack of relief from the unaltered medial brim geometry resulted in abnormal prediction of stresses on the residuum and is the main limitation of the pelvic model results in Section 4.3. As a result, this was addressed in the following section.

4.5 Secondary Methodology Method

The results from the preliminary simulations reported in Section 4.3 highlight the socket geometry as a major limitation of the study. Therefore, this section considers the use of a prosthetic liner and a prosthetic socket with proximal brim geometry (both features common in practice) to reduce this limitation. Given the intimate fit reported for a liner (Ossur 2011), the internal surface of the liner was assumed to match the external surface of the soft tissue. The liner was generated in 3Matic using the process described in Chapter 3, and was considered a ‘Boolean fit’. The liner was assigned a uniform thickness of 4mm.

The socket brim profile used to create the proximal brim geometry for each participant is shown in Figure 4-6. To ensure consistency and limit the potential for the large variations that may be introduced by using different socket geometries, the same socket brim profile was used to create the proximal brim socket geometry for all participants. For participant 2, the curve was mirrored along the sagittal plane to account for the change between residual limb sides.

The proximal brim geometry of the socket was designed as a ‘Hybrid’ form with elements of IC and Quad sockets, as detailed by Ottobock (2016). The specifications of the brim geometries were then based on the previous literatures (see Section 2.4), most notably Long (1985) and Schuch and Pritham (1990), and the best practice guidelines presented by the Steeper Group (2011) and Ottobock (2016). For this, the anterior wall of the socket was just inferior of the inguinal crease and was superior to the posterior wall. The peak of the lateral wall was set to be superior to the height of the greater trochanter. The brim of the posterior wall was an essentially flat ‘seat’, slightly inferior to the border of the ischial tuberosity. The brim of the medial wall was assigned a typical ‘v-shape’. The bottom of the ‘v’ was located at the point where the pubic ramus crosses the medial wall. There was 32.2 to 34.2mm between the bottom of the ‘v’ and the pelvic bone across all participants. The height of both the anterior and posterior sides of the medial wall was approximately 24mm higher than the bottom of the ‘v’(see Figure 4-6). This was to allow for adductus longus relief and to avoid painful contact with the ischial ramus.

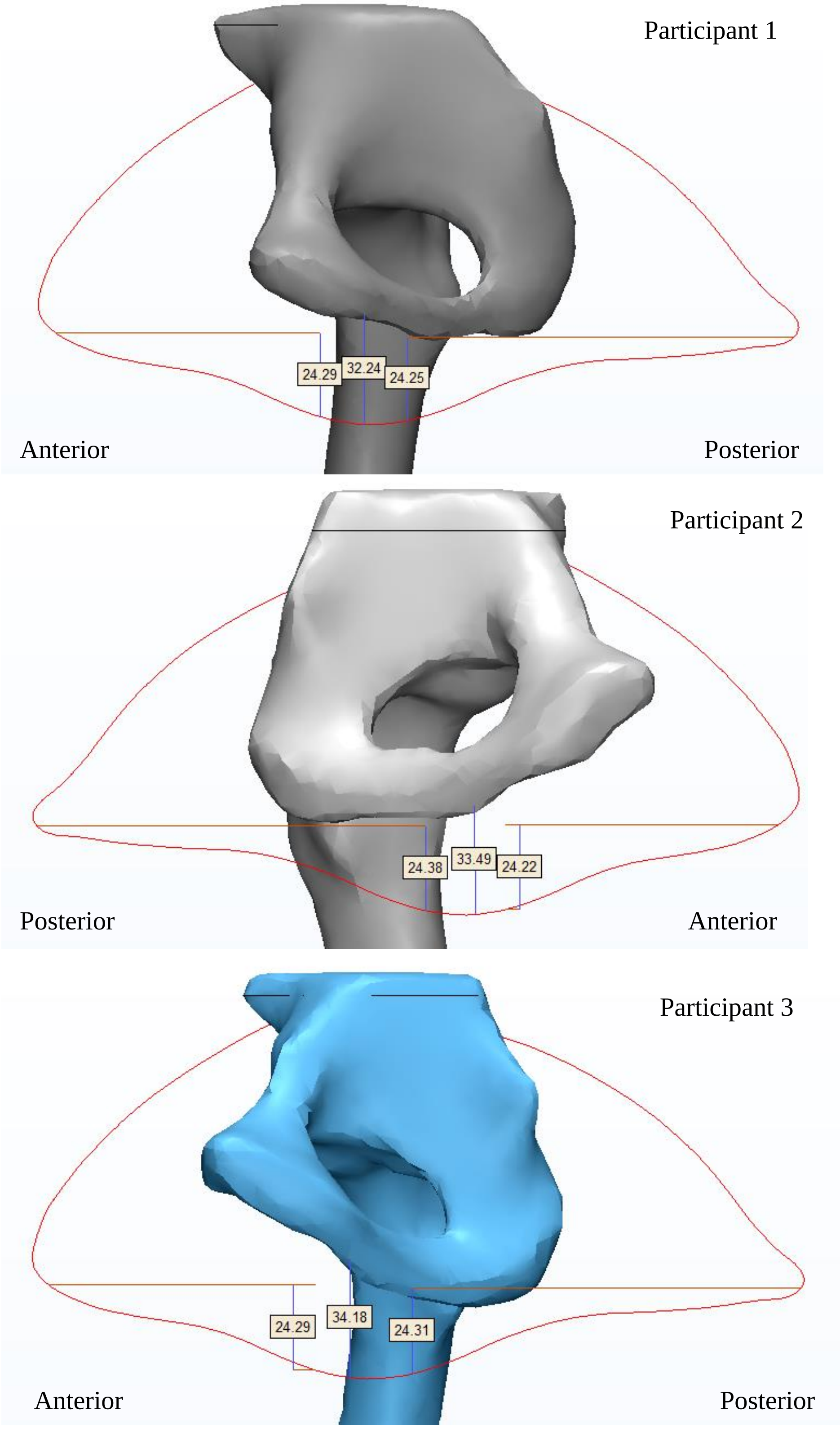

Figure 4-6: Proximal brim curves for each participant.

The process of socket creation is shown in Figure 4-7. For this, the outer surface of the liner was duplicated and the socket brim curve, with the previously mentioned specifications, was attached to the duplicated surface (a). The duplicated surface was cut using the curve and duplicated again. The second duplicated surface was scaled to provide the socket with an overall thickness of 10mm. The 'fill hole' function was applied to the two cut surfaces to create one solid part, resulting in the provisional socket (b). The inner edge of the rough socket was altered to make it more amenable to FEA (d, e, f & g) and more realistic. The inner edge of the socket brim was chamfered with an edge distance 4mm. The resulting two edges from chamfering were then smoothed with an influence distance of ± 1.5mm. This resulted in a curved inner edge of the socket brim (see Figure 4-7). Although the socket brim geometry was used in the socket creation, the remaining socket dimensions were not altered meaning the socket fit was a Boolean fit with close contact.

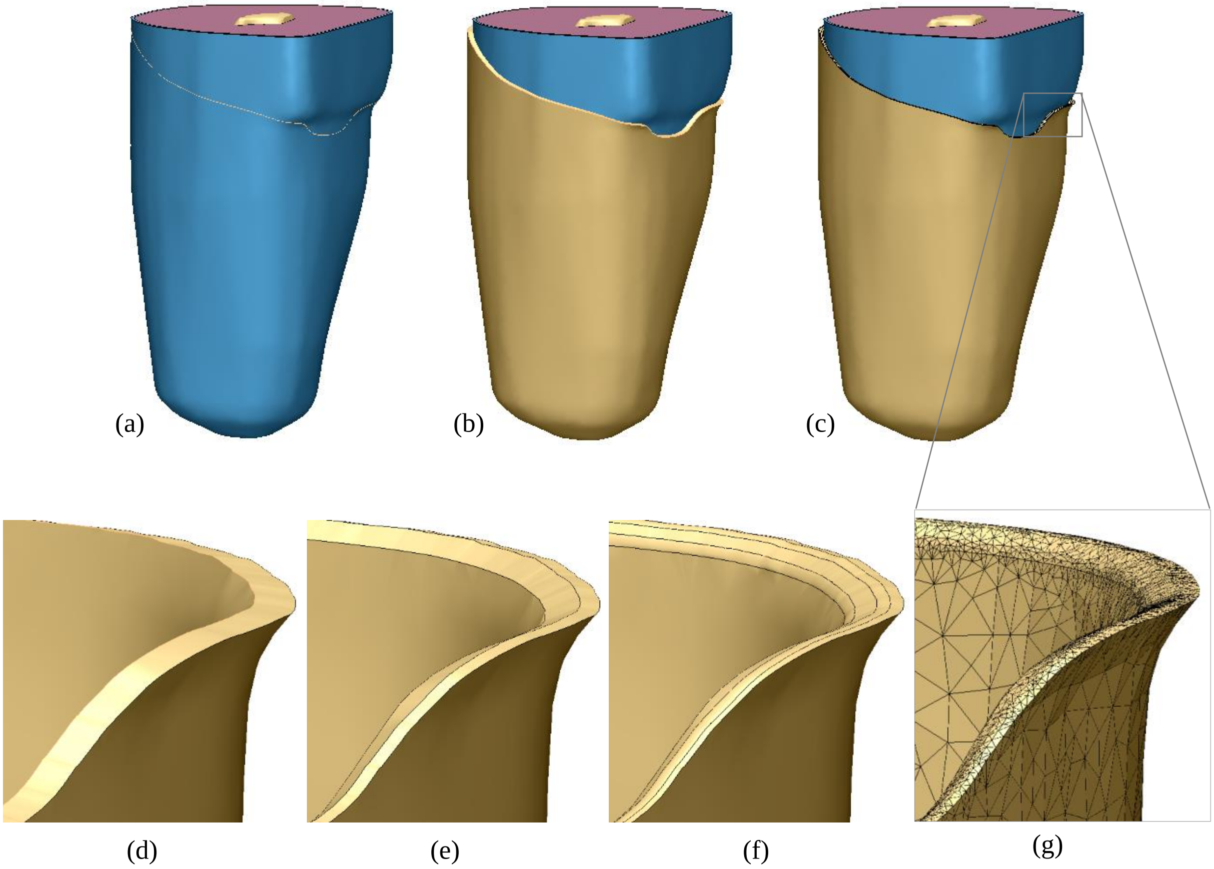

Figure 4-7: Socket geometry creation process; socket brim curve applied to outer liner surface (a), rough socket geometry (b), chamfered and smoothed socket geometry (c). Close ups showing; rough socket (d), chamfered socket (e), chamfered and smoothed socket (f) and meshed socket (g).

The new models consisted of; bone, soft tissue, prosthetic liner and prosthetic socket with proximal brim geometry (see Figure 4-8). A total of six models were created with two for each participant: (i) non-pelvic model and (ii) pelvic model. The components of the new models are shown in Figure 4-8 for participant 3 which are representative of the prosthetic socket design (see Figure 2-4 in Section 2.4).

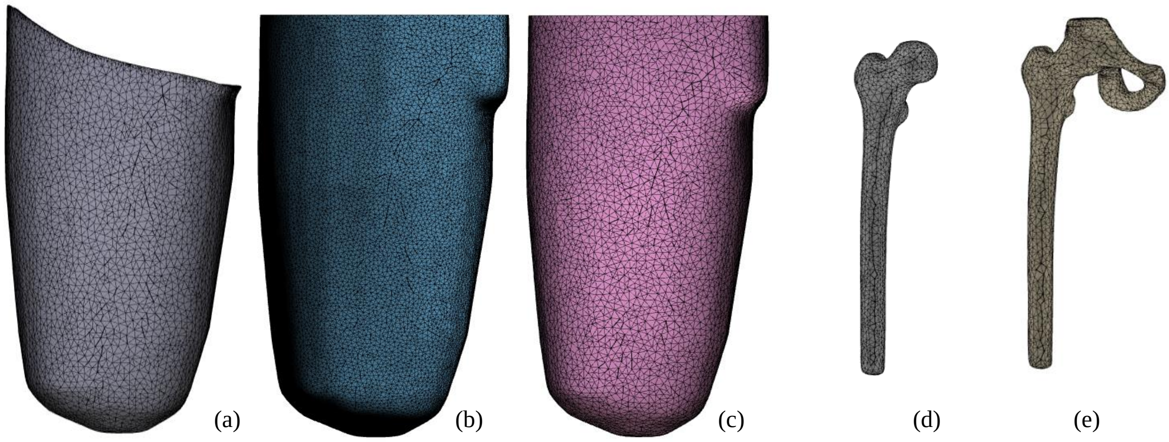

Figure 4-8: Finite element mesh of the prosthetic socket (a), prosthetic liner (b), soft tissue (c) and bone parts for the non-pelvic model (d) and the pelvic model (e).

4.5.1 Convergence Testing

The FE models were verified using the mesh convergence testing method discussed in Section 3.2.4. The resulting approximate element size was 4mm for the soft tissue, 2mm for the bone and socket and 1mm for the liner. The mesh convergence results for the models used in this study can be found in Appendix Chapter 3 Supporting Evidence.

The average run time for the models was approximately 32 hours, using a Quad Core CPU i5-4590, 3.30 GHz and 8.0 GB RAM computer.

4.5.2 Material Properties

The mechanical properties for the bone, soft tissue and socket were the same as stated in Section 4.2.2. In consideration to previous studies, the prosthetic liner was assumed to be linear elastic, isotropic and homogenous with a Young’s Modulus of 400 kPa and Poisson’s ratio of 0.4 (Sanders et al. 2004; Cavaco et al. 2015; Cagle et al. 2018).

4.5.3 Boundary Conditions and Loads

The boundary conditions and loading applied to these models followed the procedure outlined in Section 4.2.3. With regards to incorporation of the liner, the soft tissue-liner and liner-socket interfaces were modelled with surface to surface frictional contact, preventing the nodes of the slave surface in the contact pair penetrating the master surface. The selected slave surfaces were the soft tissue for the soft tissue-liner interaction, and liner for the liner-socket interaction. A friction coefficient of 0.45 (Ramirez et al. 2015) was kept for both prosthetic interfaces; the soft tissue-liner and liner-socket interfaces.

As before, the loading was performed in two phases: (i) donning and (ii) peak amputee walking load. The stresses and deformation from the donning phase were carried into the second phase.

4.5.4 Potential limitations

During the modelling process, modelling assumptions must be made with trade-offs between modelling exactness and computational solving time. These assumptions have been acknowledged in this section and reviewed objectively. Currently all previous published trans-femoral FEA studies have neglected the pelvis, however the pelvis was included in this current study. As discussed in Section 2.4; there are various types of trans-femoral prosthetic sockets which are highly variable and subject specific. Including the subject specific prosthetic socket geometry for each participant in this study would be a largely uncontrollable variable which would greatly alter the stress strain state in the soft tissue. This would limit the objectivity of examining the effect of the pelvic bone and the comparability between participant models.

As mentioned in Section 4.4, the main limitation of the initial methodology in this chapter was the unrectified socket geometry. Resulting in an unaltered proximal medial brim, which would not have realistically provided relief at the pubic ramus region. This was addressed with the subsequent methodology changes (see Section 4.5) incorporating the socket brim geometry. However, in the secondary methodology the socket was not rectified in respect to moving the socket walls closer or further way from the external surface of the soft tissue. Therefore, the counter pressures associated with alterations of the socket geometry to aid in maintaining residual limb alignment (see Section 2.4) were not included, and the socket fit allowed for distal end loading. The effect of altering the socket geometry in respect to the residuum will be considered in a later chapter. The contact interface of the residuum and prosthetic socket can be altered by the additional factors such as, gait pattern, alignment of prosthesis and prosthetic components. These were not considered for this study to limit the number of variables. Therefore, the results of this study primarily show the importance of modelling the pelvic bone.

The supine position assumed by the participants during the scans deformed the gluteal tissues to a flatter shape which may differ compared to during a standing position. The acquisition of residual limb models during supine scan position was conducted in nearly all previous studies (Dickinson et al. 2017) as it is the most widely accessible method of conducting the scan. This artefact is unavoidable unless the scans are obtained from specialised scanners which enable a standing position to be assumed during the scanning. For the pelvic models, the peak stresses and strains were located at the ischium and affected by the amount of soft tissue covering the bony prominence. The amount of musculature covering the ischial region does not change between standing and supine position (Makhsous et al. 2007). To this end, this was thought to have had a limited effect on altering the peak stresses experienced by the residuum models.

The use of a prosthetic liner changed the previous soft tissue-bone interface to soft tissue-liner and liner-socket interfaces. For this chapter, these interfaces were given fixed friction coefficients of 0.45. However, this value was reported for the interaction of skin against polypropylene socket material (Ramirez et al. 2015). In reality, the friction coefficient of prosthetic liners can vary greatly depending on a number of factors including the material, texture and condition (Cavaco et al. 2015), with different friction coefficients on the inside of the liner compared to the textured backing (Derler et al. 2007). Therefore, when incorporating a prosthetic liner into the modelling set-up, it is important to consider the impact of these changes in friction coefficients at both residuum-liner and liner-socket interfaces. This friction variant will be a consideration in the Chapter 5.

4.6 Results

The maximal stresses produced in the donning phase are shown in Table 4-4. The maximal normal stress and shear stress values from application of 110% bodyweight for both models of all participants, are shown in Table 4-5.

Table 4-4: Maximal stresses for non-pelvic and pelvic models at the soft tissue-liner interface from donning phase.

Participant and Model		**Contact pressure (kPa)**	**Circumferential shear (kPa)**	**Longitudinal shear (kPa)**
Participant 1	Non-pelvic	3.1	0.6	0.7
	Pelvic	3.9	1.1	1.1
Participant 2	Non-pelvic	4.1	0.7	0.6
	Pelvic	3.5	1.1	0.8
Participant 3	Non-pelvic	2.1	0.3	0.3
	Pelvic	3.3	1.2	1.0

For both phases, the maximal stresses were concentrated at the distal end of the residuum for all non-pelvic models and at the medial proximal region (at the ischial support region) for all pelvic models. For both phases, the pelvic bone models reported higher peak circumferential and longitudinal shear stresses compared to the non-pelvic models for all participants (see Table 4-4 & Table 4-5). The non-pelvic model showed a region of high magnitude for both shear stresses around the proximal medial region; however, this was of lesser magnitude when compared to the distal regions. The maximum pressure resulting from full loading was greater in the pelvic models compared to the non-pelvic models for all participants apart from participant 2 (see Table 4-5), who reported marginally greater maximal contact pressure for the non-pelvic model in comparison to the pelvic model.

Table 4-5: Maximal stresses at the soft tissue-liner interface for non-pelvic and pelvic models from walking loads.

Participant and Model		**Contact pressure (kPa)**	**Circumferential shear (kPa)**	**Longitudinal shear (kPa)**
Participant 1	Non-pelvic	66.6	18.2	19.9
	Pelvic	122.9	52.6	22.2
Participant 2	Non-pelvic	113.1	27.6	20.3
	Pelvic	107.0	34.4	23.7
Participant 3	Non-pelvic	75.8	12.3	18.3
	Pelvic	110.3	42.0	23.3

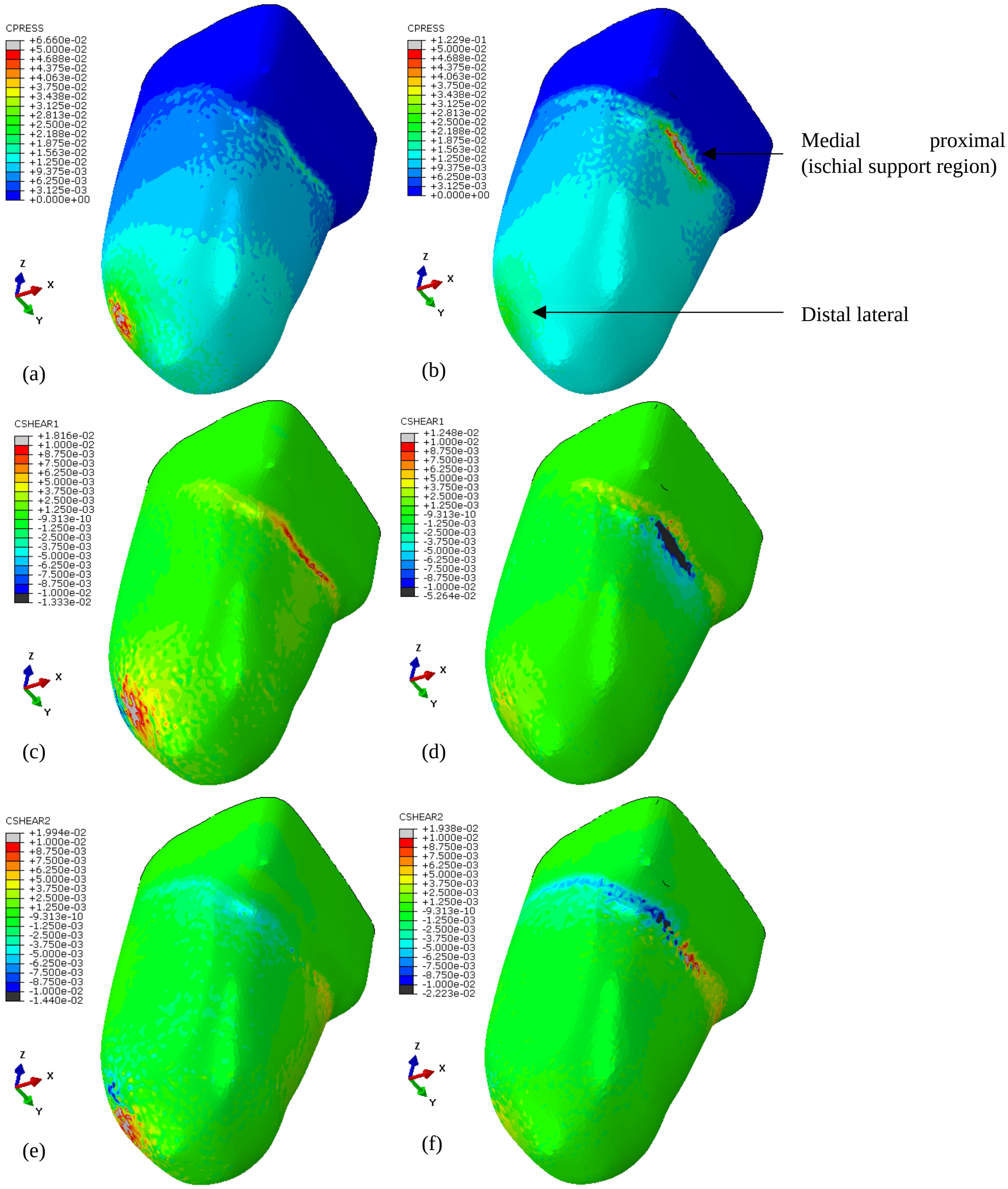

Figure 4-9: Resultant distributions of contact pressure (a, b), circumferential shear stress (c, d) and longitudinal shear stress (e, f) for the non-pelvic and pelvic model of participant 1 respectively.

Table 4-6: Peak tensile (maximum) and compressive (minimum) principal logarithmic strain.

Participant and Model		Tensile (%)	Compressive (%)
Participant 1	Non-pelvic	81.1	119.6
	Pelvic	73.1	104.4
Percentage change (%) from non-pelvic to pelvic		*-10.9*	*-14.6*
Participant 2	Non-pelvic	97.7	159.0
	Pelvic	80.1	134.1
Percentage change (%) from non-pelvic to pelvic		*-22.0*	*-18.6*
Participant 3	Non-pelvic	90.5	118.4
	Pelvic	81.6	114.8
Percentage change (%) from non-pelvic to pelvic		*-10.9*	*-3.1*

The peak tensile (maximum) and compressive (minimum) principal logarithmic strains are shown in Table 4-6. For all participants, the compressive strains were higher than tensile strains. The peak strains were located at the bone-soft tissue interface; the distal end of the residual femur for the non-pelvic models and beneath the ischial region of the pelvic bone for the pelvic models (see Figure 4-10).

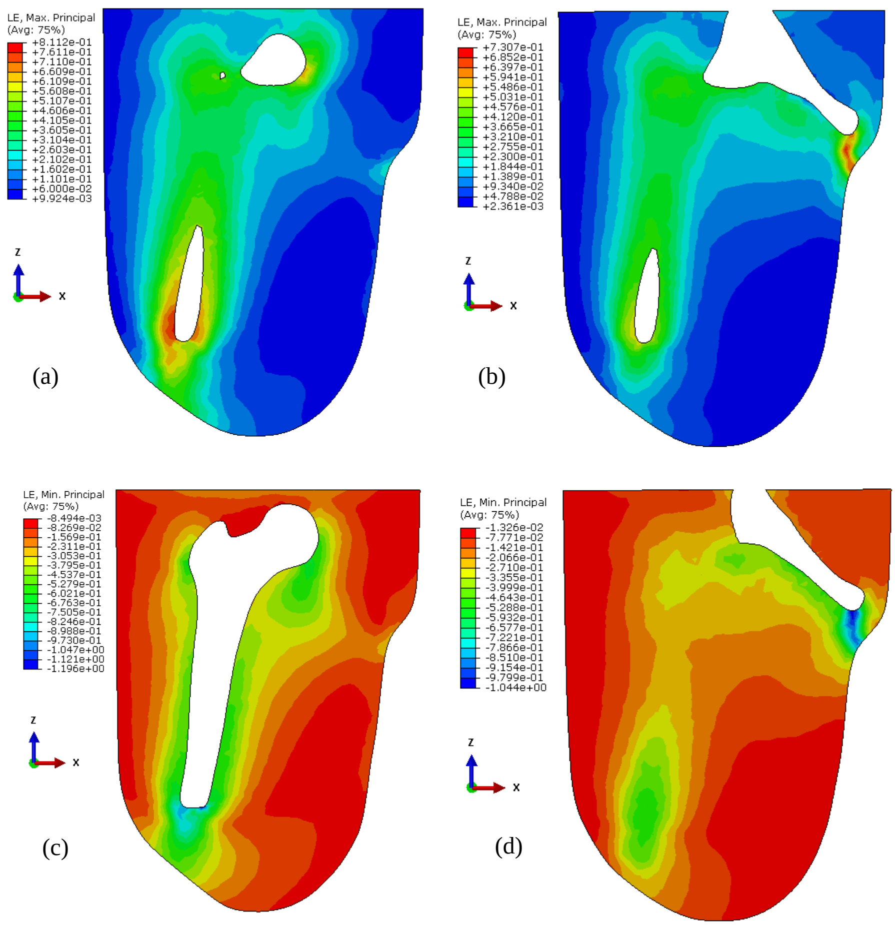

Figure 4-10: Tensile (a, b) and compressive (c, d) strains for participant 1 non-pelvic and pelvic model respectively. Cut through at location of the peak strains and varied between models.

For all the models the proximal region of the soft tissue bulk underwent larger displacement in the non-pelvic models compared to the pelvic models (see Figure 4-11).

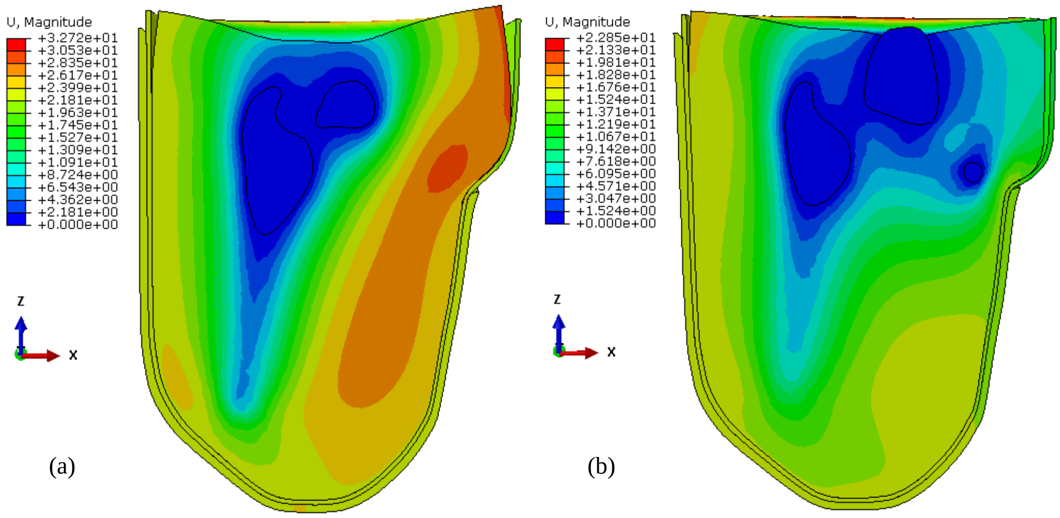

Figure 4-11: Displacement of soft tissue, liner and socket for non-pelvic (a) and pelvic (b) models of participant 1

Path plots were created to provide a visual comparison of the pressure distribution between models. The path plots ran from the proximal medial edge (normalised path ‘0’), down the ischial support region to the residuum tip (normalised path ‘~0.5’) and up the lateral side (normalised path ‘1’). The paths were normalised for ease of comparison (see Figure 4-12).

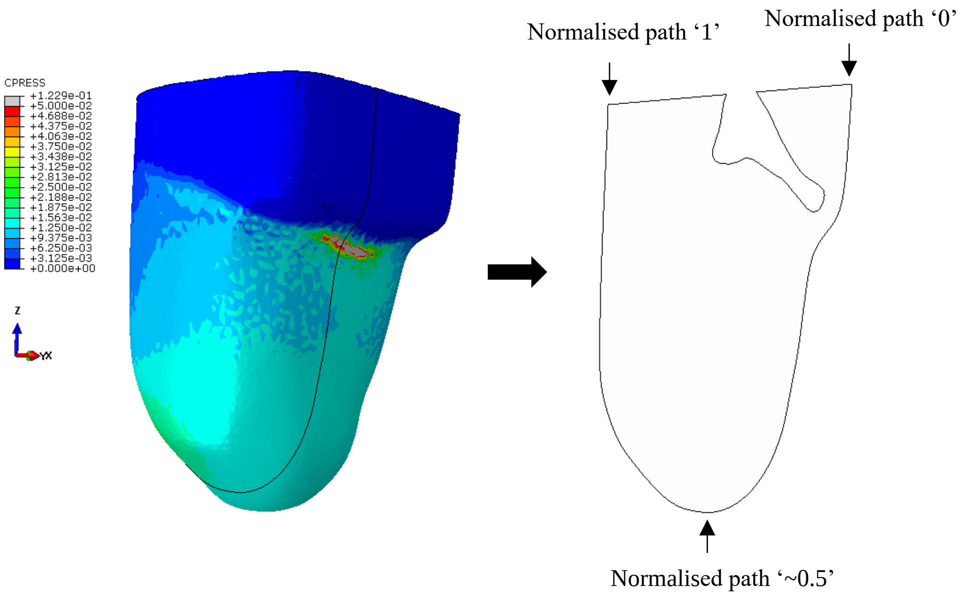

Figure 4-12: Normalised path plot route along the soft tissue surface.

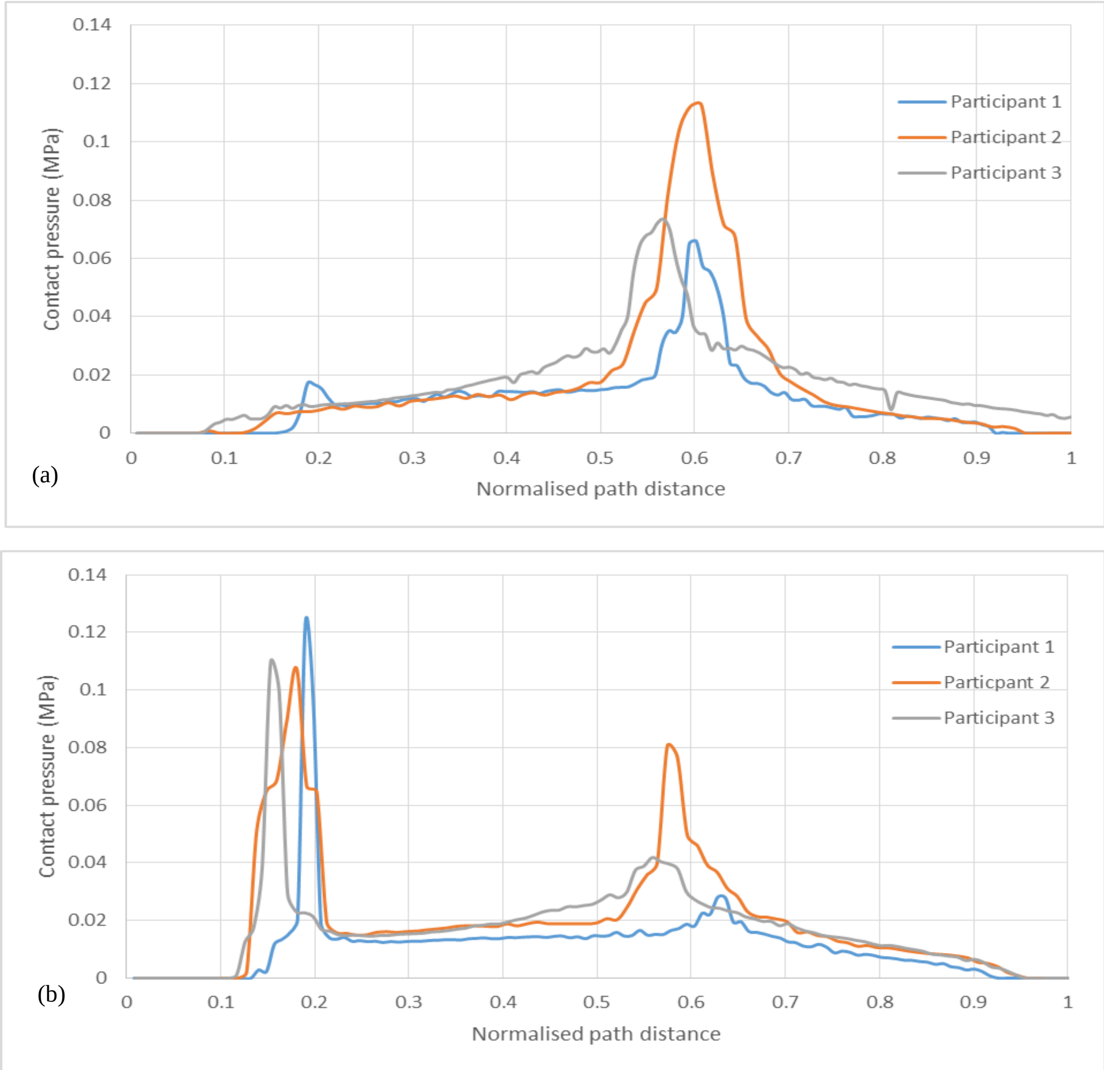

Figure 4-13: Contact pressure path plots for non-pelvic (a) and pelvic (b) models for all participants.

The resultant normalised path plots are shown in Figure 4-13. In Figure 4-13a, the peaks at ~0.6 normalised path distance are representative of the maximal contact pressure at the distal end of the residuum for the non-pelvic models. In Figure 4-13b, the greatest peaks are found at ~0.2 normalised path distance and are representative of the ischium support region of the residuum. For the pelvic bone models (Figure 4-13b) the distal end peaks are still prominent at ~0.6 normalised path distance.

4.7 Discussion

This discussion relates to the results of the simulations including the prosthetic liner and modified socket brim geometry (see Section 4.5).

The addition of the pelvic bone to the residual limb models altered the location of the maximal stresses from the distal end of the residuum to the ischial support region located at the proximal medial region of the residual limb model (see Figure 4-9) and changed the maximal contact pressure and circumferential shear stress (see Table 4-5). The models for participants 1 and 3 reported similar maximal normal stress values and changes due to the pelvic bone being introduced. Participant 2 model gave higher normal stress for the non-pelvic model and reduced normal stress for the pelvic model when compared to participants 1 and 3.

As rectifications of the socket were absent in this chapter, a 50N load was used instead to replicate the donning phase in these simulations, similar to previous studies (Lee et al. 2000; Zhang et al. 2013; Arotaritei et al. 2015). The average peak contact pressure for the non-pelvic models and pelvic models was 3.1 kPa and 3.6 kPa respectively. These values are similar to the peak contact pressure of 5.55 kPa reported by Zhang et al. (2013) who simulated donning by use of a 50N load, and the mean peak contact pressure of 4.01 ± 1.7 kPa reported by Lacroix and Patino (2011) across five FE models for which donning was solved by a push-fit method with overlap between socket and residuum. The peak circumferential (0.3 – 1.2 kPa) and longitudinal (0.3 – 1.1 kPa) shear stress range between the models in this study are similar to the ranges reported by Lacroix and Patino (2011) for peak circumferential (0.23 – 0.93 kPa) and longitudinal (0.57 – 2.00 kPa) shear stress.

For the ambulation phase, the resulting peak pressure at the distal end of the residuum for the pelvic models was 28.1, 80.4 and 41.8 kPa for participants 1, 2 and 3, respectively (see Figure 4-13b). The measured thickness of the soft tissue between the distal end of the residual femur and the liner were 56.1, 29.9 and 50.8mm for participants 1, 2 and 3, respectively. The reduced soft tissue thickness for participant 2 resulted in a greater pressure, as there was less soft tissue at the distal end of the femur to provide cushioning when compared to the models of participants 1 and 2. These measurements therefore explain the difference between peak pressures at the distal end of the residuum’s in the non-pelvic and pelvic models of the participants. For the models with a pelvic bone, a large portion of the walking load which was previously borne by the distal end of the femur was transferred to the ischium area. However, due to the lower soft tissue thickness under the distal end of the femur, a considerable portion of the load was still borne by the distal end of the femur for participant 2. This resulted in the higher pressure that was found at the distal end for the participant 2 model.

The maximal soft tissue displacement for all models and participants was located at the proximal anterior and/or posterior regions. The reporting of solely the maximal soft tissue displacement values is not an accurate measure, as the soft tissue of the non-pelvic models was displaced by a considerably larger amount compared to the pelvic models. The cut through displacement distribution shown in Figure 4-11 provides a more detailed explanation of the soft tissue displacements differences between the two model types. For all models, the soft tissue was ultimately constrained in movement by its tied interaction with the residual bone. In the non-pelvic models, the outer soft tissue in the proximal regions was able to undergo greater deformation due to it being further from the fixed interface of bone-soft tissue. For the pelvic models, the proximal soft tissue was fixed at the soft tissue-bone interface at closer proximity allowing less movement. This more limited movement of the tissues is more realistic. Without the pelvic bone present, the socket was able to undergo larger displacement (24.0mm for participant 1) as the only bearing surface was the distal end of the residuum. This caused high concentrations of stresses and strains around the distal end of the residual femur. By including the pelvic bone, the socket was bearing against the ischial tuberosity and the distal end of the residual limb. This prevented the socket, and therefore soft tissue, from being displaced as much as in the non-pelvic models and the concentration of stresses and strains were shared between the ischial tuberosity and the distal end of the residual femur. Comparably, the values of socket displacement with this chapter of 16.8 – 24.0mm (see Figure 4-11) fall within the range reported by Kahle and Highsmith (2013) reported socket displacement values of 6.0 – 45.0mm during prosthetic ambulation.

For all participants, the non-pelvic model produced greater soft tissue tensile and compressive strains in comparison to the pelvic models (see Table 4-6). For the non-pelvic models, the peak strains were located exclusively at the distal end of the residual femoral bone. In comparison, the peak strains for the pelvic models were concentrated beneath the ischium (see Figure 4-10) with secondary concentrations of lesser magnitudes located at the distal end of the residual femur. This demonstrates that the inclusion of the pelvic bone leads to load sharing between the ischium of the pelvic bone and the distal end of the residual femur. The peak tensile and compressive strains for all participants were reduced from the non-pelvic to pelvic models by 10.9% to 22.0% and 3.1% to 18.6%, respectively. This was similar to the contact pressure distributions of the pelvic models and was due to the distal loading characteristic of the prosthetic socket allowing load sharing between the distal end of the residual limb and the ischium. The peak compressive and tensile principal strains were consistently located at the soft tissue and bone interface for all participants.

Interestingly, a two-dimensional FEA study of the mechanical conditions during sitting by Linder-Ganz et al. (2007) reported a participant model with the sharpest ischial tuberosities (measured by radii of curvature for the ischial tuberosity bony prominence) had higher soft tissue compressive strains under the pelvic bone compared to the other participant models. The ischial tuberosity sharpness was measured in the pelvic models for each participant in this section for comparison. The sharpest ischial tuberosity was found for participant 3 (see Appendix Chapter 4 Supporting Evidence). Whereas the highest peak compressive strain was found for participant 2 (see Table 4-6) which was found to have the least sharp ischial tuberosity of all participants models. As such, the peak compressive strain found under the ischium was independent of the sharpness of the ischial tuberosity and therefore did not exhibit the same trend found by Linder-Ganz et al. (2007). Whilst the sharpness values achieved between studies was similar, an obvious cause for not exhibiting the same trend may be the location at which the sharpness of the ischium was measured. For this section, the ischial tuberosity sharpness was measured perpendicular to the location of peak compressive strain (see Figure 4-10) whereas Linder-Ganz et al. (2007) used a two-dimensional seating model and measured the sharpness at the point where the distance between ischial apex and external tissue surface was the smallest. To further examine the compressive strain differences between the participant models, the amount of tissue covering the ischium was measured (see Appendix Chapter 4 Supporting Evidence) and compared against the strain results. A trend of higher peak compressive strain with reduced tissue coverage over the ischium was identified, with participant 2 having the least tissue coverage and the highest peak compressive strain. Due to the reduced tissue viability from compressive strain (see Section 2.1), it could therefore be argued that individuals with less soft tissue over the bony prominence of the pelvic bone would benefit from increased external padding such as prosthetic liners or a modified prosthetic brim to compliment the pelvic bone contours (as found in the IC socket, see Section 2.4.2) in attempts to limit the compressive strain.

The magnitude of load applied to simulate ambulation was proportionate to the bodyweight of each participant (see Table 3-1). The results of interfacial stresses in this section did not identify a trend relating to the participants bodyweight. Indicating that these were not influenced by the participants bodyweight, and suggesting other factors such as residuum geometry, socket geometry and contacting material may be controlling factors for interfacial stresses. Whereas, the compressive strain did agree with the trend of higher compressive strains with increased bodyweight indicating the soft tissue compressive strain would be susceptible to changes and compensatory methods of an amputees' gait cycle due to this introducing changes in the resulting ground reaction forces (Dijkstra and Gutierez-Farewik 2015).

The contact pressure of 65 kPa in the non-pelvic model reported by Zhang and Mak (1996) is similar to the values of the non-pelvic models for participants 1 and 3 in this study (see Table 4-5). The slight differences may be associated with the use of hyperelastic material properties for the soft tissue in this study whilst Zhang and Mak (1996) used a linear elastic model with a Young's Modulus of 150 kPa and Poisson's ratio of 0.45.

For their model, Zhang et al. (2013) reported maximal contact pressures of 119.3 kPa located at the medial proximal region and 80.57 kPa located at the distal end of the residuum for their non-pelvic model. Whilst the peak contact pressures they reported were located at the ischium region, they also show much greater distal loading than the pelvic models for participants 1 and 3 of this study. As demonstrated in the comparison between the contact pressures of participants in this study, the resultant distal pressure can be altered by the thickness of the soft tissue under the distal end of the residual femur. The distance between the distal end of the residual femur and the soft tissue was not reported by Zhang and Mak (1996) or Zhang et al. (2013) preventing comparisons from being made. Velez Zea et al. (2015) examined the relationship between residual limb length (0.24 – 0.3m range) and the stress distribution on the residuum. They reported an overall trend of decreasing contact pressure with increasing residuum length and a peak contact pressure range of 81.7 – 152 kPa on the residuum. In comparison, neither the non-pelvic nor pelvic models in this chapter showed a trend relating to residuum length, as the soft tissue thickness was the dominant feature. However, this trend may have been visible with a larger sample size as Velez Zea et al. (2015) used a sample size of five participants. Conversely, the subject specific socket geometry used for each participant in their study would mostly likely have been a larger influence on pressure distribution than the residuum length.

As discussed in Section 2.5.2, the pressure distribution and peak at the ischial support region reported by Zhang et al. (2013) and Velez Zea et al. (2015) is believed to be due to the boundary conditions applied within their models. In comparison to their models, the boundary conditions applied in this model along with including the pelvic bone can be considered a more realistic representation. This is demonstrated by the maximal circumferential shear stress (135.4 kPa) compared to maximal longitudinal shear stress (25.65 kPa) on the soft tissue surface along the socket brim reported by Zhang et al. (2013). In comparison, the circumferential shear stress for both models sets in this chapter was considerably lower, whilst the longitudinal shear stress values were similar (see Table 4-5). As stated previously, the boundary conditions applied within their model would have prevented the soft tissue from displacing vertically when the socket was loaded causing bulging of the soft tissue leading to excessive circumferential shear stresses in the soft tissues.

Comparing FEA simulation results to experimental results provides a method of validating the FEA models. Therefore, the pelvic models of this study should be compared to studies with in-vivo sensors. The results of several lower residual limb sensor studies are shown in Table 4-7 along with the pelvic model results of this chapter for comparison.

Table 4-7: Peak pressure value (kPa) and location comparison between pelvic models and previous studies of Kahle and Highsmith (2013), Morotti et al. (2014) and Laszczak et al. (2016).

Study	**Kahle and Highsmith (2013)**		**Morotti et al. (2014)**	**Laszczak et al. (2016)**	**Pelvic models of this chapter**
Location / Socket type	IRC	Brimless	Not stated	Knee disarticulate	‘Hybrid’
Medial proximal	112.1 ± 80.0	109.2 ± 60.7	240.0	-	113.4 ± 6.9
Distal lateral	72.3 ± 43.7	100.1 ± 74.9	-	58.0 (distal)	50.1 ± 22.1

Kahle and Highsmith (2013) reported the peak average pressures during prosthetic ambulation for IC and brimless sockets using Tekscan transducers. The sensors were placed underneath the prosthetic liner in contact with the soft tissue, simulating the similar conditions applied to the models of this chapter (see Figure 2-12 in Section 2.5.3). For both sockets examined by Kahle and Highsmith (2013), a greater peak pressure was found at the medial proximal region (the ischial support region), with a lesser peak pressure also found at the distal lateral end of the vacuum assisted sockets. Both sockets, but most notably the IC sockets, examined by Kahle and Highsmith (2013) produced pressures of very similar values and location compared to the pelvic models in this chapter. This high correlation between their study and the pelvic models of this chapter can be used to validate that the pelvic bone geometry implemented in these models is a reasonable method for creating trans-femoral FE models.

Morotti et al. (2014) used Tekscan transducers to record a peak pressure of 240.0 kPa at the ischium area between residual limb and a non-stated type of prosthetic socket. The location of peak pressure was in agreement to the pelvic models in this chapter. However, the 240.0 kPa value reported is greater than the 113.4 ± 6.9 kPa reported in this chapter. The lower peak pressures found in this study, and that of Kahle and Highsmith (2013), can be a result of including a prosthetic liner, whereas Morotti et al. (2014) recorded pressures directly between the residuum and prosthetic socket.

Laszczak et al. (2016) reported peak pressures within a knee disarticulation socket including a prosthetic liner. They found peak pressures of 58 kPa the distal end of the residuum, 38 kPa at the posterior proximal location and 36 kPa at the anterior proximal location. Knee disarticulation amputation occurs through the knee joint, allowing for the distal end of the femur to remain intact. Therefore, distal end loading is encouraged in knee disarticulation sockets and the residual limb tissues are much less susceptible to damage compared to trans-femoral amputation (Paterno et al. 2018). The knee disarticulation socket used by Laszczak et al. (2016) thus encouraged loading and pressures at the distal end of the residuum compared to the ischial tuberosity in trans-femoral prosthetic sockets. However, the peak values reported by Laszczak et al. (2016) are considerably lower than those in this study. The reasoning for this may be considered due to the sensor size and placement. The total area for each of the three sensors were 20 x 20 mm, meaning it was only possible to record sensory information within this limited area. In addition to this, whilst the sensor placements were assumed to be over areas of peak stresses, any minor misalignment between the socket fit and the desired sensor location would result in the stresses in the anticipated location not being recorded. Therefore, the real values may be considerably greater than reported, however they were not recorded due to the sensor size and placement.

4.8 Clinical Relevance

The design of the prosthetic socket is highly related to the geometry of the patient’s pelvis. For example, in the Quad socket, the ischium seat is positioned just distal to the ischial tuberosity and in the IC socket, the medial lateral dimensions are determined by the geometry of the patient’s pelvis (Long 1985; Neuman et al. 2005). This section has shown the effect of including the pelvic bone on the interfacial stresses. This is a significant adjustment to the modelling geometry and removes a fundamental oversight from the previous geometry used, which would hinder the correct implementation of computational simulation for socket design if not corrected.

4.9 Conclusion

In this chapter, computational modelling methods were used to include the pelvic bone as an ischial support in FE models of the trans-femoral residual limb. The pelvis is an integral part of the residuum anatomy when designing a trans-femoral prosthetic socket due to its load bearing ability. However, the pelvic region had not been modelled in previous FEA studies of the trans-femoral residuum. The non-pelvic models in this section produced peak stresses at the distal end of the residuum. The location and values of these models were in accordance with previous FEA studies which also did not include the pelvis.

Adding the pelvic bone to the FE models resulted in the peak pressure location being changed from the distal lateral region to the medial proximal region. The ischial tuberosity of the pelvic bone allowed for load bearing jointly at the ischial tuberosity and the distal end of the residuum. This was shown in the reduced peak tensile and compressive strains in the pelvic models compared to the non-pelvic models. The compressive strains in the soft tissues were found to correlate to the magnitude of tissue covering the ischium but not to the sharpness of the ischial tuberosities. Whilst it is a simple change, including the pelvic bone in the FE model of the residuum is a necessary change to provide a more realistic approach of the modelling setup. This was validated by the high level of agreement when comparing the pelvic model results of this chapter to experimental data reported by Kahle and Highsmith (2013).

5. PROSTHETIC LINER PROPERTIES

5.1 Introduction

In the previous chapter, a working FE model and simulation process of the trans-femoral residuum was established. This method of numerical analysis can be developed to examine different problematic issues of the residuum.

Studies have shown the friction generated at the soft tissue and socket interface produces shear stresses within the residuum (Zhang et al. 1998; Zhang et al. 1999). The combination of normal and shear stresses is a major factor for soft tissue damage and patient discomfort (Meulenbelt et al. 2006; Li et al. 2008; Li et al. 2011). However, friction plays a vital role in supporting the load of the user's body during the stance phase of ambulation and prevents the socket slipping off the residuum during the swing phase. The correct level of friction at the residuum and socket interface will balance the production of stresses on the soft tissue whilst also limiting the amount of slip.

Optimising the interaction between residuum and socket is essential in preventing detrimental effects from ambulatory loads and providing a good level of comfort to the user. The intended purpose of a prosthetic liner is to distribute pressures over the residual limb, thus providing a higher level of comfort as opposed to direct socket and residuum contact. Studies have commonly examined the material properties of liners under different loading conditions, such as tension, compression, shear, and friction testing (Sanders et al. 1998; Sanders et al. 2004; Li et al. 2008; Li et al. 2011; Cagle et al. 2017). However, there have been few studies found in literature that investigate liner performance in human participants (Geertzen et al. 2015; Guerra-fán et al. 2018). FEA is a valuable tool as it can be utilised to examine previously reported liner data in a global simulation process due to the ease of altering the FEA inputs which may prove more problematic in an in-vivo experiment.

Due to the number of variables introduced by the prosthetic liner, this chapter is split into two. Firstly, the effect of the friction at the soft tissue-liner and liner-socket interfaces; will be examined. Secondly, the remaining variables of liner thickness and liner stiffness will be examined along with varying soft tissue stiffness.

5.2 Effect of Friction

The friction properties between a liner and human skin have been shown to be highly variable (see Section 2.3.2). Besides the liner itself, other variables such as residuum hirsuteness (Restrepo et al. 2014), surface roughness, normal force, health of skin (Li et al. 2008), and the individual and body site of testing (Zhang and Mak 1999) have all been reported to alter the measured friction coefficient. Although the frictional properties of the liner have been shown to be highly variable, the effect of this on the residuum has not yet been studied.

Therefore, the objective of this section was to conduct experimental friction coefficient testing on a range of liners and use the experimental results as friction inputs to a range of FE models to examine the effect of friction coefficient changes at both the soft tissue-liner and liner-socket interfaces on the stresses experienced by the residuum and liner.

5.2.1 Liner Friction Testing

5.2.1.1 Equipment and Method

Five prosthetic liner products were obtained from two manufacturers, covering the range of base elastomeric polymers and textured backings available from both companies. All liners were in a new condition without being previously used and showed no sign of damage. The details of these liner products can be found in Table 5-1.

Table 5-1: Experimental liner details.

Liner	Company	Product	Material	Thickness (mm)	External texture
1	Ottobock	6Y523	Polyurethane	5	Cotton
2	Ottobock	6Y70	Silicone	2.5	Cotton
3	Ottobock	6Y90	Copolymer	3	Cotton
4	Ossur	Locking	Silicone	3	Nylon
5	Ossur	Seal-in	Silicone	3	Nylon

An experimental test was developed to measure the friction coefficient using a custom-made device designed by the author and manufactured by the mechanical testing laboratory at the University of Surrey (see Figure 5-1). The device consisted of a metal frame (44 x 44 x 41cm) with linear carriage mounted (via linear bearings) on two parallel 10mm diameter bars aligned centrally which allowed axial movement. A vertical bar with adjustable height was attached to the carriage. A hollowed plastic probe was fitted over the distal end of the vertical bar. The probe end was flat with a 10mm diameter surface. Normal force was applied by the weight of the probe. A horizontal container force was applied to the probe, via a pulley system. The dragging (shear) force was applied by sand into a container to allow for greater levels of precision compared to using slit weights and their weighted increments.

The interfaces of skin-liner and liner-socket were tested. A leather surface was used as a skin substitute and a polypropylene plastic surface as a socket substitute (Cagle et al. 2017; Li et al. 2018). The liners were wrapped around the probe with the surface to be tested facing outwards, this was reversed when the opposing surface was tested.

During testing, the first operator placed the probe with the liner on the test surface, which was clamped to the table to prevent movement. The second operator applied sand at a slow and constant rate to the container, applying a dragging force an offsetting the pulley. The test was stopped as soon as movement was observed at the test liner and substitute interface. The COF ($\mu = F/N$) was calculated as a ratio of the dragging force (F), weight of the resulting sand in the container, and normal (N) force, the combined weight of the probe and liner sample. Tests were conducted six times for each interface and an average calculated. The position of the probe was reset between each test to remove any hysteresis as a result of the previous test.

A second 'wet' test set was performed on the skin-liner interfaces to replicate sweat at the liner-skin interface caused by increased humidity and lack of ventilation when using a liner. For this, distilled water was applied by spray bottle to the skin substitute surface to achieve an even distribution. The distilled water was applied to the surface of the skin substitute, then a series of tests for the wet skin-liner interface were performed for each liner material. The test surfaces were wiped dry after each liner test and the water was reapplied prior to the testing of the next liner. Tests were conducted six times for each interface and an average calculated.

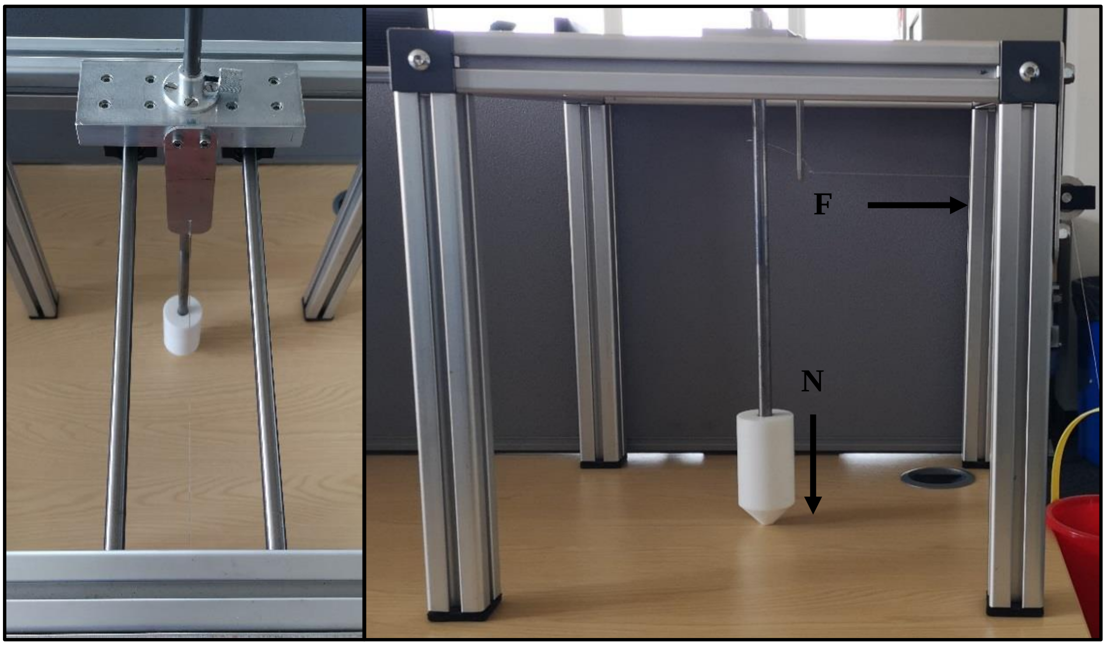

Figure 5-1: Friction coefficient testing device setup.

The coefficient of friction has been shown to alter with applied normal force (Zhang and Mak 1999; Sanders et al. 2004; Li et al. 2006; Derler et al. 2007). Therefore, to comparable to the conditions within a prosthetic socket, the normal force applied during testing should be similar to those within a socket. An average contact pressure range of 25.1 to 42.9 kPa has previously been reported within a trans-femoral prosthetic socket (Kahle and Highsmith 2013). As the probe was able to move freely over the distal end of the vertical bar, the normal force during the tests were calculated as the weight of the probe and the tested liner. The contact area over which the normal force was applied was a circle of 10mm diameter. Therefore, the contact pressure for each test could be calculated. Friction testing was conducted with contact pressures between 36.2 to 40.5 kPa (see Table 5-2). These values are within the range reported by Kahle and Highsmith (2013). Normal force applied during testing was predominantly from the weight of the probe, with a minor contributor from the weight of the sampling liner.

Table 5-2: Contact pressure applied during friction testing.

Liner	Force (N)	Area (mm^2)	Pressure (kPa)
1	3.18	78.54	40.5
2	2.84	78.54	36.2
3	2.86	78.54	36.5
4	3.04	78.54	38.7
5	2.89	78.54	36.8

5.2.1.2 Potential Limitations

The thickness profiles of the liner products tested was tapered from a thin proximal to thicker distal profile (Ossur 2011; Ottobock, 2016). The thickness values of the samples were taken from the proximal region of the products to limit the sample thickness and reduce the potential for hysteresis of the samples during testing. Liner 1 was the thickest of samples tested. During testing the amount of elastic deformation of the liner was observed for liner 1 compared to the other liners. This made it difficult to distinguish between at which point movement had occurred between the contacting surfaces rather than elastic deformation. This may have been negated by trimming the liner to reduce the thickness, however this was thought to compromise the condition of the liner and alter the results.

The hirsuteness of the skin during friction testing has been shown to produce a higher friction coefficient with reduced levels of hirsuteness (Restrepo et al. 2014). As a skin substitute was used for the testing, the effect of hirsuteness could not be included. The room temperature and humidity were not measured during this study as was done by previous studies (Sanders et al. 2004; Li et al. 2008; Li et al. 2011). Because the friction testing was performed on a skin substitute, these effects were not deemed to be as influential as they have shown to be when testing on human skin.

The friction coefficient of the ball bearing linear carriages was not factored into the friction coefficient calculations for the liners. Both ball bearing linear carriages were acquired from Automotion Components®, which provide technical information (Automotion Components 2017) stating the friction coefficient of the ball bearings produced is between 0.001 and 0.003. This value was deemed to be low enough to be negligible on the results achieved as the linear carriages appeared to run freely when a normal load was not applied. Therefore, this would not be factored into the later friction coefficient calculations.

5.2.1.3 Results

The mean coefficient of friction measured between the liner insides and skin substitute under dry conditions was 1.45 (SD 0.21), with a range between 1.24 – 1.83 (see Figure 5-2). Under wet conditions the friction coefficients for all liners were reduced, resulting in a mean coefficient of friction between the liner insides and skin substitute of 0.87 (SD 0.16), with a range between 0.64 – 1.04. The mean coefficient of friction measured between the liner outside and socket substitute was 0.38 (SD 0.13), with a range between 0.25 – 0.58. The full tables of results are shown in Appendix Chapter 5 Supporting Evidence.

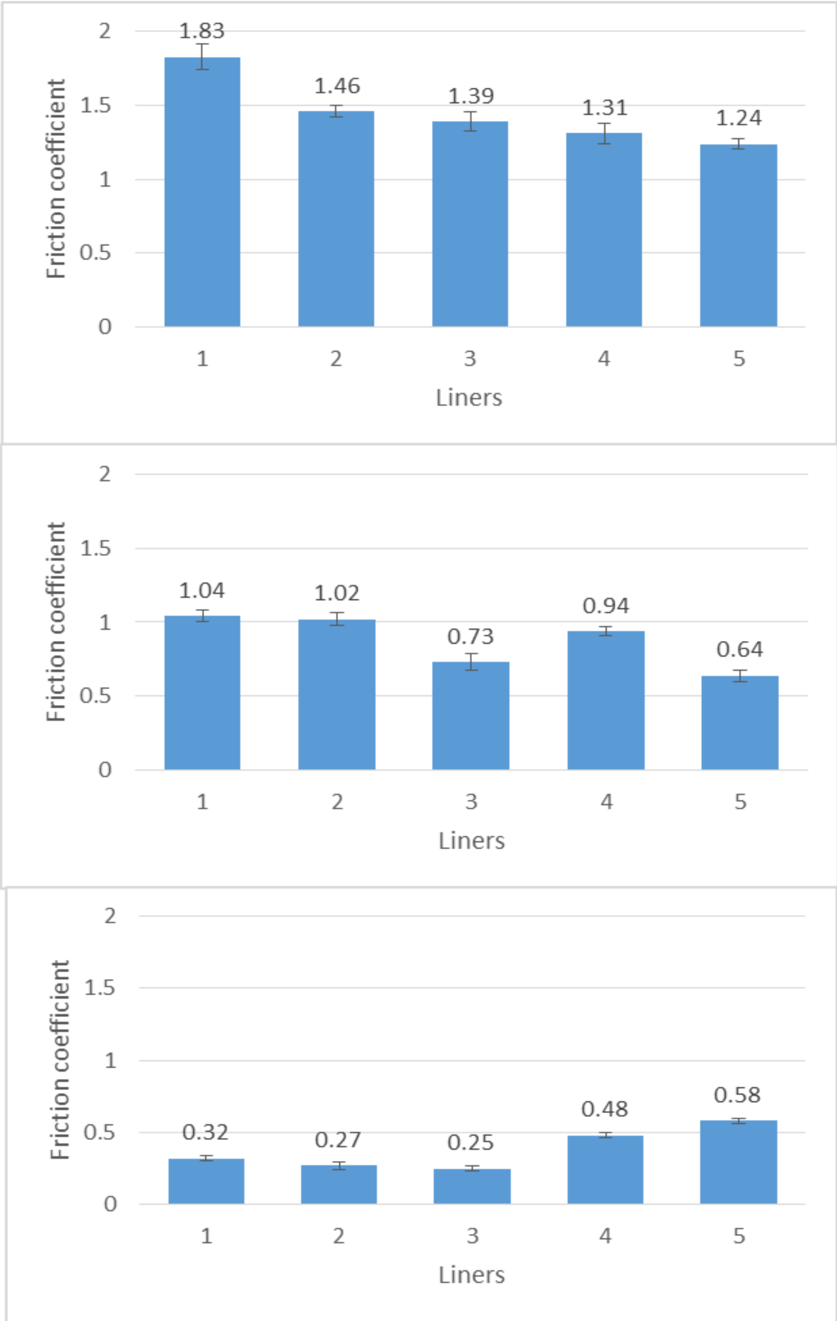

Figure 5-2: Friction coefficient results for the soft tissue-liner interface under dry conditions (top) and wet conditions (middle), and liner-socket interface (bottom).

5.2.1.4 Discussion and Conclusion

The dry conditions for the inside of the liner produced the highest friction coefficients for all liner products. The single urethane-based liner (liner 1) produced a higher friction coefficient compared to the silicone or copolymer-based counterparts. Similarly, out of the 15 liner products tested by Sander et al. (2004), the only urethane-based liner was also found to produce the highest friction coefficient compared to the silicone-based liners. It is hypothesised that the COF difference between the internal liner surfaces was a characteristic of the chemical adhesion as a result of the different liner materials (Cagle et al. 2017).

The wet condition reduced the friction coefficients for all liner products with a percentage change reduction between 28.4% and 48.1%. This would suggest, a higher friction coefficient between liner and residuum would be present during the initial period of donning a liner which would reduce over time due to sweating from the humid environment. The amount of sweat produced would be dependent on the level of ventilation, activity level and condition of the residuum and may be highly variable between individuals. A similar result to this study was reported by Li et al. (2018) who examined the effect of moisture on COF of different materials against human skin and found increased moisture levels increased the COF for texture materials but decreased the COF for polymer-based materials, which were highly similar to the inside liner materials used in this study. The difference may be attributed to the way moisture interacts with the fabrics and their absorbent capabilities which would increase the contact area (Chen 2014). Several previous studies have also reported an increased friction coefficient for a range of materials against human skin with increased lubrication levels (Gerhardt et al. 2008; Derler and Gerhardt 2012).

This is because of the bell-curved behaviour moisture has on the friction coefficient, as mentioned in Section 2.3.2.3. In which, the presence of moisture increases the COF with the transition from dry skin to moist skin. This increase occurs up to a maximum point, after which additional moisture causes a decrease in the friction coefficient. The effect of moisture on skin friction has been referred to as bell-shaped progressing through two main regimes with increasing lubrication; boundary lubrication and mixed regime lubrication (Derler and Gerhardt 2012; Adams et al. 2007; Tomlinson et al. 2009). The boundary regime is the initial transition to wet lubrication, in this regime excessive softening of the stratum corneum caused by the plasticising action of water occurs, flattening the topological features of the skin and increasing the friction coefficient (Adams et al. 2007). Past a critical amount of water, the friction coefficient reduces as it enters the mixed lubrication regime in which hydrodynamic lubrication, where complete separation of the contacting surfaces by a liquid film occurs, is developed in localised regions of the contact. The results of this study found a reduced friction coefficient with the addition of moisture. This suggests the amount of water added during the wet friction testing added sufficient water to the contacting surfaces to transition the surface into the mixed lubrication regime.

From the range of previous studies which have examined the friction between liner and human skin or a relevant substitute (leather), the most commonly reported values have been between 0.45 and 1.01 for a range of silicone gel, silicone elastomer and urethane liners (Sanders et al. 1998; Sanders et al. 2004; Zhang and Mak 1999; Emrich and Slater 1998). These previous studies were conducted under dry conditions. In comparison, the dry condition results of this study were higher than those of previous studies. These differences may be a result of numerous skin mechanics and testing parameters such as sliding speed, load and contact area (Li et al. 2006; Derler and Gerhardt 2012) and the individual liner products tested that are so different that it is not possible to establish true comparisons. For example, some previous studies have reported a constant COF regardless of normal force changes (Tomlinson and Carre 2009; Ramirez et al. 2015), whilst other studies report COF decreases with increasing normal force (Zhang and Mak 1999; Sanders et al. 2004; Li et al. 2006; Derler et al. 2007). Nonetheless, the normal force applied during this friction testing (36.2 - 40.5 kPa) was chosen to replicate the average pressure within a prosthetic socket (25.1 - 42.9 kPa) and is therefore comparable in this context.

The external textures of the liners were limited to nylon and cotton material for this study. A lower friction coefficient was found for the two liners with external cotton textured surfaces (0.25 – 0.32) compared to nylon (0.47 – 0.58) on the remaining liners. Restrepo et al. (2014) reported a friction coefficient range of 0.19 – 0.40 for a nylon textured sock against human skin, rather than against the socket material as conducted in this study. Variations in their results were caused by factors of hirsuteness and moisture levels in combination with the textured surface. Similarly, Li et al. (2011) reported a higher friction coefficient (0.18) for nylon, compared to cotton (0.06) prosthetic socks against skin. The reduced knitted density and yarn count for nylon formed a higher surface roughness creating an increase in friction coefficient (Morton and Hearle 2008).

Previous studies testing the friction coefficient of prosthetic liners have been conducted against healthy human skin (Zhang and Mak 1999; Li et al. 2006) or a skin substitute (Sanders et al. 2004). An insightful study by Li et al. (2008) concluded the friction coefficient varied depending on the condition of the human skin, with variations between healthy skin, prosthetic skin from a residual limb and scarred skin. The results showed the friction coefficient of scarred skin was higher than that of the prosthetic and healthy skin with greater amounts of fluctuation. The friction coefficient of prosthetic skin was close to healthy skin but with a greater amount of fluctuation. It was concluded the higher friction coefficient and strong fluctuations for scarred skin were due to changes of the skin histological structure and surface roughness.

Results of the three friction conditions (see Figure 5-2) showed a general trend of reducing friction coefficient standard deviation for each liner from dry, wet and outside surface. The testing involved human assessment of when slippage began. Larger amounts of elastic deformation were observed for the internal liner surface compared with the external surface. It can be assumed that human error may have had an impact on determining the point at which static friction was overcome and therefore on the standard deviations.

5.2.2 Friction Coefficient - FEA Modelling Method

The friction coefficient testing results of the previous section will be included in the FE models for this chapter. For this chapter, the pelvic models consisting of; bone (residual femur and hemi-pelvis), soft tissue, prosthetic liner, and prosthetic socket for the three participants was used. The acquisition and reconstruction of the models for each participant are detailed in Section 3.2.

5.2.2.1 Convergence Testing

The FE models were verified by the mesh convergence testing method shown in Section 3.2.4. The mesh convergence results for the models used in this study can be found in Appendix Chapter 3 Supporting Evidence.

The average run time for the models was approximately 32 hours, using a Quad Core CPU i5-4590, 3.30 GHz and 16.0GB RAM computer.

5.2.2.2 Material Properties

The mechanical properties of the bone, liner and socket were assumed to be linear elastic, isotropic and homogeneous. The soft tissues were defined using the Extended Mooney-Rivlin strain energy function with added compressibility. The material properties used in this chapter do not differ to those detailed in Section 3.2.6. This included the liner being modelled with elastic modulus of 400 kPa and Poisson's ratio of 0.4 (see Table 3-4), and the friction coefficient values from the friction testing section being incorporated into the FE models for this section. This is detailed below.

5.2.2.3 Boundary Conditions and Loads

The boundary conditions and loading applied to these models follow the procedure outlined in Section 3.2.7. This included the bone and soft tissue interface being tied, a 50N axial load used to simulate the donning process and a load equivalent to 110% of the participants bodyweight used to simulate ambulation.

To examine the effect of the friction coefficient at both liner interfaces, predetermined threshold friction values from previous studies and the friction testing carried out in Section 5.2.1 were applied to the interfaces. Thresholds values of 0.6 (*Medium*) and 1.0 (*High*) were applied to the residuum-liner (*RL*) interface in accordance with the wet internal liner tests results of 0.64 – 1.04 in the previous Section (5.2.1.3). Threshold values of 0.2 (*Low*) and 0.6 (*Medium*) were applied to the liner-socket (*LS*) interface in accordance with the external liner test results of 0.25 – 0.58 in the previous Section (5.2.1.3). This produced a total of four model variants for each participant (see Table 5-3). The models were labelled with respect to the friction values. For example, model '*RL-High/LS-Low'* refers to the residuum/liner (*RL*) with '*High*' (1.0) friction coefficient and liner/socket (*LS*) with '*Low*' (0.2) friction coefficient. The friction coefficients were applied using the Coulomb friction model (see Section 3.2.7).

It should be noted that friction coefficients up to a value of 2.0 were considered for the High friction values as the greatest dry liner friction coefficient of 1.83 achieved in the friction testing. However, this produced more instability within the FE models during simulation and for the simulations that did reach convergence, there was no real change in the relevant outputs from the input of 1.0 friction coefficient for the High threshold.

Table 5-3: Friction coefficient variations applied at the liner interfaces.

Interface	**Friction Coefficient**			
	RL-High/LS-Low	**RL-High/LS-Med**	**RL-Med/LS-Low**	**RL-Med/LS-Med**
Residuum – Liner	High	High	Medium	Medium
Liner - Socket	Low	Medium	Low	Medium

As before, the loading was performed in two phases; (i) the donning of the socket and (ii) peak amputee walking load (see Section 3.2.7). The stresses and deformation from the initial phase were carried into the second phase.

5.2.2.4 Potential Limitations

The main potential limitations observed for this section may be the Boolean fit of the prosthetic liner. The liner size is commonly decided by the distal and proximal circumferences (Ottobock, 2016), allowing a tight fit around the residuum to be achieved. Once donned, the liner and residual limb can be considered as matched in a Boolean fit. However, due to the tight fit of the liner, donning the liner pre-tensions the liner material and pre-compresses the soft tissue. Previous studies have examined the donning effect of the prosthetic socket and reported maximum pressure as low as 1.54 kPa on the residual limb (Lacroix and Patino 2011). The effect of donning the liner, and resulting magnitude of pre-loading, has not yet been fully examined (Dickinson et al. 2017). Therefore, simulating the donning of the liner and the resultant deformations and stresses was not included.

A single friction input, obtained from static friction testing, was used for both the static and dynamic element of friction with the difference between them not included. Although it is commonly established, the value of static friction is greater than that of dynamic friction, the continued pistoning of the residuum within the socket during ambulation would create a cycle of static to dynamic friction and could be considered to reduce the friction coefficient compared to the static input. The friction input was modelled using the Coulomb friction model. This model is almost exclusively used within FEA studies (Lee et al. 2004; Portnoy et al. 2008; Portnoy et al. 2009; Lacroix and Patino 2011; Zhang et al. 2013; Restrepo et al. 2014; Arotaritei et al. 2015; Velez Zea et al. 2015; Cagle et al. 2018) to model the pre-sliding (sticking) regime until the critical shear force is reached (ABAQUS 2013). A comprehensive examination of friction models within FEA by Hadji and Mureithi (2019) concluded that the Coulomb friction model is valid and applicable in models where slipping occurs, however it does not model methods of the sticking or pre-sliding condition. This is because it does not take in to account the elastic deformation prior to slipping occurring (see Figure 5-3). The elastic deformation prior to slipping would reduce the localised shear stresses, therefore the use of the Coulomb model may cause higher estimates of localised shear stresses during the period of local elastic deformation.

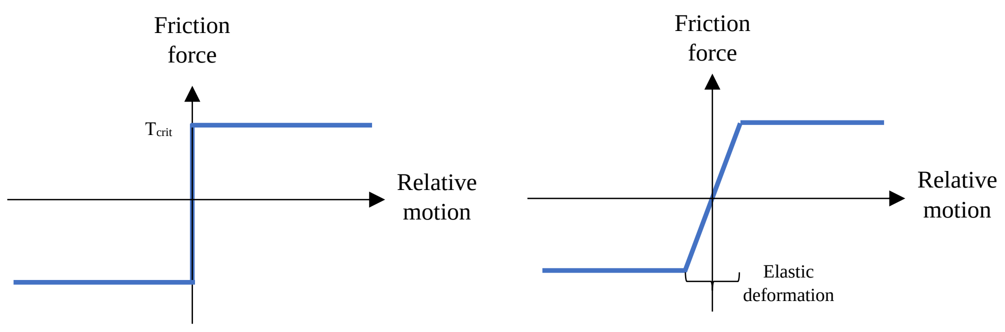

Figure 5-3: Comparison of Coulomb stick region with realistic conditions.

5.2.3 Results

The peak contact pressure, circumferential and longitudinal shear stresses on the soft tissue for the *RL-High/LS-Med* model for all participants loaded with 110% bodyweight force are shown in Figure 5-4. The peak stresses on the external surfaces of the soft tissue and liner are shown in Figure 5-5 for all participants. For all the simulations and models, the peak contact pressure on the external soft tissue surface and external liner surface were located at the ischial support region (see Figure 5-4). The peak circumferential and longitudinal shears were also found at the ischial support region and along the brim of the socket.

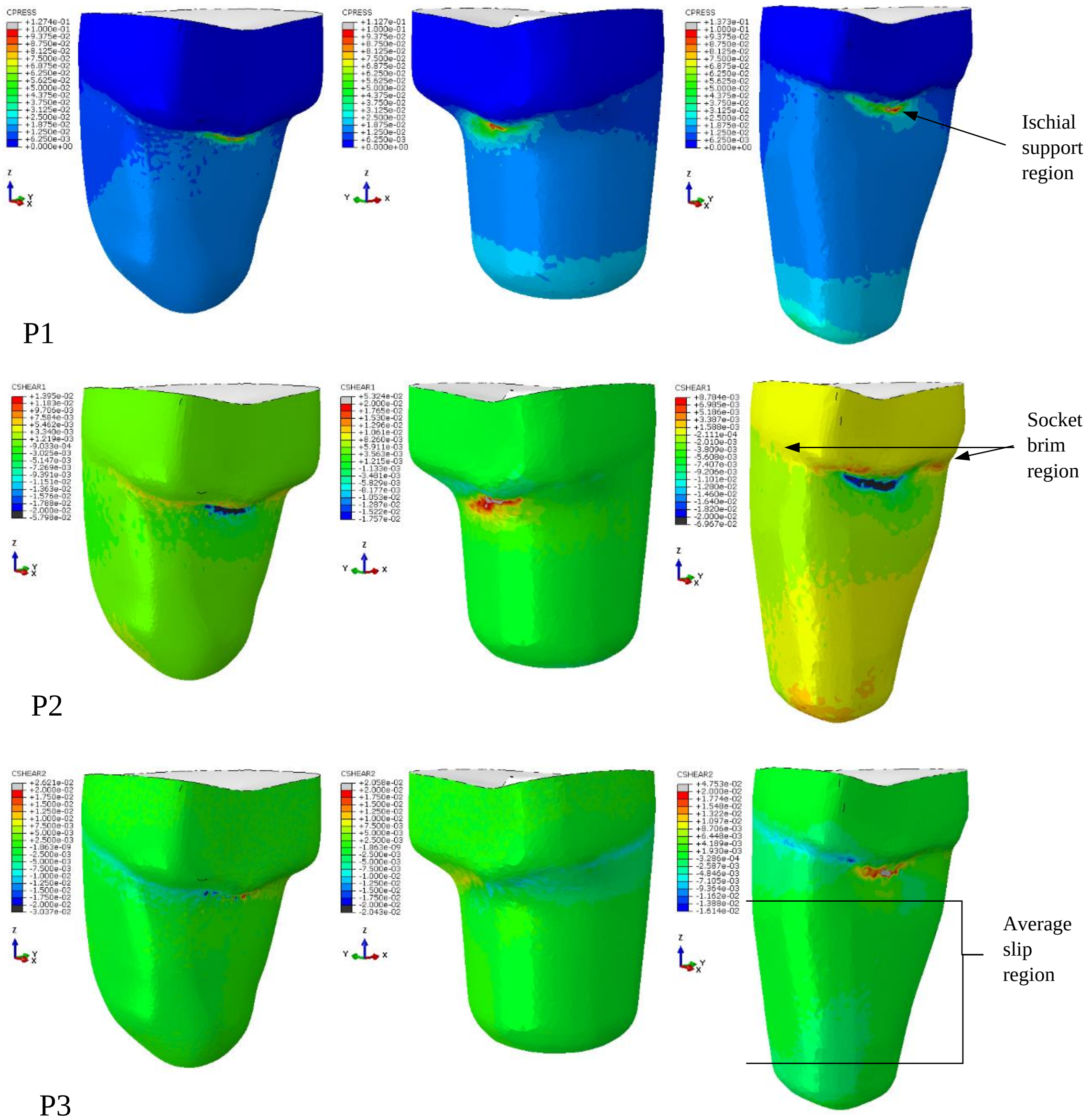

Figure 5-4: Contact pressure, circumferential and longitudinal shear stresses (left to right) on the external soft tissue surface for the RL-High/LS-Med model for participants 1, 2 & 3.

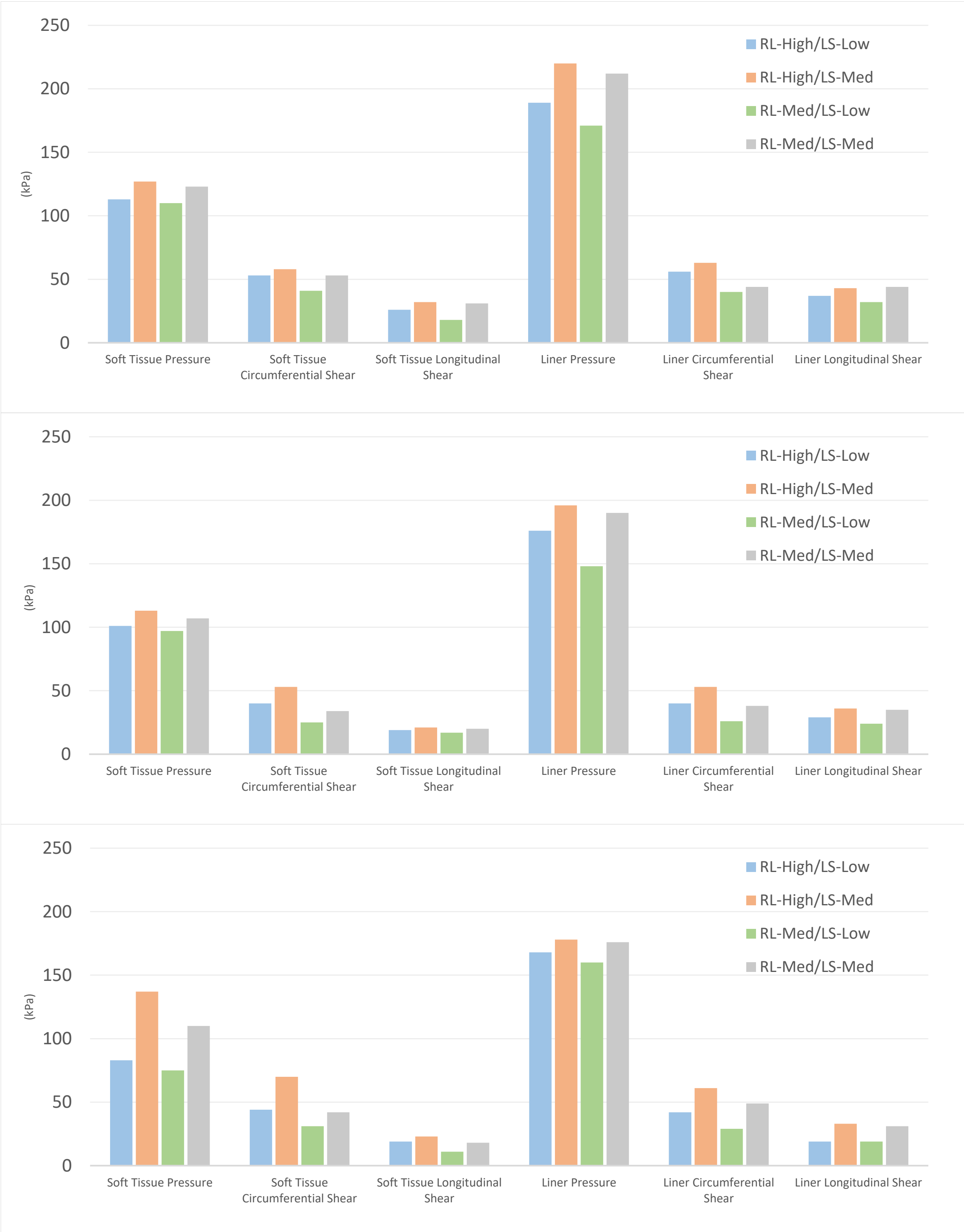

Figure 5-5: Peak contact pressure, circumferential and longitudinal shear stresses on the soft tissue and liner for participant 1 (top), participant 2 (middle) and participant 3 (bottom).

The average slip experienced between soft tissue-liner and liner-socket is shown in Figure 5-6. The average slip was taken from a band that wrapped around the thigh region of the residual limb used to represent the volume region of the residuum. The band was 4cm below the ischium and 4cm above the distal end of the residual limb. This is annotated on Figure 5-4.

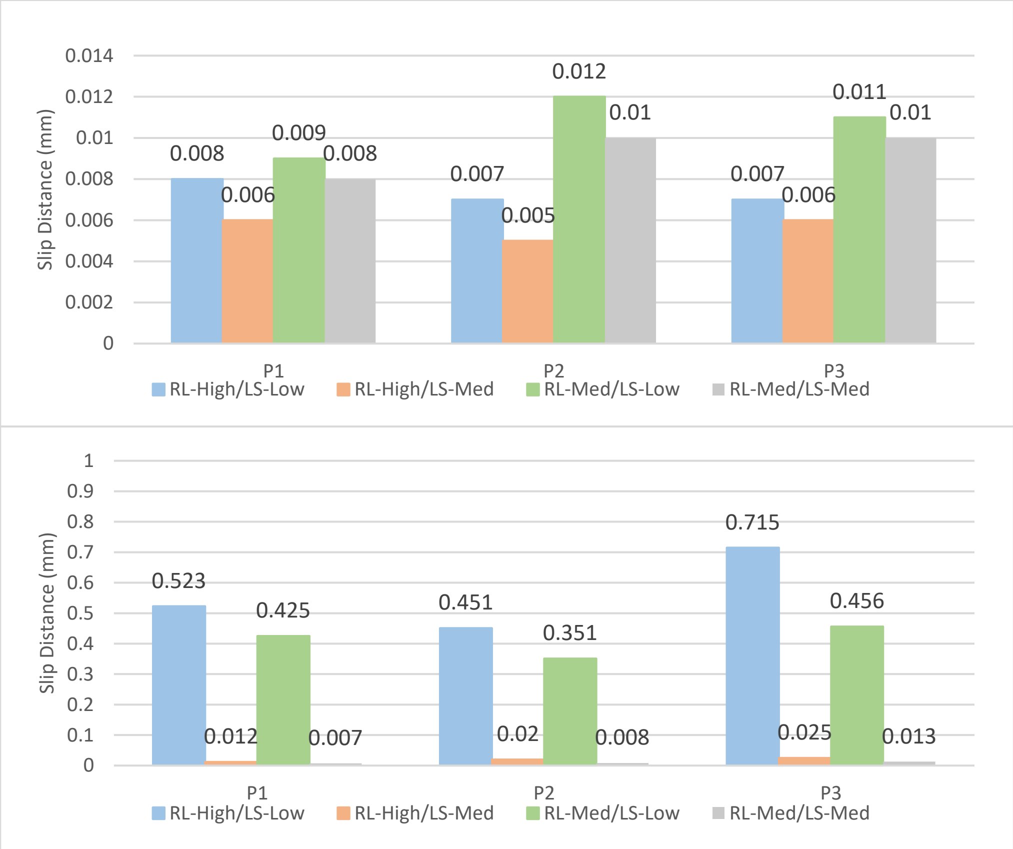

Figure 5-6: The average slip at the soft tissue-liner (top) and liner-socket (bottom) interface.

Table 5-4: Mean peak maximum (tensile) and minimum (compressive) principal logarithmic strain (LE) in soft tissues for all models of each participant.

Participant	Tensile (%)	Compressive (%)
Participant 1	73.8 ± 2.8	111.3 ± 8.1
Participant 2	84.7 ± 3.8	141.9 ± 5.6
Participant 3	83.7 ± 2.9	120.5 ± 5.5

The peak tensile (maximum) and compressive (minimum) principal logarithmic strain distribution showed a small degree of variation over the friction range for each participant (see Table 5-4).

The change in friction coefficient did not alter the location of the peak contact pressure and shear values. The pressure distribution on the residual limb is shown in Figure 5-7 with the peak pressure location remaining at the ischial support region.

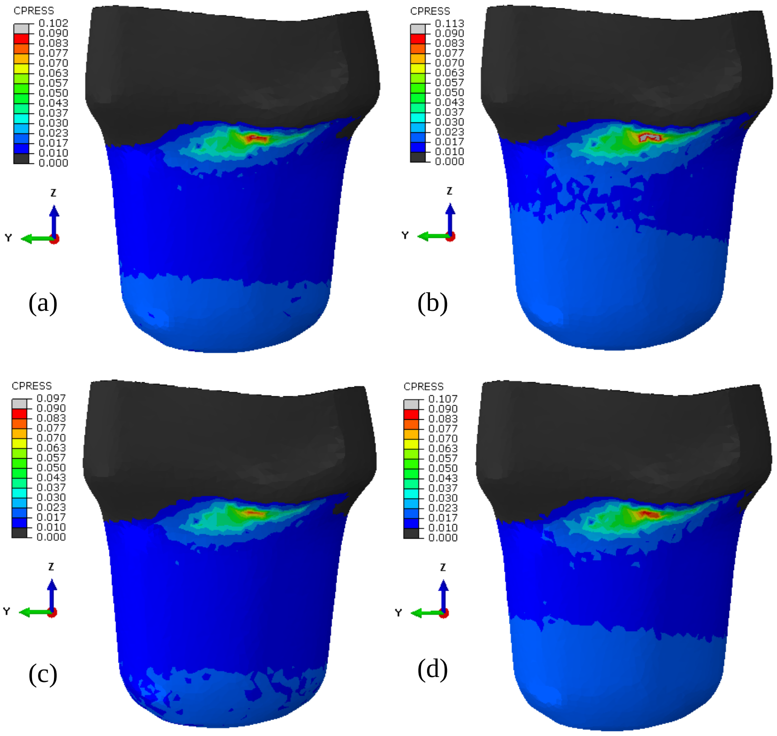

Figure 5-7: Peak contact pressure locations on the residual limb of participant 2 for models; High/Low, High/Medium, Medium/Low & Medium/Medium respectively (a, b, c & d respectively).

5.2.4 Discussion

This section demonstrates that the stresses experienced on the soft tissue and liner are influenced by the friction coefficients applied at the soft tissue and liner, as well as the liner and socket interfaces. The results of the normal and shear stresses for every participant followed the same trend, with the stresses in the *RL-Med/LS-Low* model, followed by the *RL-High/LS-Low*, *RL-Med/LS-Med* model and peaking for the *RL-High/LS-Med* model (see Figure 5-5). This trend was also observed on both the external soft tissue and liner surfaces. These trends were more pronounced for circumferential shear stress in comparison to longitudinal. Changes between Low and Medium levels of friction applied at the liner-socket interface produced more fluctuations of interfacial pressure compared to changes between Medium and High at the residuum-liner interface (see Figure 5-5). Liners with higher friction coefficients supported more of the applied load by frictional forces, reducing the movement between the contacting interfaces and encouraging localised stresses as the tissues underwent larger displacements. Liners with Low coefficient of friction at the liner-socket interface produced the lowest stresses on the residuum, these liners also allowed sufficiently more slip to occur at the liner-socket interface. Indicating that the slippage distributes the stresses over a larger area reducing localised stresses. This trend can be observed in by comparing Figure 5-5 and Figure 5-6, where the models with a ‘Low’ COF at the external liner surface resulted in lower peak stresses. So reducing the COF at these interfaces would be beneficial in reducing the potential for damage to the soft tissues due to reduced peak stresses (see Section 2.1.1), but this can also lead to negative effects during ambulation such as reduced proprioception, pistoning, and even the socket falling off during swing phase of gait in cases of sufficient slippage (Sanders et al. 2004).

The friction coefficient thresholds for the liner in the three FE models simulated was chosen from the spread of results from the friction testing performed in this chapter as well as previous studies. Table 5-5 compares the liner friction testing results to the friction thresholds used to define the four variations of friction models. This table shows all the liners tested exhibited COF values of ‘High’ or above on the internal liner surface in dry conditions. Liners 1, 2 and 3 exhibited COF values classified as ‘Low’ whilst Liners 4 and 5 were classified as ‘Medium’. Therefore, all the liners would be classified as *RL-High/LS-Low* and *RL-High/LS-Med* in their dry conditions.

However, it can be assumed that after the initial period of use the COF at the residuum/liner interface would be altered due to increased perspiration from activity to reflect the results of the wet friction testing conditions. Whilst the friction coefficient threshold for Liners 1, 2 & 4 would remain unchanged under the wet conditions, this would cause distinct differences of the stresses on the residuum for Liners 3 & 5. Under wet conditions, Liner 3 would be changed from *RL-High/LS-Low* to fall between the friction thresholds of *RL-High/LS-Low* and *RL-Med/LS-Low*, whereas Liner 5 would be changed from *RL-High/LS-Med* to *RL-Med/LS-Med*. Therefore, under the wet condition thresholds, Liner 3 would produce the lowest stresses and Liner 4 the highest stresses on the residuum of all participants in this study.

Table 5-5: Friction testing results with comparative thresholds.

Liner	Internal COF (dry)	Comparative threshold	Internal COF (wet)	Comparative threshold	External COF	Comparative threshold
1	**1.83**	High	**1.04**	High	**0.32**	Low
2	**1.46**	High	**1.02**	High	**0.27**	Low
3	**1.39**	High	**0.73**	High/Medium	**0.25**	Low
4	**1.31**	High	**0.94**	High	**0.48**	Medium
5	**1.24**	High	**0.64**	Medium	**0.58**	Medium

Participants 1 and 2 showed a smaller change in peak pressure at the residuum-liner interface as a result of friction coefficient change compared to participant 3 (see Figure 5-4). In comparison, participant 3 showed smaller changes in peak pressure at the liner-socket interface as a result of friction coefficient changes compared to the other two participants. The larger variation of participant 3 could be attributed to friction playing a larger role in supporting the residuum in the socket. This would be due to the longer conical shape of the residuum in comparison to participant 1 (short conical) and participant 2 (short cylindrical) (see Figure 5-4) allowing for a larger contact area and effective conical angle (Zhang et al. 1996). In addition, the peak stresses were located at the ischium, the pelvis geometry and amount of tissue covering the bony prominence may have justified the variations between the participant models. For all variations in friction models, the shear stresses experienced on the external soft tissue surface were lower than those experienced on the external surface of the liner. However, this change in shear stresses between the surfaces was not significant in terms of value. In comparison, the normal stresses were dissipated through the liner resulting in a reduction range of 23.0 to 53.1%

in peak pressure from the external liner surface to the external soft tissue surface across all participant models.

The highest peak contact pressure on the soft tissue for the *RL-High/LS-Med* model was 127.1, 113.4 and 137.3 kPa for participants 1, 2 and 3, respectively. These values are similar to those previously achieved in trans-femoral FE models, 119.3 kPa (Zhang et al. 2013) and 81.7 to 151.2 kPa (Vélez Zea et al. 2015). However, there are variations between this study and the comparative FEA studies, with this study including a liner and the pelvic bone in the bony geometry used. A liner reduces the peak pressures experienced by the soft tissue, and the pelvic bone has been shown to alter the value and location of pressures experienced by the trans-femoral residuum, concentrating them to the region of the ischium compared to just the residual femoral bone, as shown in Chapter 4. The peak circumferential and longitudinal shear stresses ranged from 53.3 to 70.1 kPa and 21.0 to 30.7 kPa respectively for all three participants. Comparatively, Zhang et al. (2013) simulated contact between a trans-femoral residuum and socket with a friction coefficient of 0.5 and reported peaks of 103.6 kPa circumferential and 25.7 kPa longitudinal shear stress. The values reported by Zhang and colleagues (2013) are of similar magnitude to this study, with higher circumferential shear compared to longitudinal, there are differences between the studies. The model simulated by Zhang and colleagues (2013) did not include a prosthetic liner, and applied ambulatory load recorded from a previous trans-tibial study (Lee et al. 2004) which included a horizontal load component as well as an axial load, compared to the axial load applied in this study. Cagle et al. (2018) reported a peak resultant shear stress of 50 kPa on the trans-tibial residuum with a simulated liner. The values reported within this study agree with both of these studies.

A peak pressure of up to 220.8 kPa on the external liner surface (participant 1) was reported in this study. This is of similar magnitude to previous in-vivo transducer studies, 240 kPa reported by Morotti et al. (2014) and 254.7 kPa reported by Kahle and Highsmith (2013). The pressure on the external soft tissue surface was reduced by between 23.0% to 53.1% compared to the pressure on the external surface of the liner across all models. This shows the amount by which the liner is able to reduce the pressure exerted on the residual limb as well as the variation that can occur due to studies reporting values at either the soft tissue-liner or liner-socket interface.

For all participants, the amount of average slip between soft tissue and liner can be considered negligible with a 'High' and 'Medium' friction coefficient (see Figure 5-6). Therefore, it can be assumed that no slip would occur at the residuum/liner interface for any of the liners tested under both dry and wet conditions in Section 5.2.1. The maximum slip at the liner-socket interface was 0.025mm when a 'Medium' friction coefficient was applied. This amount of slip can be considered insignificant in comparison to the slip of up to 0.715mm at the liner-socket interface for a 'Low' friction coefficient. The change in slip at the liner-socket interface when applying 'Low' and 'Medium' friction coefficients indicates that, 'Low' friction coefficient (0.2) may induce slippage in a clinical setting. Whilst the 'Low' (0.2) value is beneath the lowest friction value of 0.25 reported for the nylon external textured liners in Section 5.2.1, this indicates the two liners tested in Section 5.2.1 would be more likely to allow for slippage between liner and socket compared to their cotton counterparts, which ranged from 0.32 and 0.59 (see Figure 5-2). Upon simulation completion, a number of the models had open contact between soft tissue and liner at the most proximal regions, above the socket brim of the model. Therefore, the average slip of the volume region of the residuum (see Figure 5-4) was chosen to represent the relative slip rather than maximum slip.

The heating aspect of a liner is a contributing factor when prescribing a liner to a patient. Brienza et al. (2015) hypothesised that in the presence of slippage at the prosthetic interfaces, the shear strain would be less in magnitude but accompanied by other factors such as heating of the tissue. The results of this section agree with their statement, in that the models with less slip at the soft tissue and liner, and liner and socket interfaces resulted in greater peak magnitudes of shear stresses (see Figure 5-5) compared to the models with greater slip at the specific interface. From the results and Brienza's hypothesis, the model of *RL-High/LS-Med* would produce a reduced heating factor at the residuum-liner interface, and would therefore be more suitable paired with a highly active amputee when considering reducing the levels of perspiration during use compared to the opposing *RL-Med/LS-Low* model which would produce the highest heating factor.

Dai et al. (2006) used a FE model of the foot to examine the stresses exerted on the plantar soft tissue during flat stance phase due to the changing of friction values at the foot-socket and sock-insole interfaces in three friction scenarios. In accordance with the results of this study, Dai and colleagues reported a greater allowance for relative sliding between the foot and footwear with a lower friction coefficient. Interestingly, they reported significant reductions in shear stresses, and only minor reductions in contact pressure on the soft tissues with reduced friction coefficients. The results by Dai and colleagues are consistent with the findings in this section, in that lower friction coefficient reduces the shear stresses on the soft tissues. The results of the residual limb models in this section found significant changes in contact pressure due to changes in friction coefficient, whereas Dai et al. (2006) reported only minor changes. The reasoning for this difference may be due to the geometry of the FE models and the boundary conditions applied. The geometry of a flat stance foot provides a horizontal platform for load bearing, whilst the load within a socket is supported by the ischium in combination with the frictional action at the residuum and socket interface (Zhang et al. 1996) due to the conical shape of the residuum. Therefore, the contact pressure on the residuum would be more susceptible to variations of friction coefficients at the residuum, liner, and socket interfaces as it would affect the amount of friction action and support this provides.

For all participants, the majority of the tensile and compressive strains were located surrounding the ischium and the distal end of the residual femur. This combination of peak strain location could be attributed to the use of a Boolean fit socket, in which there was contact between the distal end of the residual limb and socket allowing for distal loading. With a non-distal loading socket, it could be hypothesised that the strains may be contained more to the ischial support region than reported in this study. For all participants, marginally higher tensile and compressive strains were found in the models with a 'High' friction coefficient between soft tissue and liner compared to a 'Medium' friction coefficient. In an above-knee FEA study, Ramírez and Vélez (2012) found 110% and 82.3% peak compressive and tensile strain, respectively. Similarly, in this study the peak mean principal logarithm strain values are 84.6% and 141.9% for participant 2 in tensile and compressive strain respectively (see Table 5-4).

Lacroix and Patiño (2011) found 53.2 ± 13.7% and 32.4 ± 16.7% mean peak compressive and tensile principal strain, comparatively the strains reported in this study were more than two-fold greater. These differences are accredited to Lacroix and Patiño (2011) simulating only the donning phase, whilst an amputee walking load was used in this study.

5.2.5 Clinical Relevance

The Seal-In liner from Ossur which was included in the friction testing had a sealing membrane ring around the distal end of the external liner surface. This membrane has been stated to increase the adhesion between liner and socket. As changes at the liner-socket interface have been shown to alter the stresses at the residuum-liner interface, the models of this section may be readily adapted to include areas of increased or decreased COF at either interface to simulate the sealing membrane. Further, this would help determine the optimum size and placement of the areas of altered friction on the external liner surface.

Changes at the liner-socket interface were shown to alter the stresses at the residuum-liner interface. As the peak stresses were located at the ischium, it may be beneficial to reduce the friction coefficient of an area on the external surface of the liner located over the ischial tuberosity. This may allow the liner area covering the ischium to provide the cushioning support inherent to the liner properties, but also to some extent reduce the stresses at the ischium due to the reduced friction and larger distribution of stresses. However, too little friction would induce slippage and have adverse effects, especially in IC sockets where the medio-lateral stability is achieved by containment of the ischium within the socket.

5.2.6 Conclusion

In this section, trans-femoral FE models were used to examine the effect of altering the friction properties at the soft tissue-liner and liner-socket interfaces. It was revealed that a change of friction at either interface affected the stresses experienced by the residuum. Higher friction coefficient led to more of the load being supported by frictional force and more localised stresses. Whereas lower friction coefficients allowed more slippage and reduced localised normal and shear stresses due to the load being more evenly distributed. Liners with higher friction coefficients supported more of the applied load by frictional forces reducing the displacement and encouraging localised stresses. Liners with ‘Low’ coefficient of friction at the liner-socket interface produced lowest stresses on the residuum, these liners also allowed sufficiently more slip to occur at the liner-socket interface. Further, it is evidence that a balance must be found between low friction to reduce peak interfacial stresses, but not too low enough to induce slipping.

The model combination of *RL-High/LS-Med* consistently produced the greatest stresses on residuum and liner whilst the *RL-Med/LS-Low* friction combination produced to the lowest. The liner reduced the peak pressures on the residuum but had a small effect on the shear stresses. Changes in friction coefficients showed only a small effect on the strains experienced by the soft tissue. This would suggest that a reduction in friction may reduce the potential for superficial soft tissue damage on the residuum, however it may not be effective in reducing the potential for deep tissue injuries which may be more suitable at determining deep tissue injury in comparison to interfacial stresses. Negligible average slip occurred at the soft tissue-liner interface, whilst a ‘Low’ friction coefficient produced much greater average slip at the liner-socket interface. This study demonstrates that the friction coefficients on both sides of the prosthetic liner varies between products and the resultant stresses on the residuum are susceptible to these changes. Therefore, the friction coefficients at both interfaces should be considered when analysing the lower limb residuum by FE modelling.

By comparing the trends from FE model results with the experimental liner friction results, it is evident that the friction values for Liner 2 would produce the highest stresses on the residuum during use but would have insignificant slip at either interface allowing for maximum control and proprioception for the user. Conversely, the friction values of Liner 5 would produce reduced stresses on the residuum due to its lower friction coefficients at both interfaces but may be susceptible to slippage at the liner/socket interface which may affect the user’s control over the prosthesis.

The friction coefficient is one key variable of a prosthetic liner and has been examined in this section. However, there are multiple differences that influence liner selection. The use of scenario analysis for the pairing between an individual’s residuum and specific liner would more greatly aid the liner selection process and will be examined in the next section.

5.3 Liner Variables

A study by Sanders et al. (2004) examining the material properties of multiple liners confirmed the idea that a bony residuum with a limited amount of soft tissue would be favourably paired with a liner of reduced stiffness to provide greater cushioning and therefore comfort. Conversely, a residuum with excessive soft tissue would be favourably paired with a stiffer and therefore less deformable liner to maintain a higher level of proprioception for the user (Sanders et al. 2004). Whilst this study provided a useful insight into the pairing between liner and residuum given the liner properties, the majority of studies that followed involving liners have focused on the mechanical properties (Klute et al. 2010) with a limited number examining their consequential effect, such as the residuum stresses (Lin et al. 2004) or biomechanics (Boutwell et al. 2012). Arguably the main properties of a liner are the stiffness and thickness as they are directly related to the liners ability to provide cushioning (Lin et al. 2004; Boutwell et al. 2012). As the liner is being matched to the residuum, the properties of the residual limb should therefore also be considered.

Matching a liner to a patient can be challenging, with the current clinical prescription practice still being primarily based on clinician experience, product literature, colleague recommendations and intuition. For example, if a certain liner appeared to be successful for a patient, the clinician would often recommend the same liner to similar patients. Therefore, there is a growing movement for scientific evidence to accompany the decisions made when providing prescription decisions (Klute et al. 2010). A survey study of prosthetists by Hafner et al. (2017) concluded that from the wide range of liners available, only a select few were regularly prescribed by the prosthetists.

The objective of this section was therefore to develop a preliminary framework for a database involving the common variables of liner stiffness, liner thickness and residual soft tissue stiffness and their impact on the stresses experienced by the residual limb. The pressures experienced by the individual on the residual limb are indicative of comfort (Lee et al. 2007) and may therefore be useful in the determining the correct pairing of liner to the residuum. This was performed with the use of a single unilateral trans-femoral FEM. This preliminary database could in turn be used to provide a more informative process of liner selection in a clinical setting.

5.3.1 Modelling Method

For this section, the model consisting of; bone (residual femur and hemi-pelvis), soft tissue, prosthetic liner, and prosthetic socket for participant 1 was used (see Figure 5-8). The acquisition and reconstruction of the model is detailed in Section 3.2.

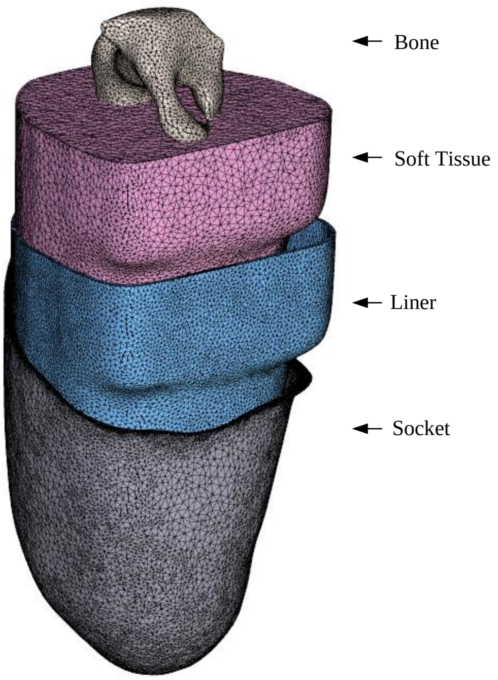

Figure 5-8: Complete residuum model with tetrahedral meshing. Positioning of parts have been modified to display all parts.

The variable parameters of liner thickness (LT), liner stiffness (LS) and muscle type (soft tissue stiffness) (MT) were examined in this study (see Table 5-6).

Table 5-6: Variable value parameters of liner thickness, liner stiffness and muscle type.

	Variable		
	Liner thickness	**Liner stiffness**	**Muscle type (hyperelastic models)**
Thresholds	1. 4 mm 2. 5 mm 3. 6 mm	1. 50 kPa 2. 100 kPa 3. 200 kPa 4. 400 kPa	1. Average flaccid muscle 2. Stiff flaccid muscle 3. Contracted muscle

Experimental studies have reported values of E 30 – 275 kPa across a wide range of urethane, TPE, silicone gel and silicone elastomer liner materials under both compression and tensile testing (Sanders et al. 2004; Cavaco et al. 2015). Across a range of 23 prosthetic liner products, Cagle et al. (2017) reported values of E 96 – 458 kPa for compression testing. This included a range of 116 – 384 kPa for the liner products from Ottobock and Ossur obtained and tested in the friction testing in Section 5.2.1 of this thesis. These studies also reported a Poisson ratio of 0.45-0.49 (Sanders et al. 2004; Cavaco et al. 2015; Cagle et al. 2018). Therefore, liner stiffness of 50, 100, 200 & 400 kPa with a Poisson ratio of 0.45 were chosen to encompass the most notable variety reported in previous studies and product literatures.

Uniform liner thicknesses of 4mm, 5mm & 6mm were chosen as these are amongst the most common thickness used for trans-femoral cases (Sanders et al. 2004; Sanders et al. 1998) and are widely available for liner products (Ossur 2011; WillowWood, 2018; Ottobock, 2015). It should be noted that a liner thickness may be as low as 2mm and have a tapered fit with a greater thickness at the distal end to provide protection over the end of the residuum. A liner thickness below 4mm was considered but proved problematic in achieving convergence due to the vast increase of elements required in the liner part to prevent element shear locking. Therefore, the lowest liner thickness was chosen as 4mm. The tapered feature of the liner can vary as required and was also not included as it created modelling difficulties with the Boolean liner and socket fit. For each liner thickness, the fit of the socket was adjusted to maintain a Boolean fit between liner and socket.

The matching process of liner to residuum should also take into consideration the properties of the residuum, as it has been hypothesised that a bulky residuum would favour a thinner liner to maintain prosthesis control, whilst a bony residuum would favour a thicker liner to provide greater cushioning. Therefore, three variations of muscle type were applied as hyperelastic representations of ‘Average flaccid muscle’, ‘Stiff flaccid muscle’ and ‘Contracted muscle’ publicised by Portnoy et al. (2009) from the works of Palevski et al. (2006) and Hoyt et al. (2008). These stiffness’s were chosen to replicate different variations of the muscle tone in the residuum, which may result from surgical myodesis and/or an individual’s activity levels (Mak et al. 1994), as this can be influential in liner selection (Hafner et al. 2017). The soft tissue equivalent modulus for the constitutive parameters were calculated by derived equations (see Section 3.2.6) and were 25.4, 37.1 & 48.3 kPa for the average flaccid, stiff flaccid and contracted muscle types respectively.

A 3-dimensional array of 3x4x3 datasets was created for results of ambulatory residuum simulations that were carried out. This involved three variations of liner thickness, four variations of liner stiffness and three variations of soft tissue stiffness. A total of 36 simulations were performed. This is shown in Figure 5-9, with the rows, columns and pages of the array being represented as liner thickness, liner stiffness and soft tissue stiffness, respectively. For example, (2,3,1) refers to the model with 5mm liner thickness, 200 kPa liner stiffness, and a muscle type of ‘Average flaccid muscle’.

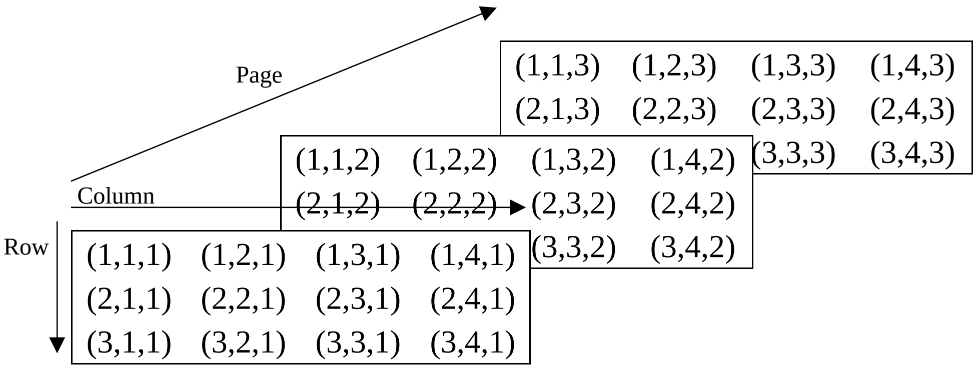

Figure 5-9: 3-dimensional array for liner thickness (row), liner stiffness (column) and muscle property (page) for a total of 36 simulations.

5.3.1.1 Convergence Testing

The FE models were verified by the mesh convergence testing method shown in Section 3.2.4. Convergence was obtained for the model variant with 4mm liner thickness, 400 kPa liner stiffness and average flaccid muscle properties. The mesh convergence results for the models used in this study can be found in Appendix Chapter 3 Supporting Evidence.

The average run time for the models was approximately 38 hours, using a Quad Core CPU i5-4590, 3.30 GHz and 16.0GB RAM computer.

5.3.1.2 Material Properties

The mechanical properties of the bone, liner and socket were assumed to be linear elastic, isotropic and homogeneous. The soft tissues were defined using the Extended Mooney-Rivlin strain energy function with added compressibility. The material properties used for this section are defined in Table 5-7.

Table 5-7: Material properties for all parts used in the liner variables simulations.

	Part	Young's Modulus (MPa)	Poisson's Ratio
	Bone	15000	0.3
	Socket	1500	0.3
	Liner	0.05, 0.1, 0.2 & 0.4	0.4
Soft Tissue	*Average flaccid muscle*	$C_{10} = 0.00425$, $C_{11} = 0$, $D_1 = 2.36$	
	Stiff flaccid muscle	$C_{10} = 0.0062$, $C_{11} = 0$, $D_1 = 1.62$	
	Contracted muscle	$C_{10} = 0.008075$, $C_{11} = 0$, $D_1 = 1.243$	

5.3.1.3 Boundary Conditions and Loads

The boundary conditions and loading applied to these models follow the details given in Section 3.2.7. The bone-soft tissue interface was modelled as tied preventing relative movement. The soft tissue-liner and liner-socket interfaces were modelled with surface to surface frictional contact, preventing the nodes of the slave surface in the contact pair penetrating the master surface. The selected slave surfaces were the soft tissue for the soft tissue-liner interaction, and liner for the liner-socket interaction. The 'Medium' COFs of 0.5 were applied at both the residuum-liner and liner-socket interfaces (*RL-Med/LS-Med*) for this section to replicate Liner 5 of the previous section.

The finite element simulation was carried out in two phases (see Section 3.2.7). The initial phase simulated donning the prosthesis and the pre-stresses produced. This was done by application of a downward 50N load on the proximal region of the bone, whilst the socket movement was constrained (Lee et al. 2004; Zhang et al. 2013; Arotaritei et al. 2015). The pre-stresses from this step were continued into the loading phase. During the loading phase, a uniaxial load equivalent to 110% of each participant's bodyweight was applied to the distal end of the socket whilst the movement of the proximal bone was constrained. The magnitude of this load corresponds to the peak ground reaction force reported for normal ambulation of prosthetic limb users (Vanicek et al. 2009).

5.3.1.4 Potential Limitations

As with all FE studies, modelling and material assumptions must be made, these assumptions must be viewed objectively and their influence on the results acknowledged. The liner stiffness values reported by previous studies to decide the threshold values in this chapter were determined from compressive elasticity testing. Differences have been observed between the compressive and tensile elasticity of liner products, with tensile modulus being lower than compressive modulus (Sanders et al. 2004; Cagle et al. 2018). Cagle et al. (2018) found the tensile modulus of liner products to be 19.5% to 34.4% of the compressive modulus of the selected liner product. The compressive modulus of the liner provides the desired cushioning ability that liners are most commonly used for. Whilst the tensile modulus of the liner would provide good suspension during swing phase, the simulations were modelled at peak ground reaction phase of the gait cycle. Therefore, the results from compressive modulus testing were chosen for the required single material property value input within ABAQUS CAE 2018®.

This study also assumed the liner variables as linear elastic whilst it has been reported that certain types of liners exhibit a non-linear response which can be modelled by a hyperelastic model fit (Cagle et al. 2017). Therefore, incorporating stress-strain data from a range of liners would allow this study type to have a direct reference to commercially available liners.

The liner profile used in this study was uniform, whereas trans-femoral liners are often available in a tapered fit. This was not modelled in this chapter as the thickness of the distal end can be altered depending on the level of distal padding required to protect the distal end of the femoral bone from loading and distal contact. The peak stresses in this chapter were continually located at the proximal medial region of the residuum, therefore it can be assumed that a tapered liner with additional distal padding would have reduced the stresses at the distal end of the residuum but would not have had a great effect on the peak stresses.

Potentially, the main limitation of this chapter is the use of a Boolean socket fit. This socket fit and design has previous used in practice as a total contact/total surface bearing socket (ICRC 2006) and subsequently FE studies have used a Boolean socket fit (Zhang and Mak 1996; Lee et al. 2004; Zhang et al. 2013; Arotaritei et al. 2015). However, recently it is often common clinical practice for the prosthetic socket to be reduced in volume and rectified, in which that socket walls are modified to lessen pressures in sensitive areas and divert it to more tolerant areas (Pirouzi et al. 2014). As these alterations would be made to lessen pressures at sensitive areas, including a rectified socket geometry would potentially reduce localised stresses and provide a more even distribution of stresses.

5.3.2 Results

The comfort acquired from the liner is a key factor in patients' choice to use a liner (Hafner et al. 2017). The perceived comfort is typically related to the pressures and shears experienced by the soft tissue (Lee and Zhang 2007). Therefore, these outputs were the main focus for this study.

The resultant contact pressure and shear stresses from 110% simulated loading with variations of liner thickness and constant liner stiffness and muscle type are shown in Figure 5-10. The resulting 3x4x3 3-dimensional array of data from the simulations are shown in Figure 5-11, Figure 5-12 and Figure 5-13 as surface plots for the contact pressure, circumferential shear stress and longitudinal shear stress, respectively. As expected, increased liner thickness and decreased liner stiffness allowed the liner to undergo greater deformation and the residual limb to displace further into the prosthetic socket resulting in reduced peak pressure and shear stresses across all muscle types. The lower stiffness of the average flaccid muscle allowed the tissue covering the location of peak loading (ischium) and socket to be displaced more compared to the contracted muscle. As a result, this caused greater ischial bearing and led to larger peak stresses for the average flaccid muscle models compared to the contracted muscle models.

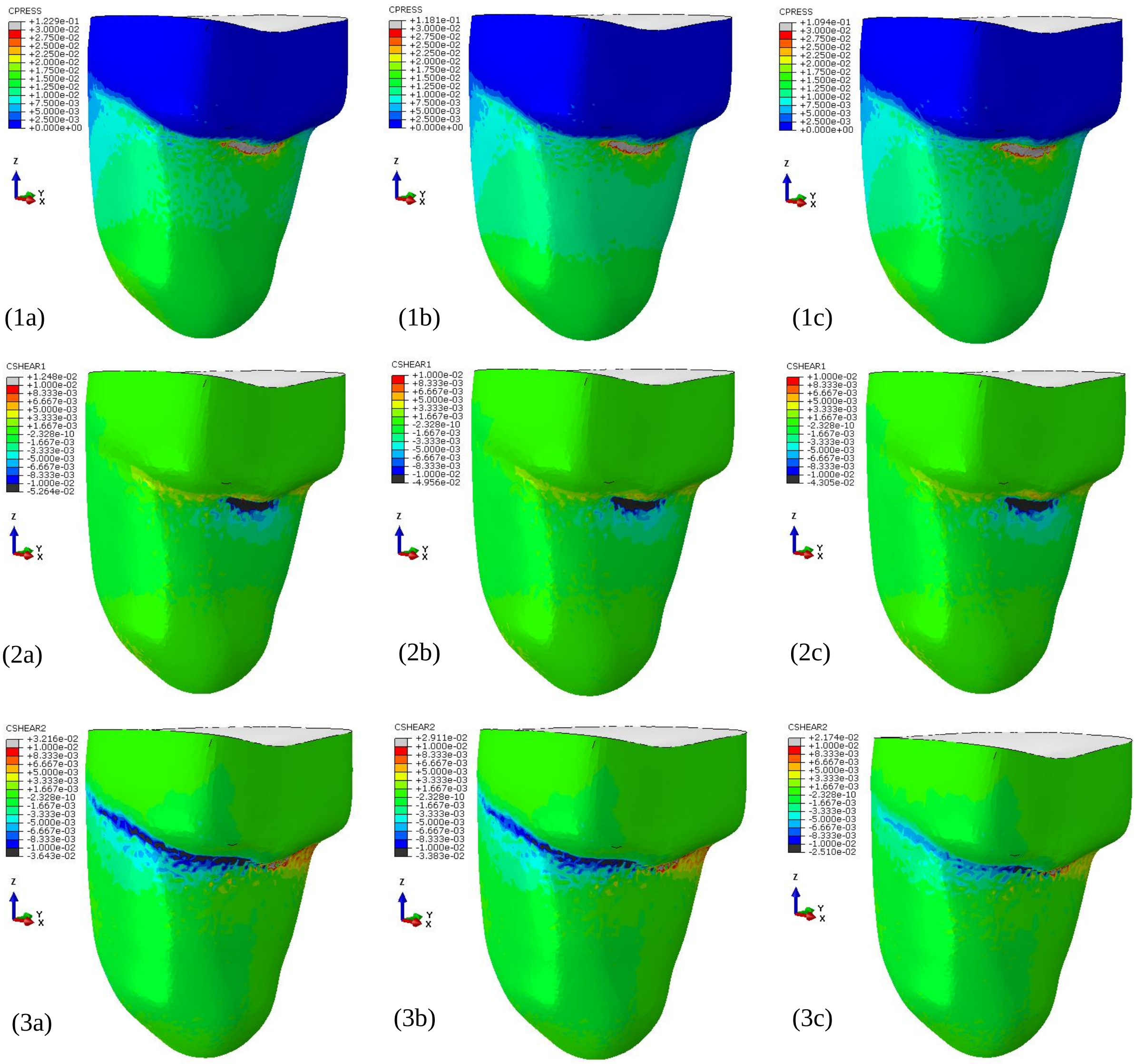

Figure 5-10: Contact pressure (1), circumferential shear (2) and longitudinal shear (3) stresses on the external soft tissue surface for the model with constant 400 kPa liner stiffness and average muscle properties and variations of 4mm (a), 5mm (b) & 6mm (c) liner thickness.

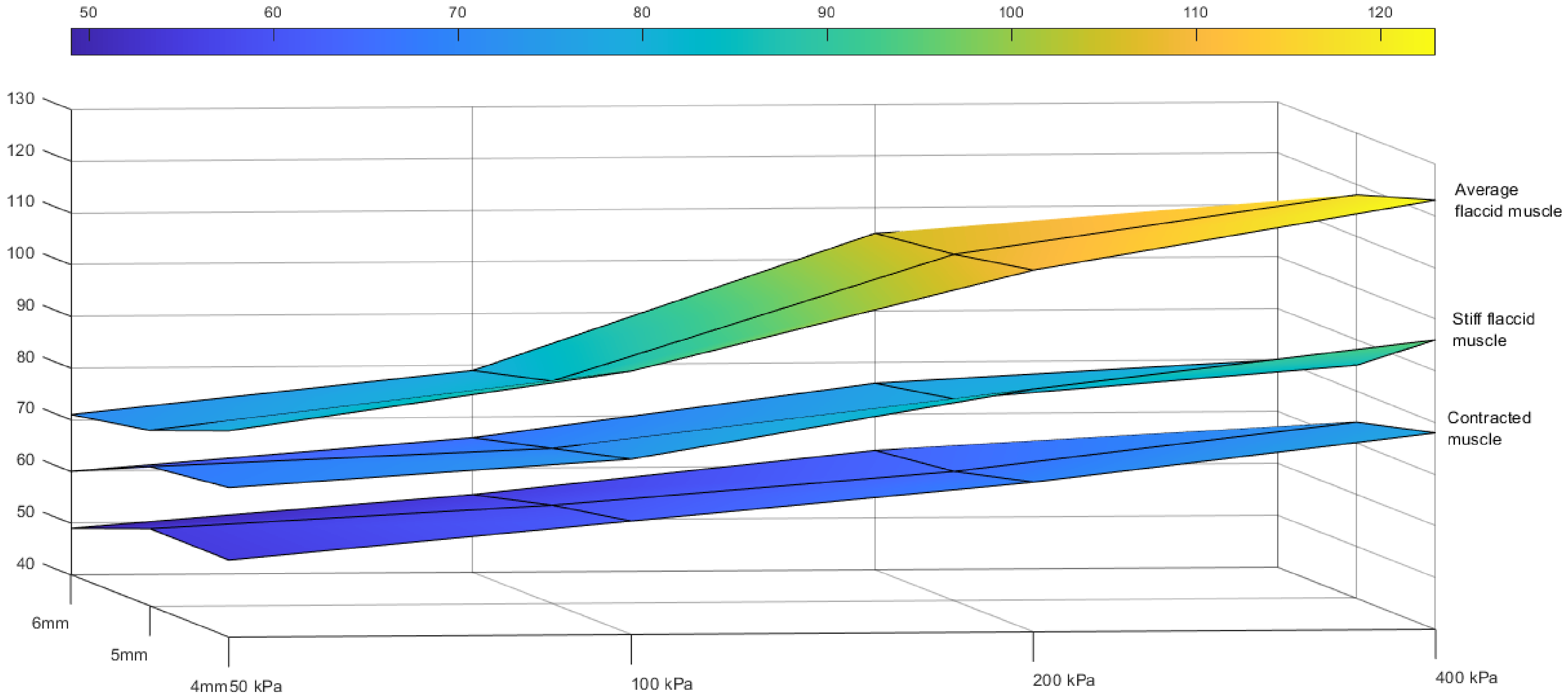

Figure 5-11: 3-dimensional surface plots of the resulting contact pressure for the 3-dimensional data array of variations in liner thickness, liner stiffness and muscle property.

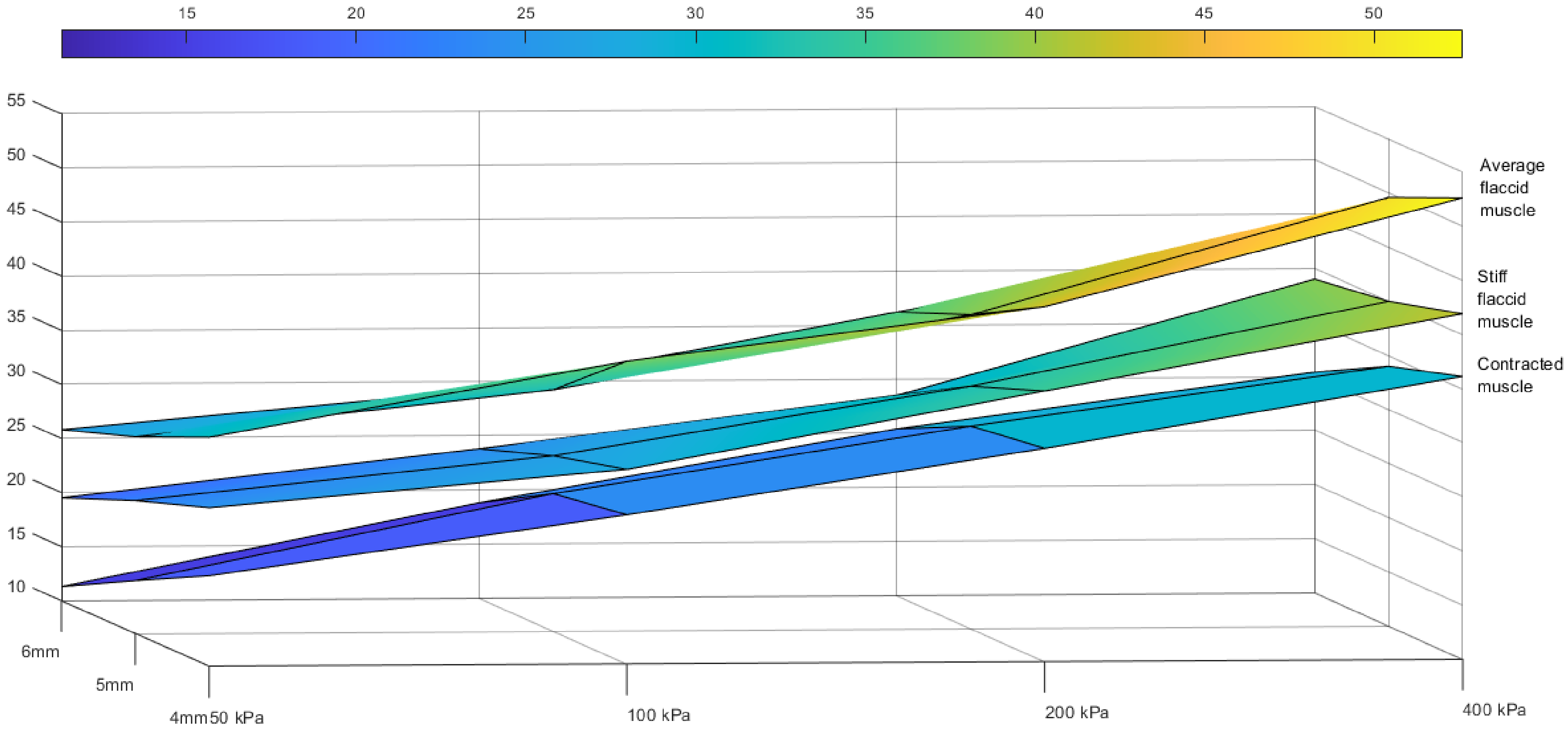

Figure 5-12: 3-dimensional surface plots of the resulting circumferential shear stress for the 3-dimensional data array of variations in liner thickness, liner stiffness and muscle property.

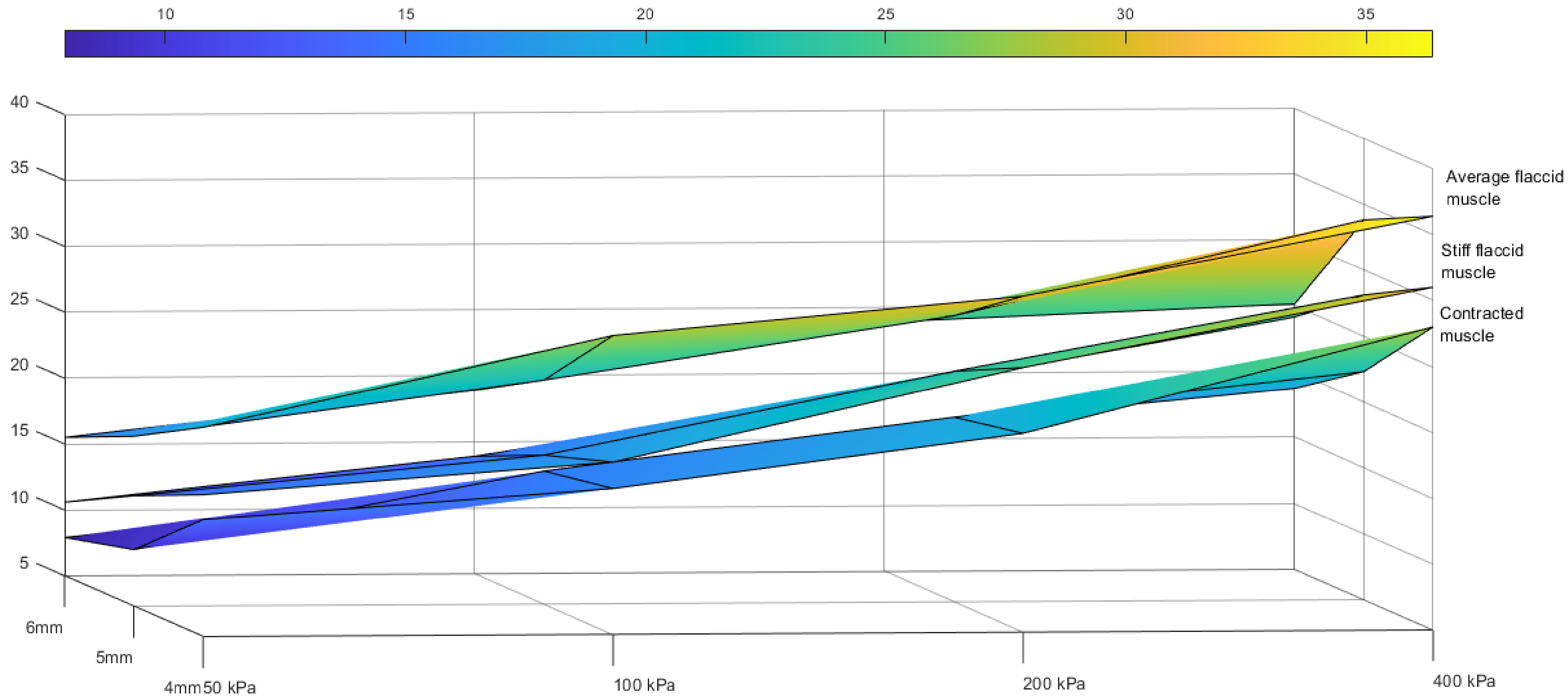

Figure 5-13: 3-dimensional surface plots of the resulting longitudinal shear stress for the 3-dimensional data array of variations in liner thickness, liner stiffness and muscle property.

.

In this section, separately for contact pressure, circumferential shear and longitudinal shear, the resultant value was analysed as the response variable, with muscle type as a categorical fixed effects with three levels (average flaccid, stiff flaccid and contracted muscle), and liner thickness and liner stiffness as continuous covariates in an Analysis of Covariance with first order interaction effects of all fixed effects. For all analyses Bonferroni corrections (significance at $p > 0.05/3$) were applied, to correctly adjust the type 1 error. The estimated marginal means for the first order interactions are shown in Figure 5-14. The full table of results used for the statistical analysis are shown in Appendix Chapter 5 Supporting Evidence.

The analysis of contact pressure gave an adjusted coefficient of determination (R2) value of 0.954, implying over 95% of the total variability in the resultant value is explained by the statistical model. The main effects of liner thickness ($p = 0.008$, ηp2 = 0.240), liner stiffness ($p = 0.001$, ηp2 = 0.334) and muscle property ($p = 0.014$, ηp2 = 0.279) were all found to be statistically significant at Bonferroni adjusted threshold. The interaction effects between liner stiffness by liner thickness and muscle property by liner thickness both showed no statistical significance ($p > 0.0166$). Conversely, the interaction effect between muscle property by liner stiffness showed strong statistical significance ($p < 0.000$, ηp2 = 0.541). Upon further inspection, the significant interaction between liner stiffness and muscle type was found to be made significant due to the contact pressure experienced by the average flaccid muscle type model ($p < 0.000$, ηp2 = 0.483). This can be evidently seen in

Figure 5-14 (1c). **Liner thickness, liner stiffness and muscle property were all found to be statistically significant in terms of contact pressure.**

The analysis on circumferential shear gave an adjusted coefficient of determination (R^2) value of 0.955. The main effects of liner thickness ($p < 0.000$, $\eta_p^2 = 0.407$), liner stiffness ($p = 0.002$, $\eta_p^2 = 0.312$) and muscle property ($p = 0.007$, $\eta_p^2 = 0.317$) were all found to be highly significant. All interaction effects showed no statistical significance ($p > 0.017$). **Liner thickness, liner stiffness and muscle property were all found to be statistically significant in terms of circumferential shear stress.**

The analysis on longitudinal shear gave an adjusted coefficient of determination (R^2) value of 0.941. The main effects of liner thickness ($p < 0.000$, $\eta_p^2 = 0.404$), liner stiffness ($p > 0.000$, $\eta_p^2 = 0.413$) and muscle property ($p = 0.006$, $\eta_p^2 = 0.322$) were all found to be highly significant. All interaction effects showed no statistical significance ($p > 0.017$). **Liner thickness, liner stiffness and muscle property were all found to be statistically significant in terms of longitudinal shear stress.**

The parameter estimates for liner thickness report a value of change in the predicted contact pressure, circumferential shear and longitudinal shear stress (B = 2.781 kPa, B = 2.729 kPa & B = 2.394 kPa respectively) for a one-unit increase (mm) in the liner thickness. This shows that an increase in liner thickness had a similar effect on the resultant contact pressure, circumferential shear stress and a marginally lower effect on longitudinal shear stress. **Changes of 1mm in liner thickness resulted in average changes of 2.781, 2.729 and 2.394 kPa for pressure, circumferential shear, and longitudinal shear stress, respectively.**

The parameter estimates for liner stiffness report B = 0.089 kPa, B = 0.05 kPa & B = 0.052 kPa for contact pressure, circumferential shear, and longitudinal shear stress respectively, for a one-unit increase (kPa) in the liner stiffness. Therefore, increasing the liner stiffness had a greater effect on the resultant contact pressure, with a lower and similar effect on both circumferential and longitudinal shear stress. **Changes of 1 kPa in liner stiffness resulted in average changes of 0.089, 0.05 and 0.052 kPa for pressure, circumferential shear, and longitudinal shear, respectively.**

The goodness of fit of the fitted models was assessed using residual plots. The plots between standardised residuals and predicted values are shown in Figure 5-15. There is no apparent pattern of these residual plots, no areas of high concentration, and an even data point spread. This suggests the use of a linear regression model is appropriate. Any outliers are not observed.

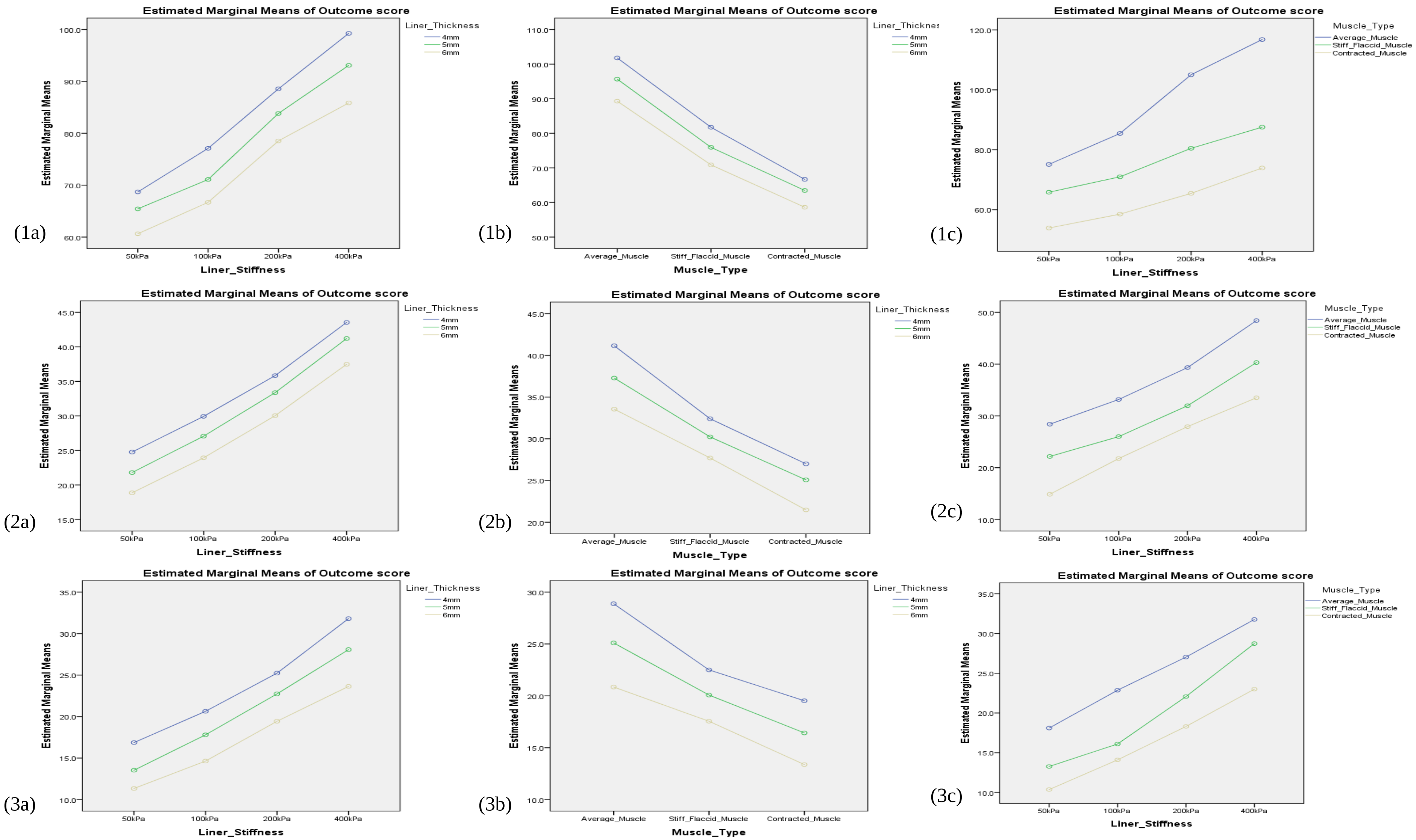

*Figure 5-14: Estimated marginal means maximal contact pressure (1), circumferential shear (2) and longitudinal shear (3) stresses for LT*LS (a), LT*MT (b) and LS*MT (c).*

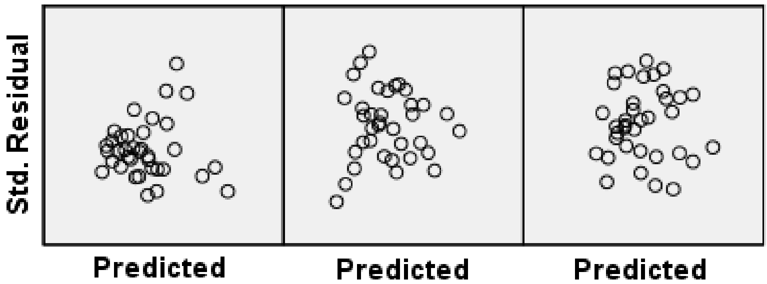

Figure 5-15: Residual plots for predicted contact pressure (left), predicted circumferential shear stress (middle) and predicted longitudinal shear stress (right) outputs.

The compressive strain within the soft tissue was susceptible to the changes in muscle type. A trend of decreasing peak compressive strain occurred as the soft tissue stiffness increased from average flaccid muscle to contracted muscle type (see Figure 5-16). The peak compressive strains were consistently located distal to the ischium, with increasing concentrations also found at the distal end of the residual femur for increased tissue stiffness.

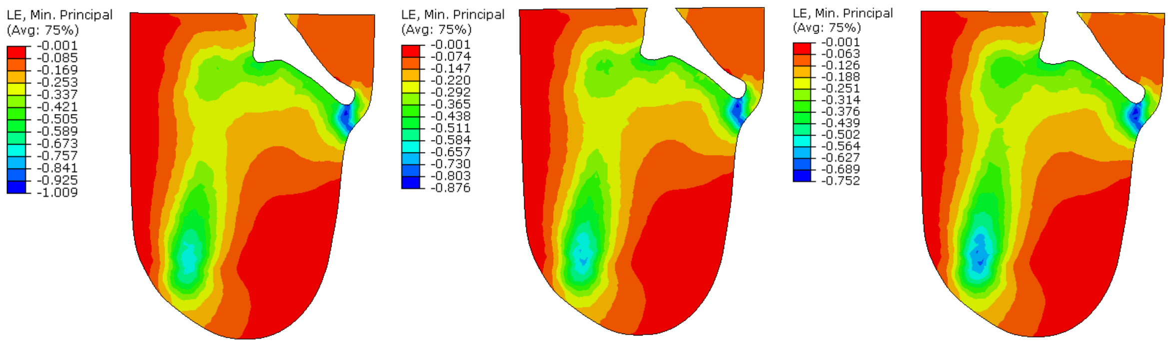

Figure 5-16: Decreasing peak compressive strain with increasing soft tissue stiffness (left: average flaccid muscle, middle: stiff flaccid muscle, right: contracted muscle). Cut through at location of the peak strains and varied between models.

5.3.3 Discussion

As expected, increasing the liner thickness, and reducing the stiffness both resulted in reduced peak pressures and shear stresses in general. An explanation for this would be the thicker and softer liner allows the soft tissue to displace more into the contours of the socket and distributes the applied loads over a large area. As a result, this has been acknowledged as providing improved shock absorption during ambulation (Boutwell et al. 2012). Because of this, a thicker and softer liner is often prescribed to a patient that requires additional cushioning over the residuum (Sanders et al. 2004). Whilst this can be beneficial to reduce the peak stresses on the residuum, which are related to both comfort and tissue viability (Lee et al. 2005; Linder-Ganz et al. 2006), this may also come with detrimental effects when understood in a clinical setting.

Focus has been placed on the liner reducing the peak stresses on the residuum to limit the potential for tissue damage and increase comfort. Conversely, increasing the liner thickness and reducing the liner stiffness to such an extent that significantly reduces the interfacial stresses, but also inhibits the individual's proprioception, would have an overall negative affect. As such, a potential upper and lower threshold of interfacial stresses may exist, where the upper threshold is denoted by the likelihood of the stresses causing discomfort or damage, and the lower threshold by a loss of control from a too loose socket fit. As the peak pressures reported in this section are within the comfort thresholds reported by Lee et al. (2007) it can be assumed that the participant would benefit from the use of the thinner and stiffer liner (i.e. 4mm & 400kPa) as this would be less likely to induce negative alterations to their normal ambulation (Boutwell et al. 2012).

Boutwell and colleagues (2012) compared 3mm and 9mm liner thickness used by bony and padded residual limbs (BRL and PRL respectively) of trans-tibial patients. For BRL patients, the 9mm liner significantly reduced peak pressures across the majority of sensor locations on the residuum compared to the 3mm liner. However, this reduction was not observed for the PRL patients indicating that the PRL patients already had an even pressure distributed present form the bulk of soft tissue which rendered the additional compliance from the thicker liner redundant. The only gait parameter that was found to be statistically significant was the GRF which was greater when patients wore the thicker liner. Interestingly, it may be hypothesised that the thicker liner caused the patient to step with greater force to obtain more sensory feedback to compensate for the reduced proprioception that came with the thicker liner. Whilst the levels of comfort were not monitored in the study, the BRL group overwhelming preferred the 9mm liner, which as it provided no changes to their gait parameter, can be assumed to be due to increased comfort due to reduced peak pressures. The PRL group had mixed preferences but expressed experiences of increased pistoning and increased energy expenditure for the 9mm liner. Pistoning can degrade proprioceptive stability (Latlief et al. 2012) and produce gait deviations that lead to trips and falls (Vanicek et al. 2009). The study by Boutwell et al (2012) highlights the importance of considering a wide variety of residuum shapes and sizes when conducting studies and considering the patients' size and shape and potential detrimental effects of these when prescribing a liner. Interestingly, their study did not consider the changes to the socket when comparing the liners, even though changing between 3mm and 9mm liner would have caused substantial volumetric changes within the socket which can alter the interfacial pressures (Sanders and Fatone 2011).

A study by Lin et al. (2004) examined the effects of liner stiffness for trans-tibial prosthesis by FEA. They found that whilst the peak pressure was almost consistently located at the anterior region of the residuum for variations of 400 – 800 kPa, a liner stiffness of 600 kPa reduced the peak stresses more than either a more or less stiff liner. The results of this study achieved a reduced peak pressure value with a less stiff liner, which appear contradictory to the results by Lin et al. (2004). Differences between these studies may be due to comparisons of trans-femoral and trans-tibial results, for example in a trans-femoral prosthetic socket the load is primarily found at the ischial support whereas for a trans-tibial prosthetic socket the loading is encouraged in multiple locations in both the Patellar Tendon Bearing and Total Surface Bearing socket designs. Therefore, Lin et al. (2004) hypothesised that the non-uniform socket shape could have been the major reason for variations in the interfacial stresses.

The maximal contact pressure range on the soft tissue was 49.5 to 122.9 kPa, with a maximal circumferential shear and longitudinal shear stresses range of 11.3 to 52.6 kPa and 7.9 to 36.4 kPa respectively. For each muscle type, the greatest normal and shear stresses were found with a combination of stiffer (400 kPa) and thinner (4mm) liner properties. Thus, the lowest normal and shear stresses were found with an opposing combination of less stiff and thicker liner. This trend is evident in Figure 5-10. Comparatively, Vélez Zea et al. (2015) reported a contact pressure range of 81.7 to 151.2 kPa for a variation of residuum lengths. The experimental results of Kahle and Highsmith (2013) reported an average peak pressure between skin and liner of 112 and 109 kPa for a variation of ischial containment and brimless trans-femoral sockets. Morotti et al. (2014) obtained a peak pressure value of 240 kPa, their study did not use a liner between socket and residuum which can be regarded the reason for the differences in values. Pressure values of these previous FEA and experimental studies agree with the results reported in this study.

Shear stresses have been less commonly reported in previous FEA, and the ability to report shear stresses in experimental studies with sensors proving costly and problematic (Laszczak et al. 2016). Laszczak et al (2016) reported a 26 kPa peak shear value for a pilot sensor test with a knee-disarticulate subject. A trans-tibial FE model study by Cagle et al. (2018) showed a mean shear value of 27 kPa. These previous shear values fall within the range reported in this study. However, frictional properties have been shown to vary between liners (Sanders et al. 2004), with variations of friction coefficients between residuum and socket altering the experienced shear stresses (Restrepo et al. 2014). Therefore, friction coefficient should also be considered as another potential variable of the liners.

The statistical analysis of this study showed that each main effect of liner thickness, liner stiffness and muscle properties were all statistically significant for the resultant normal, circumferential, and longitudinal shear stresses experienced by the residuum. Thus, they are all important considerations in the pairing process of residuum and liner. Besides the interaction effect between muscle property by liner stiffness for normal stress, no other interaction effects were found to be significant, meaning no interaction between each main effect was affecting the results above and beyond that already from the main effects.

The parameter estimates reported for liner thickness and stiffness show that, on average, a change of 50 kPa in liner stiffness alters the circumferential and longitudinal shear stress by ±2.500 kPa and ±2.600 kPa respectively from this study. Similarly, a change of 1mm in liner thickness has a similar effect on the circumferential and longitudinal shear stress by ±2.729 kPa and ±2.394 kPa respectively. However, a change of 50 kPa in liner stiffness alters the normal stress by ±4.45 kPa which is approximately double compared to the change of 1mm in liner thickness altering the normal stress by ±2.781 kPa. Therefore, when pairing a liner to the residuum geometry of participant 1, changes in liner thickness and stiffness are equally as suitable in altering the shear stress values, whilst changes in liner stiffness are the dominant factor in altering the contact pressure. This suggests, for a patient suffering from pressure sensitive areas on the residuum, it would be more beneficial to alter their liner prescription to a softer liner rather than a thicker liner. Unfortunately, it is common clinical practice for the prosthetist to prescribe a liner based on the thickness properties as this information is readily available for the commercial liners in the product information (Hafner et al. 2017). Whereas the information relating to liner stiffness is not readily available for individual products and is almost only available from previously conducted scientific research (Sanders et al. 2004). Therefore, if liner stiffness information was more available to the prosthetist, they may make more of an active decision when prescribing the products available to them.

In the previous section (5.2.2) it was shown that lower friction levels at the residuum-liner and liner-socket interface resulted in lower peak stresses on the residual limb. For the previous section, the properties of ‘Average flaccid muscle’, 400 kPa liner stiffness and 4mm liner thickness were used. The range of COFs applied at both interfaces in the previous section produced similar interfacial stresses caused by changing the liner thickness from 4mm to 6mm in this section. Alterations of the liner stiffness induced the largest magnitude of interfacial stress changes. Comparing the results from the two sections (Sections 5.2.2 and 5.3), reducing the COF at the liner-socket interface to ‘Low’ resulted in similar reductions in peak pressures and circumferential shear stress (122.9 kPa to approximately 110 kPa, and 52.6 kPa to 43 kPa respectively) as reducing the liner stiffness from 400 kPa to 200 kPa and increasing the liner thickness from 4mm to 6mm. However, the change in COF also resulted in more of a reduction to the peak longitudinal shear stress compared to changes in liner stiffness and thickness (36.4 kPa to 18.0 kPa, and 36.4 kPa to approximately 30 kPa). This is likely due to the inducing of slippage that also occurred for the ‘Low’ COF (see Figure 5-6), this indicates that reducing the liner thickness and stiffness may be more favourable for reducing the interfacial stresses without allowing slippage and potential loss of proprioception for the user.

Work has been conducted to standardise the testing protocols across commercially available liners to reduce the variations in literature (Cagle et al. 2017). Previous studies which have considered the liner properties have not also considered the muscle tone of the pairing residuum, although this has been recommended previously (Sanders et al. 2004). The properties of the residual limb have greater variation versus the liner, primarily due to differences between tissue composition (muscle, fat and skin), anatomical location, contractible muscle and individuals (Sherk et al. 2010; Pascale and Potter 2014). These variations are inherently transferred into the development of constitutive models used to describe the material behaviour. The hyperelastic muscle models applied in this study were taken from a combination of porcine and human tests (Palevski et al. 2006; Hoyt et al. 2008). These were used to more accurately describe the non-linear tissue behaviour compared to linear elastic models, and to represent the range of contractible intact musculature following surgical amputation (Portnoy et al. 2009). The hyperelastic models used could not be considered as a continuous covariate along with liner thickness and stiffness due to the intrinsic non-linear properties. The effect of the muscle properties on the interfacial stresses was found to be statistically significant.

Increasing the soft tissue stiffness substantially decreased the peak compressive strain (see Figure 5-16). Demonstrating the magnitude of compressive strain is closely coupled with the stiffness of the soft tissues, as tissues of increased stiffness transfer the strain concentrations to nearby tissues and the bony prominences. As the concentrations of compressive strains have been linked to soft tissue damage (see Section 2.1.1), this would indicate the stiffness of the residual limb would adjust the residuum’s susceptibility to strain induced damage. For example, an active individual with larger muscle composition in their residual limb would result in reduced peak compressive strains compared to a residuum with higher levels of adipose tissue. This trend agrees with previous FEA studies of the trans-tibial residuum which both reported decreased compressive strain with increasing soft tissue stiffness (Portnoy et al. 2009; Steer et al. 2019). Conversely, these studies had conflicting results for interfacial stresses, as it was reported that increased tissue stiffness produced increased stresses by Portnoy et al. (2009) and decreased stresses by Steer et al. (2019). As both studies used the same material properties used in this section (see Table 5-7) this suggests the conflicting interfacial stresses results were caused by differences in their modelling setup. The study by Steer et al. (2019) included a prosthetic liner, whereas this was not included by Portnoy et al. (2009). Furthermore, the studies used different socket geometries such as a plaster cast replica of the residuum (Boolean fit) (Portnoy et al. 2009) and a total surface bearing socket (Steer et al. 2019). As demonstrated in the current and previous section, the variables introduced when modelling a prosthetic liner (friction coefficient, liner thickness and liner stiffness) greatly affect the resultant stresses. The effect of the prosthetic socket design on the interfacial stresses is examined in Chapter 6.

Reduced peak pressure for increased soft tissue stiffness has similarly been reported for the trans-tibial residual limb models (Steer et al. 2019). Interestingly, clinical studies have shown differences in muscle activity between trans-femoral amputees and non-disabled volunteers, with greater variability in muscle activation within the trans-femoral group compared to the non-disabled group (Pantall and Ewins 2013). This contraction of residual limb muscles can result in a significant increase of 5.8% in residuum volume when the limb was contracted versus relaxed, reducing up to 3.5% when a liner was donned (Lilja et al. 1999). These implications of muscle contractions were not modelled in the contracted muscle models. Accordingly, it may be assumed the volume increase would greatly change the peak stresses and stress distribution on the residual limb.

5.3.4 Clinical Relevance

The optimal liner properties are not a 'one size fits all', providing optimal levels of stability are often achieved at the expense of comfort. This requires the prescription process to be on a more case-by-case basis than it currently is (Hafner et al. 2017). There is information on the material properties of the liners commercially available, however the resulting effects of these liners on the prosthetic interface has not been related to important characteristics of the patient's residuum, such as stiffness and geometry. The methods used in this section facilitate a more in-depth liner prescribing process, by providing more information to the prosthetist. The results of FE simulations may be used to develop a reference database, taking into consideration multiple characteristics of the prosthetic liner as well as the geometry of the patients' residuum. This would enable the prosthetist to evaluate a liner on certain features that they or the patient deem important and demonstrates the ability of an FE framework to be used to inform the prescriptive decisions of clinicians regarding prosthetic liners.

5.3.5 Conclusions

This section has performed scenario analysis to examine the effect the variables liner thickness, liner stiffness and muscle properties have on the predicted stresses on the residual limb when simulating ambulatory loading. For all simulations, the peak pressures were located at the proximal medial region beneath the ischium with peak shear stresses located along the socket brim. Variants of liner thickness, liner stiffness and muscle properties were examined. The statistical analysis of the results reported that each variant was statistically significant in terms of the resultant pressure and shear stresses exerted on the soft tissues and should therefore all be considered when pairing liner and residuum. Changes in liner stiffness and thickness had similar effects on shear stresses with liner stiffness having a greater effect on normal stress. This indicates that patients experiencing excessive pressure at the ischial tuberosity may benefit more from a tailored liner with softer material properties at the region of high pressure rather than increased liner thickness.

The main limitation of this section was the prosthetic socket geometry used. Arguably this is the most important, but also most variable factor in controlling the forces transmitted to the residual limb. Therefore, work is required to determine the extent to which modifications in a prosthetic socket geometry alter the stresses and strains experienced by the residual limb.

6. PROSTHETIC SOCKET GEOMETRY

6.1 Introduction

Throughout the previous chapters, the socket geometry used has been designed by the author using CAD software adhering to the guidelines produced by various notable resources (Long, 1985; Schuch and Pritham 1990; The Steeper Group 2011; Ottobock, 2016). Nonetheless, the main limitation of the FE models used is considered to be the socket brim geometry and Boolean fit of the prosthetic socket to the prosthetic liner.

The prosthetic socket is arguably the most important component of the lower limb prosthesis as it provides coupling between man and machine. A compromised connection between residuum and socket can create imbalances and instabilities during ambulation. To achieve a good fitting socket, the soft tissues of the residuum should be sufficiently contained within the volume of the socket. A previous study reported that a trans-tibial socket oversized by as little as 1.0% of the normal volume can be biomechanically distinguishable from an appropriately sized socket (Sanders et al. 2012). Additionally, the proximal contours of the socket are indicative of the design used by the prosthetist. For this, the proximal brim requires contouring to alleviate pressure in less tolerant areas.

The socket used to simulate the interaction with the trans-femoral residuum in previous FEA studies have been obtained by a combination of: 3D scans of either positive plaster casts of the residual limb (Lacroix and Patino 2011; Ramirez and Velez 2012; Velez Zea et al. 2015) or subject specific socket designed for the patient by a prosthetist (Morotti et al. 2015; Jamaludin et al. 2019), created using CAD (Zhang et al. 2013; Morotti et al. 2015) or unspecified (Restrepo et al. 2014; Ramasamy et al. 2018). Of these studies, only Jamaludin and colleagues (2019) reported the type of socket used. Therefore, it has not been common practice to include the information relating to the fit, such as the socket type, size, shape, and areas of rectification of the socket in comparison to the geometry of the residual limb. The lack of this information in these studies highly limits the amount of comparison that can be made between studies as the socket type and fit greatly alters the interfacial stresses and gait of the patient.

This chapter is split into two sections. Firstly, FE models will be used to examine the effect of reducing the socket volume for a fixed residual limb and liner. Secondly, FE models will be used to make comparisons between different socket geometries.

6.2 Socket Volume Reduction

Boolean fit (total contact) sockets have been used in clinical practice previously (ICRC 2006) and to simulate the interface between residual limb and socket in previous studies (Zhang and Mak 1996; Lee et al. 2004; Zhang et al. 2013; Arotaritei et al. 2015). However, recently it is common clinical practice for the prosthetic socket to be rectified, where the socket walls are modified to lessen pressures in sensitive areas and divert it to more pressure tolerant areas. The use of total contact/total surface bearing, in which all of the residuum surface is in contact with the socket in an attempt to evenly distribute the individuals' weight over the largest possible surface, is not commonly used in the modern-day socket design (The Steeper Group 2011). This is mainly due to the significant number of amputees who find it painful to weight bear at the distal end of their residuum. Instead it is common practice to remove the extreme distal loading from the socket and to modify the volume of the socket to an amount less than the volume of the patient's residual limb. Initially, global reductions of the socket size are made to sufficiently contain the volume of soft tissue within the socket which reduces the amount of socket pistoning that occurs (Sanders and Fatone 2011).

The residual limb volume can greatly affect the fit and design of a prosthetic socket (Sanders and Fatone 2011). For a trans-femoral residuum, a typical reduction between 3-6% is made in clinical practice depending on the consistency of the tissues, with the top end of up to 6% reduction for residual limbs that have a larger amount of soft tissue than normal (Kahle and Highsmith 2013; Mulroy 2018). However, there is limited availability of information which provides the recommended volume reductions, and many sources still reference the pioneering research by Radcliffe and Long. Target anterior-posterior and medial-lateral dimensions were developed by Radcliffe (1955) and Long (1985) during the conception periods of the Quad and IC sockets respectively.

This approach to socket design is a difficult task, even after the appropriate residuum volume has been decided for the socket fit, as over time the residuum may still undergo substantial changes in shape and volume. This is often during the initial 18 months post-operative recovery, but may continue for 'mature' residual limbs with many users experiencing daily volume fluctuations (Sanders et al. 2009; Sanders and Fatone 2011), commonly caused by general/post-operative oedema, muscle atrophy (Boonhong 2006) and residual muscle activity (Lilja et al. 1999). These volume changes of the residual limb can lead to problems creating and maintaining an accurate fit of a prosthetic socket.

The objective of this section was to alter the socket geometry used in the previous chapters to simulate the initial phase of prosthetic socket design determining the appropriate level of soft tissue containment within the socket.

6.2.1 Modelling Method

For this section, the model consisting of, bone (residual femur and hemi-pelvis), soft tissue, prosthetic liner, and prosthetic socket for participant 3 was used. Participant model 3 was used as it provided the greatest levels of convergence across all participant models, therefore allowing more results to be achieved. The acquisition and reconstruction of the model is detailed in Section 3.2.

For participant 3, modifications were made to the socket geometry used for previous chapters. Firstly, the distal contact between the residual limb and socket was removed to make the socket non-distal loading. To achieve this, firstly the distal end of the socket was extended axially to introduce a gap of 30mm between the distal end of the residuum to the bottom of the socket (Mulroy 2018) as shown in Figure 6-1.

Secondly, to evaluate the effect of volume change and replicate the initial phase of socket rectification, in which the correct volume containment of the prosthetic socket is determined, the socket was reduced in size. To achieve this, the socket was reduced uniformly in the medial-lateral and anterior-posterior dimensions when viewed in the transverse plane. Reduction was performed in increments of 1mm. The height of the socket was not altered. A total of ten sockets with varying degrees of volume containment were created, ranging from a 0mm (Boolean fit) to a 9mm reduction. The volume reduction of the socket was calculated for each reduction increment (see Table 6-1) with the largest reduction of 9mm equating to a 4.5% reduction in volume.

The level of overlap achieved by the socket variations was confirmed within Abaqus using the COPEN function to calculate the distance between the two interacting surfaces; the internal socket surface and the external liner surface (see Figure 6-1). The maximal overlap was obtained at the proximal level of the socket, at the medial anterior and medial posterior socket brim.

Additional socket reductions were created to reduce the socket volume by up to -6%, with a maximum overlap of up to 5.9mm. However, the simulations failed to reach convergence and are therefore not included in this study.

Table 6-1: Varying degrees of socket reduction.

	Socket reduction									
	Boolean	1mm	2mm	3mm	4mm	5mm	6mm	7mm	8mm	9mm
Maximum overlap (mm)	0	0.7	1.2	1.7	2.2	2.7	3.2	3.7	4.2	4.7
Volume change (%)	0	-0.3	-0.6	-1.0	-1.4	-1.9	-2.4	-3.0	-3.7	-4.5

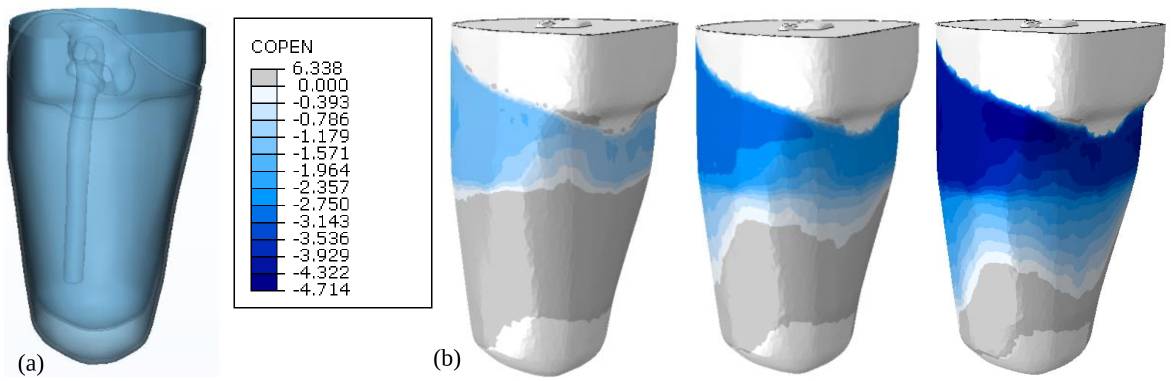

Figure 6-1: (a) Transparent model parts showing non-distal loading socket, (b) Levels of overlap between socket and liner surface for sockets reduced by -1.0% (left), -2.4% (middle) and -4.5% (right).

6.2.1.1 Convergence Testing

The FE models of this section were verified in the convergence testing of the previous chapter. The same meshing parameters were applied to the socket parts in this section.

The average run time for the models was approximately 74 hours, using a Quad Core CPU i5-4590, 3.30 GHz and 16.0GB RAM computer.

6.2.1.2 Material Properties

The mechanical properties of the bone, liner and socket were assumed to be linear elastic, isotropic and homogeneous. The soft tissues were defined using the Extended Mooney-Rivlin strain energy function with added compressibility, with values chosen to replicate average flaccid muscle. The material properties used for the bone, soft tissue and socket in this chapter do not differ from those mentioned in Section 3.2.6. The material properties for the liner in this section had minor differences. This included the liner being modelled with elastic modulus of 200 kPa, Poisson's ratio 0.4, and a thickness of 4mm. A friction coefficient of 1.0 ('High') was applied to the soft tissue and liner interface, and a value of 0.6 ('Medium') applied to the liner and socket interface. These values were chosen due to represent a silicone liner with nylon textured backing as tested in Section 5.2.1.

6.2.1.3 Boundary Conditions and Loads

The boundary conditions and loading applied to these models follow the detailing of Section 3.2.7, with minor variations explained below.

As in the previous chapters, loading was applied in two phases with the stresses and deformations of the initial phase being carried over into the second phase. The mechanisms used to apply these phases differed from the previous chapters as the models in this chapter included overlap between the socket and fixed residual limb and liner. This allowed for the donning process to be solved by a push-fit method, as mentioned in Section 3.2.7. For the second phase, an axial load equivalent to 50% of the participant's bodyweight was used to simulate bipedal stance phase.

6.2.1.4 Potential Limitations

In this chapter a load equivalent to 50% of the participants bodyweight was applied to simulate bipedal stance phase. This load is substantially lower than the amputee walking load applied in the former chapters. The increased model complexity due to the introduced overlap caused convergence difficulties when applying loads above 50% bodyweight. The bipedal stance phase loading has been applied in several previous studies (Silver-Thorn and Childress 1997; Portnoy et al. 2008; Portnoy et al. 2009; Ramirez and Velez 2012; Ramasamy et al. 2018). However, it limits the levels of peak stresses and strains that can be reported to loads from approximately half bodyweight compared to peak ambulatory loads. The loading from the heel strike and toe-off phases of the gait cycle (up to 110% BW) are more likely to cause soft tissue damage as they are of higher magnitudes (Linder-Ganz et al. 2006) compared to the stance phase.

The socket geometry used in this section was altered to replicate non-distal loading and the containment of the residual tissues within the socket. The socket was designed in accordance with guidelines published by qualified personnel (Schuch and Pritham 1999; The Steeper Group 2011; Ottobock 2016). The execution of the socket design was performed by the author within the modelling software. For the socket designs to be adequately assessed, the final designs require input to be obtained directly from qualified personnel.

6.2.2 Results

The resulting contact pressure distribution on the soft tissues from bipedal stance for the range of socket reductions is shown in Figure 6-2. The loading of the soft tissues was heavily contained around the ischial support region but was more evenly distributed with increasing socket reduction. The distal end of the soft tissues was not loaded.

To examine the changes in stresses at different locations on the residuum, pressure and circumferential and longitudinal shear stress values were obtained from the same locations from all socket reduction variations; at the medial, lateral, anterior and posterior sides at three different levels on the residuum of proximal, middle and distal (see Figure 6-3).

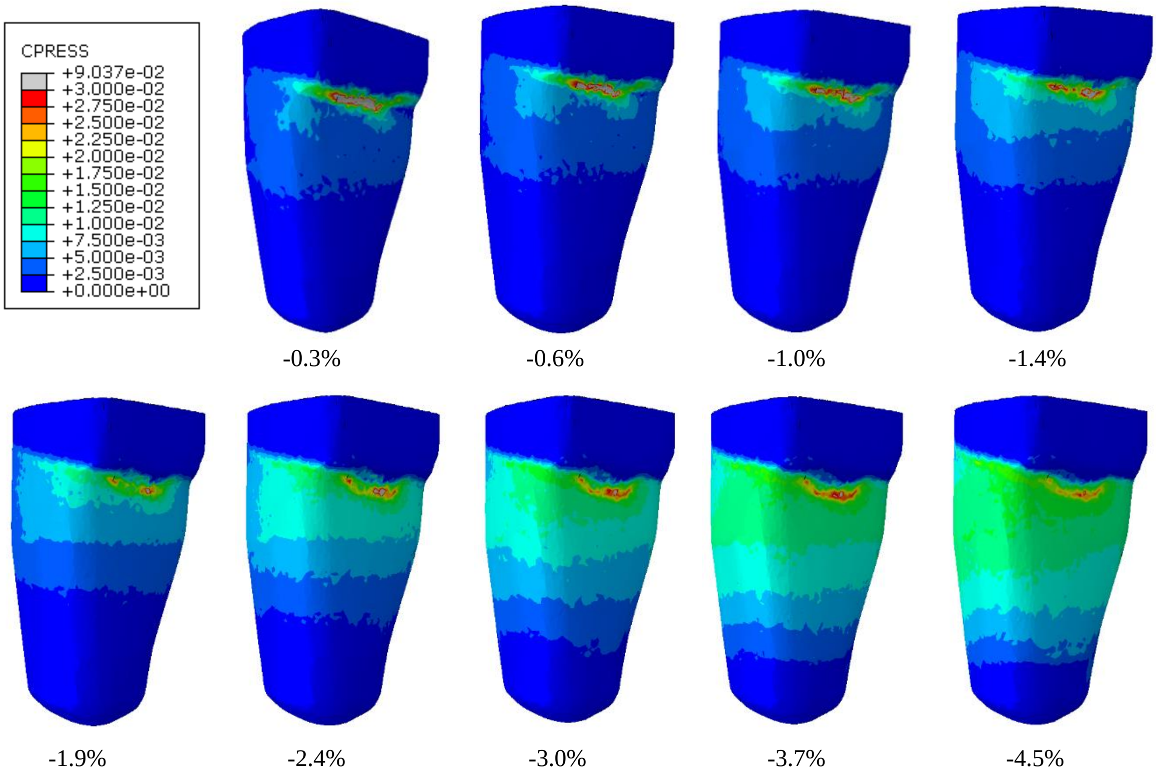

Figure 6-2: Pressure distribution for increasing levels of socket reduction.

For all volume reductions, the pressures at the proximal level are focused on the medial side. For the middle and distal levels, the distribution of pressures between the medial, lateral, anterior, and posterior regions is more evenly distributed (see Figure 6-3). As the socket volume is reduced, the pressures at the proximal level become more evenly distributed between medial, lateral, anterior, and posterior, most notably due to the reduction in medial pressure. The medial pressure is notably from the load bearing at the ischium. Reduction in volume causes increased hydrostatic loading of the residuum, reducing degree of loading applied to the ischium and increasing the pressures at both the middle and distal levels.

For both the circumferential and longitudinal shear stress, the maximal values are located at the proximal medial region. Both these maximal shear stress values are reduced overall with reducing socket volume from 0% to -4.5%. At the middle and distal levels, the medial and lateral locations experience significantly higher values of circumferential shear stress compared to the anterior and posterior locations. This is also increased with reducing socket volume.

There was a similar magnitude of circumferential and longitudinal shear stress at the middle and distal levels (see Figure 6-3). Conversely, the medial locations at the middle and distal levels provide the lowest longitudinal shear stress values compared to the lateral, anterior and posterior locations. At the middle level, the longitudinal shear appears to be unaffected by the degree of socket reduction. Whereas the lateral, anterior and posterior locations all show increasing amounts of longitudinal shear with increased socket reductions.

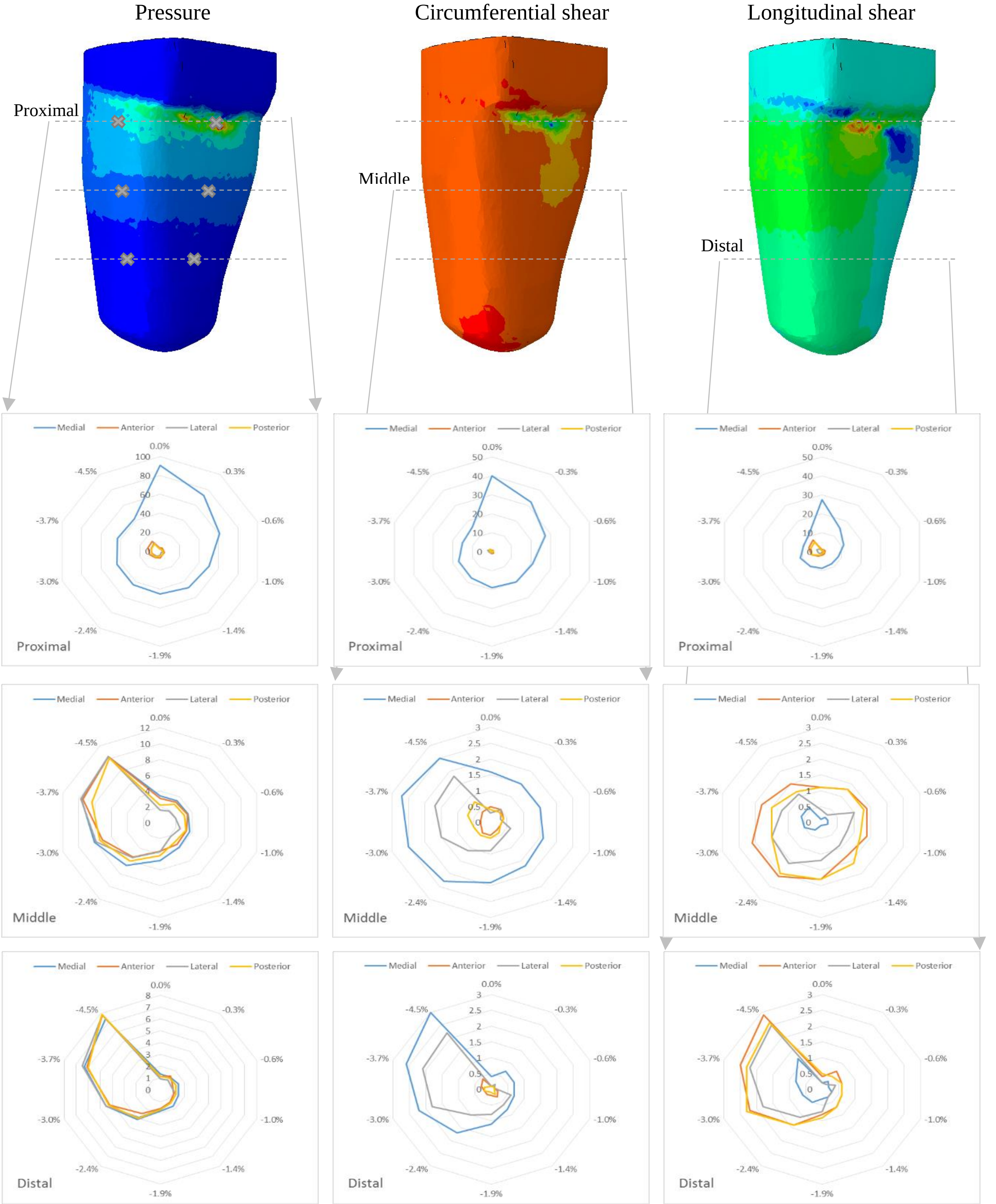

Figure 6-3: Maximal values (kPa) of pressure (left), circumferential shear stress (middle) and longitudinal shear stress (right) at Proximal (top), Middle (middle) and Distal (bottom) levels at Medial, Lateral, Anterior and Posterior location across the socket reduction range.

These variations in the shear stresses may be caused by two different factors; location of the point load used to simulate bipedal stance and the shape of the residual limb. The point load was applied to the centre of the socket distal end and the socket was not prevented from rotating. As the peak pressures were located at the proximal medial region (see Figure 6-2), this would limit the socket displacement on the medial side and may encourage the socket to undergo upward rotation on the lateral side causing higher longitudinal shear stresses on the lateral, anterior and posterior sides compared to the medial side. On the other hand, the residuum is a long conical shape with the lateral, anterior and posterior sides having a greater tapered angle leading down from the proximal to the distal end. This may have resulted in additional longitudinal shear stresses building up along these sides. These two factors may have operated individually or in conjunction with one another.

The effect of reducing the socket volume on the residuum stresses is shown in Figure 6-4. The peak pressure and shear stresses are significantly reduced between 0% and -1.4% volume reduction, after which the stress reduction starts to plateau to -4.5%. Volume reductions past -1.4% cause a minor increase in the peak longitudinal shear stress. However, reducing the socket volume does cause an overall trend of reducing the peak longitudinal shear. The average pressure was calculated from area in contact with the socket. Both the average pressure and peak donning pressure, from the push-fit method, increase substantially with volume reduction. The displacement of the socket during bipedal stance is significantly reduced by the reduction in socket volume.

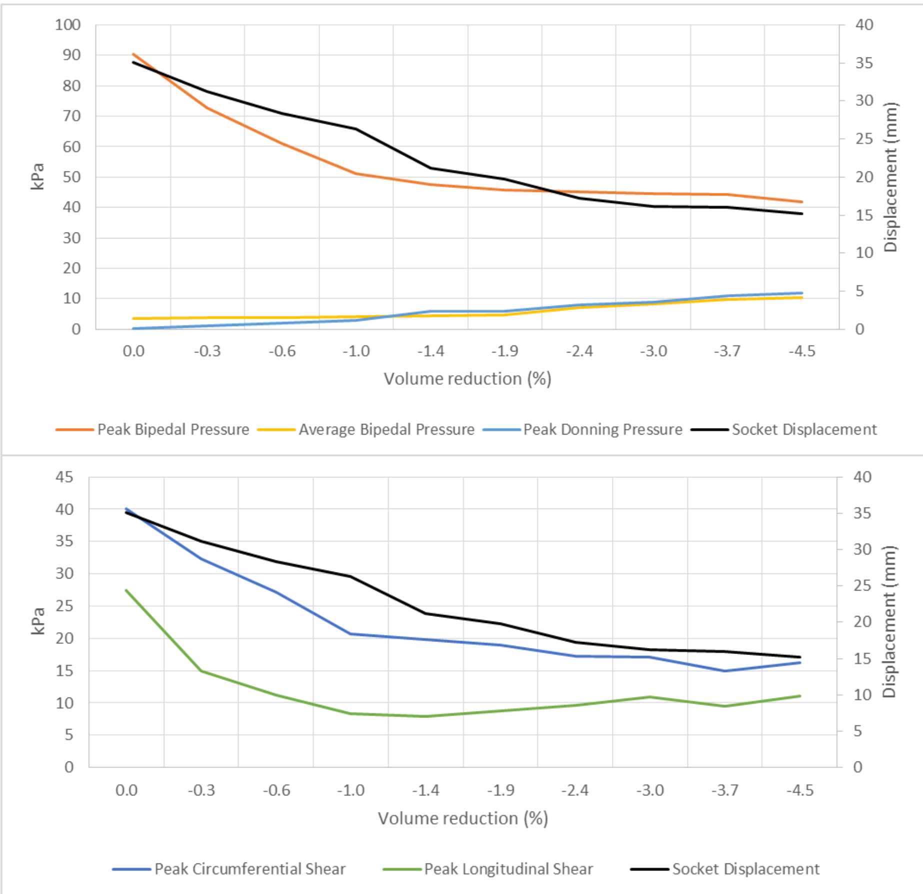

Figure 6-4: Effect on changes in socket reduction on (top) pressure and socket displacement and (bottom) shear stresses and socket displacement.

The trends of the stresses from Figure 6-4 indicate two portions to the effect of volume reduction: an initial portion (0% to -1.4%) and second portion (-1.4% to -4.5%). Therefore, Table 6-2 was developed to allow for better comparisons to be made. Overall, reducing the socket from 0% to -4.5% reduced the peak pressure, shear stresses and socket displacement by over 50%.

The initial reduction (0% to -1.4%) significantly reduced the peak pressure. After this, additional reduction resulted in further reduced peak pressure, but only by an additional -11.58% compared to the initial reduction of -47.46%. A similar result is reported for the peak circumferential shear stress from the initial (-50.37%) and secondary (-18.59%) portions. Socket displacement is reduced slightly more during the initial portion is compared to the second portion. Reducing the socket volume caused the average pressure to increase significantly (200%). This increase was minor during the initial portion of reduction but significant in the second portion. This is the reverse trend to the reducing peak pressure, which was more prominent in the initial portion compared to the second.

Table 6-2: Changes in resulting stresses and socket displacements from 0% to -4.5 % socket reduction.

Change from 0% to -4.5% volume reduction

	0%	-4.5%	Percentage change
Peak bipedal pressure (kPa)	90.4	42.0	-53.54%
Average bipedal pressure (kPa)	3.5	10.5	200.00%
Peak circumferential shear (kPa)	40.1	16.2	-59.60%
Peak longitudinal shear (kPa)	27.5	11.1	-59.64%
Socket displacement (mm)	35.1	15.2	-56.70%

Change from 0% to -1.4% volume reduction

	0%	-1.4%	Percentage change
Peak bipedal pressure (kPa)	90.4	47.5	-47.46%
Average bipedal pressure (kPa)	3.5	4.3	22.86%
Peak circumferential shear (kPa)	40.1	19.9	-50.37%
Peak longitudinal shear (kPa)	27.5	7.9	-71.27%
Socket displacement (mm)	35.1	21.2	-39.60%

Change from -1.4% to -4.5% volume reduction

	-1.4%	-4.5%	Percentage change
Peak bipedal pressure (kPa)	47.5	42	-11.58%
Average bipedal pressure (kPa)	4.3	10.5	144.19%
Peak circumferential shear (kPa)	19.9	16.2	-18.59%
Peak longitudinal shear (kPa)	7.9	11.1	40.51%
Socket displacement (mm)	21.2	15.2	-28.30%

6.2.3 Discussion

The examination of the interfacial stresses at different heights (proximal, middle, and distal) and sides (medial, lateral, anterior and posterior) of the residuum (see Figure 6-3) demonstrated that reducing the socket volume reduced the peak stresses at the proximal medial location on the soft tissue. This created a more even distribution of both normal and shear stresses over the whole contact area between the residual limb and socket.

The distribution of shear stresses over the residuum, at the middle and distal level, was shown to vary depending on the side of the residuum the value was taken from (see Figure 6-3). Two justifications for the distribution of shear stresses over the different residual heights have been given: location of point load and conical shape of the residuum. To fully understand the distribution, variations of the point load and residuum shape may be examined in later work.

For the larger socket sizes, the peak stresses were more localised. But as the socket volume is reduced there is a trade-off between the peak and average stresses. For the shear stresses, this is shown in Figure 6-3 where the peak shear stresses at the proximal level are reduced and the distal shear stresses are increased from socket reductions. For the interfacial pressures this is evident in Table 6-2 with socket volume reductions from 0 to -4.5% reducing the peak pressures by -53.54% and increasing the average pressure on the residuum by 200%.

The changes in the interfacial stresses with the volume reduction is divided into two portions. The initial portion of volume reduction is significantly effective at reducing the peak normal and shear stresses as well as reducing the socket displacement. The second portion still changes the peak stresses albeit to a lesser extent. However, it is during the second portion that the average stresses are significantly increased, and the loading of the socket is distributed more evenly on the surface of the residual limb.

The final socket size (-4.5%) can be considered the best fitting socket compared to the previous iterations of socket volume reductions. This socket greatly limited the localised stresses; the peak pressures were located along the medial brim of the socket for the larger sockets, but the maximum socket reduction of -4.5% concentrated the proximal pressures to the posterior region of the medial brim to the ischial tuberosity. This is the most advantageous location for the peak pressures to be located, as it concentrates the loading at the ischium and avoids the pressure sensitive adductor muscles at the anterior region of the medial brim. As such, this was the aim of the medial socket brim contour.

In terms of gait mechanics, the -4.5% volume reduced socket produced the least amount of socket displacement (15.2mm) compared to the unaltered socket (35.1mm) which is vital in preventing excessive socket pistoning during ambulation. Kahle and Highsmith (2013) reported an average displacement range of 14mm to 25mm for brimless and IC sockets respectively during ambulation. As they do not report the socket size in relation to the individual’s residuum size, it is difficult to draw comparisons. The socket displacement of the -4.5% socket falls within the average range reported by their study, however the displacement values reported in this study were for bipedal stance and would be expected to increase during ambulation loads. A study by Board et al. (2001) also found less pistoning occurred with a tighter fit between trans-tibial residual limb and socket, when the socket was at its ‘normal’ volume compared to a reduced volume state. They also reported greater symmetry in step length and stance duration when individuals wore a socket of tighter fit. Conversely, a previous study by Sanders et al. (2017) found trans-tibial amputees using a smaller socket fit (-3.0mm) experienced negative gait effects such as greater step time and step width asymmetries compared to when using a larger fit socket (+3.0mm). The results of this study are surprising, as it is believed a smaller socket fit would provide higher levels of proprioception causing the smaller socket to have less asymmetry (Pritkin 1997; Sanders et al. 2004; Cagle et al. 2014). Sanders et al. (2017) hypothesised the greater asymmetry may have been caused by the participants having greater confidence whilst using the smaller socket and thus would not have been focusing as intensely on their gait and have had a greater tendency to turn on the amputated side.

The health of the individual's residual limb may also be a major consideration when determining the tightness of socket fit. A sufficiently tighter socket may have beneficial gait mechanics and stress distributions, however after an amputation, the individual may experience phantom pains (Hsu and Cohen 2013) and reduced sensitivity to touch, pressure and temperature (Hains and Waxman 2006). If the amputee does not have sufficient sensation in the residual limb to confirm when too much reduction is painful this may affect the feedback from the patient during the socket fitting process causing an excessively tight socket fit. A tighter socket may consequently have negative effects such as flow occlusions which restrict the venous return and cause a build-up of cellular waste products in the residual limb and in severe cases lead to necrosis (Fenech and Jaffrin 2004).

In this study, the volume reduction of -4.5% was used to replicate the recommended global volume reduction for trans-femoral socket fitting (Kahle and Highsmith 2013; Mulroy 2018). However, the volume of the residual limb is also susceptible to substantial volume fluctuations after a previously adequate socket has been designed and fitted. A study by Sanders and Fatone (2011) reviewed several previous lower limb fluctuation studies. They reported long-term residual limb volume changes ranging from -2.0% to +12.6% across numerous studies for trans-tibial amputees. These volume changes are considerably greater than the maximum volume reduction of -4.5% achieved by the FE models in this study. However, the trans-tibial residuum is smaller than the trans-femoral residuum. Sanders and Fatone (2011) also concluded that the techniques used to measure residual limb volume lacked resolution and repeatability, as well as monitoring the entire residual limb volume rather than volume contained within the socket. Whereas the volume reduction in this study was calculated as the volume contained within the socket, which may account for the lower levels of volume reduction.

There is a very scarce amount of information available regarding the recommended amount of socket reduction. This is mainly caused by the socket design fit being largely learnt by experience and differing depending on the individual prosthetist's philosophy. The original studies by Radcliffe (1955) and Long (1985) state the recommended internal dimensions for the Quad and IC sockets respectively, given the circumference of the residuum approximately 4cm distal to the ischial tuberosity. The circumference of the residual limb used in this section was measured as 62.3cm. Measurement was made 4cm distal to the ischial tuberosity, whilst the residual limb was coupled with the liner part and under no loading conditions.

Radcliffe (1955) recommended a substantially reduced anterior-posterior (AP) dimension compared to the natural residuum geometry. However, these recommendations were made for residual limbs with a circumference between 18.0 to 22.0 inches (45.7 to 55.9cm). While the measurements provided by Radcliffe are smaller than the circumference of the residuum for the participant model in this section, an estimated goal AP dimension can be extrapolated from the goal dimensions for the smaller circumferences. As such, the goal AP dimension for the participant residuum would be approximately 10.5cm. The measured internal AP dimension of the -4.5% volume reduced socket was 21.3cm. This value is substantially higher than the extrapolated goal AP dimension. This was to be expected due to the Quadrilateral socket providing stabilisation of the residual limb by the severely reduced AP dimension. The tight socket fit has been reported as uncomfortable by several socket users (Pritham 1990; Lee et al. 1997). Furthermore, the recommendations by Radcliffe are given in a case study example but are subject to the prominence and musculature of the patients' muscle groups, notably the hamstrings, gluteal muscles, and rectus femoris.

Similar to Radcliffe (1955), Long (1985) identified recommended medial-lateral (ML) socket dimensions, which are characteristic of an IC socket. For a circumference of 25.0 inches (63.5cm) the ML dimension was 5.7 inches (14.5cm). The measured internal ML dimension of the -4.5% volume reduced socket was 19.6cm. This is considerably greater than the recommended ML of 14.5cm stated by Long (1985). This is believed to have been caused by the socket reduction being applied in both the ML and AP direction, rather than more heavily in the AP direction as is performed for IC sockets. Further, the ML dimension of the sockets, with up to 6% volume reduction, which did not achieve sufficient convergence, measured 19.0cm which was still considerably higher the Long's ML dimension.

The limited information on the socket dimensions from the rectification process severely impacts the comparisons that can be made from the FE results of this section. The volume of the sockets simulated was up to -4.5% which was within the -3% to -6% recommended reduction for the soft tissues (Kahle and Highsmith 2013; Mulroy 2018). However, this reduction resulted in AP and ML dimensions that were greater than the recommended goal dimensions stated by Radcliffe (1955) and Long (1985) respectively. This may have been a result of the volume reductions of the sockets being applied uniformly in the ML and AP directions compared to the practice of greatly reducing the ML dimension in comparison to the AP dimension as performed for IC sockets (Long 1985). Additionally, the goal dimensions of the Quad and IC sockets require significant reductions in the respective dimensions, however the computational ability used in this study was not capable of achieving the required levels of overlap to achieve these dimensions.

6.2.4 Clinical Relevance

By reducing the socket volume, the interfacial stresses were reduced, and their distribution spread more evenly over the surface of the residuum. Therefore, by reducing the peak interfacial stresses, a socket that sufficiently contains the soft tissues of the residual limb would provide greater comfort (Lee et al. 2005) to the individual compared to a socket that was larger. The initial reductions in socket volume provide greater reductions in stresses on the residuum compared to further reductions. This may be useful if the patient has less sensitive feeling in the residual limb as it would allow the benefits from the initial reduction to be obtained without putting the residual limb at risk of the detrimental effects of excessive compression and reduced blood flow.

6.2.5 Conclusion

This section simulated the effect of increasing levels of volume reduction of the prosthetic socket. Overall, reducing the socket volume by up to -4.5% significantly affected the peak pressures, shear stresses and socket displacement. It produced reductions of more than 50% and significantly increased the average pressure by up to 200%. This is the first study to have investigated the effect of reducing the volume of the trans-femoral socket from an FE perspective.

The degree of volume reduction achieved by FE simulation was within the range of typical residuum volume reduction for socket fabrication (Kahle and Highsmith 2013; Mulroy 2018). The maximum level of socket reduction simulated did not reduce the ML dimension of the residual limb enough to achieve the goal ML dimension recommended by Long (1985). However, this is primarily attributed to a further reduced AP dimension being restricted by the computational power. Nonetheless, these simulations demonstrated and quantified the effect of reducing the socket volume on the interfacial stresses which has not been previously studied.

The peak pressures on the soft tissues were exerted along the medial brim of the socket. With further reductions on socket volume, this was concentrated more at the posterior region of the medial brim, underneath the ischial tuberosity. This section has demonstrated the effect of sufficiently containing the soft tissues by reducing the global volume of the socket. The next section will look to suitably contour the proximal brim of the socket.

6.3 Socket Comparison

For the previous section and chapters, the proximal contours of the socket geometry were designed by the author using recommended guidelines (Ottobock 2016). However, in clinical practice the socket geometry can be highly variable. It not only depends on the shape and size of the patient's residuum, their surgical history and activity level but also on the prosthetist (Schuch and Pritham 1990; The Steeper Group 2011).

Section 6.2 showed the pressures along the medial brim were affected by the level of socket reduction, with increased reduction focusing the pressure at the posterior region of the medial brim. Apart from the AP and ML dimensions, the contours of the socket brim can vary with different socket concepts. The socket brim is based on recommended contours depending on the goal socket variant, these are then dependant on the ability and technique of the prosthetist to correctly apply them. Obtaining the correct contour of the medial brim in any variant of the trans-femoral socket is incredibly difficult. This is because the medial brim is the location where most of the load is transmitted between socket and residuum. Additionally, the medial border of the ischium should be loaded, but the pressure sensitive adductor longus tendon and pubic ramus which also run along the medial border are not pressure tolerant and should be alleviated as much as possible (Pritham 1990).

Therefore, the contours of the medial brim and the amount of ischium encompassed when fabricating a socket is primarily influenced by the philosophy of the prosthetist performing the fitting (Neumann et al. 2005). Previous transducer studies have been conducted to determine variations in pressure distribution, gait characteristics, patient comfort, and patient preference for trans-femoral sockets (Gottschalk et al. 1989; Lee et al. 1997; Kahle and Highsmith 2013). However, the optimal prosthetic socket brim design for a trans-femoral socket remains elusive (Lee et al. 1997; Kahle and Highsmith 2013).

The objective of this section was to alter the socket brim contours to create two distinguishable socket concepts. This would be combined with the FE model developments studied in the previous chapters of the thesis to establish two socket fits that would be plausible representations of prescribed sockets designed for a trans-femoral patient.

6.3.1 Modelling Method

For this section, the model consisting of; bone (residual femur and hemi-pelvis), soft tissue, prosthetic liner, and prosthetic socket for participant 3 was used. The acquisition and reconstruction of the model is detailed in Section 3.2. The material properties of the liner and soft tissues were the same as described in Section 6.2.

To adequately determine and design the contours and dimensions of the socket variants, collaboration with ProActive Prosthetics (Surrey, United Kingdom) was obtained and input from a qualified prosthetist provided. The initial agreement was to create two socket designs that would be distinguishable and characteristic of the Quad and IC sockets. However, input from the prosthetist at ProActive Prosthetics indicated that the amount of socket reduction that achieved convergence in Section 6.2 would not be large enough when applied in the AP dimensions to sufficiently characterise the socket as a Quad socket. Therefore, it was agreed that the socket design would have characteristics of the Quad socket, such as the brim geometry and reduced AP dimension, but it would be classified as a non-ischial containment socket instead of a Quad socket. Therefore, two distinguishably different sockets were created; a non-ischial containment (Non-IC) socket and an ischial containment (IC) socket. The dimensions of the socket geometry for both socket variations described below were created by the author from direct input from the prosthetist.

Socket wall contours

For both sockets, the medial wall was altered to provide additional relief at the adductus longus tendon, which is located at the anterior side of the medial brim. Therefore, similar distances between the pelvic bone and the bottom of the ‘v’ of the medial brim were obtained in both sockets. This was 66.8mm and 60.1mm for the Non-IC and IC sockets respectively (see Figure 6-5). For the IC socket, the medial brim contour was raised to encompass the ischial tuberosity. This was achieved by raising the posterior region of the medial brim to be above the most distal point of the ischial tuberosity. The posterior medial brim was raised by 13.0mm above the most distal region of the ischial tuberosity (see Figure 6-5) which was above the minimum of 12mm recommended by the prosthetist. Conversely, medial brim of the Non-IC socket was contoured to be a gradual slope up from bottom of the ‘v’ to the posterior wall. This involved lowering the medial wall to be 28.1mm below the ischial tuberosity, which was below the 21mm recommended by the prosthetist.

For both sockets, the height of the anterior wall was matched to the height of the inguinal crease of the soft tissues. This is required for the prosthetic socket to remain comfortable when the residual limb is raised in the sagittal plane during the swing phase and seating. Similarly, the posterior wall was set to the same height for both sockets, which was chosen as approximately the same height as the distal point of the ischial tuberosity (see Figure 6-5). For the IC socket, the lateral wall was raised to be higher than the greater trochanter of the residual femur. As this is typically done for IC sockets to provide a counter pressure on the lateral side of the femur, when coupled with a reduced ML dimension, to maintain the bony lock from the contained ischial tuberosity. Conversely, the lateral wall of the Non-IC socket was set to be below the greater trochanter.

Medial-Lateral and Anterior-Posterior dimensions

Following the guidelines for clinical practice, the sockets were reduced in the ML and AP dimensions; for the IC socket the ML dimension was reduced (by 9mm) more significantly compared to the AP dimension (by 4mm), whereas for the Non-IC socket the AP dimension was reduced (by 9mm) more significantly compared to the ML dimension (by 4mm). The reduction amounts were chosen as they were able to achieve convergence and would achieve a minimum global reduction of -1.4% volume which was the initial portion of volume reduction and significantly effective at reducing the peak normal and shear stresses as shown in the previous Section (see 6.2). As a result of the modified AP and ML dimensions, the volume of each socket was globally reduced by -2.6% and -2.8% for the Non-IC and IC sockets, respectively.

The final two socket designs; one with IC characteristics and one with non-ischial containment characteristics were agreed with, and signed off by, the prosthetist at ProActive Prosthetics and are shown in Figure 6-6. For both socket variants, there remained a 30mm gap at the distal end of the socket.

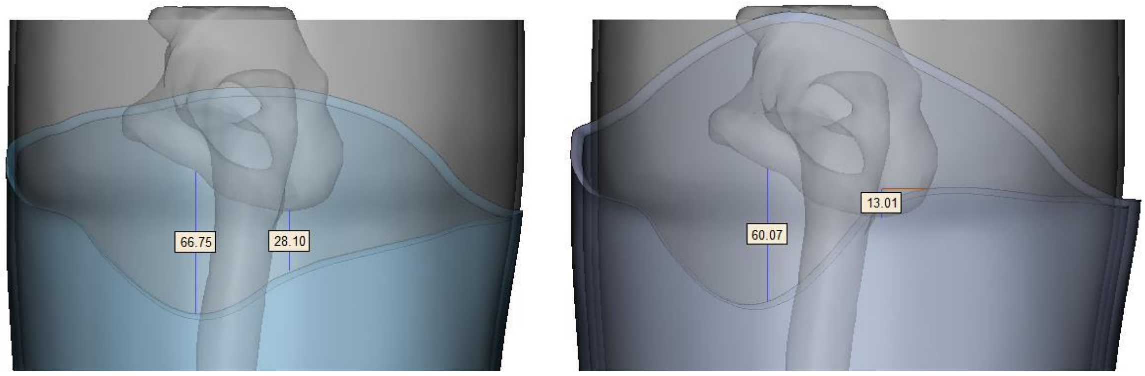

Figure 6-5: Medial socket contour dimensions for the Non-IC (left) and IC socket (right).

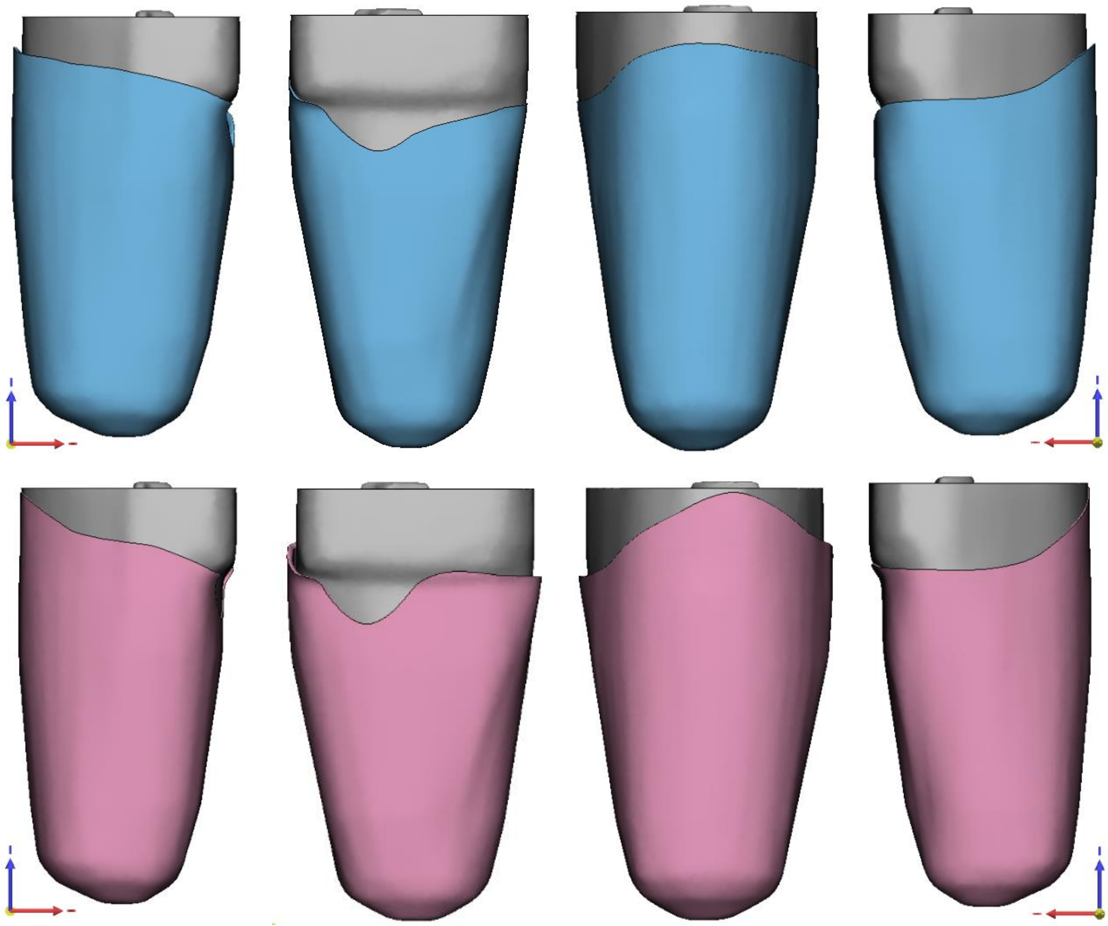

Figure 6-6: Anterior, Medial, Lateral and Posterior views of the Non-IC socket (top) and IC socket (bottom) agreed with the prosthetist.

6.3.1.1 Convergence Testing

The FE models of this section were verified in the convergence testing of the previous chapter. The same meshing parameters were applied to the socket parts in this section.

The average run time for the models was approximately 78 hours, using a Quad Core CPU i5-4590, 3.30 GHz and 16.0GB RAM computer.

6.3.1.2 Material Properties

The mechanical properties of the bone, liner and socket were assumed to be linear elastic, isotropic and homogeneous. The soft tissues were defined using the Extended Mooney-Rivlin strain energy function with added compressibility. The material properties used in this chapter do not differ to those mentioned in Section 3.2.6.

6.3.1.3 Boundary Conditions and Loads

The boundary conditions and loading applied to these models follow the detailing of Section 3.2.7, with minor variations explained in Section 6.2.

6.3.1.4 Potential Limitations

The prosthetic socket geometry used in this section was an improvement on the socket geometry used in the previous section as it was obtained through collaboration with a prosthetist at ProActive Prosthetics who approved the final socket designs. But as with any socket designed by a prosthetist, there is a potential limitation that the design fabricated was not optimal. The socket geometries used were after initial consultation with the prosthetist, therefore it can be assumed that more socket rectifications would further improve the fit of the socket.

The results of the FE models of this section have been related to the soft tissue damage models of previous literature to compare and infer the locations of damage on the residual limb. However, the soft tissue in the FE models was modelled as a bulk material, whereas realistically the material properties of skin, adipose tissue, muscle, tendons, and ligaments all have varying material properties. To improve this limitation the individual components of the soft tissue should be modelled, such as skin, fat and muscle, and their respective material properties applied. This can be problematic, as firstly a very high-resolution scan is required to accurately define the contours between these sections of the soft tissues (Prompers et al. 2006), and secondly the literature containing the information regarding the properties of these materials is limiting and conflicting (Dickinson et al. 2017).

As mentioned in Section 3.2.7, the previous chapters used a simplified peak axial load (110% BW), which excluded transverse plane forces and joint moments. However, the loading applied to the simulations in this section was only up to bipedal stance (50% BW). Whilst standing in bipedal stance, there are no transverse plane forces or joint moments applicable. Convergence at higher loads to simulate the peak loads from ambulation as simulated in the previous chapters could not be obtained. The results of the bipedal stance simulations in this section will be compared with previous literature on soft tissue damage to evaluate the socket designs and equate the outputs to potential soft tissue damage.

6.3.2 Results

For each of the models, pressure, circumferential shear, and longitudinal shear values were taken at varying levels (proximal, middle, and distal) on the residuum, with four locations (anterior, posterior, medial and lateral) at each level. These planes and locations are the same as those examined in the previous section (see Figure 6-3). Further, the stresses at the distal end of the residuum were also reported. These are reported as bar charts in Figure 6-7 and Figure 6-8 for the Non-IC and IC socket models respectively, along with the contour graphs showing the stress distributions on the residual limb surfaces at bipedal stance. The full table of these results are shown in Appendix Chapter 6 Supporting Evidence.

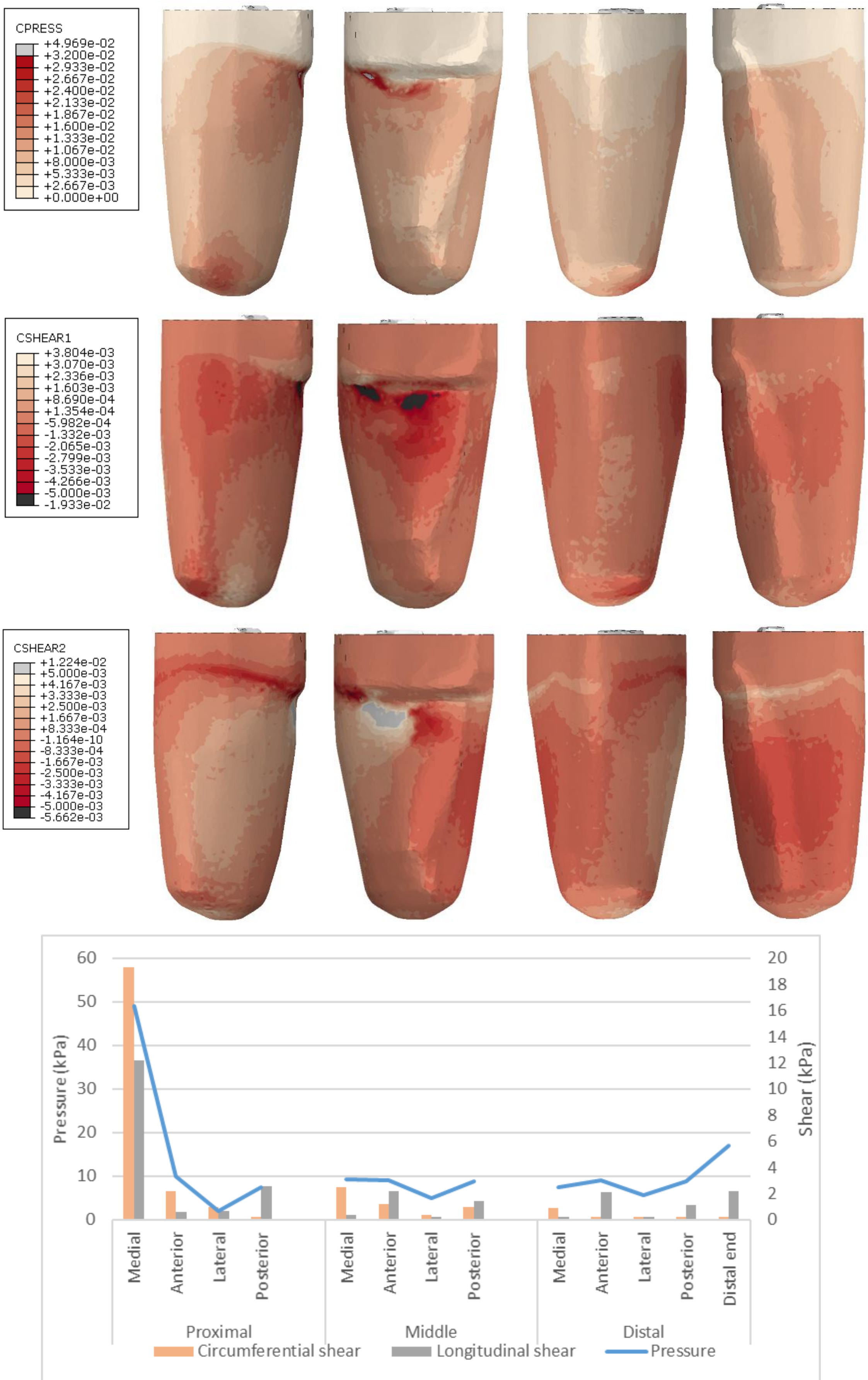

Figure 6-7: Pressure, circumferential shear and longitudinal shear stress distributions for the Non-IC socket during bipedal stance. Views of anterior, medial, lateral and posterior.

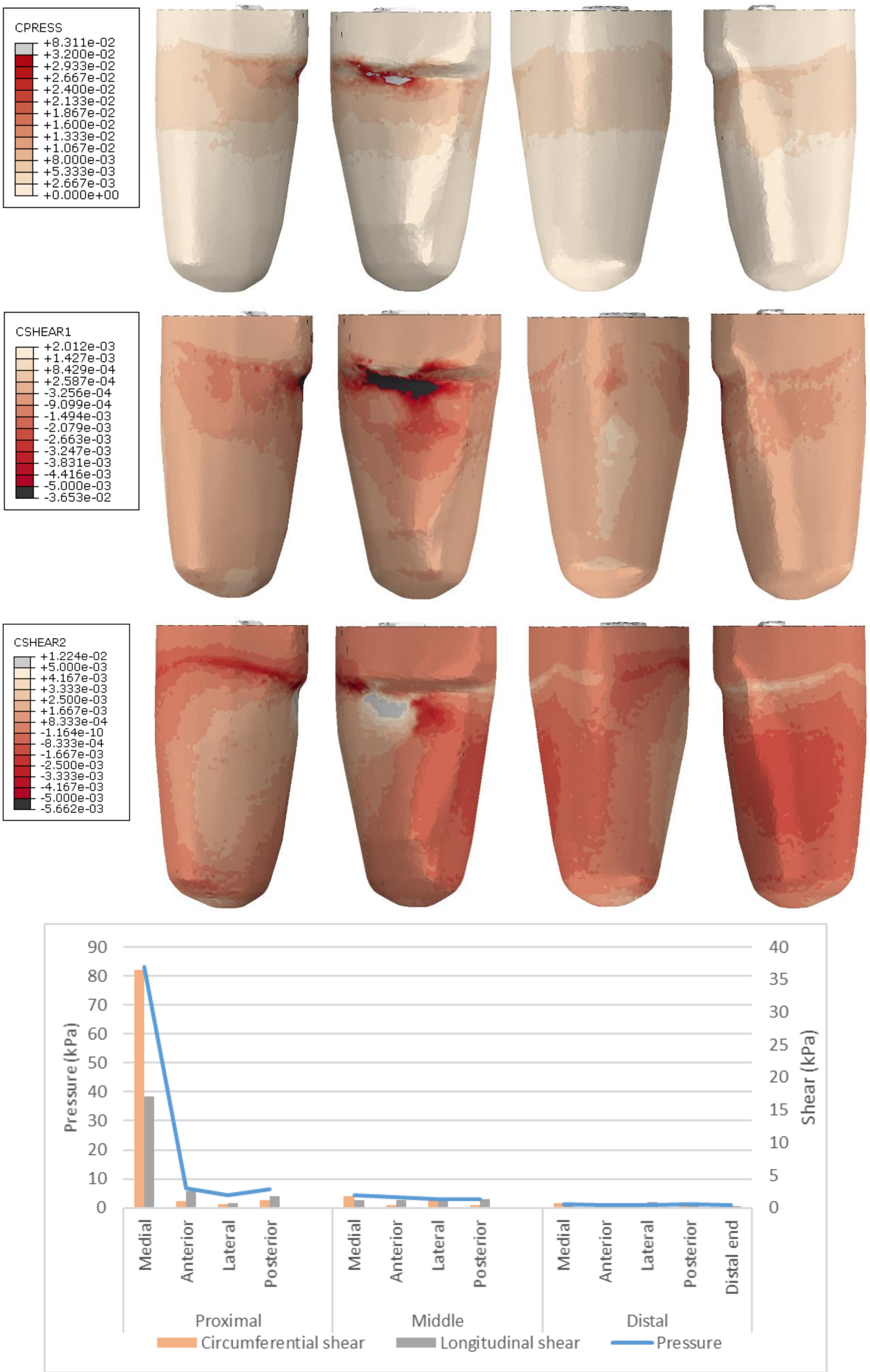

Figure 6-8: Pressure, circumferential shear and longitudinal shear stress distributions for the IC socket during bipedal stance. Views of anterior, medial, lateral and posterior.

For both models, the peak pressures and shear stresses were located at the medial brim of the socket. The peak pressure and shear stresses were greater in the IC socket in comparison to the Non-IC socket. The bar graphs of Figure 6-7 and Figure 6-8 show the pressures and shears were more evenly distributed over the surface of the residuum for the Non-IC socket (average pressures of 7.3 kPa) in comparison to the IC socket (average pressures of 3.8 kPa). The average pressure was calculated from area in contact with the socket.

The models used in this section were the result of continual development throughout this thesis and were therefore the most accurate representations of the trans-femoral residual limb, prosthetic liner, and prosthetic socket interaction. Thus, these simulations may be used to inform comparisons to previous soft tissue damage models. A study by Linder-Ganz et al. (2006) correlated pressure and durations (minimum of 15 minutes) to inform a soft tissue damage model from the results of previous studies (see Figure 2-1). As the loading applied in the simulations of this section were from bipedal stance, they may be assumed to be applied for longer durations, such as stationary standing, as opposed to the instantaneous ambulatory loads of the previous chapters. The solid black line indicates the level of pressure at the histopathology that always showed cell death. The value for this was 32 kPa from 15 to 60 minutes, which drops down to 9 kPa just after 100 minutes. Whereas, the dashed line specifies the pressure at which cell damage was never identified. The value for this was 26 kPa from 15 to 60 minutes, which drops down to 5 kPa just after 100 minutes. Between these two levels, exists a region of uncertainty in which the authors believed cell death may or may not occur.

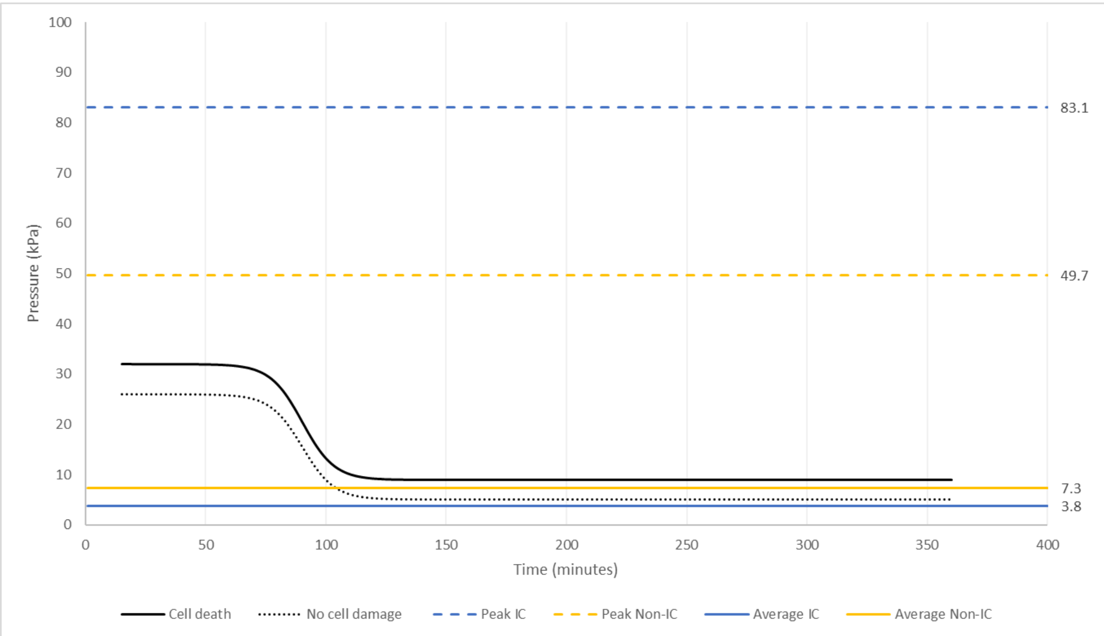

Figure 6-9: Comparison of peak (red) and average (blue) pressure values from Non-IC (dashed lines) and IC (solid lines) sockets with soft tissue damage models reported by Linder-Ganz et al. (2006).

The peak and average pressure for both socket types have been plotted over the top of the results for tissue damage from a study by Linder-Ganz et al. (2006) (see Figure 6-9). The peak pressure from both socket variants is larger than the limit for which certain tissue damage will occur. The threshold value of 32 kPa applied to the pressure distributions contours (see Figure

6-7 and Figure 6-8) was chosen as it represents the upper-most level of pressure at which certain cell death occurred for durations below 60 minutes. The average pressure on the residual limb surface was calculated as 7.3 kPa for the Non-IC socket and 3.8 kPa for the IC socket. The average pressure within the Non-IC socket remains under the dashed line for the whole duration. Whereas, the average pressure within the IC socket remains under the dashed line for the initial approximate 100 minutes, after which it is within the region of uncertainty. The area of tissue that is exposed to pressures greater than the threshold limits for cell death (32 kPa and 9 kPa) are shown in Figure 6-10.

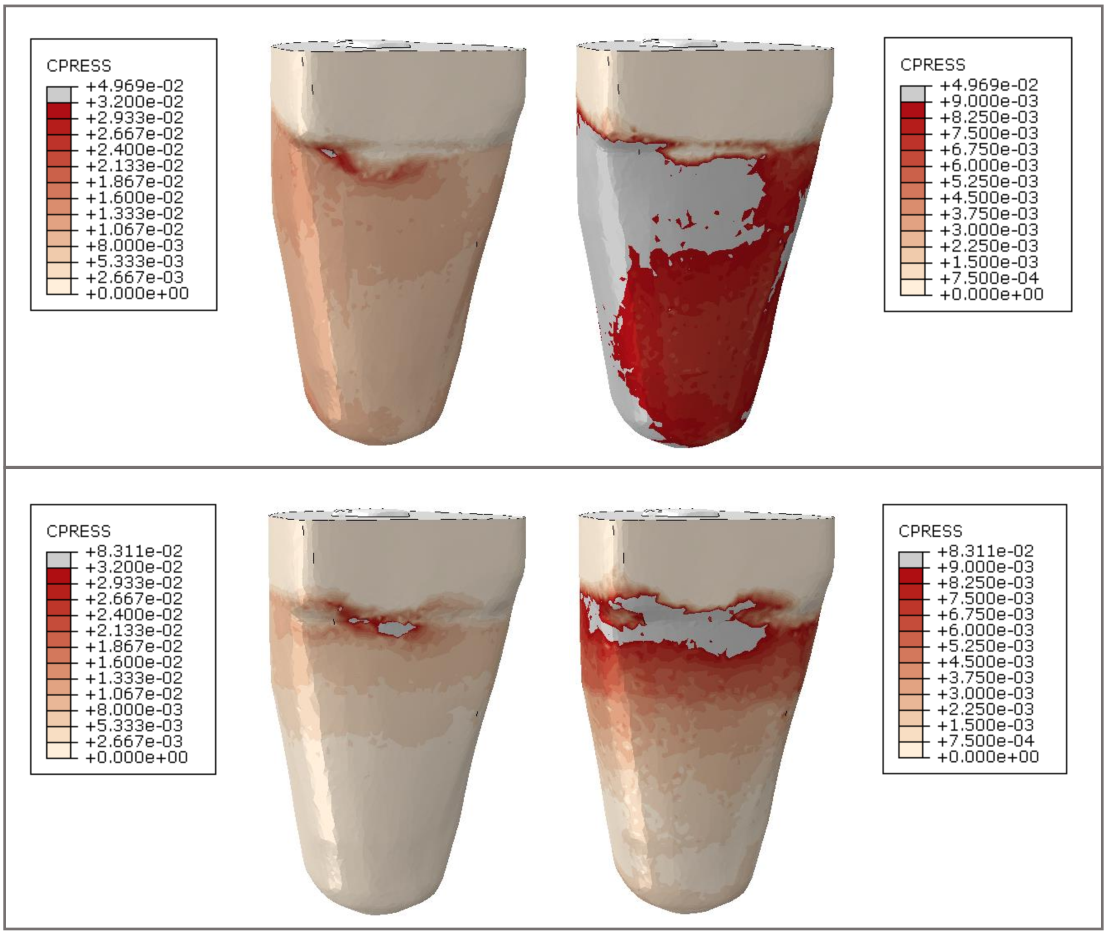

Figure 6-10: Area of tissue of Non-IC (top) and IC (bottom) socket model with interfacial pressure greater than the amount required to cause certain cell death

Both sockets had a distal gap of 30mm between the end of the residuum and the socket. The Non-IC socket underwent socket displacement of 37.6mm as a result of bipedal loading. This resulted in contact between the distal end of the residuum and socket being made for the Non-IC socket, with pressures up to 17.0 kPa occurring at the distal end of the tissues. In comparison, the IC socket was displaced by a lesser amount of 23.9mm, which did not result in distal end contact between residuum and socket and minimal distal end pressure of up to 1.6 kPa due to contact between the soft tissue and liner.

To fully assess the pressure distribution along the proximal brim of the socket models as a result of changing the containment of the ischial tuberosity, comparisons between the two socket models were also performed at a lower bodyweight loading of approximately 25% (see Figure 6-11). This was the point prior to which to the Non-IC socket did not have distal loading from the socket, meaning the loading was concentrated around the ischium and not supported at the distal end of the residuum. At approximately 25% bodyweight load, the Non-IC socket had high pressures concentrated around the anterior medial side of the socket brim with a peak of 19.6 kPa. Whereas, the IC socket had a more evenly distributed pressure along the medial brim of the socket with a lower peak of 14.0 kPa.

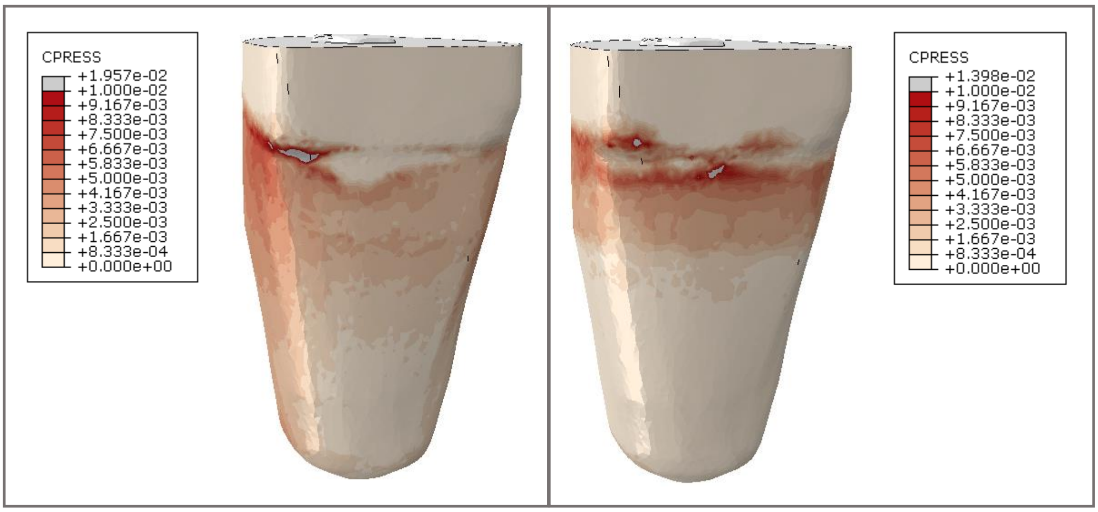

Figure 6-11: Comparison of Non-IC (left) and IC (right) socket models contact pressures at ~25% bodyweight load.

After the donning phase, the peak compressive (minimum) and tensile (maximum) principal logarithmic strain for each socket model was 10.0% and 8.7%, and 11.8% and 10.5% for the Non-IC socket and IC socket models, respectively. After bipedal loading, the peak compressive and tensile strains for each socket model were 169.7% and 123.5%, and 163.5% and 96.4% for the Non-IC socket and IC socket models, respectively. The strain distribution for each of the models at bipedal loading is shown in Figure 6-12. For both models, the maximal strains were located around the medial part of the pelvic bone, with high levels of compressive and tensile strain were also located around the femoral shaft and at the distal end for the Non-IC socket. It should be noted, substantially high strain concentrations were found at the top surface of the soft tissues at the interface with the bone. The elements containing the concentrated strains were deemed an artefact of the tied interface between the bone and soft tissue. These elements were removed and not included in the results reported.

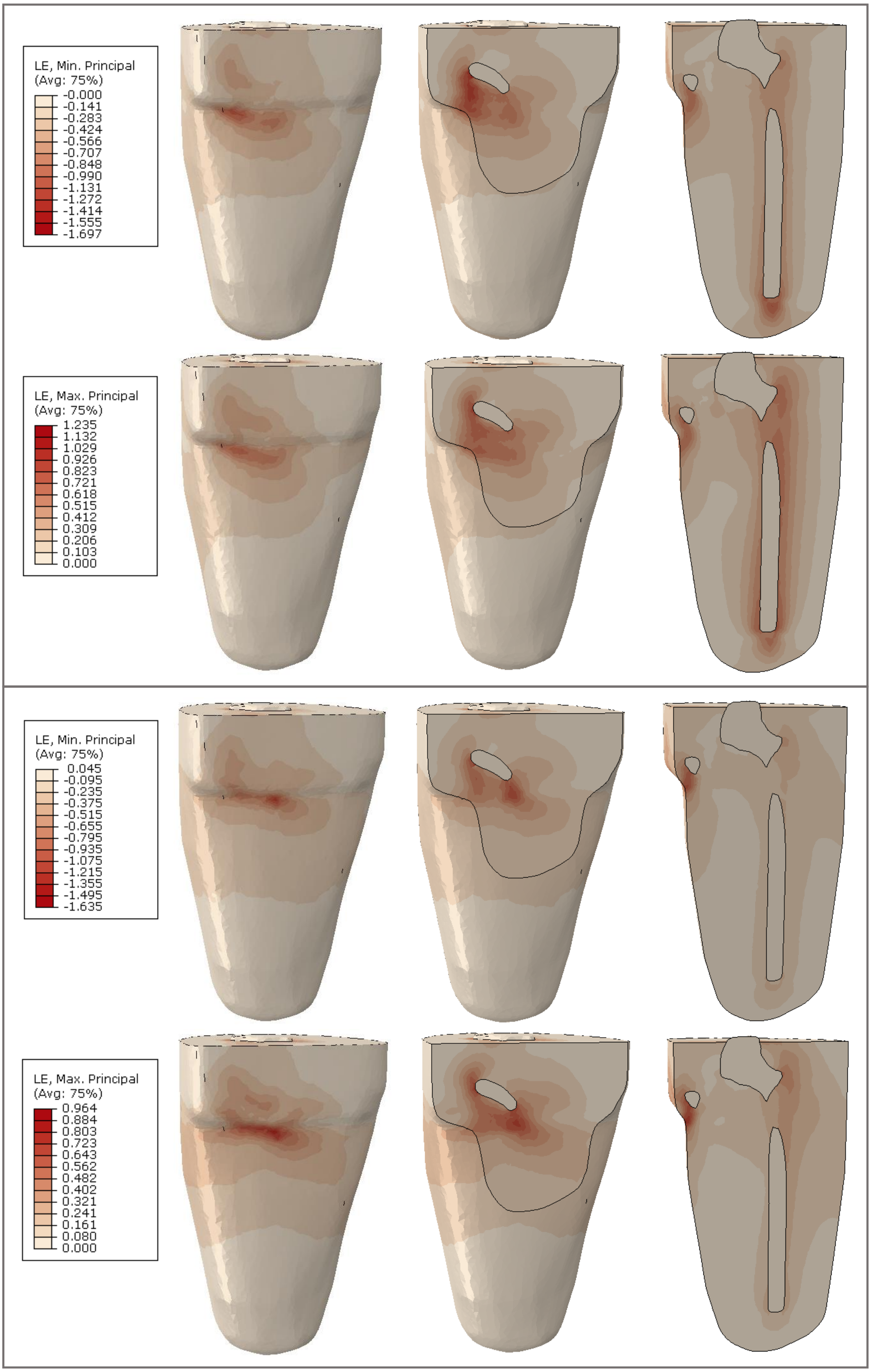

Figure 6-12: Non-IC socket (top) and IC socket (bottom) compressive (minimum) and tensile (maximum) principal logarithmic strain distribution.

The strain results were compared to the results of a study by Gefen et al. (2008) who defined a strain-time cell death threshold for bio-artificial muscle (BAM) specimens under true compressive strain (see Figure 6-13), which is the same as the logarithmic principal strain output. Similar to the results of Linder-Ganz et al. (2006), the results of Gefen and colleagues indicated a strain-time sigmoid curve, with the BAM cultures being able to tolerate compressive strains below 57% for up to approximately 60 minutes, with the tolerable compressive strains dropping to 42% after a duration of approximately 180 minutes. Subsequently, the threshold values of 57% and 42% compressive strain were applied to both model outputs (see Figure 6-14) to demonstrate the areas of tissue that exceeded these thresholds for potential bipedal stance durations of 60 and 180 minutes, respectively.

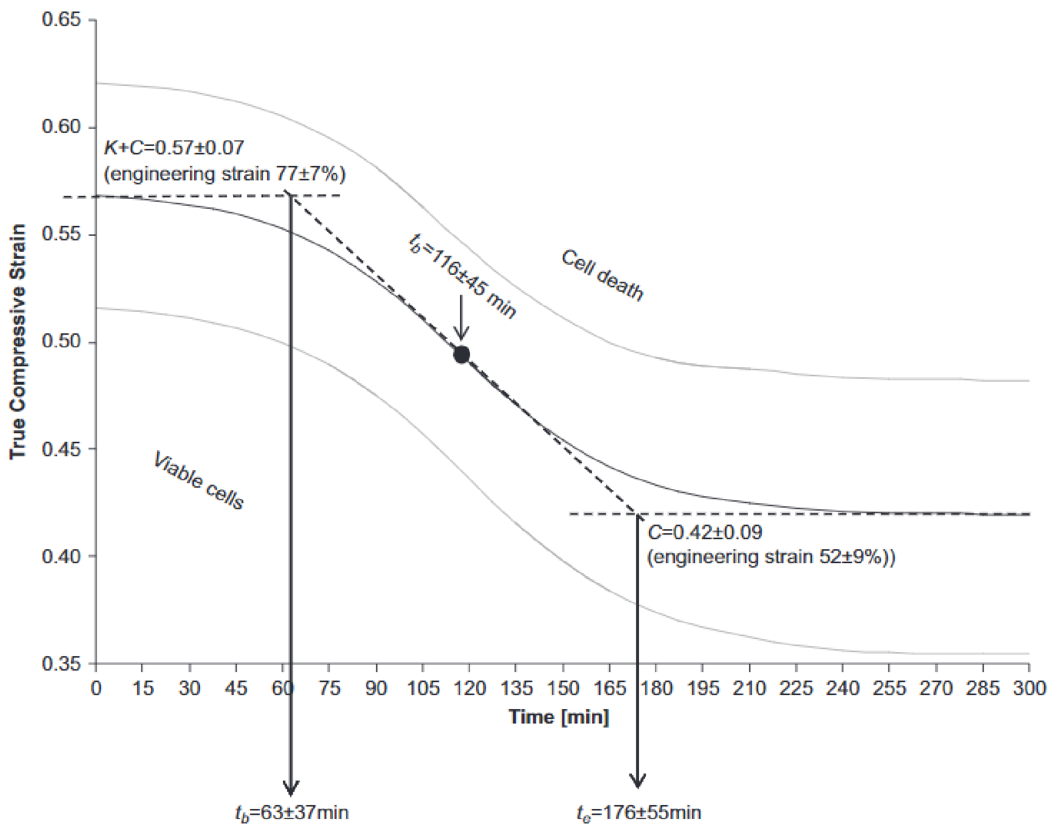

Figure 6-13: The strain-time cell death threshold for bio-artificial muscle specimens under compressive strain reported by Gefen et al. (2008). The 0.95-confidence limits are depicted as solid grey lines.

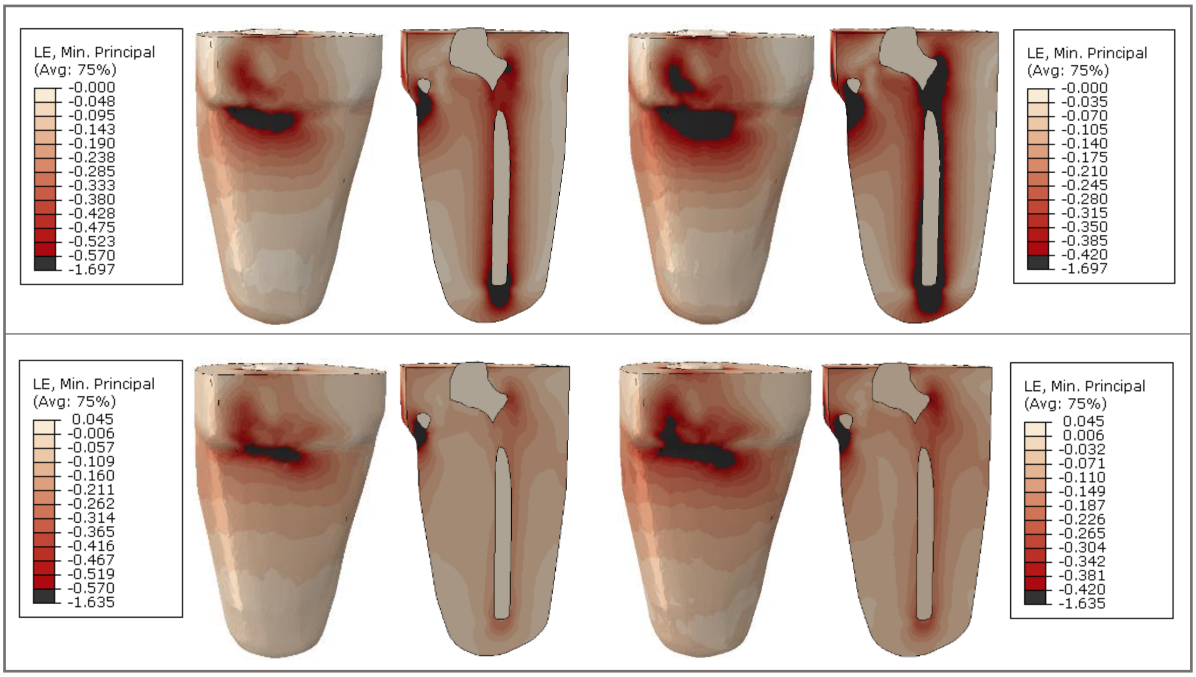

Figure 6-14: Area of tissue of Non-IC (top) and IC (bottom) socket model with strains greater than 57% (left) and 42% (right) required to induce cell death.

6.3.3 Discussion

6.3.3.1 Model Comparisons

The Non-IC socket resulted in a lower peak normal and shear stresses in comparison to the IC socket. The stresses were more evenly distributed over the residuum surface. The bipedal loading displaces the Non-IC socket to such an extent that the 30mm gap between the distal end of the residuum and the socket bottom is breached and distal loading occurs on the sensitive tissues at the distal end of the residuum. This may be a result of the AP dimension of the socket not being reduced as significantly as it would be in clinical practice for a socket that does not contain the ischial tuberosity. Further reductions of the AP dimension would have enabled more of the bodyweight to have been supported by hydrostatic loading of the soft tissue and friction. It is hypothesised that this would have reduced the socket displacement, which in turn would cause an initial increase in the peak stresses (due to the reduced socket displacement removing the distal loading), but these would reduce with further AP dimension reductions (see Section 6.2).

Conversely, the socket displacement for the IC socket was more limited, and did not allow for distal loading to occur, with the axial support being provided mostly by the pelvic bone. This was due to the encompassing of the ischial tuberosity and the greater reduction of the ML dimension. Whilst this did result in greater peak stresses in the IC socket compared to the Non-IC, the peak pressures were contained more to the ischial tuberosity at the posterior region of the medial brim. The ischial tuberosity is a pressure tolerant region and is the region of the pelvis that withstands the greatest loads while an individual is seated (Sonenblum et al. 2013). On the other hand, the peak pressures were located at the anterior region of the medial brim in the Non-IC socket (see Figure 6-7). This region contains pressure sensitive muscles and tendons; notably the adductor longus muscle, which is often the major muscle left intact after amputation, providing adduction of the residual limb. Pressure sensitive muscles require the pressure to be alleviated for them to function properly. Thus, the peak pressure occurring in the anterior region of the medial brim is not optimal for the socket design.

Comparisons between socket types (Quad, brimless and IC) has been conducted by transducer studies previously (Lee et al. 1997; Kahle and Highsmith 2013). These studies have provided varying results in terms of pressure distributions and participant preferences.

Lee and colleagues (1997) compared the pressure distributions of a Quad and IC socket for two participants during standing and walking. For standing conditions, the highest pressure was recorded at the ischial tuberosity for both sockets; approximately 34 kPa for the Quad socket and approximately 23 kPa for the IC socket. The IC socket produced a more even pressure spread during standing. This was also true for walking conditions, where the Quad socket produced higher pressures at the proximal medial and proximal posterior walls (over 90 kPa). Lee and colleagues hypothesised that the ML stability provided by encompassing the ischial tuberosity in the IC socket played a significant role in reducing the peak pressures at both proximal medial and distal lateral regions. Their justification was, during prosthetic leg stance phase, the pelvis will naturally rotate toward to the unsupported side. Adductor muscles on the prosthetic side work harder to maintain alignment but also push the distal end of the residual femur laterally against the socket wall, causing increased pressures in the distal lateral region and subsequently proximal medial region. This was deemed to be more present in the Quad sockets due to the reduced ML stabilisation (this is shown in Figure 2-3). It was noted that the test sockets were constructed with holes to fit the strain gauges for pressure measurements, this may have compromised the socket and influenced the pressures experienced as well as participant preference. Nonetheless, both participants in the study by Lee and colleagues expressed a preference for the IC socket compared to the Quad socket.

Kahle and Highsmith (2013) investigated the effect of brimless compared with IC socket design on the skin pressure of nine participants during ambulation. They used a coronal plane pelvic x-ray to make manual measurements for medial wall height of the sockets. The brimless socket’s mean was 33mm distal to ischial tuberosity, whereas the medial wall of the IC mean was 11mm proximal to ischial tuberosity. These measurements were taken from medial-most proximal aspect of both sockets to most distal aspect of ischial tuberosity. These were very similar to the Non-IC (28.1mm distal to ischial tuberosity) and IC (13.0mm proximal to ischial tuberosity) sockets simulated in this section. The brimless socket geometry used by Kahle and Highsmith (2013) is comparable to the Non-IC socket used in this section. Their results showed greater mean vertical displacement (pistoning) for the IC socket (15mm to 45mm) compared to the brimless socket (0.6mm to 31mm), which was the opposite to the findings of this section that showed greater displacement for the Non-IC (37.6mm) compared to IC (23.9mm) socket. Reasoning for this may be the greater volume reduction of 6% used by Kahle and Highsmith compared to the 2.6% to 2.8% reduction in this section, as further reduction would reduce the amount of socket displacement (see Section 6.2.2). For the brimless socket, they reported maximal average pressures in the medial proximal and distal lateral region as 25.3 ± 13.7 kPa and 30.0 ± 15.1 kPa, respectively. For the IC socket, these values were 43.0 ± 28.0 kPa and

25.1 ± 9.3 kPa, respectively. Their pressure results indicate a more even pressure distribution for the brimless socket compared to IC socket.

As both sockets examined by Kahle and Highsmith (2013) were reduced by the same amount, it can therefore be hypothesised that the socket displacement may have been caused by differences in gait characteristics by the individuals when wearing the sockets. For example, all participants in the study preferred the brimless socket, with a common narrative of the brimless socket providing increased comfort during standing and seating. The IC socket has been previous noted to have associated perineal discomfort (Gottschalk and Stills 1994). This would suggest the participants may have experienced gait abnormalities due to discomfort when wearing the IC socket, however no significant difference in the gait characteristics recorded were observed between the socket types (Kahle and Highsmith 2013). However, in their study a reduced medial proximal pressure in the brimless socket compared to IC socket may also account for the unanimous preference of the brimless socket.

There are discrepancies between these two studies (Lee et al. 1997; Kahle and Highsmith 2013). The IC socket produced a more even pressure distribution in the study by Kahle and Highsmith (2013) but not in the study by Lee et al. (1997). Whilst there are several variables that may have influenced this, such as testing protocols, sensor placement, study population, surgical scars, and previous socket use. But the largest influence is the socket design itself. This is directly related to the work, and capability of the prosthetist.

Nonetheless, the studies both found the only characteristic directly related to socket preference was the ability to evenly distribute pressure over the residuum. This would suggest the Non-IC socket would be preferable over the IC socket for the residuum simulated in this section, as it produced a more evenly spread pressure distribution and lower peak pressures (see Figure 6-7 and Figure 6-8). However, this was achieved by the socket undergoing greater displacement causing distal loading to occur, both of which have been stated as undesirable properties of prosthetic sockets (Lee et al. 1997; Neuman et al. 2005; The Steeper Group 2011; Boutwell et al. 2012). While distal loading is to be avoided, as the distal end of the residual trans-femoral limb is very sensitive to pressure (Mulroy 2018) causing pain, the amount of pressure at the distal end of the residuum did not exceed the minimum pain threshold of 350 kPa reported by Lee et al. (2005) at the distal end of the trans-tibial residuum. As there has not been a study directly relating the amount of displacement to detrimental effects such as loss of proprioception or stability, it is not possible to state whether the amount of socket displacement would have a negative effect on the individual’s gait. The amount of socket reduction for the Non-IC socket was -2.6% compared to the recommended range of -3% to -6% (Mulroy 2018). By reducing the socket volume further, the amount of displacement would be reduced (as shown in Section 6.2).

At a lower magnitude of loading, approximately 25% bodyweight, both sockets were primarily loaded through the pelvis, meaning a more direct comparison of the pressure distribution is possible due to the differences in socket brim contours. As a result, the peak pressure was greater in the Non-IC socket compared to the IC socket, with the IC model producing a more even pressure distribution (see Figure 6-11). This contrasts with the results of bipedal stance for which the IC socket produced the greatest peak pressures.

As mentioned above, the Non-IC model was considered more favourable due to its ability to more evenly distribute the pressure over the residual limb surface at bipedal stance, however this was only due to the socket reduction not sufficiently containing the soft tissues enough to prevent distal loading occurring. The addition of the results comparisons at approximately 25% bodyweight load indicate that if the Non-IC socket reduction had been greater to the extent it had prevented distal loading, the peak pressures would likely have been greater than those achieved by the IC socket at bipedal stance. Further, the location of the peak pressures was anterior to ischial tuberosity and at less tolerable locations compared to the IC socket.

6.3.3.2 Stress Damage Model

The pressures reported in this section from bipedal stance load, and by the studies of Lee et al. (1997) and Kahle and Highsmith (2013) throughout the gait cycle, did not exceed the lower limits of pain threshold reported by Lee et al. (2005). Indicating that in terms of pain, the socket designs for these studies was suitable. Research on a model for pressure-duration related to cell death was reported by Linder-Ganz et al. (2006) using the histopathology results from muscle tissue of albino rats, which had been exposed to pressures between 11.5 and 70 kPa for various durations. Their results were combined with the results of similar studies also conducted on albino rats (Hussain 1953; Kosiack 1961; Nola and Vistnes 1980; Salcido et al. 1995) and two sigmoid curve functions were fitted to the results (R^2=0.98, R^2=0.88). A normal abled person experiences pressures up to 40 kPa on the ischial tuberosity during sitting (Sussman and Bates-Jensen 2012). With the use of a lower limb prostheses, the trans-femoral socket will be applying pressures to the tissues around the ischium not only during sitting, but also during bipedal standing (Kahle and Highsmith 2013). This suggests that continual pressures will be applied around the ischium during the whole time the prosthesis is being used and may have a significant impact as the tissue viability considerably reduces with the duration of pressure applied.

If the results of the study by Linder-Ganz et al. (2006) are to be taken as quantifiably comparable to tissue damage in the residual limb, the region of the soft tissues where the pressure exceeds 32 kPa pressure (the area of tissues shown in grey in Figure 6-10) would be at serious risk of cell death occurring if the patient was to wear either of the sockets for bipedal stance durations greater than 15 minutes (this was the minimum amount of pressure-duration recorded for cell death). However, the average pressures of both sockets do not exceed the level of certain cell death over the entire duration. The amount of soft tissue exposed to pressures which exceed the threshold of 32 kPa is larger for the IC socket compared to the Non-IC socket simulated in this study. This implies a smaller area of soft tissue within the Non-IC socket would be susceptible to cell death (above 32 kPa) for durations up to 60 minutes (see Figure 6-10). Whereas, for durations above 110 minutes, the Non-IC socket would expose larger areas of soft tissue to potential cell death (above 9 kPa) compared to the IC socket.

The soft tissue model put forward by Linder-Ganz et al. (2006) may not be suitable to draw direct comparisons to the pressures recorded on the residual limb. Pressures on human soft tissue have commonly been reported above the threshold of 32 kPa by multiple lower residual limb transducer studies (Krouskop et al. 1987; Lee et al. 1997; Neumann et al. 2005; Kahle and

Highsmith 2013). None of these studies reported any tissue damage along with the pressures experienced. The participants of the lower limb socket studies commonly reported the sockets which exerted these pressures as being a comfortable fit, with the sockets being worn for in excess of 6 hours during the testing (Neuman et al. 2005). A study by Basboom et al. (2001) applied pressures of up to 70 kPa, for durations up to 6 hours, to the hind legs of Norway rats. Their results indicated these pressures did not cause soft tissue damage. But, pressures of 250 kPa did cause damage when applied for durations of up to 2 hours. The findings by Basboom and colleagues were acknowledged by Linder-Ganz et al. (2006) but were not included in the damage model. More recently, Stojadinovic et al. (2013) found continuous loads of 300 kPa for durations of 4 hours on ex vivo human tissue caused subepidermal separation (tissue damage) in both aged and young tissue. This suggests human tissue is not as susceptible to tissue damage as reported by Linder-Ganz and colleagues (2006).

Furthermore, the soft tissue damage model (see Figure 6-9) is solely based on pressure, whereas in reality due to the fit of the socket over the soft tissues, there will always be an aspect of shear stress exerted on the residual limb. For the models of this section, the peak shear stresses are often exerted on the soft tissues at similar locations to the peak pressures (see Figure 6-7 and Figure 6-8). Consequently, the effect of shear on the soft tissue damage should also be considered as the combination of pressure and shear reduces the amount of pressure required to cause vascular occlusion leading to significant tissue damage occurring earlier. For example, Goldstein and Sanders (1998) reported tissue breakdown with pressures of 250 kPa and shear stress of 45 kPa, however when increasing the shear stress to 71 kPa, a pressure of only 125 kPa was required to induce the same tissue breakdown. The minimum amount of shear recorded to reduce the required pressure to cause tissue damage was 36 kPa. In this section, the peak shear stresses on the IC model simulation was 36.5 kPa, also located at the medial proximal region along with the peak pressure of 83.1 kPa. This combination of peak shear and pressure can be assumed to reduce the tissue viability in this region, leading to a greater potential for damage. A study by Cagle et al. (2018) correlated the areas of trans-tibial FE models with pressures above 95 kPa and shear stresses above 33 kPa from simulated ambulation to the same areas the patients had experienced previous skin damage whilst wearing the prosthetic socket.

The available literature provides inconsistent values in terms of the amount of pressure and shear required to cause tissue damage. The premise that damage occurs from large amounts of pressure applied over a short period, but also when less pressure is applied over a longer period is agreed by more recent studies (Nguyen et al. 2008; Bhattacharya and Mishra 2015). As a result, the soft tissue damage model reported by Linder-Ganz and colleagues (2006) may not provide quantitative data comparable to the pressures achieved at the prosthetic interface but may provide a qualitative input to the capabilities of soft tissues to withstand pressures over longer durations. Thus, it is possible to propose the regions highlighted in Figure 6-10 would be the most susceptible to potential damage from the pressure and shear exerted on the residual limb. Furthermore, the tissues of the residual limb are able to self-adapt to the applied loads (Li et al. 2008; Li et al. 2011) reducing their vulnerability. It could be argued, that the threshold for potential damage would be greater for the tissues of the residual limb compared to animal and human tissues previously tested (Goldstein and Sanders 1998; Basboom et al. 2001; Linder-Ganz et al. 2006; Stojadinovic et al. 2013) that were not continually exposed to the loads exerted from the prosthetic socket.

6.3.3.3 Strain Damage Model

The peak compressive strains reported by both models were very similar (169.7% for Non-IC and 163.5% IC model). The peak compressive strains were also located around the ischium for both models; for the IC socket model, the compressive strains were focused underneath the posterior region of the ischium, whereas for the Non-IC socket model they were focused underneath the anterior region of the ischium (see Figure 6-12). Interestingly, at the soft tissue and liner interface, the compressive strain distribution showed similarities to the interfacial pressures for each model (see Figure 6-12). However, the AP and ML dimensional differences between the model variants changed the peak interfacial pressure but the compressive strains remained similar. This indicates that the interfacial pressures may be suggestive of the strain distribution, but the magnitude of pressure cannot be directly correlated to the strain magnitude. The pelvic geometry, notably the soft tissue covering the ischium, may account for the similarities in compressive strain values, as this was unchanged between the model types. This would suggest that the level of tissue covering the bony prominences is a critical factor in the compressive strain produced. This is in agreement with Sopher et al. (2010) who found significant increases in peak compressive strain in the tissue covering the ischial tuberosity when increasing the patients' BMI (soft tissue thickness and composition of adipose and muscle tissues) from 15 to 25 in two-dimensional FE models. Increases above a BMI of 25 were not reported to cause changes in the peak compressive strains.

Significant differences in tensile strain were found between the model variants. The tensile strain for the IC model showed a similar distribution to the compressive strain, with the peak strain (96.4%) being focused at the ischium, and lower magnitudes around the lateral side of the pelvis. On the other hand, significant magnitudes of both compressive and tensile strain were found at the distal end of the residual femur for the Non-IC model. This is a result of the excessive socket displacement in the model variant as mentioned previously. Further, the Non-IC model variant showed significant tensile strain along the shaft of the residual femur. This is also a result of the socket displacement as the soft tissue elements at the interface with the bone would have undergone large amounts of displacement whilst also constrained due to the tied constraint used at this interface.

As shown in this section, FE modelling has regularly predicted the highest strains occur internally near the bony prominences as opposed to the interface of the skin and supporting surface, consistent with the findings of others (Stekelenberg et al. 2007; Portnoy et al. 2009; Sopher et al. 2010; Ramirez et al. 2012; Traa et al. 2018; Traa et al. 2019). As mentioned previously, the peak pressures and strains on the external surface of the soft tissue shared similar locations but at varying magnitudes. Indicating interface pressure is not an appropriate parameter to define a damage threshold for deep tissue injury, such as pressure ulcers (Oomens et al. 2010) which is more susceptible to internal local deformations (strain) (Leopold and Gefen 2013), suggesting strain may be a more suitable parameter.

Similar to the pressure-duration threshold model reported by Linder-Ganz et al. (2007), Gefen et al. (2008) developed a strain-duration cell-death threshold using bio-artificial muscles (BAM) cultured from murine (rat) cells. Their study used an indentor to apply strain distributions within the BAM and induce deep tissue injuries (DTIs). Following indentation, the necrotic cells were stained with iodine, due to their increased permeability compared to healthy cells (see Section 2.1.1) to specify the volume of tissue damage and correlate to oedema, necrosis, haemorrhage, fibrosis and fatty infiltration (Fleckenstein 1996; Stekelenburg et al. 2007, Oomens et al. 2010).

The strain-duration damage model developed by Gefen and colleagues (2008) can be used to infer locations of potential strain induced damage. From Figure 6-14, it is evident the tissue covering the ischium for both model variants would be the primary location for potential tissue viability risk for strains exceeding 57% for durations up to 60 minutes. Further, the tissue at the distal end of the residuum for the Non-IC model also exceeds the strain threshold due to the distal loading introduced from excessive socket displacement. This highlights the importance of a sufficient socket fit and implies that further socket corrections would remove the potential for such displacements, and therefore reduce the amount of tissue at risk. For durations above 180 minutes, the volume of tissue at risk increases for both models. The longer duration and lower strain threshold increase the volume of tissue at risk along the medial side of the residuum at a level beneath the ischium. The additional volume of tissue exceeding the lower threshold of 42% compressive strain are located along the shaft of the residual femur for the Non-IC model and at the medial aspect of the pubic symphysis. Whilst the strains at both of these regions may be an accurate representation, as no other studies have modelled the trans-femoral residuum with the pelvis bone, they may also be influenced by the modelling techniques used, notably the tied interface between soft tissue and bone.

Nonetheless, the amount of tissue at risk due to deep tissue injury from compressive strains was primarily around the ischium for both models and the distal end of the femur for the Non-IC model. In comparison, the volume of tissue identified as being at risk due to the stress damage model developed by Linder-Ganz et al. (2007) was also focused around the ischium (see Figure 6-14), highlighting that this volume of tissue is exposed to the greatest stresses and strains and therefore has the highest vulnerability risk. As expected in both models, the amount of tissue at risk increased as the duration increased and threshold for damage decreased due to the sigmoid curve fit. However, the stress damage varied due to the different traits of the two sockets modelled, notably the reduced AP dimension for the Non-IC socket and the ML dimension for the IC socket. Whereas, the difference in volume of damage due to strain was a result of the excessive Non-IC socket displacement leading to distal loading. The damage inferred from the stress damage model is limited to the interfacial pressures and contact area. It has been demonstrated that strain damage has the potential to propagate along the muscle fibres to encompass an area of tissue significantly greater than the area of initial contact (Nelissen et al. 2018). This suggests that strain induced damage may propagate to tissues not contained within the prosthetic socket if they undergo enough localised deformation required to cause damage. Interestingly, both damage models reported a transition period after approximately 60 minutes where the amount of stress or strain required to induce damage was significantly reduced (see Figure 6-9 and Figure 6-13). Indicating a potentially inherent physiological time dependent limit on the duration soft tissues can withstand mechanical loading at a cellular level. If accurate, this would prove valuable information that may be used to inform the prosthesis user of the increased risk of extended prosthesis use.

For both socket models, the peak compressive strains from the donning phase were below the threshold of strain recorded to induce strain damage in the study by Gefen and colleagues (2008) (see Section 6.3.2). Conversely, after bipedal loading both socket models contained tissue regions with about 3 times the required threshold. Similarly, as found when drawing comparisons to the stress threshold damage model, strain values above the strain threshold used have commonly been reported in FE studies of the lower limb residuum.

A study by Lacroix and Patino (2011) performed FE modelling to simulate the trans-femoral socket donning phase. Their study used the same hyper elastic material properties for the soft tissues as this work. They reported mean peak compressive strains of 53.2% (±13.7%) and tensile strains of 32.4% (±16.7%), with the strain distribution varying for each participant model, but was most intense around the distal end of the residuum. The maximum overlap between socket and residuum reported in their study ranged between 10.3mm to 30.4mm. In contrast, the peak compressive and tensile strains of the socket models in this chapter were marginally lower but of the same magnitudes to those reported by Lacroix and Patino (2011). This was to be expected as the socket models in this chapter also had a lower level of maximum overlap of up to 4.7mm (see Table 6-1).

By comparing the results of this section with those of Lacroix and Patino (2011), it is evident that the low level of strains produced from the donning phase are highly influenced by both the socket geometry and the participant's residual limb geometry. This means the peak strains after the donning phase would be located at the areas where the socket was tighter and displaced the greatest amount of soft tissue. After the donning phase with the load applied to the socket from bipedal stance, the distribution of the peak strains shifts to the areas of peak load support, as demonstrated in this section. However, as a single participant residuum geometry was used in this study, and only the donning phase was simulated by Lacroix and Patino (2011), it cannot be determined whether the location of the peak strains from the donning phase remain at their initial distribution, shift to another location, or propagate throughout the tissue and become more uniform when increased loads are applied.

As mentioned previously, the potential increase in strain experienced by the soft tissue at the bone interface was the focus of a study by Ramirez and Velez (2012). Their study examined the effect of changing the boundary condition between bone and soft tissue within trans-femoral FE models. They reported the use of a friction coefficient at the bone and soft tissue interface resulted in increased peak compressive (85.1% to 133% for tied, 118% to 163% for friction) and tensile (26.1% to 82.3% for tied, 48.8% to 118% for friction) strains for all participant models compared to a tied boundary condition when simulating bipedal stance. For the tied condition in their study, the peak compressive and tensile strains were concentrated primarily at the top surface of the soft tissue, at the interface with the bone. This may have been as a result of the soft tissue deformation and the tied interface between bone and soft tissue causing artefacts at the top surface of the soft tissues as also found in this study. The friction boundary condition altered the strain distribution, focusing the peak strains at both the top surface of the soft tissue and underneath the distal end of the residual femur. This was even found for participant models which had long residual limbs and short residual femur bones covered with sufficient soft tissue padding at the distal end.

Ramirez and Velez applied a friction coefficient of 0.3 at the bone and soft tissue interface. The value was taken from a study by Shacham et al. (2010) which is the only study known to have reported on the friction between bone and muscle. However, their study was conducted in vitro and did not replicate in vivo conditions such as the hydrostatic pressure interacting between tissues within the body (Zhang et al. 2019). Whilst the assumption of a tied interface between bone and soft tissue may not be correct and therefore a potential modelling oversight, it is commonly used for lower limb FE models and allows for better comparisons between studies. Further, there has not been sufficient study into the in vivo interaction between bone and soft tissue to confirm the friction properties as these would alter with patient BMI, pressure applied from the socket fit, and interstitial fluid causing lubrication (Gebeshuber and van Aken 2017). Overall, the strains reported by Ramirez and Velez (2012) were less than those in this work. Besides, the differences in participant model geometry between the study by Ramirez et al. (2012) and this work and their use of linear elastic properties (200 kPa) to simulate the soft tissue material may have resulted in an over or under estimation of the resulting internal strain.

Both studies by Ramirez and Velez (2012) and Lacroix and Patino (2011) did not include the pelvis geometry, nor information on their socket geometry, such as whether the sockets were total surface bearing (distal loading), therefore comparisons that can be made of the strain distribution between their studies and this section are limited. Chapter 4 demonstrated that including the pelvic bone in the residual limb model reduced the peak compressive and tensile strains by up to 18.6% and 22.0% respectively. However, the FE model used in this section was developed further in comparison to the FE model initially used in Chapter 4. The sockets used in this section were designed by the prosthetist to provide additional relief underneath the ischium (60.07 to 66.75mm, see Figure 6-5) compared to the relief provided by the socket used in Chapter 4 (32.24mm, see Figure 4-6). Further, the models in this section were loaded for bipedal stance, whereas 110% bodyweight load was used in the previous chapters. Both of these factors would have reduced the peak compressive strains. On the other hand, the sockets in this section were not distal loading, and this might explain the increased compressive strain reported in this section (163.5% and 169.7%) compared to Chapter 4 (104.4%) as the load was only supported at the ischial tuberosity.

Furthermore, work conducted in previous chapters has demonstrated the magnitude of compressive strain is susceptible to changes in amount of tissue coverage over bony prominences, increased bodyweight (see Section 4.7), and reduced soft tissue stiffness (see Section 5.3.3). As a result, fluctuations in the individual's bodyweight due to diet and exercise regimes may have a positive or negative effect on the vulnerability of the tissues depending on weight loss or gain. Similarly, a stiffer residuum with more musculature may be less susceptible to strain-induced tissue damage compared to a less stiff residuum with a smaller amount of musculature when subjected to the same magnitude of loads. Thus, the daily lifestyle choices of an amputee may highly influence the potential for tissue breakdown.

FE studies on the biomechanics of sitting (Linder-Ganz et al. 2007; Sopher et al. 2010) have reported peak compressive strains underneath the ischial tuberosity that also exceed the strain threshold reported by Gefen et al. (2008). Linder-Ganz et al. (2007) used a reverse engineering approach to calculate the strain distribution by matching the material properties to best agree with the deformation change between undeformed buttock tissue and the deformed buttock tissue during sitting. The reverse engineered FE models reported compressive and tensile strains of 70-84% and 68-83% respectively across six healthy sitting humans. Sopher et al. (2010) simulated the loading conditions around the ischial tuberosities during sitting with a range of body mass indices (BMIs) and reported a peak compressive strain range of approximately 80% to 100% underneath the ischial tuberosity for all BMI models. They found the compressive strain in the muscle tissue to be approximately two-fold greater than in fat. Although the tolerances for injury are not well characterized for muscle versus fat tissue, it can be hypothesized from the results of Sopher et al. (2010) study that the onset of damage would primarily occur in the muscle tissue underneath the ischial tuberosity. The strain values reported by these studies (Linder-Ganz et al. 2007; Sopher et al. 2010) are marginally lower than those reported within this section. It can be assumed the change in angle and loading point of the ischium between standing and sitting can account for these differences. During sitting, the loading point would be at the posterior angle to the ischium, where the gluteal muscles would provide additional cushioning.

In addition to the pelvic bone, further surgical and morphological factors of the residual limb FE model have been shown to affect the reported strain (Portnoy et al. 2009). In reference to a trans-tibial residuum, the mean compressive strain at the bone-soft tissue interface were shown to increase with decreased bevelment of the tibial distal end, increase with increased bone length (thus decreased tissue covering the distal end) and decrease with increased muscle stiffness. The superficial factors such as size and depth of surgical scarring was not shown to affect the resultant strains. These morphological factors indicate the resultant strains in the residuum model are inherently highly influenced by the geometry and properties of the patient's residuum. The comparison of the two socket variants in this section showed minimal variation in resultant strain, this may indicate that the socket design is not a primary factor in the resultant strains. However, as only a single residuum geometry was used in this section, wider research is required across a range of residuum geometries and varying socket designs.

Besides the primary impact of tissue damage from the effect of strain (deformation) on the soft tissues, it may also have a secondary impact in the potential to alter the length-tension relationship of the muscles in the region of high strain. Muscles have an optimal length for which they can contract and relax most efficiently, but when the muscles are deformed beyond their contractible range the sarcomeres within the muscle fibres can be damaged. Overstretched sarcomeres can leave the muscle more susceptible to damage and involves individual muscle fibres failing to contract leading to reduced muscle force (Yeung et al. 2002; Morgan and Proske 2004; Gavin et al. 2018) and, as a result, have also been shown to induce changes in gait patterns (Schutte et al. 1997; Arnold and Delp 2011). The threshold amount of muscle lengthening required to induce these affects has not been researched. Nonetheless, the adductor longus, adductor magnus and pectineus are the primary muscles responsible for maintaining adduction of the residual limb following trans-femoral amputation (Gottschalk and Stills 1994). These muscles originate at locations along the ischium and pubic ramus and attach along the length of the femur. This muscle group runs along the medial side of the pelvis and residual limb and would therefore be the most likely to be affected from the high strains reported in this region by the FE models of this section. As a result, it can be assumed that the patient's ability to maintain sufficient adduction may potentially be compromised. The health of this muscle group should be prioritised considering the adductor muscles are already less efficient considering they are reduced in length following amputation.

In the same way to the stress model previously discussed, the results of Gefen et al. (2008) are not suitable for drawing conclusive comparisons - in terms of strain tissue death. Strains from previous studies of the residual limb (Portnoy et al. 2009; Ramirez and Velez 2012), the biomechanics of sitting (Linder-Ganz et al. 2007; Sopher et al. 2010) and this work have been consistently greater than the strain threshold values. Instead their results may be used to highlight locations of potential tissue viability risk, and imply the qualitative effect of strain over certain durations rather than definitive threshold indicators for human tissue damage which may prove a successful indicator for the evaluation of socket fit for sockets designed by computational design.

As acknowledged by Gefen and colleagues (2008), a limitation of using the BAM to determine the strain levels of simulated DTI is the tissue-engineered muscles lacking the hierarchical organisation of native tissue, such as a capillary bed. A capillary bed would significantly aid in the oxygen supply to the cells and removal of cellular waste that would have contributed to the acidosis aspect of ischemia. Potentially meaning the level of strain threshold to cause DTI by ischemia would be higher than that reported.

The strain damage model only takes into consideration the compressive strains. The high magnitudes of compressive and tensile strains in this study occurred at similar locations within the soft tissues, both of which affect the muscle length and thus the contracting capabilities. A study by Stekelenburg et al. (2007) used uniaxial indentation testing applying strains of up to 37% compressive and 170% tensile to the hindlegs of Brown Norway rats. They found irreversible damage to muscle tissue after two hours of the applied pressure. However, the compressive strains applied in their study fall within the ‘viable cells’ region reported by Gefen et al. (2008) (see Figure 6-13). This suggests that the use of purely compressive strain for cell damage may not be accurate and a more holistic approach to tissue damage involving multiple factors may be required.

More recently, Traa et al. (2019) conducted work similar to that of Gefen et al. (2008) comparing the tissue damage from indentation testing on rats to the internal deformations evaluated by FE modelling. Their work indicated that there is no distinct damage threshold at specific strain values, but rather a vague transition zone between ‘safe’ and ‘danger’ regions. Further, their analysis showed a subject specific tolerance to the compressive strain induced tissue damage between the range of rats tested, with the volume of damaged tissue varying by approximately 3.5-fold between rats when indentation was performed under the same conditions.

In this section damage models from both normal stress and compressive strain were examined due to their prevalence in previous literature and high potential to cause tissue damage (see Section 2.1). As mentioned previously, shear stresses at the surface of the soft tissues have been well documented in relating to tissue damage. However, there are large discrepancies in the recorded levels of shear stress required to cause damage, with limited information proclaiming threshold values. To this end, the shear stresses were not examined in relation to their potential to cause damage.

6.3.4 Clinical Relevance

This study offers an insight into the techniques used to contour the brim of the prosthetic socket in clinical practice. The design of prosthetic sockets is highly specific to the patient's pelvic geometry. The use of CAD to design the socket contours, allowed direct feedback on the distances between the socket contours in relation to the patient's pelvic geometry, allowing the prosthetist to use their knowledge in determining the favourable contours of the socket brim without having to fabricate the socket and obtain feedback from the patient. In comparison to conventional techniques, using socket models to design the socket contours would allow for easier collaboration and communication of socket designs between prosthetists, as it provides direct comparisons between the geometry of the patient and the socket.

The sockets simulated in this section were the initial designs, whereas on average at least nine socket iterations are performed by the prosthetist in the first 12 months following amputation (Prezzin et al. 2004). This shows the significant information that can be gathered from the use of FE modelling for the first iteration alone. Subsequent iterations of the socket models design would provide further improvements to the socket design.

The application of both a stress threshold model (Linder-Ganz et al. 2006) and a strain threshold damage model (Gefen et al. 2008), are capable of being comparative tools, providing qualitative information about the tissues that may potentially be compromised as a result of the stresses and strains experienced. As demonstrated in this section, both of these may successfully be used as an indicator for the evaluation of socket fit for sockets designed by computational design, and additionally inform the areas required for modification throughout the socket fitting process to limit the potential for tissue damage.

The ischium is often the site of the greatest stresses but has a limited amount of surrounding soft tissue. Therefore, adaptations to the socket brim contour may be made to reduce the peak pressures and even move their locations as shown in this section. The use of interfacial stress as an indicator to determine an appropriate socket fit has recently been the focus of innovative socket design solutions such as the EU Horizon 2020 Socket Master project (Xu et al. 2018). Whilst interfacial sensors can provide real-time feedback and can be related to patient comfort (Lee et al. 2005), internal tissue strain has commonly been acknowledged as a more determinant indicator of non-superficial tissue damage compared to interfacial pressure (Oomens et al. 2010). The internal tissue strain is only obtainable from FE modelling and not from experimental sensors, and therefore demonstrates a critical advantage of incorporating the use of FE modelling into the socket design process.

The study methodologies used to develop, simulate, and compare socket designs in this chapter have covered a significant portion of the work towards developing a standardised approach for socket design. This is demonstrated by the computational section of the flow chart shown in Figure 6-15. For further development, it is suggested that a combination of computational modelling (CAD and FEA) and experimental testing would be performed concurrently.

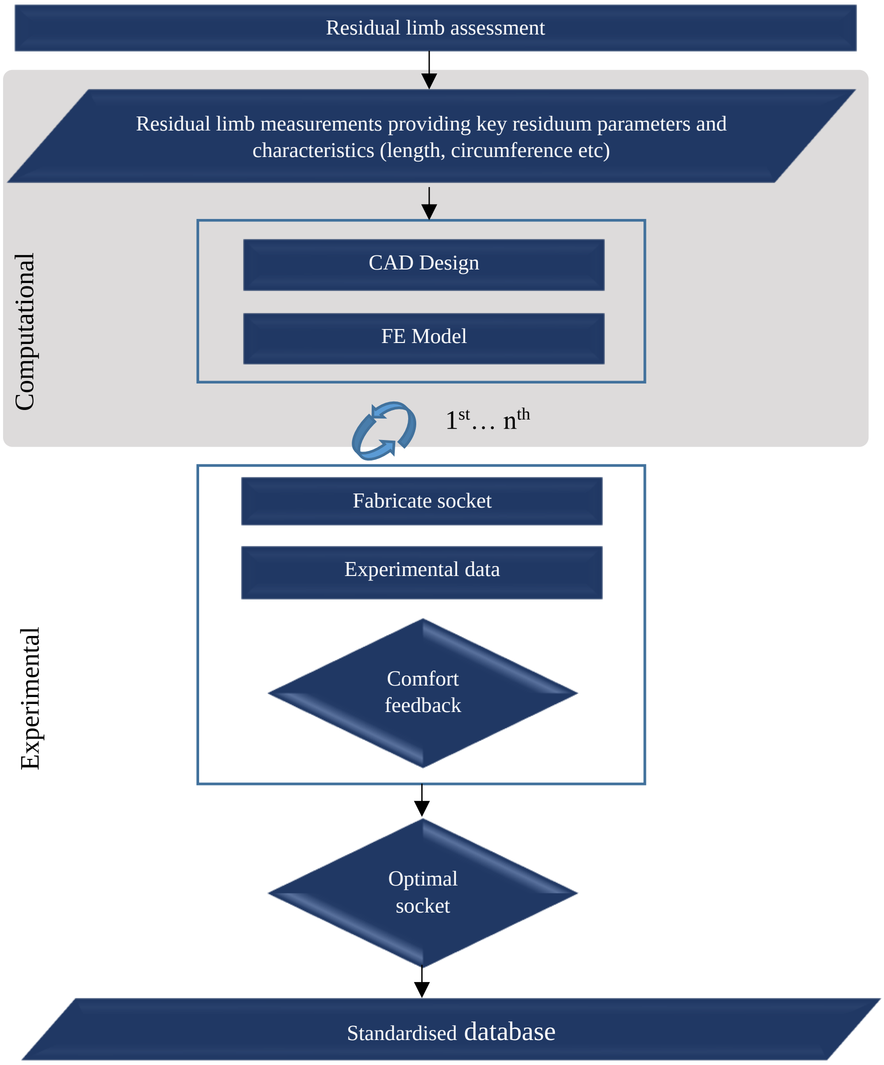

Figure 6-15: Flow diagram demonstrating implementation of computation design combined with experimental study and prosthetist input. This study covers the highlighted area, with the potential to cover the remaining area by further study.

To enhance the current iterative process of socket design, initial socket model iterations would be designed within CAD, with input from the prosthetist, and solved within FEA. This would be used to inform subsequent sockets which would be fabricated from the socket models and experimental testing used to obtain validation of the subject specific FE models and direct feedback from the patient regarding the socket comfort during testing. This would be performed numerous times until the socket fit is deemed comfortable and appropriate by both the patient and prosthetist. In this chapter, the computational section of Figure 6-15 highlighted within the grey box, was followed for a single residual limb geometry, deemed 'long and thin' by the prosthetist. To be applicable in a clinical setting, the work should cover a larger study population with varying residuum circumferential and longitude lengths.

6.3.5 Conclusion

In this chapter the main limitation of the previous chapters, the socket geometry, was addressed. The socket volume reduction was assessed, and collaboration with ProActive Prosthetics was performed to create two distinctly different sockets.

At bipedal stance, the IC socket exposed the residual limb to greater pressures and shear stresses compared to the Non-IC socket. The Non-IC socket achieved a more even pressure distribution which has been directly related to patient comfort and socket preference, but this was also combined with greater socket displacement and distal loading. This section indicates the choice of socket brim contours and the approach taken by the prosthetist to design the socket directly influences the comfort of the socket. Further work should be conducted to apply this methodology across a wider residuum study population of varying bulks, heights, and shape. This work on FE models may be used to help standardise the work conducted by the prosthetist, allowing better socket fits to be more readily achieved and the techniques of the prosthetist to be better understood and more widely shared.

As it was not possible to obtain direct feedback from the patient whose residuum was used to create the FE model, the FE outputs of normal stresses were used to define a favourable socket fit by inferring potential tissue damage. The IC socket subjected a larger amount of tissue to stresses potentially capable of causing tissue damage for durations up to 60 minutes. Conversely, for durations above 110 minutes, it was the Non-IC socket which would have subjected larger amounts of tissues to these stresses as the threshold decreased with duration. Whilst there is a known premise that damage occurs from large amounts of pressure applied over a short period, but also when less pressure is applied over a longer period, the literature on soft tissue damage is often varied due to a variety of testing protocols, leading to boundaries which are not well established. This produces difficultly in performing direct comparisons to assess the potential viability of the residual limb tissues of the FE models simulated.

Further comparisons were made to a strain threshold damage model. Both the Non-IC and IC socket models continually reported compressive strain values considerably higher than the threshold values reported to have caused cell death. In both of these damage models, the peak stresses and strains occurred at similar locations indicating that the soft tissue around the ischium (the area of load support) had the highest potential for cell damage. The prediction of injury from these models is reliant on the accurate characterisation of the soft tissue properties. Further, it has been shown that the tissues of the residual limb adapt and stiffen as they become more established at the prosthetic interface. Coupled with the critiques of the examined damage models, this demonstrates the difficulty and required caution when defining a tissue damage threshold.

The sockets designed and simulated in this section were obtained after the initial consultation and design input from the prosthetists at ProActive Prosthetics. The results of this initial design were comparable to the results achieved by studies which used sockets fabricated using the conventional design process and multiple socket design iterations. Without direct testing by a patient and feedback being provided, it is not possible to confirm that the socket geometry designed in this section would be suitable for the individual.

Due to the iterative process of socket design, it may be assumed that additional rectifications to the socket models in this chapter enable the socket to be optimised. As the boundaries for soft tissue damage and pain threshold are not well established and subjective, these rectifications should be combined with the fabrication and testing of the socket in a clinical environment. Direct testing of the current socket design, and feedback from the individual who the socket was designed for, should be used to rectify the socket. This method of socket design falls outside the scope of the current thesis, but methods for approaching this are shown in Figure 6-15 and discussed in the next chapter.

7. CONCLUSIONS AND FUTURE WORK

7.1 Research Summary

The research presented in this thesis provides an insight into aspects of the interface between the residual limb and prosthetic socket which had not previously been examined in detail. The narrative across chapters four, five and six was the objective evaluation of important variables for FE modelling of the trans-femoral residuum. Throughout these chapters the residual limb model increased in complexity with each chapter building on the previous. By developing the modelling method used to simulate the lower limb residuum, there is potential to further the developments in socket design by integrating computational modelling into the current process. The work performed has highlighted the susceptibility of the prosthetic interface to the various aspects examined. The FE modelling setup developed can be used to measure qualitative results of prosthetic liners and sockets which should enable both FE models and clinical comparisons. The second chapter literature review highlighted aspects of the modelling setup overlooked in previous studies. These aspects were identified as the pelvic bone, prosthetic liner, and prosthetic socket. The third chapter of this thesis detailed the process used to create the FE models, and the subsequent chapters four, five and six examined the modelling aspects individually. The main findings of these chapters are summarised as follows:

Pelvic Bone.

The addition of the pelvis geometry to the FE models provided support for the proximal medial wall of the socket to bear against the ischium, shifting the peak stresses from the distal end of the residuum to the proximal medial region (ischial support region). This method of supporting the loading has been known and used by prosthetists in the socket design, but it has not been modelled in previous FE simulations before. Previous models had used external boundary conditions to encourage the proximal tissues to support the load and prevent them from displacing axially (Zhang et al. 2013; Velez Zea et al. 2015). The compressive strains were found to correlate to the amount of tissue covering the ischium but not to the sharpness of the ischial tuberosities. The pelvic bone allowed the support of the load and the deformation of the proximal tissues of the residual limbs to be more truly represented.

Prosthetic Liner.

Friction testing of the liners obtained from Ossur and Ottobock showed that the friction coefficient for all liners decreased in wet conditions (0.87 ±0.16) compared to dry conditions (1.45 ±0.21). Urethane produced higher COF on the internal surface of the liner compared to the silicone or copolymer-based counterparts. The external surfaces of the liners with a textured backing of nylon, had a higher COF compared to the liners with a cotton backing. When incorporated in the FE modelling a general trend was found with higher peak normal and shear stresses occurring with higher COF levels at both the residuum-liner and liner-socket interfaces. But the changes were not entirely consistent and were believed to be caused by the variation of the residuum shape and size between the participant models. The resultant tissue strains were not found to be highly susceptible to changes in friction coefficient at either interface.

Statistical analysis showed tissue stiffness, liner stiffness and liner thickness were all statistically significant in terms of the resultant pressures and shear stresses exerted on the soft tissues. Changes in liner stiffness and thickness were shown to have similar effects on shear stresses, whereas the liner stiffness had a greater effect on pressure compared to liner thickness. Therefore, to reduce the peak pressures more effectively at certain locations it would be more effective for the prosthetist to prescribe the patient a softer liner rather than a thicker liner.

Prosthetic Socket.

Reducing the volume of the socket significantly reduced the peak stresses and socket displacement (by over 50% for -4.5% volume reduction) and significantly increased the average pressures (by 200% for -4.5% volume reduction). The effect of socket volume reduction was observed over two phases; the initial phase (0 to -1.4% volume reduction) was effective at reducing the peak pressure and shear stresses, and socket displacement, whilst the increased average pressures were observed during the second phase (-1.4% to -4.5% volume reduction.

Collaboration with ProActive Prosthetics resulted in two distinguishably different socket designs: IC and Non-IC sockets. Incorporating the ischium within the medial socket brim was found to localise the peak pressures to the pressure tolerant ischial tuberosity. Not containing the ischium in the Non-IC socket led to pressures occurring at the pressure sensitive anterior region of the medial brim (see Figure 2-5). The tissues in both models experienced similar magnitudes of compressive strains. At bipedal stance, higher peak stresses were reported on the residuum from the IC socket compared to the Non-IC socket. The Non-IC socket achieved a more even pressure distribution which has been reported as a primary factor for socket preference by patients.

The results from both socket simulations in Section 6.3 were compared to two damage models to infer locations of potential tissue damage on the residuum. For the stress damage model, higher peak normal stresses exerted on the residuum from the IC socket caused a larger area of tissue to be potentially compromised for shorter durations of bipedal standing. Whereas, for longer durations of bipedal stance, the Non-IC socket would potentially risk the viability of a larger area of tissue, due to it having higher average pressures on the residuum compared to the IC socket. The peak compressive strains were not found to vary significantly between the two socket designs. As a result, this indicated similar levels of potential tissue damage at durations under 60 minutes. Conversely, a larger volume of tissue was found to be potentially compromised for the Non-IC socket for longer durations. As expected, both damage models indicated the proximal medial tissues of the residuum as having the highest potential for damage due to this being the prime location of load support.

Due to the continual developments that were made to the FE models throughout the process of this thesis, it is difficult to conduct direct comparisons between the changes caused by the variables examined in chapters four, five and six. Nonetheless, the addition of the pelvic bone to the geometry of the residuum model is a simple and accurate modification and has arguably the largest impact on the FE models examined in this thesis. In various fields of study, the results of FEA are commonly accepted and trusted, however throughout this study, the FE models have been highly susceptible to the multiple variables considered. This therefore demonstrates the required complexity needed for the FE model of the lower residual limb to be able to accurately simulate the real-life loading conditions. This directly links to the "solving the right equations" aspect of validation, where the simulations being validated would need to be accurately replicating experimental data where all the known variables are recorded. Consequently, there may be potential difficulty in using FE as a practical tool without direct methods of validation.

The research aim of this thesis, was to evolve the FE modelling of the trans-femoral residual limb for simulation of the interaction between the lower limb prosthetic components. The FE models have been evolved throughout the development of chapters four, five and six, with the study methodologies used in Chapter six providing significant work towards standardising the socket design method utilising computational design (see Section 6.3.4). However, additional work may be required for this to be fully realised. This is discussed in the following sections.

7.2 Further Work

This section outlines the further work that may be done to progress the work conducted in this thesis. The further work has been split into two sections: future research, which requires substantial work to be carried out to examine the potential for integrating FE modelling into clinical design application, and recommendations, these are additional aspects of socket modelling which have not been previously examined and would require a smaller amount of work to research.

7.2.1 Future Research

The future vision of this work, enabled by future research, is that FE modelling could be readily adapted to facilitate the existing socket modelling procedure to further explore clinical questions. For example, providing an insight into how the alterations made between the iterative socket rectifications leads to a comfortable fit for the patient would be very attractive for a prosthetist.

As mentioned in Section 6.3.4, this approach would be conducted using a combination of FE modelling and experimental testing performed concurrently (as displayed in Figure 6-15). This would provide potentially useful information regarding the interfacial stresses for each socket iteration leading up to an 'optimal' socket. This may include informative criteria in terms of pressure and strain at certain regions of the residuum. To be widely applicable in a clinical setting, the work should cover a larger study population with varying residuum lengths and circumferential dimensions (as displayed in residual limb measurements section of Figure 6-15). Subsequently, this would create a standardised approach for the selection and creation of an initial socket design for an individual whose residuum possesses characteristics within the study population. The end goal would be to correlate the development of socket geometry, interfacial stresses, and patient comfort to significantly reduce the number of socket design iterations required for new patients. Fundamentally, this rationalisation of the current process would provide increased levels of knowledge sharing and reduce the reliability on the tacit knowledge from the individual prosthetist. However, it would still require knowledge provided by the prosthetist to determine physiological aspects of the patient and locations of previous tissue damage during the initial assessment.

7.2.2 Recommendations

In both the analysis of previous literature and simulations performed in this study, there are assumptions that have been made in the modelling process that are recommended to be considered in future studies. To the best of the authors' knowledge, these two recommendations have not been examined or even considered by any current study. These are explained separately below.

a) During the donning of the liner, the liner is pre-tensed which will affect its stress-strain state. This was not simulated in this study, neither has it been simulated in previous FE studies nor considered during liner mechanical testing studies. A liner is available in a range of sizes and is chosen by measuring the residual limb of the patient to determine the appropriate fit. However, the residual limb often undergoes minor to larger volume fluctuations which would change the fit of the single liner. Examining the effect of different levels of pre-tensed liner by FE study would provide greater information available to prosthetists when determining the appropriate liner combined with the volume fluctuation history of the patient's residuum.

b) The peak ground reaction forces occur at either heel strike or toe off depending on the individuals gait characteristics. During these phases, the stance leg would either be flexed or extended altering the positioning of the joints. This has not been considered by any previous studies including this study, all of which modelled the alignment between the pelvis and residual femur from the digital scans obtained from the patient in the supine position. While this may be representative of the lower limb alignment during bipedal stance, it is not representative of the alignment during heel strike or toe off. The angle of the hip joint varies by approximately 40 degrees throughout the gait cycle (Lewis and Sahrmann 2015). This change of angle is likely to alter the peak pressures along the brim of the socket and apply a moment to residuum from the socket. Therefore, examination should be performed to consider how the different stages of stance phase alters the positioning of the hip joint and its effect on the required brim contours to potentially alleviate or consolidate pressure in certain areas.

8. REFERENCES

ABAQUS (2011) ABAQUS Documentation', Dassault Systèmes, Providence, RI, USA

ABAQUS User's Manual (2013) Version 6.12, vol. 5

Adams, M., Briscoe, B., Johnson, S. (2007) Friction and lubrication of human skin. Tribol. Lett. 26(3) pp 239–253

Agam, L., Gefen, A. (2007) Pressure ulcers and deep tissue injury: a bioengineering perspective. Journal of Wound Care 16(8) pp 336-342

Ahmad, A., (2009) Prosthetic problems of transtibial amputee. J. Postgrad. Med. Inst. 23(2) pp 155–158

Al-Fakih, E.A., Osman, N.A.A., Adikan, F.R.M. (2016) Techniques for interface stress measurements within prosthetic sockets of transtibial amputees: A review of the past 50 years research. Sensors 16(7) pp 1119

Ali, S., Osman, N., Arifin, N., Gholizadeh, H., Razak, N., Aba, W. (2014) Comparative study between Dermo, Pelite and Seal-In X5 liners: Effect on patient’s satisfaction and perceived problems. The Scientific World Journal. Article ID769810, 8 pages

Andre´, T., Lefe`vre, P., Thonnard, J.L. (2009) A continuous measure of fingertip friction during precision grip. J. Neurosci. Methods 179(2) pp 224–229

Andrysek, J., Eshraghi, A. (2017) Influence of prosthetic socket design and fitting on gait. In: Müller B. et al. (eds) Handbook of Human Motion. Springer, Cham

Appoldt, F.A., Bennett, L.M., Contini, R. (1969) Socket pressure as a function of pressure transducer protrusion. Bull Prost Res 10-11 pp 236–49

Appoldt, F.A., Bennett, L.M., Contini, R. (1970) Tangential pressure measurements in above-knee suction sockets. Bull Proshet Res 10(13) pp 70-86

Arnold, E.M., Delp, S.L. (2011) Fibre operating lengths of human lower limb muscles during walking. Philos Trans R Soc Lond B Biol Sci. 366(1570) pp 1530-1539

Arotaritei, D., Turnea, M., Filep, R., Ilea, M., Rotariu, M. (2015) Analyze of liner influence in transtibial prosthetic taking into account tribiological aspects. In: 9th International Symposium on Advanced Topics in Electrical Engineering, pp 299-302. Bucharest, Romania

Automotion Components® (2017) Linear Ball Bushings [Online] (Available at: https://www.automotioncomponents.co.uk/media/files/datasheet/lin.lspb.pdf)

Bader, D. (1990) Pressure sores – Clinical practice and scientific approach. MacMillan Press Scientific & Medical, London

Bader, D., Bouten, C., Colin, D., Oomens, C. (2005) Pressure ulcer research: Current and future perspectives. Springer Science & Business Media.

Berry, D., Olson, M., Larntz, K. (2009) Perceived stability, function and satisfaction among transfemoral amputees using microprocessor and nonmicroprocessor controlled prosthetic knees: A multicentre survey. Journal of Prosthetics and Orthotics 21(1) pp 32-42

Bhattacharya, S., Mishra, R.K. (2015) Pressure ulcers: current understanding and newer modalities of treatment. Indian J Plast Surg. 48(1) pp 4-16

Blatchford (2019) Caring for your lower limb prosthesis: Information for patients. Imperial College Healthcare. NHS Trust. [Online] (Available at: Blatchford.co.uk/documents/caring-lower-limb-prosthesis.pdf/)

Board, W.J., Street, G.M., Caspers, C. (2001) A comparison of trans-tibial amputee suction and vacuum socket conditions. Prosthetics and Orthotics International 25 pp 202-209

Boonhong, J. (2006) Correlation between volumes and circumferences of residual limb in below knee amputees. J Med Assoc Thai 89 pp S1-S4

Bouten, C.V., Oomens, C.W., Baaijens, F.P., Bader, D. (2003) The aetiology of pressure ulcers: skin deep or muscle bound? Arch Phys Med Rehabil 84(6) pp 616-619

Boutwell, E., Stine, R., Hansen, A., Tucker, K., Gard, S. (2012) Effect of prosthetic gel liner thickness on gait biomechanics and pressure distribution within the transtibial socket. Journal of Rehabilitation Research & Development 49(2) pp 227-240

Bower, A. (2009) Applied Mechanics of Solids. CRC Press 1st edition

Buis, A., Kamyab, M., Hillman, S., (2017) A preliminary evaluation of a hydro-cast trans-femoral socket, a proof of concept. Pro Ort Open J. 1(7)

Cagle, J,C., Hafner, B. J., Taflin, N.B., Sanders, J.E. (2018) Characterisation of prosthetic liner products for people with transtibial amputation. Journal of Prosthetics and Orthotics, 30(4) pp 187-199

Cagle, J.C., Reinhall, P.G., Allyn, K.J., McLean, J., Hinrichs, P., Hafner, B.J., Sanders, J.E. (2018) A finite element model to assess transtibial prosthetic sockets with elastomeric liners. Medical & Biological Engineering & Computing 56(7) pp 1227-1240

Cagle, J.C., Reinhall, P.G., Hafner, B.J., Sanders, J.E. (2017) Development of standardized material testing protocols for prosthetic liners. Journal of Biomedical Engineering 139(4) 0450011–04500112

Cavaco, A., Duraes, L., Pais, S., Ramalho, A. (2016) Friction of prosthetic interfaces used by transtibial amputees. Biotribology 6 pp 36-41

Cavaco, A., Ramalho, A., Pais, S., Durães, L. (2015) Mechanical and structural characterization of tibial prosthetic interfaces before and after aging under simulated service conditions. Journal of the Mechanical Behaviour of Biomedical Materials 43 pp 78-90

Chen, G. (2014) Fundamentals of contact mechanics and friction. Handbook of Friction-Vibration Interactions. Woodhead Publishing pages 71-152

Chen, G. (2014) Handbook of Friction-Vibration Interactions. Woodhead Publishing Elsevier, London

Chihuri, S., Wong, C.K. (2018) Factors associated with the likelihood of fall-related injury among people with lower limb loss. Inj Epidemiol 5(42) 8 pages

Choi, A.P.C., Zheng, Y.P. (2005) Estimation of Young's modulus and Poisson's ratio of soft tissue from indentation using two different-sized indentors: finite element analysis of the finite deformation effect. Medical & Biological Engineering & Computing 43 pp 258-264

Colombo, G., Filippi, S., Rizzi, C., Rotini, F. (2010) A new paradigm for the development of custom-fit soft sockets for lower limb prostheses. Comput. Ind. 61 pp 513-523

Cutti, A., Osti, G., Migliore, G., Cardin, D., Venturoli, F., Verni, G. (2018) Clinical Effectiveness of a Novel Hydrostatic Casting Method for Transfemoral Amputees: Results From the First 64 Patients. [Online] (Available at: https://www.researchgate.net/publication/331075453_Clinical_Effectiveness_of_a_Novel_Hydrostatic_Casting_Method_for_Transfemoral_Amputees_Results_From_the_First_64_Patients)

Dai, X., Li, Y., Zhang, M., Cheung, J. (2006) Effect of sock on biomechanical responses of foot during walking. Clinical Biomechanics 21(3) pp 314-321

Davie-Smith, F., Hebenton, J., Scott, H. (2018) A Survey of the Lower Limb Amputee Population in Scotland: Full Report. Research report for Scottish Physiotherapy Amputee Research Group. University of Strathclyde & NHS Scotland. 59 pages

Defloor, T. (1999) the risk of pressure sores: a conceptual scheme. J Clin Nurs 8(3) pp 206-216

Derler, S., Gerhardt, L.C. (2012) Tribology of skin: review and analysis of experimental results for the friction coefficient of human skin. Tribology Letters 45(1) 1-27

Derler, S., Rossi, R.M., Rotaru, G. (2015) Understanding the variation of friction coefficients of human skin as a function skin hydration and interfacial water films. J Engineering Tribology 229(3) pp 285-293

Derler, S., Schrade, U., Gerhardt, L.C (2007) Tribology of human skin and mechanical skin equivalents in contact with textiles. Wear 263 pp 1112-1116

Dickinson, A.S., Steer, J.W., Worsley, P.R. (2017) Finite element analysis of the amputated lower limb: A systematic review and recommendations. Medical Engineering Physics 43, 1-18

Dijkstra, E. J., Guteirrez-Farewik, E. M. (2015) Computation of ground reaction force using Zero Moment Point. Journal of Biomechanics 48 pp 3776-3781

Dinsdale, S.M. (1973) Decubitus ulcers in swine: light and electron microscopy study of pathogenesis. Arch Phys Med Rehabil 54. pp 51-56

Duchemin, L., Bousson, V., Raossanaly, C., Bergot, C., Laredo, J.D., Skalli, W., Mitton, D. (2008) Prediction of mechanical properties of cortical bone by quantitative computed tomography. Med. Eng. Phys. 30(3) pp 321-328

Dudek, N.L., Marks, M.B., Marshall, S.C., Shardon, J.P. (2005) Dematologic conditions associated with use of a lower-extremity prosthesis. Arch. Phys. Med. Rehabil. 86(4) pp 659-663

Emrich R, Slater K. (1998) Comparative analysis of below-knee prosthetic socket liner materials. J Med Eng Technol 22(2) pp 94–98

Erdemir, A., Guess, T.M, Halloran, J., Tadepalli, S.C., Morrison, T.M. (2012) Considerations for reporting finite element analysis studies in biomechanics. Journal of Biomechanics 45(4) 625-633

Esquenazi, A. (2004) Amputation rehabilitation and prosthetic restoration: From surgery to community reintegration. Disabil Rehabil 26 pp 831-836

Faustini, M., Neptune, R., Crawford, R. (2006) The quasi-static response of compliant prosthetic sockets for transtibial amputees using finite element methods. Med Eng Phys 28 pp 114-121

Fenech, M., Jaffrin, M.Y. (2004) Extracellular and intracellular volume variations during postural change measured by segmental and wrist-ankle bioimpedance spectroscopy. IEEE Trans Biomed Eng 51(1) pp 166-175

Fleckenstein, J. (1996) Skeletal muscle evaluated by MRI. Encylopedia of Nuclear Magnetic Resonance, Edited by Grant, D., Harris, R. Chichester, United Kingdom. Wiley pp 4430-4436

Freutel, M., Schmidt, H., Durselen, L., Ignatus, A., Galbusera, F. (2014) Finite element modelling of soft tissues: Material models, tissue interaction and challenges. Clinical Biomechanics 29(4) pp 363-372

Frossard, L., Berg, D., Merlo, G., Quincy, T., Burkett, B. (2017) Cost Comparison of Socket-Suspended and Bone-Anchored Transfemoral Prostheses. Journal of Prosthetics and Orthotics 29(4) 11 pages

Garrick, R.J., Fatone, S. (2013) Marlo Anatomical Socket studied for coronal plane stability. Northwestern University Prosthetic Orthotics Center for Education and Research, Capabilties, Winter pp 1-8

Gavin, J.P., Cooper, M., Wainwright, T.W. (2018) The effects of knee joint angle on neuromuscular activity during electrostimulation in healthy older adults. J Rehabil Assist Technol Eng 5 pp 1-10

Gebeshuber, I. C., van Aken, G. (2017) Friction and Lubricants Related to Human Bodies. Lubricants 5(4) 4 pages

Geertzen, J., Van Der Linde, H., Rosenbrand, K., Conradi, M., Deckers, J., Koning, J. (2015) Dutch evidence-based guidelines for amputation and prosthetics of the lower extremity: rehabilitation process and prosthetics. Part 2. Prosthetics and Orthotics International 39(5), 361-371

Gefen, A. (2018) The future of pressure ulcer prevention is here: Detecting and targeting inflammation early. EWMA Journal 19(2) pp 7-13

Gefen, A., van Nierop, B., Bader, D.L., Oomens, C.W. (2008) Strain-time cell-death threshold for skeletal muscle in a tissue-engineered model system for deep tissue injury. J Biomech 41(9) pp 2003-2012

Gefen, A., Weihs, D. (2016) Cytoskeleton and plasma-membrane damage resulting from exposure to sustained deformations: A review of the mechanobiology of chronic wounds. Med Eng Phys 38(9) pp 828-33

Gerhardt LC, Strässle V, Lenz A, Spencer ND, Derler S. (2008) Influence of epidermal hydration on the friction of human skin against textiles. J R Soc Interface 5(28) pp 1317–1328

Goh, J., Lee, P., Toh, S., Ooi, C. (2005) Development of an integrated CAD-FEA process for below-knee prosthetic sockets. Clinical Biomechanics 20 pp 623-629

Goldstein, B., Sanders, J. (1998) Skin response to repetitive mechanical stress: A new experimental model in pig. Arch Phys Med Rehabil. 79 pp 265-272

Gottschalk, F., Stills, M. (1994) The biomechanics of trans-femoral amputation. Prosthetics and Orthotics International 18(1) pp 12-17

Gottschalk, F.A., Kourosh, S., Stills, M., McClellan, B., Roberts, J. (1989) Does socket configuration influence the position of the femur in above-knee amputation? J Prosthet Orthot. 2(1) pp 94–102

Gottschalk, F.A., Stills, M. (1994) The biomechanics of trans-femoral amputation. Prosthet Orthot Int. 18(1) pp 12–17

Guerra-fán, E., Nunez, J.H., Sanchez-Raya, J., Crespo-Fresno, A., Angles, F., Minguell, J. (2018) Prosthetic limb options for below and above knee amputations: Making the correct choice for the right patient. Current Trauma Reports 4 pp 247-255

Hadji, A., Mureithi, N. (2019) Validation of friction model parameters identified using the IHB method using finite element method. Shock and Vibration. Article ID 3493052, 19 pages

Hafner, B.J., Cagle, J.C., Allyn, K.J., Sanders, J.E. (2017) Elastomeric liners for people with transtibial amputation: Survey of prosthetists' clinical practices. International Society for Prosthetics and Orthotics 41(2) pp 149-156

Hains, B.C., Wasman, S.G. (2006) Activated microglia contribute to the maintenance of chronic pain after spinal cord injury. J Neuroscience 26(16) pp 4308-4317

Hall, C.B. (1964) Prosthetic socket shape as related to anatomy in lower extremity amputees. Clin Orthop 37 pp 32-46

Henao, S., Orozco, C., Ramirez, J. (2020) Influence of gait cycle loads on stress distribution at the residual limb/socket interface of transfemoral amputees: a finite element analysis. Scientific Reports 10 pp 4985

Heyer, K., Debus, E.S., Mayerhoff, L., Augustin, M. (2015) Prevalence and Regional Distribution of Lower Limb Amputations from 2006 to 2012 in Germany: A Population based Study. Eur J Vasc Endovasc Surg. 50(6) pp 761-766

Hoyt, K., Kneezel, T., Castaneda, B., Parker, K. J. (2008) Quantitative sonoelastography for the in vivo assessment of skeletal muscle viscoelasticity. Physics in Medicine & Biology 53(15) pp 4063-4080.

Hsu, E., Cohen, S.P. (2013) Postamputation pain: epidemiology, mechanisms and treatment. J Pain Res 6 pp 121-136

ICRC, International Committee of the Red Cross (2006) Manufacturing Guidelines – Trans-femoral prosthesis physical rehabilitation programme [Online] (Available at: https://www.icrc.org/en/doc/assets/files/other/eng-transfemoral.pdf)

Jamaludin, M.S., Hanafusa, A., Shinishirou, Y., Agarie, Y., Otsuka, H., Ohnishi, K. (2019) Analysis of pressure distribution in transfemoral prosthetic socket for prefabrication evaluation via the finite element method. Bioengineering 6(98) 12 pages

Javidinejad, A. (2012) FEA practical illustration of mesh-quality-results difference between structured mesh and unstructured mesh. ISRN Mechanical Engineering. 2012, 7 pages

Jensen, J.S., Nilsen, R., Zeffer, J. (2005) Quality benchmark for trans-tibial prostheses in low-income countries Prosthet. Orthot. Int., 29 pp 53-58

Jia, X., Zhang, M., Lee, W. (2004) Load transfer mechanics between trans-tibial prosthetic socket and residual limb – dynamic effects. Journal of Biomechanics 37 pp 1371-1377

Jordan, R.W., Marks, A., Higman, D. (2012) The cost of major lower limb amputation: a 12-year experience. Prosthetics and Orthotics International 36(4) pp 430-434

Kahle, J. (2002) A case study using fluoroscope to determine the vital elements of transfemoral interface design. J. Prosthet. Orthot. 14 (3) pp 121-126

Kahle, J., Highsmith, M.J. (2013) Transfemoral sockets with vacuum-assisted suspension comparison of hip kinematics, socket position, contact pressure, and preference: Ischial containment versus brimless. Journal of Rehabilitation Research & Development 50(9) pp 1241-1252

Kerr, M., Rayman, G., Jeffcoate, W. (2014) Cost of diabetic foot disease to the National Health Service in England. Diabetes Med. 31 pp 1498-1504

Kistenberg, R.S. (2014) Prosthetic choices for people with leg and arm amputations. Phys Med Rehabil Clin N Am. 25. pp 93-115

Klute, G. K., Glaister, B. C., Berge, J. S. (2010) Prosthetic liners for lower limb amputees: A review of the literature. Prosthetics and Orthotics International 34(2) pp 146-153

Koc, E., Tunca, M., Akar, A., Erbil, A.H., Demiralp, B., Arca, E. (2008) Skin problems in amputees: a descriptive study. Int J Dermatol 47(1) pp 463-466

Kokate, J.Y., Leland, K.J., Held, A.M., Hansen, G.L., Kveen, G., Johnson, B., Wilke, M.S., Sparrow, E.M., Iaizzo, P. (1995) Temperature-modulated pressure ulcers: a porcine model. Arch Phys Med Rehabil 76(7) pp 666-673

Kosiak, M. (1961) Etiology of decubitus ulcers. Archives of Physical Medicine and Rehabilitation 42 pp 19-29

Kristinsson, O. (1993) The ICEROSS concept: a discussion of a philosophy. Prosthetics and Orthotics International 17(1) pp 49–55

Krouskop, T.A., Muilenberg, A.L., Doughtery, D.R., Winningham, D.J. (1987) Computer-aided design of a prosthetic socket for an above-knee amputee. Journal of Rehabilitation Research 24(2) pp 31-38

Lacroix, D., Patiño, J.F.R. (2011) Finite element analysis of donning procedure of a prosthetic transfemoral socket. Annals of Biomedical Engineering 39(12) pp 2972-2983

Laszczak, P., McGrath, M., Tang, J., Gao, J., Jiang, L., Bader, D.L., Moser, D., Zahedi, S. (2016) A pressure and shear sensor system for stress measurement at lower limb residuum/socket interface. Med. Eng. Phys. 38(7) pp 695-700

Latlief, G., Elnitsky, C., Hart-Hughes, S., Phillips, S. L., Adams-Koss, L., Kent, R., Highsmith, M. J., (2012) Patient safety in the rehabilitation of the adult with an amputation. Phys Med Rehabil Clin N Am, 23 (2) pp 377-392

Lawrence, R.B., Knox, W., Coombes, A., Greenwood, C.D., Davies, R.M. (1983) The A/K-B/K Rapidiform socket fabrication system. Bioengineering Centre Report, University College London, Roehampton, London

Lawrence, R.B., Knox, W., Mack, A., Crawford, H.V., Saunders, C.G. (1984) A computer-controlled carving machine. Bioengineering Centre Report, University College London, Roehampton, London

Lee, V.S.P, Solomonidis, S.E, Spence, W.D. (1997) Stump-socket interface pressure as an aid to socket design in prostheses for trans-femoral amputees —a preliminary study. Journal of Engineering in Medicine 211 Part H pp 167-180

Lee, W., Zhang, M., Boone, D., Contoyannis, B. (2004) Finite element analysis to determine effect of monolimb flexibility on structural strength and interaction between residual limb and prosthetic socket. J. Rehabil. Res. Dev. 41(6A), pp 775-786

Lee, W.C., Zhang, M., Mak, A.F. (2005) Regional differences in pain threshold and tolerance of the transtibial residual limb: Including the effects of age and interface material. Archives of Physical Medicine and Rehabilitation 86(4) pp 641-649

Lee, W.C.C., Zhang, M. (2007) Using computational simulation to aid in the prediction of socket fit: A preliminary study. Medical Engineering & Physics 29(8) pp 923-929

Lee, W.C.C., Zhang, M., Jia, X., Cheung, J.T.M. (2004) Finite element modelling of the contact interface between trans-tibial residual limb and prosthetic socket. Medical Engineering & Physics 26(8) pp 655-662

Legro, M., Reiber, G., del Aguila, M., Ajax, M., Boone, D., Larsen, J., Smith, D., Sangeorzan, B. (1999) Issues of importance reported by persons with lower limb amputations and prostheses. Journal of Rehabilitation Research & Development 36(3) pp 155-163

Lenka, P., Choudhury, A. (2011) Analysis of trans tibial prosthetic socket materials using finite element method. Journal of Biomedical Science and Engineering 4 pp 762-768

Leopold, E., Gefen, A. (2013) Changes in permeability of the plasma membrane of myoblasts to fluorescent dyes with different molecular masses under sustained uniaxial stretching. Med Eng Phys 35(5) pp 601-7

Lewis, C.A., Sahrmann, S.A. (2015) Effect of posture on hip angles and moments during gait. Man Ther. 20(1) pp 176-182

Li, G., Carrera, E., Cinefra, M., Miguel, A., Kulikov, G., Pagani, A. (2019) Evaluation of shear and membrane locking in refined hierarchical shell finite elements for laminated structures. Advanced Modelling and Simulation in Engineering Sciences 6(8) 24 pages

Li, W., Kong, M., Liu, X.D., Zhou, Z.R. (2008) Tribological behaviour of scar skin and prosthetic skin in vivo, Tribol. Int. 41 (7) pp 640–647

Li, W., Liu, X.D., Cai, Z.B., Zheng, J., Zhou, Z.R. (2011) Effect of prosthetic socks on the frictional properties of residual limb skin, Wear 271(11) pp 2804-2811

Li, W., Qu, S.X., Zhou, Z.R. (2006) Reciprocating sliding behaviour of human skin in vivo at lower number of cycles Tribol. Lett., 23 pp 165-170

Li, W., Shen, H., Hung, J., & Shih, C. (2018). The effect of moisture on friction coefficient of fabrics used on taekwondo personal protective equipment. Proceedings of the Institution of Mechanical Engineers, Part J: Journal of Engineering Tribology, 233(1) pp 87–94

Lilja, M., Johansson, S., Oberg, T. (1999) Relaxed versus activated stump muscles during casting for trans-tibial prostheses. Prosthet Orthot Int 23 pp 13-20

Lin, C., Chang, C., Wu, C., Chung, K., Liao, I. (2004) Effects of liner stiffness for trans-tibial prosthesis: a finite element contact model. Medical Engineering & Physics 26(1) pp 1-9

Linder-Ganz, E., Gefen, A. (2007) The Effects of Pressure and Shear on Capillary Closure in the Microstructure of Skeletal Muscles. Annals of Biomedical Engineering 35 pp 2095-2107

Linder-Ganz, E., Gefen, A. (2007) The effects of pressure and shear on capillary closure in the microstructure of skeletal muscle. Annals of Biomedical Engineering 35(12) pp 2095-2107

Linder-Ganz, E., Shabshin, N., Itzchak, Y., Gefen, A. (2007) Assessment of mechanical conditions in sub-dermal tissues during sitting: A combined experimental-MRI and finite element approach. Journal of Biomechanics 40(7) pp 1443-1454

Linder-Ganz, E.L., Engelberg, S., Scheinowitz, M., Gefen, A. (2006) Pressure-time cell death threshold for albino rat skeletal muscles as related to pressure sore biomechanics. Journal of Biomechanics 39(14) pp 2725-2732

Liu, Z., Fan, Y., Qian, Y., Zhang, M. (2007) Biomechanical research of the endoskeletal trans-tibial monolimb. IEEE/ICME International Conference on Complex Medical Engineering pp 1267–1271

Long, I.A. (1975) Allowing normal adduction of femur in above-knee amputations. Orthotics and Prosthetics 29(4) pp 54-54

Long, I.A. (1985) Normal shape-normal alignment (NSNA) above-knee prosthesis. Clinical Prosthetics & Orthotics 9(4) pp 9-14

Lyon, C., Kulkarni, J., Zimerson, E., Van Ross, E., Beck, M. (2000) Skin disorders in amputees. J Am Acad Dermatol. 42 pp 501-507

Mak, A.F.T., Liu, G., Lee, S.Y. (1994) Biomechanical assessment of below-knee residual limb tissue. Journal of Rehabilitation Research and Development 31(3) pp 188-198

Mak, A.F.T., Zhang, M., Boone, D.A. State-of-the-art research in lower-limb prosthetic biomechanics-socket interface: A review. Journal of Rehabilitation Research and Development. 38(2) pp.161-174

Makhsous, M., Lim, D., Hendrix, R., Bankard, J., Rymer, W., Lin, F. (2007) Finite element analysis for evaluation of pressure ulcer on the buttock: development and validation. IEEE Trans Neural Sys Rehabil Eng 15(4) pp 517-525

Marghoub, A., Libby, J., Babbs, C., Ventikos, Y., Fagan, M.J., Moazen, M. (2019) Characterizing and Modeling Bone Formation during Mouse Calvarial Development. Physical review letters, 122(4)

Masen, M., (2011) A system based experimental approach to tactile friction. J Mech Behav Biomed Mater 4(5) pp 1620-1626

Meulenbelt, H., Geertzen, J., Jonkman, M., Dijkstra, P. (2011) Skin problems of the stump in lower limb amputees: a clinical study. Acta Derm Venereol 91(45) pp 173-177

Meulenbelt, H.E, Dijkstra, P., Marcel, F., Geertzen, J.B. (2006) Skin problems in lower limb amputees: a systematic review. Disability and rehabilitation 28(10) pp 603-608

Meulenbelt, H.E., Geertzen, J.H., Jonkman, M.F., Dijkstra, P.U. (2009) Determinants of skin problems of the stump in lower-limb amputees. Arch Phys Med Rehabil 90(1) pp 74-81

Moerman, K., van, Vijven, M., Solis, L., van Haaften, E., Leonen, A., Mushahwar, V., Oomens, C. (2017) On the importance of 3D, geometrically accurate, and subject-specific finite element analysis for evaluation of in-vivo soft tissue loads. Comput. Methods Biomech. Biomed. Eng. 20(5) pp 483-491

Moore, Z., Patton, D., Rhodes, S.L., O'Connor, T. (2017) Subepidermal moisture (SEM) and bioimpedance: a literature review of a novel method for early detection of pressure-induced tissue damage (pressure ulcers). Int Wound J 14(2) pp 331-337

Morgan, D.L., Proske U. (2004) Popping sarcomere hypothesis explains stretch-induced muscle damage. Clinical and Experimental Pharmacology and Physiology 31 pp 541-545

Morotti, R., Rizzi, C., Regazzoni, D., Colombo, G. (2014) Numerical simulations and experimental data to evaluate residual limb-socket interaction. IMECE, Quebec, Canada

Morris, C.D., Potter, B.K., Athanasian, E.A., Lewis, V.O. (2015) Extremity amputations: principles, techniques, and recent advances. Instructional Course Lectures 64, pp 105-117

Morton, W.E., Hearle, J.W.S. (2008) Physical Properties of Textile Fibres, vol. 4. Woodhead Publishing in Textiles and CRC Press, Boca Raton

Mulroy, S. (2018) Seal-Options Webinar – Clinical Prosthetics. 25 March 2018 [Online] (Available at: https://assets.ossur.com/library/38908)

Munarriz, R., Kulaksizoglu, H., Hakim, L., Gholami, S., Nehra, A., Goldstein, I. (2003) Lower extremity above-knee prosthesis-associated erectile dysfunction. International Journal of Impotence research 15 pp 290-292

Murdoch, G. (1965) The Dundee socket for below knee amputation. Prosthet Int. 3(4) pp 12-14.

Narres, M., Kvitkina, T., Claessen, H., Droste, S,. Schuster, B., Rumenapf, G. (2017) Incidence of lower extremity amputations in the diabetic compared with the non-diabetic population: A systematic review. PLoS One 12(8)

National Pressure Ulcer Advisory Panel/ European Pressure Ulcer Advisory Panel (2009) Pressure Ulcer Prevention & Treatment: Clinical Practice Guidelines. Washington DC, USA: National Pressure Ulcer Advisory Panel

Nelissen, J., Traa, W., de Boer, H., de Graaf, L., Mazzoli, V., Savci-Heijink, C., Nicolay, K., Froeling, M., Bader, D., Nederveen, A., Oomens, C., Strijkers, G. (2018) An advanced magnetic resonance imaging perspective on the etiology of deep tissue injury. J. Appl. Physiol. 124 pp 1580-1596

Neumann, E.S., Wong, J.S., Drollinger, R.L. (2005) Concepts of pressure in an Ischial Containment Socket: Measurement. Journal of Prosthetics and Orthotics 17(1)

Ng, P., Lee, P.S.V., Goh, J.C.H. (2002) Prosthetic sockets fabrication using rapid prototyping technology. Rapid Prototyping Journal. 8(1) pp 53-59

Nguyen, P., Smith, A., Reynolds, K. (2008) A literature review of different pressure ulcer models from 1942-2005 and the development of an ideal animal model. Australasian Physical & Engineering Sciences in Medicine 31(3) pp 223-225

Ning, X., Lovell, M., Slaughter, W. (2006) Asymptotic solutions for axisymmetric contact of a thin, transversely isotropic elastic layer. Wear 260(7) pp 693-698

Noala, G., Vistnes, L. (1980) Differential response on skin and muscle in the experimental production of pressure sores. Plast Reconstr Surg. 66(2) pp 728-733

Oomens, C.W., Loerakker, S., Bader, D.L. (2010) The importance of internal strain as opposed to interface pressure in the prevention of pressure related deep tissue injury. J Tissue Viability 19(2) pp 35-42

Össur (2011) Össur® UK Prosthetics Catalogue. [Online] (Available at: https://assets.ossur.com/library/14489/ossur-uk-prosthetics-catalogue-2011.pdf).

Ossur (2017) Iceross Seal-In Liner: Instructions for use [Online] (Available at: assets.ossur.com/library/7732/Iceross%20Transfemoral%20Seal-In%c2%a0%20Instructions%20for%20use.pdf)

Ottobock (2015) Liner selection tool. Brochure. (Available at: https://professionals.ottobock.com.au/document?mediaPK=8923929640990&attachment=true)

Ottobock (2015) Prosthetics Lower Limbs Catalogue. [Online] (Available at: https://www.ottobock.es/media/cat%C3%A1logo-de-prot%C3%A9sica-miembro-inferior-(gb).pdf).

Ottobock (2016) Service Fabrication: Customized Solutions. [Online] (Available at https://www.ottobock.co.uk/media/local-media/brochures/prosthetics/catalogues/service-fabrication-646k71-en-03-1301w.pdf).

Packman, D.E. (2011) Theories of fundamental adhesion. Handbook of Adhesion Technology. Springer, Berlin, Heidelberg

Palevski, A., Glaitch, I., Portnoy, S., Linder-Ganz, E., Gefen, A. (2006) Stress relaxation of porcine gluteus muscle subjected to sudden transverse deformation as related to pressure sore modelling. J Biomech Eng. 128(5) pp 782-787

Pantall, A., Ewins, D. (2013) Muscle activity during stance phase of walking: Comparison of males with transfemoral amputation with osseointegrated fixations to nondisabled male volunteers. JRRD 50(4) pp 499-514

Pascale, B.A., Potter, B.K. (2014) Residual Limb Complications and Management Strategies. Curr Phys Med Rehabil Rep 2 pp 241–249

Patel, S., Knapp, C.F., Donofrio, J.C., Salcido, R. (1999) Temperature effects on surface pressure-induced changes in rat skin perfusion: implications in pressure ulcer development. J Rehabil Res Dev 36(3) pp 189-201

Paterno, L., Ibrahimi, M., Gruppioni, E., Menciassi, A., Rico, L. (2018) Sockets for limb prostheses: A review of existing technologies and open challenges. IEEE Transactions on Biomedical Engineering 65(9) pp 1996-2010

Peery, J.T., Klute, G.K., Blevins, J.J., Ledoux, W.R. (2006) A three-dimensional finite element model of the transibial residual limb and prosthetic socket to predict skin temperatures. IEEE Trans Neural Syst Rehabil Eng 14(3) pp 336-343

Pezzin, L.E., Dillingham, T.R., MacKenzie, E.J. (2004) Use and satisfaction with prosthetic limb devices and related services. Arch Phys Med Rehabil 85 pp 723–729

Physiopedia (2018) Lower limb prosthetic sockets and suspension systems. [Online] (Available at: https://www.physio-pedia.com/Lower_Limb_Prosthetic_Sockets_and_Suspension_Systems#cite_note-:7-1)

Pirouzi, G., Abu Osman, N.A., Eshraghi, A., Ali, S., Gholizadeh, H., Wan Abas, W.A.B. (2014) Review of the socket design and interface pressure measurement for transtibial prosthesis. Sci. World J. 2014

Portnoy, S., Siev-Ner, I., Yizhar, Z., Kristal, A., Shabshin, N., Gefen, A. (2009) Surgical and morphological factors that affect internal mechanical loads in soft tissues of the transtibial residuum. Ann. Biomed. Eng. 37(12) pp 2583-2605

Portnoy, S., Yizhar, Z., Shabshin, N., Itzchak, Y., Kristal, A., Dotan-Marom, Y., Siev-Ner, I., Gefen, A. (2008) Internal mechanical conditions in the soft tissues of a residual limb of a trans-tibial amputee. J. Biomech 41 pp 1897-1909

Pritham, C. H. (1990) Biomechanics and shape of the above-knee socket considered in light of the ischial containment concept. Prosthetics and Orthotics International 14(1) pp 9-21

Pritkin, M.R. (1997) Effects of design variants in lower-limb prostheses on gait synergy. J Prosthet Orthot 9 pp 113-122

Prompers, J., Jeneson, J., Drost, M., Oomens, C., Strijkers, G., Nicolay, K. (2006) Dynamic MRS and MRI of skeletal muscle function and biomechanics. NMR Biomed 19 pp 927-953

Radcliffe, C. W. (1977) The Knud Jansen Lecture: Above knee prosthetics. Prosthetics and Orthotics Int. 1, pp 146-160

Radcliffe, C.W. (1955) Functional considerations in the fitting of above-knee prostheses. Artificial Limbs 2(1) pp 35-60

Ramasamy, E., Avci, O., Dorow, B., Chong, S., Gizzi, L., Steidle, G., Schick, F., Rohrle, O. (2018) An efficient modelling-simulation-analysis workflow to investigate stump-socket interaction using patient-specific, three-dimensional, continuum-mechanical, finite element residual limb models. Frontiers in Bioengineering and Biotechnology. 6 pp 126

Ramirez, J. F., Pavon, J., Toro, A. (2015) Experimental assessment of friction coefficient between polypropylene and human skin using instrumented sclerometer. J Engineering Tribology 229(3) pp 259-265

Ramirez, J.F., Velez, J.A. (2012) Incidence of the boundary condition between bone and soft tissue in a finite element model of a transfemoral amputee. Prosthet. Orthot. Int. 36(4) pp 405-414

Restrepo, V., Villarraga, J., Palacio, J.P. (2014) Stress reduction in the residual limb of a transfemoral amputee varying the coefficient of friction. Journal of Prosthetics and Orthotics 26(4) pp 205-211

Reynolds, D. (1998) Shape design and interface load analysis for below-knee prosthetic sockets [PhD Thesis] University of London.

Reynolds, D.P., Lord, M. (1992) Interface load analysis for computer-aided design of below-knee prosthetic sockets. Medical & Biological Engineering & Computing 30 pp 419-426

Reynolds, D.P., Rodwell, T.R.T. (1984) Socket production modelling using Finite Element Analysis. Bioengineering Centre Report, University College London, Roehampton, London.

Röhrle, O., Sprenger, M., Schmitt, S. (2017) A two-muscle, continuum-mechanical forward simulation of the upper limb. Biomech Model Mechanobiol 16(3) pp 743-762

Sabolich, J. (1985) Contoured adducted trochanteric-controlled alignment method: Introduction and basic principles. Clinc Prosthet Orthot 9 pp 15-26

Safari, M., Rowe, P., McFadyen, A., Buis, B. (2013) Hands-off and hands-on casting consistency of amputee below knee sockets using magnetic resonance imaging. The Scientific World Journal. Article ID 486146. 13 pages

Salcido, R., Donofio, J., Fisher, S., LeGrand, E., Dicky, K., Carney, J., Schosser, R., Liang, R. (1995) Histopathology of pressure ulcers as a result of sequential computer-controlled pressure sessions in a fuzzy rat model. Advances in Wound Care 7 pp 23-28

Sanders, J.E., Cagle, J.C., Harrison, D.S., Myer, T.R., Allyn, K.J. (2013) How does adding and removing liquid from socket bladders affect residual-limb fluid volume? Journal of Rehabilitation Research & Development 50(6) pp 845-860

Sanders, J.E., Fatone, S. (2011) Residual limb volume change: Systematic review of measurement and management. J Rehabil Res Dev 48(8) pp 949-986

Sanders, J.E., Greve, J.M., Mitchell, S.B., Zachariah, S.G. (1998) Material properties of commonly-used interface materials and their static coefficients of friction with skin and socks. Journal of Rehabilitation Research and Development 35(2) pp 161-176

Sanders, J.E., Harrison, D., Allyn, K., Myers, T. (2009) Clinical utility of in-socket residual limb volume change measurement: Case study results. Prosthet Orthot Int 33 pp 378-390

Sanders, J.E., Nicholson, B.S., Zachariah, S.G., Cassisi, D.V., Karchin, A., Fergason, J.R. (2004) Testing of elastomeric liners used in limb prosthetics: Classification of 15 products by mechanical performance. Journal of Rehabilitation Research and Development 41(2) pp 175-186

Sanders, J.E., Severance, M.R., Allyn, K.J. (2012) Computer-socket manufacturing error: how much before it is clinically apparent? J Rehabil Res Dev 49 pp 567-582

Sanders, J.E., Youngblood, R., Hafner, B., Cagle, J., Mclean, J., Redd, C., Dietrich, C., Ciol, M., Allyn, K. (2017) Effects of socket size on metric and socket fit in trans-tibial prosthesis users. Med Eng Phys 44 pp 32-43

Saunders, C.G. (1982) Reconstruction of anatomical shapes from Moire Contourographs. Biosterometrics '82. SPIE Proceedings, August.

Schuch, C. M., Pritham, C. H. (1999) Current transfemoral sockets. Clinical Orthopaedics and Related Research 361 pp 48-54

Schuch, M.C. (1992) Transfemoral amputation: Prosthetic Management, in Atlas of Limb Prosthetics: Surgical, Prosthetic and Rehabilitation Principles Chapter 20B. Rosemont, IL, American Academy of Orthopedic Surgeons.

Schutte, L.M., Hayden, S., Gage, J. (1997) Lengths of hamstrings and psoas muscles during crouch gait: Effects of femoral anteversion. Journal of Orthopaedic Research 15(4) pp 615-621

Seguchi, Y., Tanaka, M., Nakagawa, A., Kitayama, I. (1989) Finite element analysis and load identification of above-knee prosthesis socket. Proceedings of 4th Int ANSYS Conf Exhib, Pittsburgh pp 12.31–12.44

Shacham, S., Castel, D., Gefen, A. (2010) Measurements of the static friction coefficient between bone and muscle tissues. Journal of Biomechanical Engineering 132(8) 4 pages

Shaked, E., Gefen, A. (2013) Modelling the effects of moisture-related skin support friction on the risk for superficial pressure ulcers during patient repositioning in bed. Frontiers in Bioengineering and Biotechnology 1(9) pp 1-7

Sherk, V.D., Bemben, M., Bemben, D. (2010) Interlimb muscle and fat comparisons in persons with lower-limb amputation. Arch Phys Med Rehabil 91 pp 1077-1081

Silver-Thorn, M.B. and Childress, D.S. (1997) Generic, geometric finite element analysis of the transtibial residual limb and prosthetic socket. Journal of Rehabilitation Research and Development 34(2) pp171-186

Smith, D.G., Fergason, J.R. (1999) Transtibial amputations. Clinical Orthopaedics and Related Research 361 pp 108-115

Sonck, W.A., Cockrell, J.L., Koepke, G.H. (1970) Effect of liner materials on interface pressures in below-knee prostheses. Archives of Physical Medicine and Rehabilitation 51(11) pp 666-669

Sonenblum, S. E., Sprigle, S. H., Cathcart, J. M., Winder, R. J. (2013) 3-dimensional buttocks response to sitting: a case report. Journal of Tissue Viability 22, pp 12-18

Sopher, R., Nixon, J., Gorecki, C., Gefen, A. (2010) Exposure to internal muscle tissue loads under ischial tuberosities during sitting is elevated at abnormally high or low body mass indices. Journal of Biomechanics 43(2) pp 280-286

Sparks, J., Vavalle, N., Kasting, K., Long, B., Tanaka, M., Sanger, P., Schnell, K., Conner-Kerr, T. (2015) Use of silicone materials to simulate tissue biomechanics as related to deep tissue injury. Advances in Skin & Wound Care 28(2) pp 59-68

Steege, J.W., Childress, D.S. (1988) Finite element prediction of pressure at the below-knee socket interface. Report of ISPO Workshop on CAD/CAM in Prosthetics and Orthotics. pp 71–82.

Steer, J.W., Worsley, P.R., Browne, M., Dickinson, A. (2019) Predictive prosthetic socket design: part1 – population-based evaluation of transtibial prosthetic sockets by FEA-driven surrogate modelling. Biomechanics and Modelling in Mechanobiology. e-pub ahead of publication.

Stekelenberg, A., Strijkers, G., Parusel, H., Bader, D., Nicolay, K., Oomens, C. (2007) Role of ischemia and deformation in the onset of compression-induced deep tissue injury: MRI-based studies in a rat model. Journal of Applied Physiology 102 pp 2002-2011

Stojadinovic, O., Minkiewicz, J., Sawaya, A., Bourne, J.W., Torzilli, P., de Rivero Vaccari, J.P., Dietrich, W.D., Keane, R.W., Tomic-Canic, M. (2013) Deep tissue injury in development of pressure ulcers: a decrease of inflammasome activation and changes in human skin morphology in response to aging and mechanical load. PLoS One 8(8)

Sugimoto, S. (2013) Characteristic of stump shape and stress during gait cycle for transfemoral prosthesis 345 socket. MSc Thesis. Shiaura Institute of Technology, Tokyo, Japan

Sussman, C.B., Bates-Jensen, B.M. (2012) Wound care: A collaborative practice manual for health professionals. 4th ed. Philadelphia, Wolters Kluwer Health, Lippincott Williams & Wilkins

The Steeper Group (2011) Prosthetic: Best practice guidelines. [Online] (Available at https://www.steepergroup.com/SteeperGroup/media/SteeperGroupMedia/Additional%20Downloads/Steeper-Prosthetic-Best-Practice-Guidelines.pdf?ext=.pdf)

Tomlinson, S., Lewis, R., Carre, M.J. (2007) Review of the frictional properties of finger-object contact when gripping. Engineering Tribology, Part J, pp 221

Tomlinson, S.E., Lewis, R., Carre, M.J. (2009) The effect of normal force and roughness on friction in human finger contact. Wear 267 pp 1311-1318

Tomlinson, S.E., Lewis, R., Liu, X. (2011) Understanding the friction mechanisms between human finger and flat contacting surfaces in moist conditions. Tibol Lett 41(1) pp 283-294

Torres-Moreno, R., Jones, D., Solomonidis, S.E., Mackie, H. (1999) Magnetic resonance imaging of residual soft tissues for computer-aided technology applications in prosthetics—a case study. J Prosthet Orthot 11(1) pp 6–11

Torres-Moreno, R., Saunder, C.G., Foort, J. (1990) Computer-aided design and manufacture of an above-knee amputee socket. J. Biomed. Eng. 13 pp 3-9

Torres-Moreno, R., Solomonidis, S.E., Jones, D. (1992) Three-dimensional finite element analysis of the above-knee residual limb. Proceedings of 7th World Congress ISPO pp 274

Traa, W., Turnhout, M., Moerman, K., Nelissen, J., Nederveen, A., Strijkers, G., Bader, D., Oomens, C. (2018) MRI based 3D finite element modelling to investigate deep tissue injury. Computer Methods in Biomechanics and Biomedical Engineering 21(14) pp 760-769

Traa, W., Turnhout, M., Nelissen, J., Strijkers, G., Bader, D., Oomens, C. (2019) There is an individual tolerance to mechanical loading in compression induced deep tissue injury. Clinical Biomechanics. 63 pp 153-160

Untaroiu, C., Darvish, K., Crandall, J., Deng, B., Wang, J. (2005) Characterisation of the lower limb soft tissues in pedestrian finite element models. In Proceedings of the 19th International technical conference on the Enhanced Safety of Vehicles, Washington DC, USA, 6-9 June pp 124-131

Van Heesewijk, A., Crocombe, A., Cirovic, S., Taylor, M., Xu, W. (2018) Evaluating the effect of changes in bone geometry on the trans-femoral socket-residual limb interface using finite element analysis. In: Lhotska, L., Sukupova, L., Lacković, I., Ibbott, G. (eds) World Congress on Medical Physics and Biomedical Engineering IFMBE Proceedings 68(2) Springer, Singapore

Vanicek, N., Strike, S., McNaughton, L., Polman, R. (2009) Gait patterns in transtibial amputee fallers vs. non-fallers: Biomechanical differences during level walking. Gait & Posture 29(3) pp 415-420

Veijen, N. (2013) Skin friction: a novel approach to measuring in vivo human skin. PhD Thesis, University of Twente, The Netherlands

Vélez Zea, J.A., Goez, L.M.B., Ossa, J.A.V. (2015) Relation between the length of the residual limb length and stress distribution over stump for transfemoral amputees. Revista EIA (Spanish) 12(23) pp 107-115

Viceconti, M., Olsen, S., Burton, K. (2005) Extracting clinically relevant data from finite element simulations. Clinical Biomechanics 20 pp 451-454

Watson, P.J., Dostanpor, A., Fagan, M.J., Dobson, C.A. (2017) The effect of boundary constraints on finite element modelling of the human pelvis. Medical Engineering & Physics 43 pp 48-57

Wentink, E., Prinsen, E., Rietman, J., Veltink, P. (2013) Comparison of muscle activity patterns of transfemoral amputees and control subjects during walking. Journal of Neuroengineering and Rehabilitation 10(87) 11 pages

Wernke, M. M., Schroeder, R. M., Haynes, M. L., Nolt, L. L., Albury, A. W., & Colvin, J. M. (2017). Progress Toward Optimizing Prosthetic Socket Fit and Suspension Using Elevated Vacuum to Promote Residual Limb Health. Advances in wound care, 6(7) pp 233–239

Wheeler, J., Mazumbar, A., Marron, L., Dullea, K., Sanders, J., Allyn, K. (2016) A Pressure and Shear Sensing Liner for Prosthetic Sockets. Conf Proc IEEE Eng Med Biol Soc pp 2026-2029

Whiteside, S.R. (2015) Practice Analysis of Certified Practitioners. American Board for Certification in Orthotics, Prosthetics & Pedorthotics, Inc

WillowWood (2018) WillowWood 2018 Product Catalog. [Online] (Available at: https://www.willowwoodco.com/wp-content/uploads/2017/10/WillowWood-2018-English-Catalog-Digital-11-2018-NC.pdf)

World Health Organisation (2017) Standards for Prosthetics and Orthotics. Part 1: Standards. [Online] (Available at: https://apps.who.int/iris/bitstream/handle/10665/259209/9789241512480-part1-eng.pdf)

Wu, C., Chang, C., Hsu, A., Lin, C., Chen, S., Chang, G. (2003) A proposal for the pre-evaluation protocol of below-knee socket design - integration pain tolerance with finite element analysis. Journal of the Chinese Institute of Engineers. 26(6) pp 853-860

Wyss, D., Lindsay, S., Cleghorn, W.L., Andrysek, J. (2015) Priorities in lower limb prosthetic service delivery based on an international survey of prosthetists in low- and high-income countries Prosthet. Orthot. Int., 39 pp 102-111

Xu, D.H., Crocombe, A., Xu, W. (2016) Numerical evaluation of bone remodelling associated with trans-femoral osseointegration implant--A 68-month follow-up study. Journal of Biomechanics 49(3) pp 488-492

Xu, W., Robinson, K. (2008) X-ray image review of the bone remodeling around an osseointegrated trans-femoral implant and a finite element simulation case study. Annals of Biomedical Engineering 36(3) pp 435-443

Xu, W., van Heesewijk, A., Tayler, M., Zhu, X., Lorenzelli, L., Papadimtriou, V., Haidar, A., Gao, J. (2018) Surface Pressure Reconstruction for a Prosthetic Socket Design System – a Numerical Case Study. 14th IEE International Conference on Control & Automation. June 12-15, Alaska

Yeung, E.W., Balnave, C.D., Ballard, H.J., Bourreau, J.P., Allen, D.G. (2002) Development of T-tubular vacuoles in eccentrically damaged mouse muscle fibres. J. Physiol. 540 pp 581–92

Zachariah, S.G., Sanders, J.E. (2000) Finite element estimates of interface stress in the trans-tibial prosthesis using gap elements are different from those using automated contact. Journal of Biomechanics 33(7) pp 895-899

Zhang, L., Zhu, M., Shen, L., Zheng, F. (2013) Finite element analysis of the contact interface between trans-femoral stump and prosthetic socket. In: 35th Annual International Conference of the IEEE EMBS, pp 3-7. Osaka, Japan

Zhang, M., Lord, M., Turner-Smith, A.R., Roberts, V.C. (1995) Development of a nonlinear finite element modelling of the below-knee prosthetic socket interface. Med Eng Phys 17(8) pp 559–66

Zhang, M., Mak, A.F.T. (1996) A finite element analysis of the load transfer between an above-knee residual limb and its prosthetic socket – Roles of interface friction and distal-end boundary conditions. IEEE Transactions on Rehabilitation Engineering 4(4) pp 337-346.

Zhang, M., Mak, A.F.T. (1999) In vivo friction properties of human skin. Prosthetic and Orthotics International 23(20) pp 135-141.

Zhang, M., Mak, A.F.T., Roberts, V.C. (1998) Finite element modelling of a residual lower-limb in a prosthetic socket: a survey of the development in the first decade. Med. Eng. Phys. 20, pp 360-373.

Zhang, M., Roberts, C. (2000) Comparison of computational analysis with clinical measurement of stresses on below-knee residual limb in a prosthetic socket. Med Eng Phys 22(9) pp 607-612

Zhang, M., Turner-Smith, A.R., Roberts, V.C., Tanner, A. (1996) Frictional action at lower limb/prosthetic socket interface. Med Eng Phys 18(3) pp 207-214

Zhang, M., Turner-Smith, A.R., Tanner, A., Roberts, V.C. (1998) Clinical investigation of the pressure and shear stress on the transtibial stump with a prosthesis, Med. Eng. Phys. 20 188–198.

Zhang, M., Zheng, Y.P., Mak, A.F.T. (1997) Estimating the effective Young's modulus of soft tissues from indentation tests – nonlinear finite element analysis of effects of friction and large deformation. Med Eng Phys 19 pp 512-517

Zhang, X., Chan, F., Parthasarathy, T., Gazzola, M (2019) Modeling and simulation of complex dynamic musculoskeletal architectures. Nature Communications 10 Article number 4825

9. APPENDIX

9.1 Chapter 3 Supporting Evidence

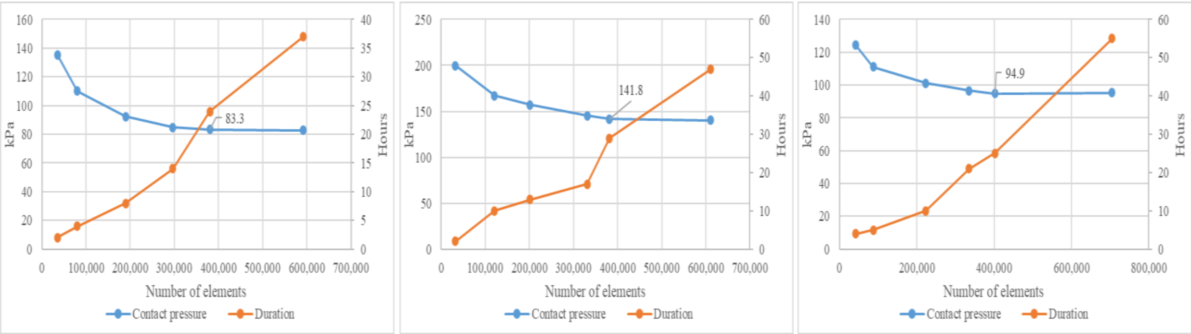

Figure 9-1: Non-pelvic model convergence testing for participant models 1, 2 and 3 (left to right respectively) with the contact pressure for the converged model shown.

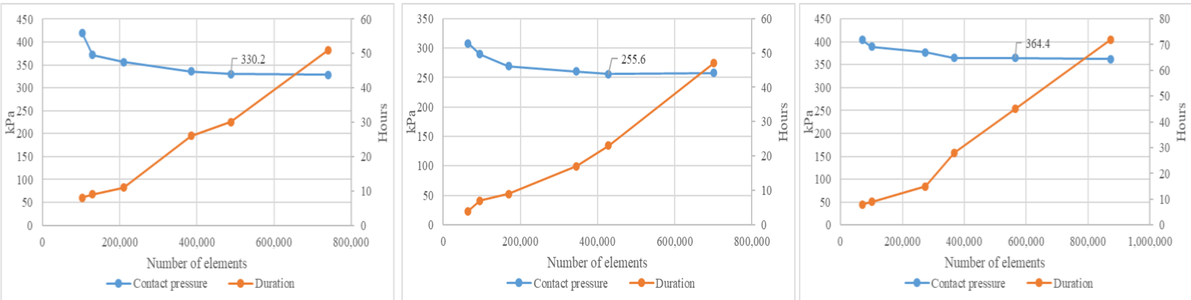

Figure 9-2: Pelvic model convergence testing for participant models 1, 2 and 3 (left to right respectively) with the contact pressure for the converged model shown.

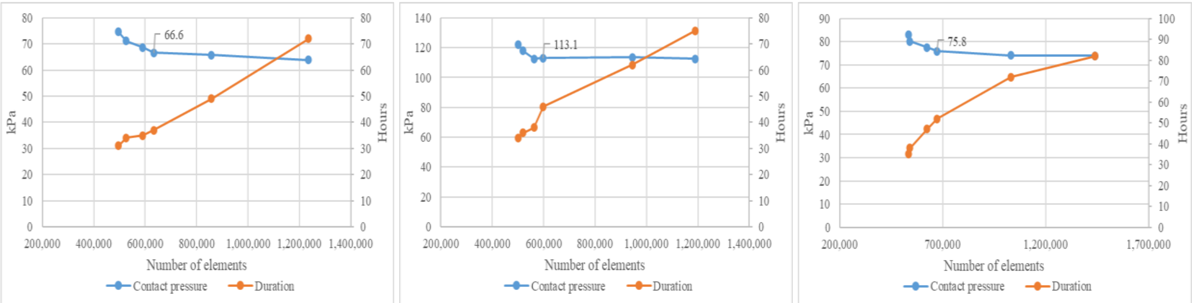

Figure 9-3: Non-pelvic model with liner convergence testing for participant models 1, 2 and 3 (left to right respectively) with the contact pressure for the converged model shown.

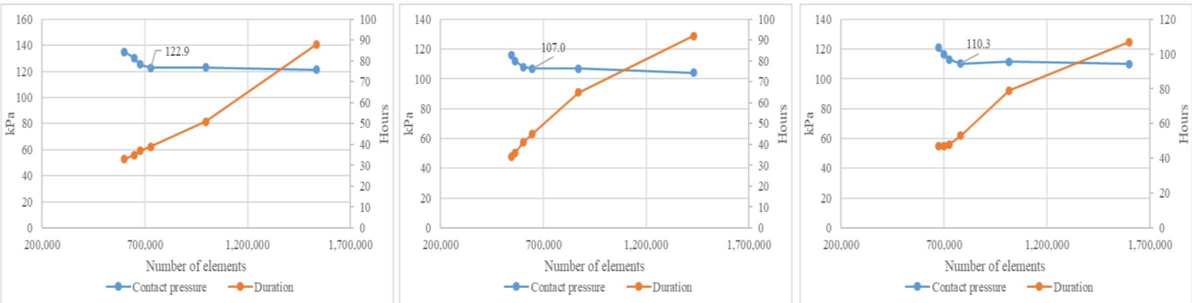

Figure 9-4: Pelvic model with liner convergence testing for participant models 1, 2 and 3 (left to right respectively) with the contact pressure for the converged model shown.

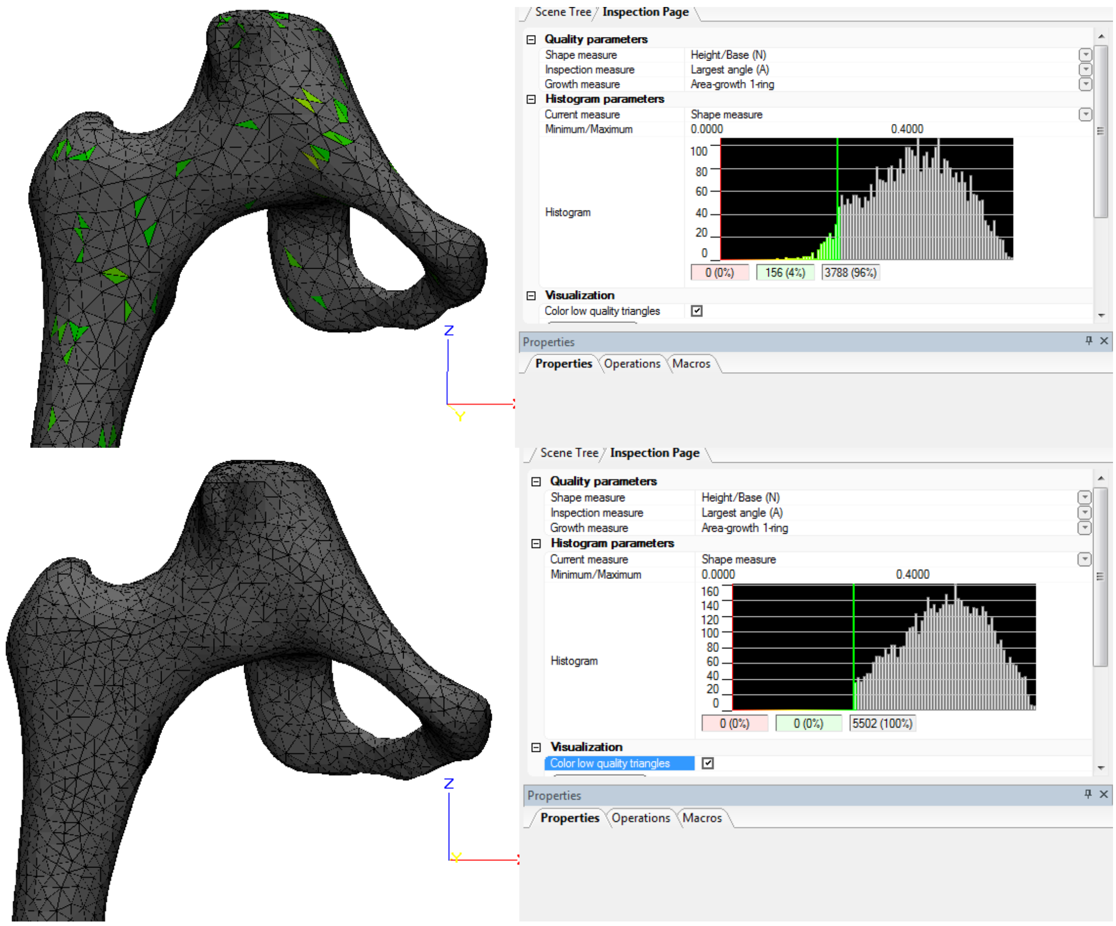

Figure 9-5: Results of adaptive meshing performed within 3-matic showing the spread of elements below the height/base ratio (top) and all elements above the threshold (bottom).

9.2 Chapter 4 Supporting Evidence

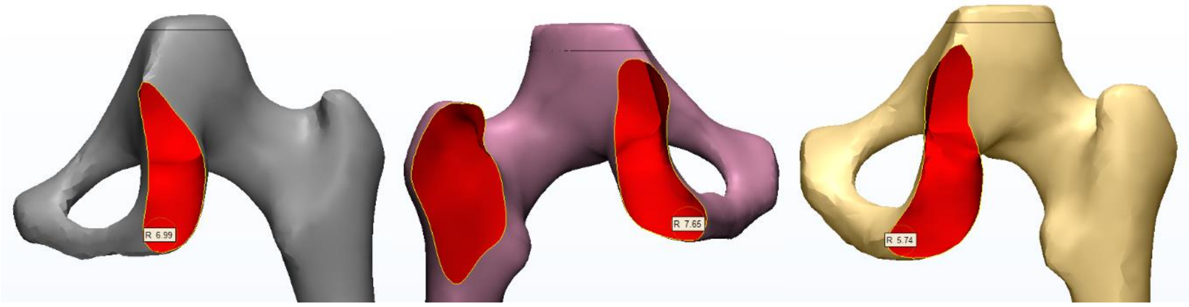

Figure 9-6: Measure of ischium sharpness (measured by best fit radii of curvature for the ischial tuberosity) for participants 1 (left), 2 (middle) and 3 (right).

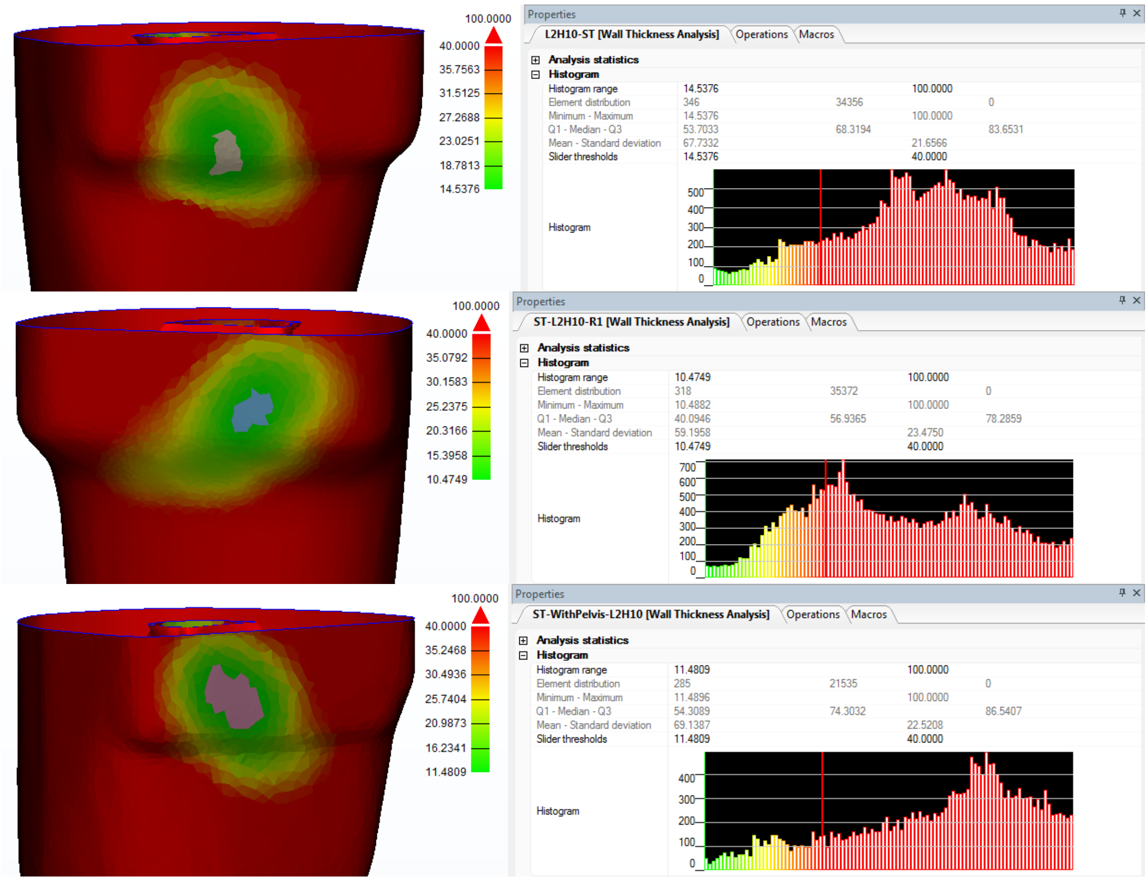

Figure 9-7: Measure of soft tissue coverage over the pelvic bone. Participants 1 (top), 2 (middle) and 3 (bottom) had percentages of 12%, 25% and 14% respectively, of soft tissue with a thickness of 40mm of less over the surface of the residual limb.

9.3 Chapter 5 Supporting Evidence

Table 9-1: Liner inside (dry) friction coefficient results.

Liner	Normal weight (g)	Liner inside/skin substitute tests (dry) Shear weight (g)					Average (g)	Standard deviation	Friction coefficient
		Test 1	Test 2	Test 3	Test 4	Test 5			
1	324	603	634	601	557	569	592.8	27.26	**1.83**
2	290	445	423	419	423	411	424.2	11.28	**1.46**
3	292	397	411	375	413	433	405.8	19.21	**1.39**
4	310	413	432	410	367	409	406.2	21.31	**1.31**
5	295	375	350	374	355	369	364.6	10.21	**1.24**

Table 9-2: Liner inside (wet) friction coefficient results.

Liner	Normal weight (g)	Liner inside/skin substitute tests (wet) Shear weight (g)					Average (g)	Standard deviation	Friction coefficient
		Test 1	Test 2	Test 3	Test 4	Test 5			
1	324	350	347	319	342	323	336.2	12.73	**1.04**
2	290	303	301	287	310	277	295.6	11.93	**1.02**
3	292	241	209	118	220	209	213.2	16.94	**0.73**
4	310	296	279	295	281	304	291.0	9.53	**0.94**
5	295	208	173	191	185	189	189.2	11.29	**0.64**

Table 9-3: Liner outside friction coefficient results.

Liner	Normal weight (g)	Liner outside/socket substitute tests Shear weight (g)					Average (g)	Standard deviation	Friction coefficient
		Test 1	Test 2	Test 3	Test 4	Test 5			
1	324	101	104	106	94	109	102.8	5.12	**0.32**
2	290	87	69	68	81	79	76.8	7.28	**0.27**
3	292	69	81	75	77	68	74.0	4.90	**0.25**
4	310	149	146	139	151	154	147.8	5.12	**0.48**
5	295	169	166	173	172	182	172.4	5.39	**0.58**

Table 9-4: Supporting evidence for statistical analysis of liner variables.

Peak Pressure (kPa)

	Average Flaccid Muscle					Stiff Flaccid Muscle					Contracted Muscle			
	50 kPa	100 kPa	200 kPa	400 kPa		50 kPa	100 kPa	200 kPa	400 kPa		50 kPa	100 kPa	200 kPa	400 kPa
4mm	80.0	94.2	110.1	122.9	4mm	69.1	75.8	86.2	95.9	4mm	57.0	61.4	69.4	79.0
5mm	74.2	83.1	107.3	118.1	5mm	67.0	71.1	79.0	86.7	5mm	55.1	59.1	65.2	74.5
6mm	71.1	79.0	97.7	109.4	6mm	61.3	66.0	76.2	80.0	6mm	49.5	55.1	61.7	68.2

Peak Circumferential Shear Stress (kPa)

	Average Flaccid Muscle					Stiff Flaccid Muscle					Contracted Muscle			
	50 kPa	100 kPa	200 kPa	400 kPa		50 kPa	100 kPa	200 kPa	400 kPa		50 kPa	100 kPa	200 kPa	400 kPa
4mm	31.2	38.0	42.8	31.2	4mm	24.7	28.0	35.0	41.9	4mm	18.4	23.8	29.7	36.1
5mm	28.2	32.3	39.0	28.2	5mm	22.3	26.2	32.4	40.0	5mm	14.9	22.7	28.7	34.0
6mm	25.8	29.2	36.2	25.8	6mm	19.5	23.8	28.5	39.0	6mm	11.3	18.8	25.4	30.4

Peak Longitudinal Shear Stress (kPa)

	Average Flaccid Muscle					Stiff Flaccid Muscle					Contracted Muscle			
	50 kPa	100 kPa	200 kPa	400 kPa		50 kPa	100 kPa	200 kPa	400 kPa		50 kPa	100 kPa	200 kPa	400 kPa
4mm	20.9	27.7	30.5	36.4	4mm	15.8	18.1	25.1	31.0	4mm	13.9	16.1	20.1	28.0
5mm	17.9	22.0	26.7	33.8	5mm	13.4	16.3	22.5	28.1	5mm	9.3	15.1	19.0	22.3
6mm	15.5	18.9	23.9	25.1	6mm	10.6	13.9	18.6	24.1	6mm	7.9	11.1	15.8	18.7

9.4 Chapter 6 Supporting Evidence

Table 9-5: Supporting evidence for Non-IC and IC socket comparison

		Non-IC			IC		
		Pressure (kPa)	Circumferential shear (kPa)	Longitudinal shear (kPa)	Pressure (kPa)	Circumferential shear (kPa)	Longitudinal shear (kPa)
Proximal	Medial	49	19.3	12.2	83.1	36.5	17.1
	Anterior	10	2.2	0.6	6.7	1	2.5
	Lateral	2	1	0.7	4.2	0.5	0.7
	Posterior	7.5	0.2	2.6	6.5	1.1	1.8
Middle	Medial	9.4	2.5	0.4	4.3	1.8	1.2
	Anterior	9	1.2	2.2	3.8	0.4	1.2
	Lateral	4.9	0.4	0.2	3	1.1	1.1
	Posterior	8.9	1	1.4	3	0.4	1.3
Distal	Medial	7.4	0.9	0.2	1.3	0.7	0.4
	Anterior	9	0.2	2.1	0.9	0.2	0.4
	Lateral	5.6	0.2	0.2	1	0.6	0.8
	Posterior	8.9	0.2	1.1	1.3	0.2	0.7
	Distal end	17	0.2	2.2	0.8	0.2	0.2

9.5 List of Publications

Conferences

Van Heesewijk, A., Crocombe, A., Cirovic, S., Xu, W. (2018) Evaluating the effect of changes in bone geometry on the trans-femoral socket-residual limb interface using finite element analysis. World Congress on Medical Physics and Biomedical Engineering (IUPESM) IFMBE Proceedings, Prague, vol 68(2) pp 587-591

Van Heesewijk, A., Crocombe, A., Cirovic, S., Taylor, M., Xu, W. (2018) A finite element study of the contact interface between trans-femoral prosthetic socket and residual limb, Proceedings of 8th World Congress of Biomechanics (WCB), Dublin, pp 1654

Van Heesewijk, A., Crocombe, A., Cirovic, S., Xu, W. (2018) Effect of prosthetic liner properties on residual limb stresses. Proceedings of BioMedEng18, London, pp 398